

2011

Saad A. A. Jabir

PhD Electrical Engineering-
Thick Film Sensors

[THICK FILM ELECTRONIC CERAMIC SENSORS FOR CIVIL STRUCTURES HEALTH MONITORING]

The main aim of the proposed research project is to investigate the possibility of using thick-film technology stress sensors in masonry, concrete and building materials in general to monitor overstress throughout the life of the structures and roads.

Saad A. A. Jabir

PhD Electrical Engineering- Thick Film Sensors

2011

**THICK FILM ELECTRONIC CERAMIC SENSORS FOR CIVIL
STRUCTURES HEALTH MONITORING**

BY

Saad Abdul-Ameer Jabir
BSc Electrical Engineering

A Thesis Submitted in Partial Fulfilment of the Requirements of
Edinburgh Napier University
For the Award of Doctor of Philosophy PhD
May 2011

*To the memory of my friend and
teacher*

Dr. Fouad M. Khalaf

CONTENTS

ABSTRACT	16
NOMENCLATURE	18
ACKNOWLEDGEMENTS	20
1. INTRODUCTION.....	21
1.1 Objectives of the Research	22
1.2 Stress – Strain for Structural Health Monitoring	22
1.3 Stress – Strain Mechanical Relationship.....	23
1.4 Thick Film Piezoresistivity.....	26
1.5 Basic Strain Gauge Concepts and Relationships.....	27
1.6 Strain Gauges Historical Summary	29
1.7 Suitability of Thick Film Technology for Sensor Manufacturing.....	30
1.8 Research Methodology.....	32
1.9 Outline of the Thesis	34
1.10 Thick Film (TF) Technology.....	36
1.10.1 Thick-Film (TF) Manufacturing Process	37
1.10.2 STEP 1: Schematic and Artwork.....	37
1.10.3 STEP 2: Screen Printing.....	38
1.10.3.1 Screen Fabric Mesh.....	38
1.10.3.2 Screen Frame	39
1.10.3.3 Ink or Paste.....	39
1.10.3.4 Substrate.....	40
1.10.3.5 Substrate Holder.....	41
1.10.3.6 The Squeegee	41
1.10.4 STEP 3: Firing.....	41
1.10.5 Further Necessary Steps	42

2. STATE OF THE ART	43
2.1 Structural Health Monitoring Overview	44
2.1.1 Structural Health Monitoring Objective Levels.....	46
2.1.2 SHM Sensing Techniques	48
2.1.2.1 Local and Global SHM.....	49
2.1.2.1.1 Acoustic Vibration Based Techniques	51
2.1.2.1.1.1 Active and Passive Ultrasonic Sensing.....	54
2.1.2.1.1.2 Piezoelectric Sensors	55
2.1.2.1.1.2.1 Piezoelectric Polymer Films	56
2.1.2.1.1.3 Lamb Wave and Acoustic Emission Sensors	58
2.1.2.1.2 Strain Measurement Techniques.....	61
2.1.2.1.2.1 Fibre Optic Strain Sensor	61
2.1.2.1.2.2 Classification of Fibre-Optic Sensors.....	62
2.1.2.1.2.2.1 Intensity-Based Sensors.....	62
2.1.2.1.2.2.2 Fibre Optic Bragg Gratings Strain Sensor	63
2.1.2.1.2.2.3 Phase Modulated Optical Fibre Sensors, or Interferometers	64
2.1.2.1.2.3 Foil Strain Gauges (FSG)	65
2.1.2.1.2.4 Self-Sensing Materials.....	67
2.1.2.1.2.5 Magnetostrictive Sensors Including Amorphous Wire Sensors.....	69
2.1.3 Some Universities Research on the Subject.....	71
2.1.3.1 Bristol University.....	71
2.1.3.2 University of Delaware	71
2.1.3.3 Berkeley University.....	72
2.1.3.4 The University of Michigan	73
2.2 Summary.....	73
3. SENSOR DESIGN AND VALIDATION TESTS	75
3.1 Piezoresistive Thick Film Sensors.....	75
3.2 The Designed Thick Film Piezoresistive Sensor.....	77
3.2.1 Sensor Description and Properties	78
3.2.1.1 Resistor Value.....	79
3.2.1.2 The per Square Concept.....	79

3.2.1.3	Thick Film Conductor.....	81
3.2.1.4	Substrate Material and Thickness.....	81
3.2.2	Sensor Mechanical Simulation	83
3.2.2.1	Simulation Tool.....	84
3.2.2.2	Simulation Results.....	85
3.2.2.2.1	Gluing Sensor on the Material.....	85
3.2.2.2.2	Embedding Sensor in Building Material	86
3.2.3	Thick Film versus Foil Metal Strain Gauges.....	91
3.2.3.1	Metal Foil Strain Gauge (FSG).....	91
3.2.3.2	System 5000.....	92
3.2.3.3	Circuit Electronics Used to Interface System 5000.....	93
3.2.3.4	Four Point Bending Test (4PBT)	95
3.2.3.4.1	Test Results.....	99
3.2.3.4.2	TF Sensor Gauge Factor Calculation.....	100
3.2.4	Test of SMT Mounted Sensor	101
3.2.4.1	Maximum Allowable Supported Load	104
3.3	Direct Load Application of TFS.....	105
3.4	Summary.....	105
4.	SENSOR INTERFACE.....	107
4.1	Sensor Definition.....	107
4.2	Sensor Classes and Specification	109
4.3	Choice of Suitable Interface Circuit.....	112
4.3.1	The Quarter Wheatstone Bridge	113
4.3.2	Operational Amplifier as Current Source	114
4.3.2.1	Wheatstone Bridge Versus Op-Amp Outputs.....	116
4.3.2.1.1	Verification by Simulation.....	117
4.3.2.1.2	Saber Simulator.....	117
4.3.2.1.3	Wheatstone Bridge Simulation.....	118
4.3.2.2	Op-Amp Simulation.....	120
4.3.2.3	Full Bridge with Amplifiers Simulation	123
4.3.3	Sensor Array Interface Circuit.....	125
4.3.4	Sensor Array Simulation.....	128

4.4	Application of TF Sensor on Building Materials	128
4.4.1	Experimental Result	131
4.4.1.1	Overview of the Experiment	131
4.5	Proportionality of Response	135
4.6	Summary:	137
5.	SENSOR APPLICATION ON BUILDING MATERIALS	138
5.1	Thick Film Piezo-resistive Sensor Intrinsic Discrepancies	138
5.2	Gauge Factors in a Thick Film Piezoresistive Sensor	139
5.3	Experimental Comparison between Response of Two TF Sensors	140
5.4	TF Sensor Characterization	143
5.4.1	Three Point Bending Test	143
5.4.1.1	Testing Method	143
5.4.1.2	Summary of Beam Theory	144
5.4.1.3	Strain Calculation in 3 PBT	147
5.4.1.4	Pressure Chamber Characterisation	148
5.5	Application of TF Sensor on Building Material	150
5.5.1	Gluing on Material Surface	150
5.5.1.1	On Wood	150
5.5.1.2	On Gypsum Plaster	151
5.5.1.3	TF Gauge Factor When Glued on Material	153
5.5.1.4	Methodology for Finding GF	153
5.5.2	Embedding in Structures	154
5.5.2.1	Embedding in wood	156
5.5.2.2	Embedding in Gypsum Plaster	159
5.5.2.3	Embedding in Concrete	161
5.5.3	Direct Force Application	163
5.5.3.1	Four Different Sensors on a Steel Block Angels	164
5.5.3.2	Effect of Cushion Material Test	166
5.5.3.3	Current Source to Sum Effect of TF Array	169
5.6	Summary	171
6.	THICK FILM FOR PRACTICAL SHM APPLICATION	172

6.1	The Environment.....	172
6.2	Hybrid Technology for Packaging and Long Term Functionality	173
6.2.1	Technology Overview	173
6.2.2	Commercial Applications	174
6.2.3	Military and Space Applications.....	175
6.2.4	Hybrid Technology Reliability	175
6.2.5	Packaging.....	176
6.2.6	Low-Temperature Co-Fired Ceramic, LTCC Technology	178
6.3	Structural Stability in SHM.....	180
6.3.1	Column Stability.....	181
6.3.2	TF Sensors Glued on Surface for Structures Stability.....	182
6.3.3	Mechanical Simulation of the Column Structure.....	185
6.3.4	Current Source to Improve Signal	187
6.3.5	Sensitivity to Lateral Strain.....	188
6.3.6	Embedded TF for Structure Stability.....	189
6.3.7	Direct Load Application for Structure Stability	191
6.4	Floor Stability	192
6.5	Microcontroller Based System.....	193
6.6	Power in Structural Health Monitoring	195
6.7	Summary.....	197
7.	DISCUSSION, CONCLUSIONS AND RECOMMENDATIONS.....	198
7.1	Discussion	198
7.1.1	Contributions to knowledge	205
7.2	Conclusions and Recommendations.....	208
7.2.1	Conclusions	208
7.2.2	Recommendations.....	209
8.	REFERENCES.....	212
9.	APPENDIX A-BASICS OF STRAIN GAUGES	224
9.1	Resistance of a Conductor	224

9.2	Strain Gauge Schematic	225
9.3	Strain Gauge Operation.....	225
9.4	Relationship between Resistance and Strain	226
9.5	Relationship between Resistance and Strain (2)	228
9.6	Signal Conditioning	229
9.7	Wheatstone Bridge Circuit	229
9.8	Output of a Wheatstone bridge	230
9.9	Characteristics of Quarter Bridge Strain Gauge Sensors	232
9.10	Temperature Compensation (1).....	232
9.11	Strain Gauge Installation	234
9.12	Measurement of Bending Strain.....	235
10.	APPENDIX B-MODULUS OF ELASTICITY	237
11.	APPENDIX C- PUBLICATIONS AND ACHIEVEMENTS.....	238
12.	APPENDIX D – GLOSSARY OF TERMS	241

LIST OF FIGURES

Figure 1.1 Homogeneous isotropic bar stretched by force [Webster et al 1969].....	24
Figure 1.2 Shear force, shear stress, shear strain, and shear modulus	25
Figure 1.3 Thick Film sensors on PCB for in material embedding	33
Figure 1.4 Typical hybrid circuit (Hypro Enterprise Co.)	36
Figure 1.5 Screen printer.....	38
Figure 1.6 Mesh of stainless steel screen.....	39
Figure 1.7 Complete hybrid circuit device (Clec Group)	42
Figure 2.1 The four levels of structural damage assessment	47
Figure 2.2 Graphical representation of concrete hardening in time and relative sound pulse velocity (POPOVICS 2001)	52
Figure 2.3 Piezo Electric effect.....	56
Figure 2.4 Ceramic particles in polymer matrix (LEVASSORT 1998).....	57
Figure 2.5 Symmetrical and anti-symmetrical Lamb waves.....	59
Figure 2.6 SMART Layer™ interfaced with the SMART Suitcase™ (Acellent Inc.).....	60
Figure 2.7 Light propagates through FBG, spectral response in reflection (a) and transmission (b) (FIXTER 2006).....	64
Figure 2.8 Multi-component strain stress transducer.....	67
Figure 3.1 Ceramic pressure transducer membranes (Metalux).....	76
Figure 3.2 Thick Film Sensor glued on sample building block under stress	76
Figure 3.3 Thick Film force sensor embedded in building material.....	77
Figure 3.4 (a) Thick Film piezoresistor on ceramic (b) only the resistive part without terminals (c) one connection terminal (d) magnified side view.....	78
Figure 3.5 Thick film ceramic sensor (TFCS) compared to the tip of a pencil.....	79
Figure 3.6 TF sensor 4.9X4.9X0.275mm 275GPa loaded with 100N	85
Figure 3.7 Sensor with applied 100N has a change in length of $\Delta x=0.0013\text{mm}$	86

Figure 3.8 Distributed load on sensor area.....	87
Figure 3.9 Constrained TF sensor response to 7N/mm distributed load	88
Figure 3.10 Constrained TF sensor bending moment diagram.....	89
Figure 3.11 TF sensor sensitivity enhancements by soldering only one side	90
Figure 3.12 Bending moment diagram of the sensor soldered on one side.....	91
Figure 3.13 Typical Foil Strain Gauge (FSG).....	92
Figure 3.14 Data acquisition unit of System 5000	93
Figure 3.15 Quarter Wheatstone bridge	95
Figure 3.16 Four point bending test	96
Figure 3.17 TFCS orientation.....	96
Figure 3.18 Four point bending test simulation results	97
Figure 3.19 Image of TF sensors together with foil strain gauge in 4 PBT.....	98
Figure 3.20 TFCS bridge circuit connection to the steel bar and system 5000	99
Figure 3.21 Thick-Film ceramic Sensor in tension and compression.....	100
Figure 3.22 Test of TF sensor mounted on PCB in SMT.....	102
Figure 3.23 SMD mounted TF sensor response to uniform load	102
Figure 3.24 Circular edge-clamped diaphragm Response (Measurement Group).....	103
Figure 3.25 Direct application of load on Thick Film substrate	105
Figure 4.1 Sensor interface to measure a physical phenomenon	108
Figure 4.2 Wheatstone bridge Circuit	113
Figure 4.3 Op amp as current source.....	115
Figure 4.4 Wheatstone bridge voltage amplified by an inst. Amp.....	119
Figure 4.5 V_{out} vs. TF R_t change, ΔY should be divided by 10	120
Figure 4.6 TF sensor resistor in op-amp LMC6482 configuration	121
Figure 4.7 Output of op-amp with R_t stepping by 10 Ω	122
Figure 4.8 Op-amp boosted Wheatstone bridge.....	124

Figure 4.9 Op-amp driven Wheatstone bridge max output voltage swing.....	125
Figure 4.10 Two arrays of four TF sensors mounted on PCB.....	126
Figure 4.11 Array of four TFCS driven by one current source.....	127
Figure 4.12 TF sensor array output response , $\Delta Y=3.56$ V	128
Figure 4.13 Differential amplifier with offset balance	129
Figure 4.14 Sample brick 12.4x16.7x34.7 mm.....	130
Figure 4.15 Sample concrete block 23.3x22.3x50 mm	130
Figure 4.16 Concrete block sample stressed on a linear scale.....	132
Figure 4.17 S_1 response vs. compressive force	133
Figure 4.18 S_2 response vs. compressive force	133
Figure 4.19 S_1 and S_2 response vs. compressive force.....	134
Figure 4.20 S_3+S_4 on concrete	134
Figure 4.21 TF sensors response on red brick and concrete.....	135
Figure 5.1 Circuit used to compare two TF sensors response	141
Figure 5.2 Response of two TF sensors subject to same strain.....	142
Figure 5.3 Difference response of two TF sensors subject to same stress.....	142
Figure 5.4 Three Point Bending test to measure sensor GF.....	144
Figure 5.5 Deformation of a beam subject to force.....	145
Figure 5.6 Three point bending to measure TF sensor GF	148
Figure 5.7 An array of TF sensors mounted in SM technology	149
Figure 5.8 response of an array of TF sensors subject to uniform pressure.....	149
Figure 5.9 20x20x20 wood block under compression and tension.....	151
Figure 5.10 TF sensor on sample plaster compressive stress	152
Figure 5.11 Embedded TF sensor for column stability.....	155
Figure 5.12 TF sensor embedded in wood with bi-component adhesive	156
Figure 5.13 Surface Mounted sensor embedded in wood	157

Figure 5.14 Load unbalance with one sensor in wood.....	158
Figure 5.15 Load increase at +20 cm from centre	158
Figure 5.16 Load increase at -20 cm from centre	159
Figure 5.17 Plaster column with two embedded TF sensors	160
Figure 5.18 Response of embedded TF sensor in Plaster column.....	161
Figure 5.19 Mould and concrete cube with embedded TF sensors	162
Figure 5.20 TF resistance change during concrete cure time	163
Figure 5.21 Four TF sensors on upper surface of steel cube.....	164
Figure 5.22 Direct load application in steel cube compression test.....	165
Figure 5.23 Four sensors response in direct load application on steel cube.....	166
Figure 5.24 Sample-building materials with TF glued	167
Figure 5.25 TF on steel cube loaded with Teflon pin.....	168
Figure 5.26 Response of TF directly loaded on wood, plaster, steel.....	168
Figure 5.27 Array of four TFCS driven by one current source.....	169
Figure 5.28 Silicon rubber on TF sensors on the angles of sample red brick.....	170
Figure 5.29 Response of silicone and hard rubber in direct load on brick.....	170
Figure 6.1 Example of Hybrid circuit (Sanchez Hybrids).....	176
Figure 6.2 Liquid level sensor.....	179
Figure 6.3 3D structure of LTCC and example of possible features (JACQ 2009)	180
Figure 6.4 Sketch of the column stability test setup.....	182
Figure 6.5 Circuit to observe column stability.....	183
Figure 6.6 Brick column response as function of load movement	184
Figure 6.7 TF sensors on sides of Brick column with moving load	184
Figure 6.8 Simulation of brick column loaded with 2Kg at 30mm.....	185
Figure 6.9 Column side loading behavior	186
Figure 6.10 Current source to monitor column stability	188

Figure 6.11 Rosette Foil Strain Gauge.....	189
Figure 6.12 An experiment on a column supporting a floor.....	190
Figure 6.13 TF sensors embedded and on surface of plaster column	190
Figure 6.14 Response to load of two embedded TF sensors in plaster column	191
Figure 6.15 Four TF sensors used to monitor load and stability.....	192
Figure 6.16 Block diagram of load and stability measuring system.....	193
Figure 6.17 Microcontroller system to monitor structure stability	196
Figure 7.1 TF Ceramic sensor glued on sample Brick.....	201
Figure 7.2 Bulge occurs in the middle in relatively flexible material.....	203
Figure 7.3 Edge clamped Diaphragm.....	210
Figure 7.4 TF sensor embedded parallel to load	211

LIST OF TABLES

Table 1.1 Characteristics of strain gauges materials (PRUDENZIATI 1994)	27
Table 3.1 Alumina Substrate Properties (Accutatus)	83
Table 5.1 TF sensor GF calculation table.....	154

ABSTRACT

Buildings, roads, bridges and structures in general suffer many kinds of damages due to overstress caused by settlements of foundations, high winds, dynamic forces, passing traffic, vibration and unexpected external loads beyond the safe design forces. The damages manifest itself by cracks, falling of plaster and render uneven roads and some time complete collapse. The cost of maintaining and fixing damages caused by the above is quite high for the building and construction industry. The same phenomenon is common to many other structures like airplanes, wind turbine and machinery in general.

Structural Health Monitoring (SHM) is the engineering branch, which aims to give, at every moment during the life of a structure, a diagnosis of the "state" of the constituent materials, of the different parts of a structure. The state of the structure must remain in the domain specified in the design, although this can be altered due to usage or due to normal aging by the action of the environment, and by accidental events. By using special electronic sensors to monitor the unexpected high concentration of stresses or changes of these stresses throughout the life of the structure and pavement, reduces the cost of maintenance and repair. Historic buildings would also benefit from using such sensors to monitor the overstress in the old and frugally stones and bricks. The sensors can be embedded in the lime mortar joints and an electronic meter is used periodically to check for any unusual overstress during the life of the building.

The main aim of the proposed research project is to investigate the possibility of using thick-film technology stress sensors in masonry, concrete and building materials in general to monitor overstress and instability throughout the life of the structures. The sensors could be used

in brick, block, stone, and concrete and they could be mounted on the surface or embedded in the materials.

There are many research studies on strain gauge devices in structural monitoring; Thick Film (TF) piezo-resistive sensors are proposed as a direct alternative to the widely used metal Foil Strain Gauges (FSG). Due to the low cost of TF sensors, their ease of use, suitability to integrate electronics on board, and to have different geometrical shapes, they could be deployed at different locations in a building, road or be distributed in arrays. This offers the continuous monitoring of stresses at any time by using a data logger on two points on the surface or by using wireless electronic transmission.

In this research, new thick film screen-printed ceramic piezo-resistive sensor has been developed and characterized as discrete device for deployment on surface of a structure and embedded into the structure during building material curing or after structure erection. The sensor response on different building materials has been experimented and compared. Mechanical and electronic simulation tools were used to characterise the sensor and to choose an adequate interface electronic circuit.

The experimental results of the simulated sensor and circuitry, showed the suitability of the sensor to be embedded in building materials during curing period and on erected structures. Materials used were wood, concrete, brick and plaster. In addition, the overall linearity of response of the sensors applied on building material surface was asserted which makes the technology a candidate for a more wide deployment in SHM field.

NOMENCLATURE

Symbol	Unit	Name
A	Metre	Wire radius of loop coil
A	Metre ²	Area
b	Metre	Width
c	Metre	Distance from neutral axis to beam surface
C	Farad	Capacitance
CSHM	-	Civil Structural Health Monitoring
δ	millimetre	beam deflection
E	N/mm ² or (GPa)	Young's modulus
E	Volts per Metre	Electrical field strength
f	Hertz	Frequency
FSG	-	Foil Strain Gauge
P	Newton	Force
g	Metre	Width of air gap
G	-	Gain of an amplifier
G	N/mm ² or (GPa)	Shear modulus
GF	-	Gauge factor of a strain gauge
h	mm	Thickness
H	Ampere per Metre	Magnetic field strength
i	Ampere	Electrical current
J	-	Complex operator
I	Metre ⁴	Moment of inertia of beam cross-section
K	N/m	Stiffness
l	Metre	Length
M	N-metre	Bending moment
Δl	Metre	Length change
Op-amp	-	Operational Amplifier

c	Columb	Charge
Q	-	Radius of curvature of a beam
R	Ohm	Resistance
r	Metre	Radius
σ	N/mm ² or (GPa)	Stress
T	Second	Period
TF	-	Thick Film
TFS	-	Thick Film Sensor
TFCS	-	Thick Film Ceramic Sensor
θ	Degrees	angle of beam deflection
V	Volt	Electrical voltage
x	Metre	Distance
Y	Metre	distance from beam neutral axis
Z	Ohm	Impedance
α	Coulombs per metre	Charge density
β	-	Phase constant
δ	Neper per metre	Dielectric losses
ϵ	Farad per Metre	Dielectric permittivity
ϵ	-	Strain
γ	-	Shear strain
η	-	Metal ratio
λ	Metre	Spatial wavelength
μ_0	Henrys per Metre	Free space magnetic conductivity
ω	Hertz	Angular Frequency
ρ	Ω - metre	Resistivity
τ	Newton/ Metre ²	Shear stress
σ	Newton/ Metre ²	Stress on material bulk
ν	-	Poisson's ratio

ACKNOWLEDGEMENTS

I would like to take this opportunity to thank various staff members at Edinburgh Napier University, In particular, I would like to thank my Director of Studies Dr Naren K Gupta and my supervisor; Dr. Sam Wamuziri, for their advice encouragement and patience throughout the duration of present research. My thanks also go to Mr. Willie Laing, who always made himself available for the various practical investigations of this research, His friendship and support is highly appreciated.

This study idea was originated by Dr. Fouad M. Khalaf. I will never forget him as a friend and teacher. His scientific contributions will remain in the memory of the civil engineering community worldwide.

1. Introduction

For the purpose of improving safety and reduce the maintenance costs of infrastructures, novel inspection and damage detection techniques need to be developed, tested and implemented on various structures including buildings, bridges, aircraft, and railroads. One such technique that has gained much attention in the research and industrial communities over the past years is Structural Health Monitoring (SHM). The concept behind structural health monitoring is that every structure has certain properties that change as the structure degrades or becomes damaged. The health of the structure can be monitored by measuring these properties and looking for changes in them over time. An important property of a structure is the stress-strain relationship, which determines many important physical quantities indicating structure health like bending moments, torques, loads, etc.. The SHM involves the complete process of obtaining and analysing dynamic response data including implementing an array of sensors/actuators on the structure, periodically obtaining structural response measurements, analyzing the measurements and extracting damage sensitive properties, and statistically analyzing the extracted properties to describe the current state of the structure (STEVEN 2008).

One of the used techniques to assess the structure health is the measurement of strain caused by loading stresses on the structure and the changing envelop in time of these strains that might be caused by structure degradation.

Thick Film is a strain consolidated measuring technology, used widely for vessel pressure measurements and is deployed in many industrial sectors among which are automotive, hydraulic-lifts, hydraulic moving machines

and power tools ,etc. The subject of the study is to apply this technology to Structural Health Monitoring. As the subject is all about stress-strain the first chapter will start describing the stress-strain relationship for solids after introducing the objectives of the research and how these objectives could be achieved. At the end, it gives an overview of Piezoresistivity effect and goes through a step-by-step description of the Thick Film manufacturing process.

1.1 Objectives of the Research

The main objective of this study is to investigate the suitability of thick film strain piezoresistive sensors for load and strain measurements on building materials. The evaluation of the technology is in light of providing a new aid to Civil Structural Health Monitoring (CSHM). The study will extend to examine different possible deployment methodologies on civil engineering structural materials like concrete, steel, timber, gypsum and clay. Reference will be made during this work to the other widely used piezoresistive sensor; the metal Foil Strain Gauge. In General, the study will try to answer the following questions:

- 1- Is piezo-resistive thick film sensor suitable for measuring strain on building materials?
- 2- How to interface TF sensors to measure loads in a reliably way and for a period comparable to the civil structures life?
- 3- What are the advantages of using such technology?
- 4- How can these sensors be employed?
- 5- What are the limitations of the technology and what are the recommendations to improve the usage?

1.2 Stress – Strain for Structural Health Monitoring

Structural Health Monitoring of civil structures by measuring strains is adapted by using many techniques and sensor technologies. Among these

sensor technologies are metal foil strain gauges, metal wires, fibre optics, and others, which will be discussed in the literature review of chapter two.

Strain sensing technology has become one of the most critical areas required for structural health monitoring (SHM), damage detection, condition-based maintenance, failure prevention and non-destructive evaluation. This because strain, is one of the key performance parameters that affects the life of mechanical components and civil structures. Stress, fatigue strength, material internal damage and load-history of structure, can be interpreted from strain information (SUN 2006). The purpose of this chapter is to introduce Thick Film piezoresistive stress sensor technology as viable and effective sensor technology for civil structural health monitoring.

1.3 Stress – Strain Mechanical Relationship

The terms stress and strain are used to describe deformations of solid materials. The simplest types of solids to describe are homogeneous and isotropic. Homogeneous means the material properties are the same at different locations and isotropic means the material properties are independent of direction in the material. Most building materials have these properties. E.g. An annealed steel bar is homogeneous and isotropic. When the properties are different along the length and and/or along the cross section the material is said to be non-isotropic, an example is the animal bone which is not homogeneous because the marrow which has different properties and it is not isotropic because these properties are different along the length and along the cross-section [Webster et al 1969].

The concepts of stress and strain are introduced in the context of a long homogeneous isotropic subjected to a tensile load in **Figure 1.1**,

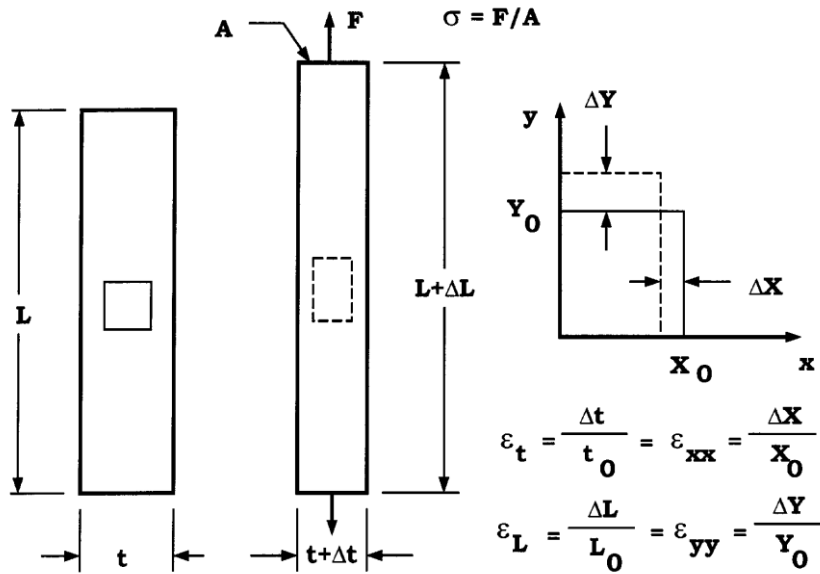


Figure 1.1 Homogeneous isotropic bar stretched by force [Webster et al 1969]

The stress σ , is the applied force F , divided by the cross-sectional area A . The resulting strain ϵ , is the length change ΔL , divided by the initial length L . The bar elongates in the direction of the pulling force generating longitudinal strain ϵ_L , and contracts in the direction perpendicular to the force with a transversal strain ϵ_t .

In **Figure 1.1**, ΔL could be positive or negative depending on whether the applied force is a tensile or compressive force. Δt will also change sign correspondingly.

When the strain is not too large, like many solid materials, building materials behave like linear springs; i.e. displacement is proportional to the applied force. If the same force is applied to a thicker piece of material, the spring is stiffer and the displacement is smaller. This leads to a relation between force and displacement that depends on the dimensions of the material. Material properties, such as the density and specific heat, must be defined in a manner that is independent of the shape and size of the specimen. Elastic material properties are defined in terms of stress and

strain. In the linear range of material response, the stress is proportional to the strain and the ratio of stress to strain for the bar under tension is an elastic constant called the Young's modulus; E . The ratio of the transverse strain to longitudinal strain is the Poisson's ratio ν . This ratio has a negative sign because ϵ_T is negative for axial tension.

Forces can be applied to a material in a manner that will cause distortion rather than elongation (**Figure 1.2**). A force applied tangent to a surface divided by the cross-sectional area is described as a shear stress τ . The distortion can be measured by the angle change produced. This is the shear strain γ . when the angle change is small then the relation between shear stress and shear strain is linear and the ratio of the shear stress to shear strain is the shear modulus G .

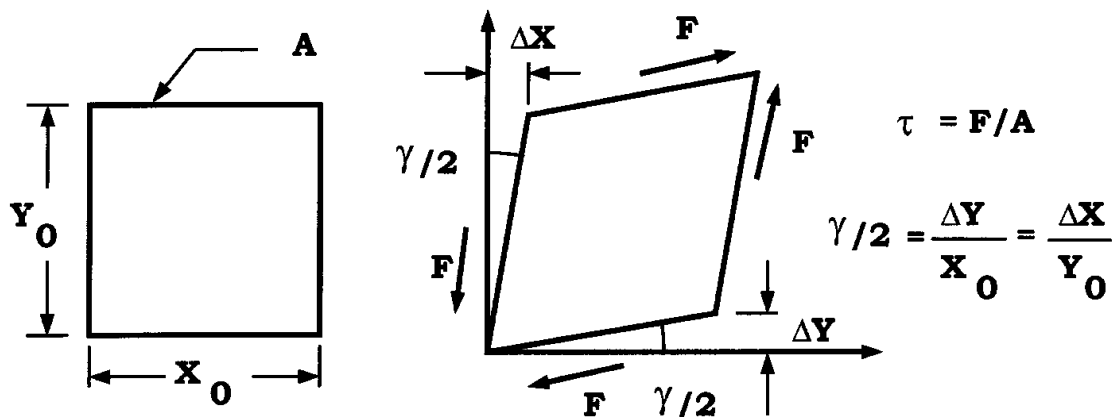


Figure 1.2 Shear force, shear stress, shear strain, and shear modulus

Several types of sensors are used to measure strain. These include piezoresistive gauges (foil or wire strain gauges and semiconductor strain gauges), piezoelectric gauges (polyvinylidene fluoride (PVDF) film and quartz) fibre optic gauges, birefringent films and materials, and Moiré grids (see Appendix-D for definitions). Each type of sensor requires its own specialized signal conditioning. Selection of the best strain sensor for a given measurement is based on many factors, including specimen

geometry, temperature, strain rate, frequency, magnitude, as well as cost, complexity, accuracy, spatial resolution, time resolution, sensitivity to transverse strain, sensitivity to temperature, and complexity of signal conditioning. Appendix A gives an overview of a metal foil strain gauge usage and circuit implementation.

1.4 Thick Film Piezoresistivity

Piezoresistivity is a reversible phenomenon wherein under the influence of an externally applied stress a resistor exhibits a change in resistance. This change in resistance persists as long as the applied stress prevails. This fractional change in resistance is proportional to the applied stress. The constant of proportionality is defined as the Gauge Factor (GF).

Piezoresistive materials used for strain gauge applications are classified into three groups: thin metal films, thick film resistors and semiconductors. Over the past two decades several commercial as well as potential applications of thick film strain gauges have been studied. Device performance characteristics with advantages and limitations of such applications have been reported by (STECHEER et al 1987). (DELL'ACQUA 1986), and (PUDENZIATI et al 1994). The thick film strain gauges are an excellent compromise between the performance characteristics of the other two types of strain gauges, thin metal films and semiconductors. Also, the in-line print and fire thick film manufacturing is simple, economical and reliable. High GF thick film resistors are used in a wide variety of low cost, high reliability strain gauge and sensor applications. These applications include acceleration, force, pressure, weight, computer joy stick or pointing stick. Some high gauge factor thick film pastes exhibits Gauge Factors in the 14 to 20 range for sheet resistance in the 1k Ω /sq to 10k Ω /sq range (CHITALE et. al 1989) and exhibit low temperature dependence.(CHITALE 1996)

Table 1.1 shows the main characteristics of TF strain sensors with respect to metal foil and silicon strain gauges. The combination of relatively high

gauge factor (GF) and temperature stability in addition to mass production capability and low cost are the major factors justifying implementing this technology to build reliable force and pressure sensors in general.

Table 1.1 Characteristics of strain gauges materials (PRUDENZIATI 1994)

Material	GF	TCR - PPM/degree	TCGF - PPM/degree	Stability
Metal sheets and films	1 to 2	20	100	Excellent
Silicon Single crystals	50 to 80	1000	-1500	Good
Thick Film Resistor	2 to 35	50 to 200	-300	Very good

Table 1.1 terms definitions:

GF: Gauge factor [$GF = (\Delta R/R) / \epsilon$]

TCR: Temperature coefficient of resistor [$TCR = (\Delta R/R)/\Delta T$]

PPM: Parts per million

TCGF: Temperature coefficient of gauge factor [$TCGF = GF/\Delta T$]

1.5 Basic Strain Gauge Concepts and Relationships

Like foil metal strain gauges, TFCS obeys equation 1.1,

$$R = \rho (L/A) \quad 1.1$$

By considering a change in conductor length only:

$$\Delta R = \frac{\rho \Delta l}{A} \quad 1.2$$

Dividing by R then we obtain the partial change in resistance (R) due to change in length (L):

$$\frac{\Delta R}{R} = \frac{\frac{\rho \Delta l}{A}}{\frac{\rho l}{A}} = \frac{\Delta l}{l} \quad 1.3$$

In general the resistance variation is not only due to change in length but also due to variation in the other parameters (L, A, and ρ). Similar relation can be obtained for change in resistivity, $\Delta\rho$, i.e.

$$\frac{\Delta R}{R} = \frac{\Delta\rho}{\rho} \quad 1.4$$

In general, if the effect of all variables on resistor is considered:

$$\frac{\Delta R}{R} = \frac{\Delta\rho}{\rho} - \frac{\Delta A}{A} + \frac{\Delta l}{l} \quad 1.5$$

It may be noted that as A is in the denominator of (1.1), the positive change in area by ΔA will decrease resistance; hence, the negative sign.

A solid body, which is under stress, changes its dimension in the direction of force. However, it will not change in volume. A change in one dimension will be compensated by an opposite change in the other dimension within the elasticity limit of the material.

In this context $\Delta L/L$ is the strain and $\Delta A/A = -2\nu\epsilon$ in an isotropic material stressed within its elastic behaviour and characterized by a Poisson's ratio ν (MORTEN 1994).

The change in area can be related to the change in length via Poisson's effect. If the cross section is rectangular of initial width B, then as the area

goes from A to A+ΔA, B will change from B to B+ΔB. If the axial strain is defined as $\epsilon_a = \Delta l/l$, and the transverse strain as $\epsilon_t = \Delta B/B$ then

$$\epsilon_t = \frac{\Delta B}{B} = -\nu \epsilon_a = -\nu \frac{\Delta l}{l} \quad 1.6$$

Where, ν is Poisson's ratio.

Accordingly, the following relationship is obtained:

$$GF = \frac{\Delta R}{R\epsilon} = \frac{\Delta \rho}{\rho\epsilon} + 1 + 2\nu \quad 1.7$$

The gauge factor is dependent on two terms, one is due to change in resistivity with strain and the other is for geometrical alteration. Solids may have a poisson's ratio ν of 0.2 to 0.45. Hence, even if the term dependent on resistivity of the material is zero, the geometrical contribution will give rise to a gauge factor of 1.5 to 1.9. Gauge factor for TF piezoresistive sensors ranges from 2 to 35 as indicated in **Table 1.1**.

1.6 Strain Gauges Historical Summary

The history of strain gauges has roots in the nineteenth century. Lord Kelvin's report (1857) was on the change of resistance of strained conductors (PRUDENZIATI 1977).

In 1939 strain gauges consisting of supported metal wires and metal grids obtained by photo etching of laminated metals were introduced. Gauges of this type have been and are used in huge quantities for the measurement of strain in buildings, aircraft wings, prototypes of new machines etc (Norton 1996). These kinds of sensors have small change of signal with strain, nevertheless they have no real competitor for a combination of suitable characteristics including small size, possibility to be bonded,

glued to any type of surface. They also have large strain range and low cost.

Sensors of strain-related mechanical quantities, which rely on the piezoresistive properties of thick-film resistors, came in the late 1970s when this phenomenon was noticed during reliability considerations of hybrid microelectronic circuitry.

A collection of many suitable properties was noticed. These are high strain sensitivity, low temperature coefficients of resistance, low temperature coefficient of gauge factor, high stability and reproducibility were suitable for the implementation of novel classes of sensors for strain-related physical quantities (PRUDENZIATI 1994). Since then piezoresistive properties of thick film, resistors have attracted a great deal of scientific and technological interest and applications have rapidly spread in sensors for many diversified applicative areas.

1.7 Suitability of Thick Film Technology for Sensor Manufacturing

Thick film technology is defined by a particular manufacturing process. This process is screen-printing and firing. The range of materials available, therefore, is determined by their capability of being both printed and fired. Research and development brought all sorts of new materials that reveal sensitivities to various physical and chemical phenomena. Besides the availability of materials, TF fabrication technology allows physical forms to be realized which by constitution and shape facilitates appropriate interaction with the physical world.

Thick-film hybrid technology is also an interconnection technology that allows different electronic components of various degrees of complexity to be assembled to form systems capable of signal elaboration. This process does not require big investment compared for example to semiconductor manufacturing. An estimation of the cost of small size semiconductor production line is from 1 to 2 million USD compared to 0.1 million USD of

thick film. The process of semiconductor manufacturing often requires hundreds of sequential steps, each one of which could lead to yield loss. Consequently, maintaining product quality in manufacturing facility often requires the strict control of hundreds or even thousands of process variables. Production in thick film technology has much less parameters and hence yield is less susceptible to process variation.

Thick film technology has many advantages over other sensing techniques which make it adequate for Structural Health Monitoring and here are some remarkable advantages:

- Availability of different materials suitable to build sensors and electronic components (capacitances, resistors, etc).
- Different geometrical forms can be realized.
- Production process provides interconnectivity of the components of the built geometries. It also provides connectivity to external systems.
- Cheap process in terms of material and equipment investment.
- Low material and process running cost.
- Mass production capability, which is an important factor to have cheap sensors.
- Suitable for integration with amplifying, driving, or compensating electronics on the same substrate.
- Thick-Film Technology can be used to build different kinds of sensors to measure various physical and environmental entities relevant to building security monitoring like temperature measurement [FERRARI 2002], (MAHAYEER 2001), Gas (DAE 2002)], and chemical biosensors (VOSKERICIAN 2005).
- Materials developed specifically for sensor applications have included magneto-resistive and piezoelectric inks (PRODUNZIATI 1992) (WHITE 1991). In all these cases, the printing and processing techniques are compatible with conventional thick film hybrid

circuit fabrication techniques. This provides a convenient and flexible technology for manufacture and enables the sensors to be integrated with hybrid electronic circuits.

- An important topic in SHM is the power supply for the intelligent sensors. The supply is necessary to drive electronics and the networking to monitor a structure. It is well known that cadmium sulphide can be screen printed and sintered to form films that display photosensitivity. Such sintered films have been used to produce photoconductive sensors (NICOLL 1955) and more recently for photovoltaic solar cells (VOJDANI 1973). In this last paper, photoconductive sensors based on screen printed cadmium sulphide and cadmium selenide thick films printed over standard silver-palladium conductors are described. The process is such that the sensor could be readily integrated into a hybrid circuit. Simple photoconductive arrays and a potentiometric position sensor have been fabricated (ROSS 1994).
- Substrate made of ceramic material or steel has outstanding mechanical and thermal properties which make them adequate on one hand to have stable electronic circuits and to withstand harsh environmental conditions on the other.

1.8 Research Methodology

To achieve the prefixed objectives, following research milestones were covered:

- 1- To develop a Thick Film sensor to be applied on building materials in various requirements suitable for structures monitoring.
- 2- To verify the response of the designed sensor on different building materials compared to foil metal strain gauges using same driving circuitry.
- 3- To choose suitable driving circuitry with the aid of simulation tools.

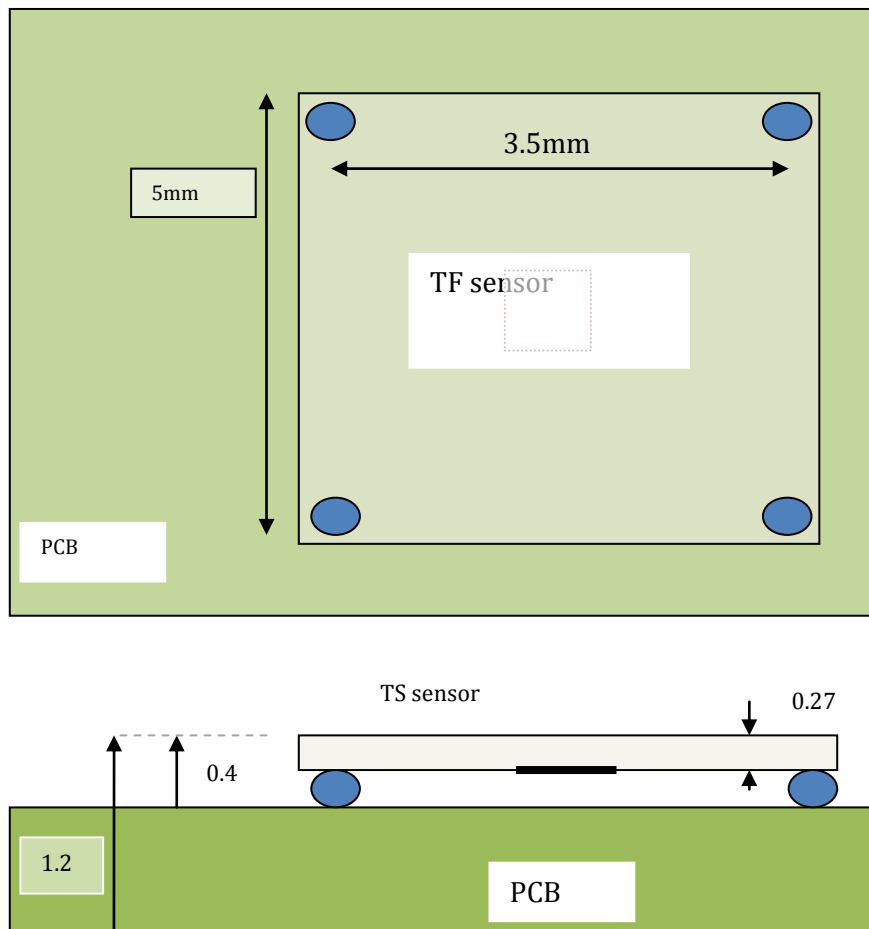


Figure 1.3 Thick Film sensors on PCB for in material embedding

- 4- Application of the sensor in the following deployment methodologies:
 - a. Glued on the material like foil metal strain gauge,
 - b. Mounted on Printed Circuit Board (PCB) for the purpose of embedding in the building material as in **Figure 1.3**.
- 5- To investigate any possible system level deployment that might contribute to Civil Structural Health Monitoring. In this case, a circuit for column stability has been considered.

1.9 Outline of the Thesis

The structure of the thesis can be summarized as follows:

- Chapter 1 Introduces the stress-strain in solids and derive the basic equations for Piezoresistivity. Historical overview of strain gauge and thick film technologies are given outlining the advantages of thick film and hybrid technology. A step-by-step TF production procedure is described. The chapter defines the research objectives and methodology adapted.
- Chapter 2 Introduces the subject of Structural Health Monitoring and subdivides its various adoption methods. Thick film technology is placed in the right classification of application area, describes the state of the art of the technology, and presents a literature review on the subject inherent to the kind of application similar to Thick Film technology
- Chapter 3 Sensor development and validation tests. TF sensor development, parameters effecting sensor response, mechanical simulation and derivation of the sensor response in its deployment methods is given.
- Chapter 4 Sensor interface and application on building materials. Comparison between Wheatstone bridge and Op-Amp configuration is derived and simulated then used to drive TF sensors on building materials.
- Chapter 5 In this chapter, a comparison between different TF sensors coming from same production lot are experimented and a method to measure TF GF before deployment is proposed. TF sensors are applied on different materials and in different methodologies.

- Chapter 6 Practical considerations and an overview of the electronic hybrid circuit technology and its advantages which make it suitable for Civil Structural Health Monitoring. Experiment for how to use thick film sensors for structure stability like a column and a circuit with microcontroller to monitor the stability and load of the column is proposed.
- Chapter 7 Discussion of the achieved objectives and the contributions made to knowledge through this work. At the end conclusions and recommendations for future work and researches are given.

1.10 Thick Film (TF) Technology

Thick-film technology history can be followed back to the fifties of the last century. This was when hybrid technology was considered as a replacement of Printed Circuit Technology to provide mechanical assembly support for electronic circuits. In the sixties and with the advent of semiconductor integrated circuits and the appearance of palladium based resistor, hybrid circuit technology became a reality. It became clear that with hybrid technology, different technologies could be assembled together to produce new class of electronic systems.

A thick-film circuit comprises layers of special inks or pastes deposited and fired onto an insulating substrate. Thick-film components are conductive, resistive, capacitive and dielectric film patterns on a substrate surface. These materials are in the form of ink composed of various metal, oxides, ceramic and glass powders suspended in an organic vehicle.

Pastes and substrate in a thick-film circuit form capacitors and resistors which are the fundamental parts of electronic circuits and with the addition of integrated circuits, complete electronic systems could be manufactured. A hybrid circuit example is given in **Figure 1.4**.

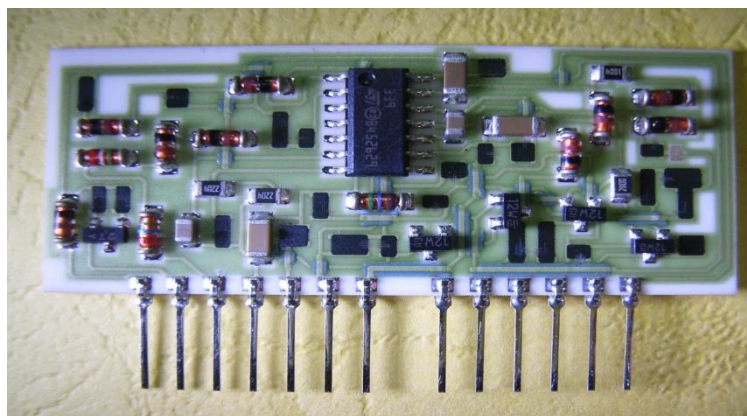


Figure 1.4 Typical hybrid circuit (Hypro Enterprise Co.)

1.10.1 Thick-Film (TF) Manufacturing Process

Thick-film Technology is distinguished by depositing inks on the substrate surface by screen-printing through stainless steel masks. The deposited inks are then fired in a kiln. The steps to produce a TF piezoresistive sensor are the same to produce hybrid circuits. The steps are described in (PRODUNZIATI 1994) of which here is a summary:

1.10.2 STEP 1: Schematic and Artwork

Similar to that done for Printed Circuit Board (PCB), computers are used to draw the schematics to be eventually simulated to prove correct functionality. Software packages are available to transfer the schematic to screen layouts.

There are some sophisticated software packages available specifically for thick film hybrid circuit design, which provide amongst other facilities, the ability to automatically check the layout against a set of design rules. These design rules are dictated by production line machines manufacturing precision capabilities to maintain high yield. The layout can be modified to suit each individual user processing or assembly needs. Assuming the computer layout conforms to the design rules then the next phase in the design process is to generate a hard copy of the design. The exact form of this copy can take one of several forms depending on the equipment available to the user. For example, many thick film screen manufactures will accept artwork in either positive or negative film scaled up by 2, 4, 5 or 10 times the required size. Successive reduction will reduce errors.

With the advent of accurate photo plotters, it is now possible to take the layout and accurately reproduce it on photographic film directly so that it can be developed to be ready for screen manufacture.

1.10.3 STEP 2: Screen Printing

One of the most distinguishing aspects of the thick film process is the method used for deposition of the films. Screen-printing traditionally recognized, as art (like that done for pottery) has had to be modernised and transformed into a more scientific tool for thick film technology.

A print occurs first, and then firing in an oven, second print is next and firing in the oven again, etc. This cycle depends on the complexity of the hybrid circuit. Printing and firing multiple layers consists of conductors, resistors, insulators and surface protection glass. **Figure 1.5** shows the constituent parts of a screen printer.

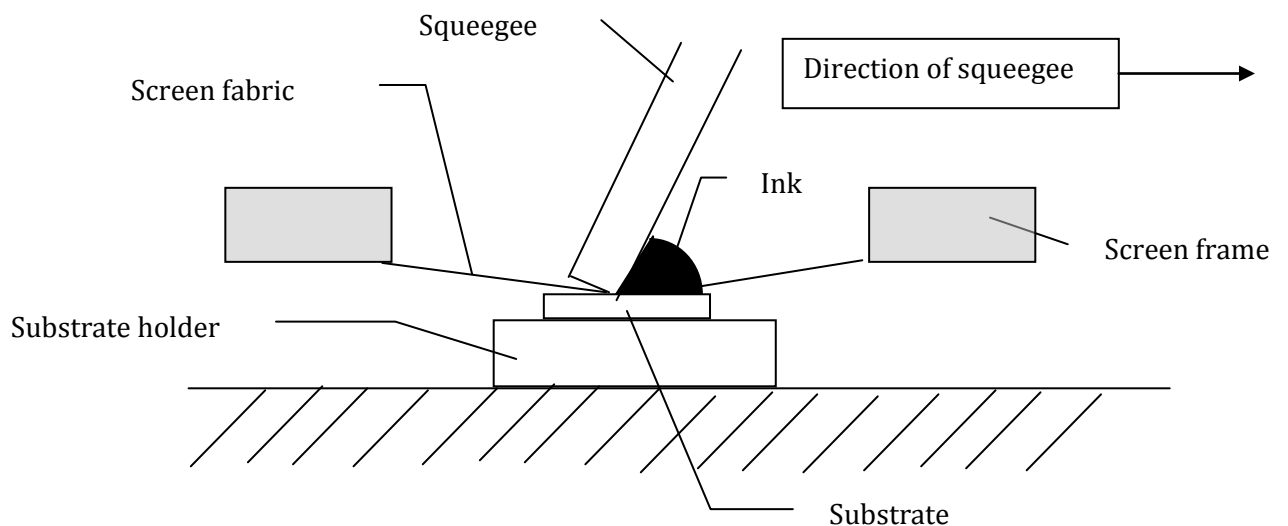


Figure 1.5 Screen printer

Here is a description of the parts in **Figure 1.5**:

1.10.3.1 Screen Fabric Mesh

A typical TF screen consists of a finely woven mesh of stainless steel, nylon, or polyester mounted under tension on a metal frame (**Figure 1.6**). The screen acts as a metering device to control print thickness, and hence it is essential to ensure that the mesh material achieves uniformity of the

printed deposit. This uniformity is responsible for components matching and reproducibility. Therefore, the mesh material must be precisely and evenly woven and possesses uniform mesh apertures. The fabric should also have suitable flexibility to enable good contact over all areas of the substrate particularly when this is not exactly flat. There are other mechanical characteristics necessary for good screen-printing like resilience, smoothness, resistance to chemical agents, etc.

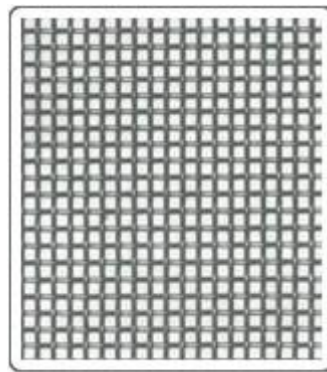


Figure 1.6 Mesh of stainless steel screen

1.10.3.2 Screen Frame

Holds the screen and is to be fixed firmly by the printing machine chassis. The screen frame is usually made of cast aluminium and serves to hold the mesh fabric taught and also to allow the stencil to be held firm and precisely located during printing. The mesh is attached to the frame by either crimping it around the frame edge or by using adhesives.

1.10.3.3 Ink or Paste

A composed paste containing various metal, oxide, ceramic and glass powders suspended in an organic vehicle. When this ink is screen-printed, dried and fired on an appropriate substrate, like ceramic, forms a unified solid structure of various geometries and shapes.

The composition takes advantage of knowledge acquired and accumulated in several disciplines, like polymer chemistry, electrochemistry and solid-state physics. Any paste for electronic thick film passive component or sensing element contains at least two ingredients, an organic vehicle and a functional material or active ingredient that is intended to dominate the electric and sensing properties of the layer. There is a third ingredient, which is usually present, made of either a glass frit or an oxide. This last serves as a bonding agent of the fired film to its substrate, so it affects directly the mechanical response in case of sensor manufacturing.

One fundamental aspect of the TF technology is the flexibility and the myriad of materials of a wide spectrum of properties that can be generated to form different kinds of sensors and components that serves wide range of applications.

1.10.3.4 Substrate

Substrates mainly provide the mechanical support and electrical insulation for the TF hybrid devices. The properties of the substrate can affect both the processes and the final characteristics of the devices. The substrate properties must meet the applications requirement. These are dielectric constant, dielectric strength, dissipation factor, thermal conductivity, thermal expansion coefficient, resistivity, mechanical strength, modulus of elasticity, etc.. These are important properties to be considered for each specific application. The majority of substrates used in TF technology consist of ceramic materials such as Alumina, Beryllia, Magnesia, and Zirconia.

For specific applications, glass and enamelled steel substrates have also been quite successful. Glass-ceramic materials are going to be widely used because of their low sintering temperature, which enables the manufacture of multilayer circuit structures with low resistivity conductors. Even plastic substrates are sometimes used in combination with polymeric or metal organic pastes.

1.10.3.5 Substrate Holder

The function of the substrate holder is to register the substrate accurately below the screen and also to keep it firmly fixed in position during printing. The two most common ways of holding the substrates are with a vacuum chuck or a recessed jig. The alternative is a recessed chuck that is fitted with locating pins and a clamping edge. The vacuum alone is usually sufficient to hold the substrate in position without the need for mechanical clamping (PRUDENZIATI 1977, 1994).

1.10.3.6 The Squeegee

The squeegee is essentially a flexible blade whose function is to transfer the paste through the screen and onto the substrate. During printing the squeegee forces ink through the open areas of the mesh by virtue of the surface tension between the film and substrate, the required pattern is transferred to the substrate as the screen and substrate separate. The squeegee's shape, material and pressure are all factors, which dictate the life of the screen and the squeegee.

1.10.4 STEP 3: Firing

After film deposition, the substrate is to be fired in a kiln. The films themselves contain fine powders which must be exposed to a high temperature in order to form a solid composite material. This is often referred to as sintering and is achieved in a belt furnace. Sintering is defined as a method for making objects from powder by increasing the adhesion between particles as they are heated. Sintering traditionally serves for manufacturing ceramic objects and has also found use in such fields as powder metallurgy.

The furnace operator has control over a number of parameters including peak temperature, dwell time and throughput speed. Some ink is very sensitive to variations in these parameters whilst other types show little dependence on process parameter variations. All thick film inks contain

glass and during the firing cycle the glass melts and forms a mechanical key at the film substrate interface and also provides a suitable matrix for the active material of the film. The result is a fired composite film that is finally bonded to the substrate. Further screen-printed layers may be added after firing if necessary.

1.10.5 Further Necessary Steps

The necessary steps to form a thick film layer on a substrate has been described. By repeating this process to add different TF layers, a complete circuit or device as shown in **Figure 1.7** can be realised. However, there are usually some other steps to complete a usable device. These are laser trimming, surface mounting and pin attachment for external connectivity. Hybrid circuit technology makes also use of Surface Mounted Technology (SMT) useful for automatic pick and place of components like the integrated circuits, diodes, etc.

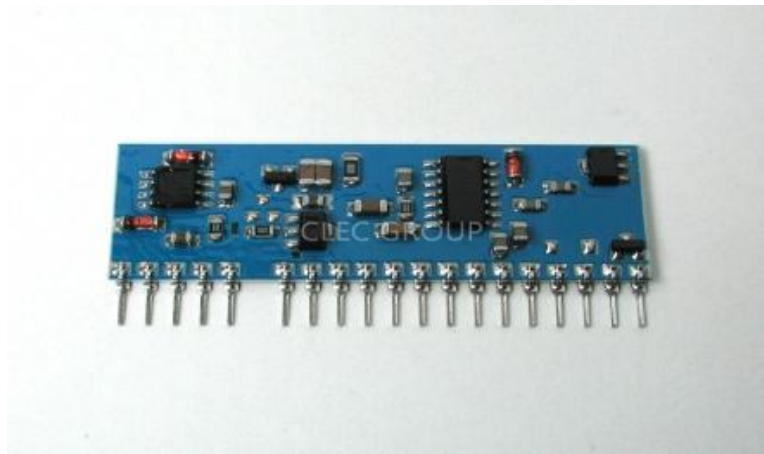


Figure 1.7 Complete hybrid circuit device (Clec Group)

The finishing industrial process includes soldering of large components, washing, inspection, encapsulation, labelling, testing, burn-in, quality assurance, packing and shipping. Hybrids using semiconductor processes have the additional steps of semiconductor die attach, wire bonding and semiconductor encapsulation.

2. State of The Art

Structural health monitoring has gained interest throughout the research community over the past two decades. The field of SHM developed through the combination of non-destructive evaluation (NDE) methods and novel sensing and actuation techniques to create intelligent monitoring systems permanently installed on structures. Non-destructive testing (NDT) or evaluation is a wide group of analysis techniques used in science and industry to evaluate the properties of a material, component or system without causing damage (CARTZ 1995). Since NDT does not permanently alter the article being inspected, it is a highly valuable technique that can save both money and time in product evaluation, troubleshooting, and research.

Upon its conception, many researchers working on SHM projects presented papers at NDE conferences first. The first conference devoted to SHM was created by Professor Fu-Kuo Chang in 1997, called the International Workshop on Structural Health Monitoring (IWSHM). A summary of the results of the presentations and panel discussions held at the first IWSHM conference was presented by Professor Chang at the second IWSHM (CHANG 1999). Today, there are several journals and conferences throughout the world that include sections devoted to SHM.

Since the concept of structural health monitoring first arose, there has been a significant amount of research conducted in the field. Researchers have studied many areas of SHM, some of which include sensor/actuator design, data analysis techniques, and the implementation of SHM systems to real world structures. The vast amount of research conducted on SHM

has given rise to several review articles summarizing the trends and developments in SHM (STEVEN 2008).

2.1 Structural Health Monitoring Overview

Structural Health Monitoring (SHM) is a vast subject, which aims in principle to give diagnoses of the condition of a structure at any moment in time and under various working and environmental conditions. Structures are of different types and usage purposes. The structure of a ship is different from the structure of a motor or a civil structure like buildings and houses. A structure may drift out of the initial design specification due to normal aging, environmental action, or to accidental events. Monitoring the status of a structure in time to build historical database can provide prognosis for the evolution of the damage. It is evident how variant are the conditions of these diagnoses. Different working conditions, different environments, different constituent materials make the SHM a vast field rich of new technologies, which are evolving to provide SHM with means to achieve the mentioned objectives. Part of these efforts is the present work; a feasibility study for the introduction of Thick Film technology for strain management in civil structures.

SHM has the potential to reduce the human error involved in monitoring structures and to improve the effectiveness of monitoring systems and the overall safety of structures. SHM system installed on a bridge, for example, could be used to continuously monitor the condition of the bridge and maintenance could be performed as soon as the beginning stages of damage are detected. On an aging aircraft, SHM could be used to reduce the amount of scheduled time-based maintenance and allow the aircraft to be repaired on a condition-basis when the SHM system indicates potential problems. In a seismic area SHM for civil structures will give a precise picture of damages due to earthquakes. In all cases, the cost of maintenance and repair could be decreased and the safety of the structure

could be improved. The advantages realized through the use of SHM can also be observed on railroads, buildings, and other infrastructure. (Steven 2008).

Today, the prevalently used method of structural health monitoring is visual inspection. There are however, significant drawbacks to visual inspection. First, visual inspection is very time intensive. It requires the time of a skilled and knowledgeable inspector both to travel to site and to perform the inspection. Some structural elements are difficult to see or access. Gaining access to the structural elements of interest can be a time consuming and costly procedure. Moreover, visual inspection is very subjective. Signs of damage that one inspector may consider to be significant may be missed entirely by another. Finally, effects of damage below the surface, especially in concrete or composite structures are extremely difficult to discern visually (SWARTZ 1995). Another important aspect is the consideration of durability and reliability of the monitoring system which should be comparable to building life duration which cannot be achieved by human beings inspections.

The civil engineering community has studied vibration-based damage assessment of bridge structures and buildings since the early 1980s. Modal properties and quantities derived from these properties, such as mode shape curvature and dynamic flexibility matrix indices, have been the primary features used to identify damage in bridge structures. Environmental and operating condition variability presents significant challenges to the bridge monitoring application. The physical size of the structure also presents many practical challenges for vibration-based damage assessment. Regulatory requirements in Asian countries, which mandate that the companies that construct the bridges periodically certify their structural health, are driving current research and commercial development of bridge SHM systems. In light of this, articles by

(BROWNJOHN 2007) and (Lynch 2008) discuss further the applications of SHM to civil engineering infrastructure.

In summary, the review of the technical literature presented by (DOEBLING et al. 1996) and (SOHN et al. 2003) shows an increasing number of research studies related to damage identification. These studies identify many technical challenges to the adaptation of SHM that are common to all applications of this technology. These challenges include the development of methods to optimally define the number and location of the sensors, identification of the features sensitive to small damage levels, the ability to discriminate changes in these features caused by damage from those caused by changing environmental and/or test conditions; the development of statistical methods to discriminate features from undamaged and damaged structures and performance of comparative studies of different damage identification methods applied to common datasets. These topics are currently the focus of various research efforts by many industries including defence, civil infrastructure, automotive and semiconductor manufacturing where multi-disciplinary approaches are being used to advance the current capabilities of SHM (FARRAR 2007).

2.1.1 Structural Health Monitoring Objective Levels

According to (RYTTER 1993), SHM has four levels. Each level classified by the objective to achieve and for the kind of information it provides for damage assessment. More information about the damage can be obtained by moving down the flow chart in **Figure 2.1** ; while level one gives the information that the damage is present in the structure, level two provides more information about the localization of the damage. The information about the extent of the damage can be obtained in level three. Example the amount of change of strain in certain location which has a specific model derived from the structure static load analysis, gives an indication of the amount of damage did the structure undergo.

Level four is the highest and most sophisticated stage of monitoring which gives prognosis of the remaining lifetime of the structure. This may be based on the same model in level three or a combination between global structural models with

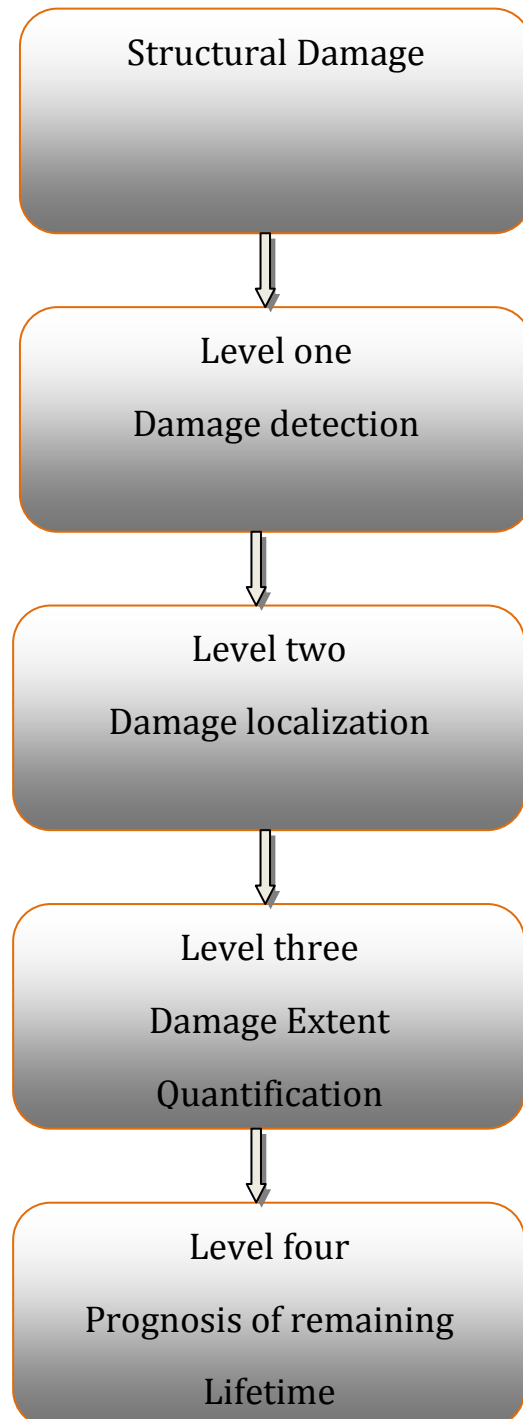


Figure 2.1 The four levels of structural damage assessment

local continuum damage models or fractural mechanics models which are able to describe the evolution of damage (BALAGEAS 2006). Many studies were conducted for reliability of systems, material, and linear damage accumulation, which can be found in (CHEDLIZE et. Al 2001 and 2003), (WEDMAN et. All 2001), (WALLASCHEK 2002), (WOLTERS 2003), (SOEFFKER 2001) and (PEIL 2002).

There are still many unsolved problems at all levels. Example ; at the lowest level of damage detection , the challenges are to increase the sensitivity, detect small amounts of damage in an early state without getting false alarms, and separate the effects of the damage from the effects of the changes in environmental conditions.

2.1.2 SHM Sensing Techniques

Currently, an immense number of techniques exist for the identification and location of damage in structures. (FIXTER & WILLIAMSON 2006) report on the state of art of SHM covers and describes all these techniques. Because all the techniques have their own advantages and disadvantages, there is no general method that allows the resolution of all kinds of problems in all kinds of structures. Every technique tends to have damage related sensitivities; i.e., a very sensitive technique may produce false-positives, while a less sensitive technique may lead to false-negatives, the latter case being more problematic. Generally, only damage above a certain size can be detected. The quantification of damage and prediction of the remaining lifetime are beyond any doubt the most difficult issues, as well the most desirable capabilities.

The basic premise of SHM feature selection is that damage will significantly alter the stiffness, mass or energy dissipation properties of a system, which, in turn, alter on one side the measured dynamic response of that system and on the other side the static force distribution and strains. Although the basis for feature selection appears intuitive, its actual application poses many significant technical challenges. The most fundamental challenge is the fact that damage is typically a local phenomenon and may not significantly influence the lower-frequency

global response of structures if only vibration technique is used. Here comes the need for the static feature extraction necessity like strain in particular for civil structures. Local sensors are normally measured during system operation and should be correlated to the global phenomenon.

2.1.2.1 Local and Global SHM

As mentioned before, there exists within the evaluation of any structure, two distinct positions from which to view the response, namely, a global view and a local view. Local view inspects the structure in a relatively small area with different techniques; ultrasonic waves, magnetic fields in amorphous wires, eddy current and strain measurement methods. In ultrasonic, Lamb waves are used (will be described further). These waves are a type of ultrasonic waves which can be generated by a transducer bonded to the surface of a thin plate. For local detection in Lamb acoustic application a local dense number of sensors are required to cover the local area to be inspected. Other possibility is to have combined technologies, e.g. local strain measurement. Lamb Waves are generated by permanent installed actuators, which are either mounted on the surface or embedded into the material. The actuator generates frequencies in the range of hundreds of KHz, which are high frequency Lamb acoustic waves as explained in (IHM 2003 and 2004) and (STASZEWSKI 2004). The size of the possible detected structural defect is proportional to the Lamb wavelength according to the relation $c=\lambda f$ where λ , f and c are the wavelength, the frequency, and the phase velocity of the wave respectively. For example, 100 KHz frequency has a wavelength of 20mm for longitudinal wave with a velocity of 5000 m/s (BALAGEAS 2006). In Low frequency range, waves work with modes, which are proportional to the dimensions of the complete structure.

The global view uses the fact that the local damage has repercussion overall the structure or at least part of it. An example is the change of stiffness of columns, which will produce instability, and change of strain in

other structure locations. Locally, strain sensors to monitor instability can be installed on the column directly.

The same global effects which are result of change of structural property can be observed also with Lamb vibration waves, examples by observing the shift in resonant frequencies or change in vibration modes. The combination between local and global methods is discussed in (SOHN 2004).

The global model-based damage identification can be considered as a special application of system identification methodology (CHANG 1999) (FRITZEN 1998) (DOEBLING 1996). The damage causes characteristic local changes in stiffness, damping and/or mass, and, because of these changes, shifts of the dynamic characteristics, such as Eigen-frequencies, modal damping and mode shapes, occur. The deviations between the actual dynamic properties and the undamaged state can be used to detect the damage and diagnose its location and extent. The system is generally represented by the finite element (FE) method. In the finite element method, the behaviour (stresses, strains and displacements resulting from load conditions) of large-scale structures is approximated and predicted by an FE model consisting of structural elements (members) connected at structural node points. These points are the array of acoustic sensors localized on the structure or could be the array of any kind of strain sensors like metal foil strain gauges, thick film gauges, fibre optics strain sensors, etc..

In general, two Techniques can be distinguished, one is related to a global vision of the structure, where features of the structure is measured by a radar similar technique using acoustic waves, the other is by directly measuring structure properties like strain stress relationship monitoring.

2.1.2.1.1 Acoustic Vibration Based Techniques

Since the early 1980s there has been an increasing awareness of the deterioration and lack of performance of civil infrastructure systems. As the world's infrastructure grows and existing infrastructure ages, evaluating the condition of existing structures and monitoring the engineering behaviours of new structures become more significant. To be efficient, economical and convenient, improved inspection methods must be devised to assess the deterioration of infrastructure. Non-destructive testing (NDT) has grown into a reliable alternative to meet these requirements (WANG 2009). The main benefit of such Non Destructive Evaluation systems (NDE) is that the structure need not be altered in any way while being monitored. The ND testing started initially with concrete lab test as will be here after explained.

Acoustic emission testing is an important technology for evaluating structural materials, especially for detecting damage in concrete and it is associated in the literature with non destructive testing (NDT) as opposed to the common destructive testing used to measure concrete strength. Concrete is unique in that it is the only engineering material in which strength determination is attempted from ultrasonic measurements. If the concrete is not strong enough (for instance, it has deteriorated) the consequence can be shortened service life and, in extreme cases, collapse of the structure (POPOVICS 2001).

The setting and hardening process of concrete is considered to be the most critical time period during the life of a concrete structure. Research has been conducted on an ultrasonic wave reflection method that utilizes a steel plate embedded in the concrete to measure the reflection loss of shear waves at the steel-concrete interface. The reflection loss has been shown to have a linear relationship to compressive strength at early ages (VOIGT 2003). The procedure was for strength prediction based on measured loss (pulse velocity test ASTM C 597-83). The investigations and

research was also to examine the fundamental relationship between the reflection loss, measured with shear waves and the hydration kinetics of Portland cement mortar represented by setting time, dynamic elastic modulus, compressive strength and degree of hydration. Dynamic modulus elasticity is measured by fundamental resonant frequency and ultrasonic pulse velocity using compression and shear waves.

The water/cement (w/c) ratio was varied for the tested mixture composition. The velocity of ultrasonic waves in concrete was used (VOIGT 2003). Experiments and studies have shown a good relationship between longitudinal and shear sound waves and concrete strength.

Figure 2.2 shows two curves relative to concrete age. One is sound pulse velocity (V) in concrete; the other is concrete compressive strength (f).

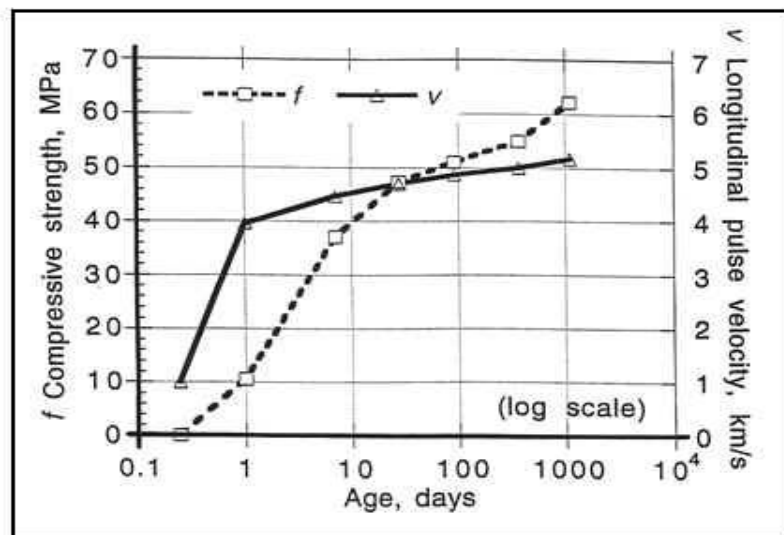


Figure 2.2 Graphical representation of concrete hardening in time and relative sound pulse velocity (POPOVICS 2001)

Concrete compressive strength increases in concrete cure time. More is the compressive strength higher is the speed propagation.

No derived formula can represent or reproduce the experimental results. Therefore, the existing need has forced engineers to use other empirical formulas obtained by curve fitting for the calculation of the concrete strength solely from the longitudinal pulse velocity. The most popular such formula is

$$f = a * \exp (bV)$$

Where:

f = Compressive strength in MPa

V = longitudinal pulse velocity of sound

a and b = empirical parameters determined by curve fitting (POPOVICS).

The American Society for Testing and Materials (ASTM) standard Nr. C597 covers the determination of the propagation velocity of longitudinal stress wave pulses through concrete. It is a standard test method for pulse velocity through concrete to determine its quality.

The functions of generation and sensing of ultrasound waves can be achieved by MEMS. MEMS are Micro-Electro-Mechanical-Systems, which is the integration of mechanical elements, sensors, actuators, and electronics on a common silicon substrate through semiconductor micro fabrication technology.

Developing MEMS transducers for acoustic emission testing includes permanent bonding or embedment for superior coupling, greater density of transducers, and a bundle of transducers on each device tuned to different frequencies. Additional advantages include capabilities for maintenance of signal histories and coordination between multiple transducers. An array of such sensors are distributed and put in

synchronization to produce a general view of structure health condition. Here we distinguish two kinds of acoustic sensing: active and passive.

2.1.2.1.1.1 Active and Passive Ultrasonic Sensing

Analysis of actively transmitted ultrasonic signals is a conventional NDT methodology that has long been used to detect and assess damage. However, such approaches use sensors that are scanned over the structure to provide a point-by-point representation of material properties and/or damage locations. An array of permanently attached or embedded ultrasonic transducers, which act dually as transmitters and receivers, is being researched (PROSER 2002). Neighbouring transducers within an array detect ultrasonic signals generated by one transducer. Damage along paths between the transducers can be detected and with more complex analysis methods, material along secondary propagation paths that include reflections from structural boundaries can also be evaluated. The development of the Stanford Multi Actuator Receiver Transduction (SMART) layer is an excellent example of recent efforts in this area. Ongoing areas of research in active ultrasonic sensing technology for structural health monitoring include: (1) the further improvement and characterization of miniaturized, rugged, embeddable sensors. (2) Analysis methodologies for optimized sensor placement to enable characterization of damage throughout the entire structure rather than just along direct propagation paths; and. (3) modelling of ultrasonic guided wave propagation that occurs when such sensors are attached to structures (PROSSER 2002).

Passive ultrasonic monitoring, also known as acoustic emission (AE), utilizes an array of ultrasonic sensors. The sensor array is used to passively monitor acoustic signals generated by damage mechanisms such as crack growth. AE is widely used as a conventional method for off-line structural assessment and can also be implemented in-situ testing (PROSSER 2002).

The transducers which transfer mechanical force to an electronic signal and vice versa, are the piezo-electric transducers or sensor which are introduced in the coming paragraph.

To mention here is that fibre optic sensors can also be used to detect cracks in the structure. The acoustic sound perturbation generated because of a crack propagates through the structure and generates small strain energy at the air gap of the sensor which causes the laser light to fluctuate. The light fluctuations are picked up by the photodiode converting it to electrical signal proportional to the entity of the generated disturbance. Fibre optic sensors are much more sensitive to the small strain changes produced by AE (MARTIN 1988). Acoustic generated strain is not a static permanent strain. TF sensors can detect the static change of load and strains through the structure.

2.1.2.1.1.2 Piezoelectric Sensors

Piezoelectric sensors convert mechanical energy into electrical energy (and vice versa), and they can be used to convert the displacements from sound vibrations or an impact event into an electrical signal.

Piezoelectric materials are either inherently piezoelectric or they have to be poled to enable polarization of the domains, and this can be achieved by applying an electric field, to align the domains. **Figure 2.3** shows the principle of converting mechanical energy into electrical energy, the phenomenon that enables piezoelectric material to be used to detect impacts and deformations in a structure. If a compressive force is applied to the piezoelectric material in the same orientation as the electric field used to pole the material, then a voltage of the same polarity is produced [http://www.americanpiezo.com/piezo_theory/]. Piezoelectric materials are more responsive to high frequency events such as an impact event or acoustic vibrations; they are not suitable for measuring static strain. By resonating a piezoelectric element, acoustic waves can be generated.

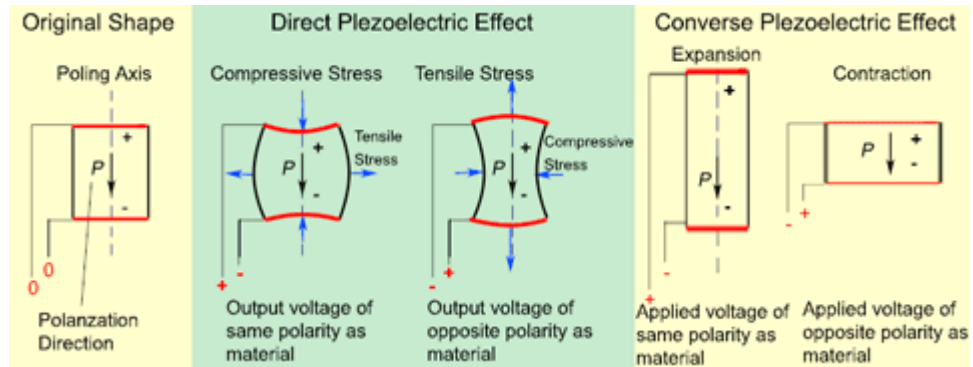


Figure 2.3 Piezo Electric effect

A common piezoelectric material is Lead Zirconate Titanate (PZT), which is commonly used as a bulk material in transducers. It is a very hard ceramic material structurally weak in tension and not always compatible with the process of embedding into structures. The following piezoelectric materials have been used for SHM purposes for various applications.

2.1.2.1.1.2.1 Piezoelectric Polymer Films

PZT in its powder form can be incorporated into a resin matrix to form a 0-3 composite. Ceramic particles in polymer matrix are connected as in **Figure 2.4**. The 0-3 composite can act as an impact damage sensor [BADCOCK 1996]. A tape-casting method allows the 0-3 slurry to be cast into a thin film, which is then cured. To make the 0-3 composite active; the material has to be poled.

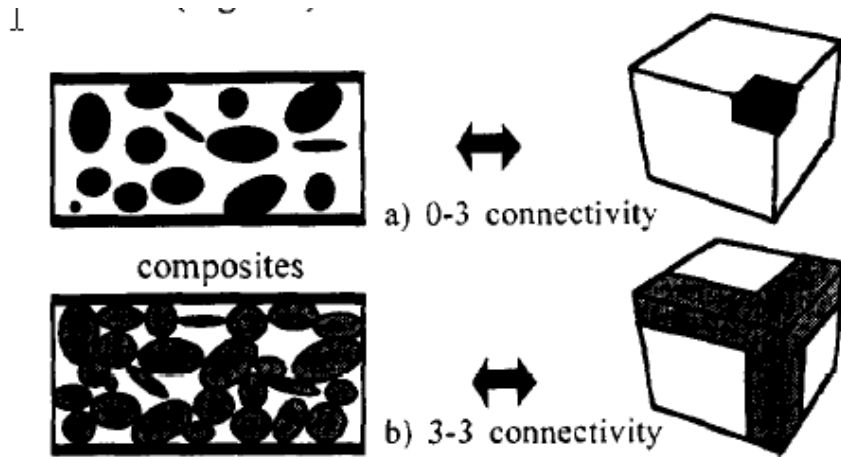


Figure 2.4 Ceramic particles in polymer matrix (LEVASSORT 1998)

To ascertain the sensitivity of the material; strain coefficient (d_{33} charge sensitivity) (Appendix-D)¹ measurements were made and values of 18pC/N (pico-Colomb/Newton) were obtained, which makes it comparable with PVDF (Polyvinylidene Fluoride film)(Appendix-D). The 0-3 composite either can be surface-mounted to a structure or embedded into a composite, but the cure temperature of the composite has to be below the Curie temperature of the 0-3 piezoelectric polymer or the material will become inactive. The Curie temperature is the temperature above which the material loses its piezoelectricity due to random alignment of the electric dipoles within the material due to thermal excitation.

An alternative piezoelectric film uses Polyvinylidene Fluoride (PVDF) of which two other co-polymers are available: P(VDF-TrFE) and P(VDF-TeFE), where the Tr and Te stand for Tri and Tetra. PVDF is weakly piezoelectric unless drawn to orientate the molecules. The greater the orientation, the stronger the piezoelectric response. The strongest effect is found in the plane that the material is drawn in. The d_{33} response of PVDF

¹ Appendix-D contains a glossary of definitions of terms and words

is typically 33pC/N and it has a Curie temperature of 110°C. The co-polymers no longer need to be stretched mechanically to achieve crystalline state and typically exhibit a d_{33} of 12 pC/N and a Curie temperature of 130°C. It is essential to ensure that the cure temperature resin system is compatible with the PVDF or co-polymer to ensure the material stays active (NASA 2001 and COHEN 1996).

0-3 piezoelectric polymer composite and PVDF materials have both been used for SHM sensors, either as an impact sensor or as a transducer for detecting acoustic emission or Lamb waves.

2.1.2.1.1.3 Lamb Wave and Acoustic Emission Sensors

As mentioned before, Lamb waves are a type of ultrasonic wave that can be generated by a transducer bonded to the surface of a thin plate. It is a type of elastic perturbation that can propagate across large areas of a free-free solid plate with low dispersion of energy, even in materials with a high attenuation ratio. This type of wave was first described in theory by (Lamb 1917), although he never tried to produce them. (ALLEYNE AND CAWLEY 1992) were among the first to discuss interaction of Lamb waves with defects for non-destructive testing. (SARAVANOS et al. 1994) presented a procedure for delamination (Appendix-D) detection in composite materials using Lamb Waves and embedded piezoelectric sensors. (KESSLER et al. 2002) maintain that techniques using Lamb waves have proven to provide more information about damage type, severity and location than previously tested methods using FRFs (frequency response function), since Lamb waves are more sensitive to local structural defects. Piezo-ceramic patches were used to excite the first anti-symmetric Lamb wave (A_0 mode). The PZT actuators were chosen because of their high force output at relatively low voltages and also due to their good response qualities at low frequencies. (KESSLER et al. 2002) explored the optimization of Lamb wave methods for damage detection in composite materials, covering the problems of choosing the appropriate

actuating frequency, pulse shape and sensor geometry for Lamb wave application. The results were compared by performing a wavelet decomposition using the Morlet wavelet (Appendix-D), and plotting the magnitude of the coefficients at the driving frequency. Although Lamb waves display great capabilities in damage detection and localization, these authors point out that the major disadvantage of this method is that active sensing is necessary for its implementation; i.e., it requires a voltage supply and a generated signal. The high data acquisition rate needed to gain useful signal resolution is also an awkward requirement. Finally, the Lamb wave method should most likely be placed into a SHM system in conjunction with other passive detection methods, such as frequency response function (FRF) method, in order to conserve power and data storage space and because the Lamb wave data can be more difficult to interpret. Damage in composites and disbands in joints can be detected, as they interfere with the propagating Lamb waves; which would otherwise travel over a long distance in an undamaged composite. The Lamb waves are made up of shear and longitudinal modes, and these can either be symmetric or anti-symmetric, (**Figure 2.5**).

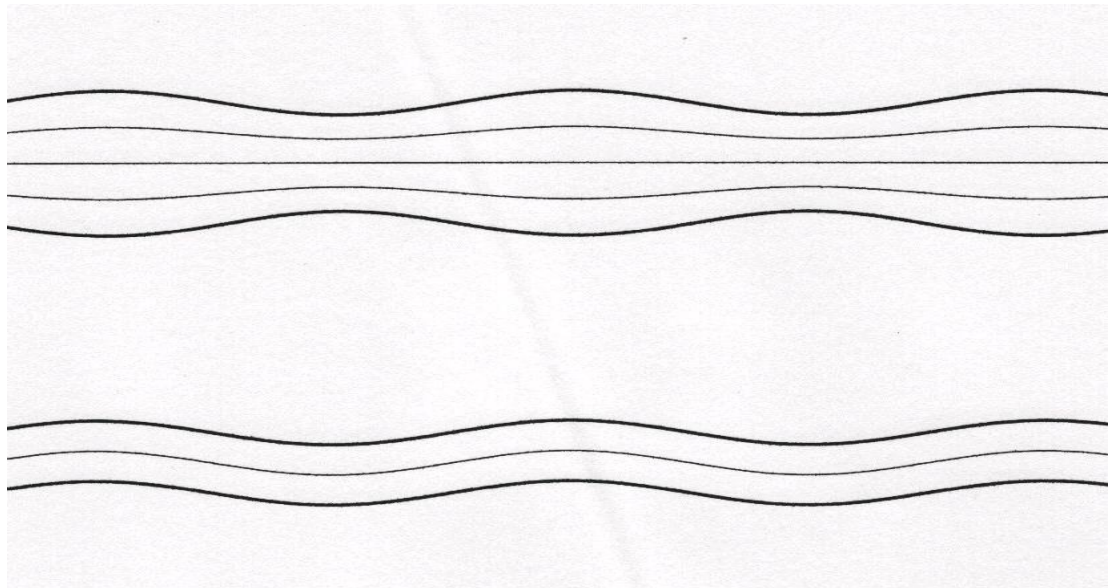


Figure 2.5 Symmetrical and anti-symmetrical Lamb waves

A transducer is used to generate the Lamb waves, and the same transducer or another transducer can be used to receive the signal (pulse echo mode). Any perturbations in the attenuation of the generated waves can be indicative of damage.

The transducers used, have to be designed specifically to match the waveguide structure and defect type, and propagation of ultrasonic modes can be limited if there is a high density of structural features. The anisotropic nature of composite materials adds complexity to the usage of Lamb wave sensors and they are often best suited to localize damage detection of vulnerable areas, (DALTON 2001 and BIRT 1996).

Acoustic emission sensors operate in the same way, except that the disturbances detected by the transducers are generated by the damage event itself as mentioned in 2.1.2.1.1.1 (FINLAYSON 2000).

These sensors can be incorporated into films such as the "SMART layer", (Stanford Multi Actuator Receiver Transduction layer) (LIN 2005). The SMART layer comprises of piezoelectric discs that are networked together to provide a sensing and active layer suitable to transmit and receive Lamb acoustic waves. The discs integrated on a polymer sheet can take different shapes (**Figure 2.6**) and can be embedded into composite. The PZT discs range in diameter from 3.17mm to 6.36mm (0.125 to 0.25 inches) and are distributed to provide a method for detecting damage

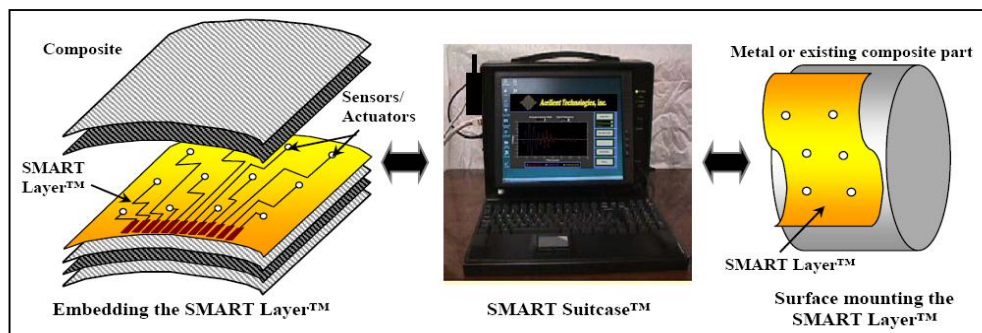


Figure 2.6 SMART Layer™ interfaced with the SMART Suitcase™ (Acellent Inc.)

2.1.2.1.2 Strain Measurement Techniques

Structural Health Monitoring regards the mechanical quality and stability of a structure. However, the methods used to reveal and quantify the structure quality could be of different natures. Strain change is however the common structural parameter indicating structure condition in time. Strains can give rise to cracks in the structure that will grow exponentially in time.

There are different techniques to measure strain by measuring a parameter affected by strain change giving rise to different kinds of sensors. Strain sensors are divided into piezo-resistive, piezo-electric, piezo-magnetic, piezo-resonant and piezo-optic strain sensors Which indicates variability of a parameter like electric, magnetic, resistive ,etc with pressure (piezo is derived from the Greek word “piezein” which means pressure) .

2.1.2.1.2.1 Fibre Optic Strain Sensor

Optical fibre (OF) is a pipe for light, transmitting information, but it may also be sensitive to changes in the external environment surrounding the fibre, such as temperature, strain or chemical composition. It becomes a sensor for these parameters if this change can be quantified and measured. A simple example is when a very narrow pulse of light is launched along an OF, the back-scattered radiation dispersed inside the OF is proportional to its temperature. By means of equipment called an OTDR (Optical Time Domain Reflectometer), it is possible to measure the light back-scattered along the fibre length, returning to the emitter after the time of flight. From the signal of intensity collected as a function of time, the temperature distribution along the length can be measured. Two operating modes are distinguished; the *intrinsic mode* is when the OF property is changed because of change in the host environment like temperature or strain, OF in this case is the sensor. The other mode is the *extrinsic mode* when OF is used for data transmission. An approach based

on a combination of the two modes is commonly used, a small local sensor sensible to strain or other parameter, is included in the data transmission path.

Common advantages of all kinds of optical fibre sensors arise from their small size and weight and their non-electrical nature, making them immune to electromagnetic interference and to electrical noise, also allowing them to work in explosive environments; they usually have a very high sensitivity and a wide operating temperature range. For smart structures, local intrinsic sensors are the most commonly used, because of their simplicity, the minimal perturbation of the host material and the accuracy of measurement. Multiplexing capability, or the possibility to excite several sensors on the same optical fibre, is another highly desirable feature. A single optical fibre, 0.25 mm in diameter, can provide strain readings from 10 to 20 different points in the structure. When compared to the four leads required by each electrical strain gauge, a clear advantage can be seen (GUEMES et. Al 2006).

2.1.2.1.2.2 Classification of Fibre-Optic Sensors

A basic classification of optical fibres sensors may be made in terms of the optical parameters. The external environment to be monitored must change some of the parameters, which define the optical wave: intensity, phase, wavelength and polarisation. Based on the type of change, different kinds of optical sensors have been developed.

2.1.2.1.2.2.1 Intensity-Based Sensors

These are the simplest fibre optic devices, and consequently they were among the first available; they are still in use as proximity sensors, for damage detection, cure monitoring and hydrogen detection. The components of the measurement system are a stable light source (white or monochromatic), an optical fibre (preferably multimode for higher power transmission) and a sensitive photo detector.

Commercially available proximity sensors are used for non-contact monitoring of the displacement of rotating shafts with accuracy better than $3\mu\text{m}$. The distance between the cleaved fibre-optic end and the moving surface is related to the amount of light reflected by this surface, and captured again by the optical fibre.

2.1.2.1.2.2 Fibre Optic Bragg Gratings Strain Sensor

Fibre Bragg Grating is a short length of optical fibre that filters out a particular wavelength. Periodically spaced zones in the fibre core are altered to have different refractive indexes slightly higher than the core. This structure selectively reflects a very narrow range of wavelengths while transmitting others.

The Bragg Gratings based fibre optic strain sensor is fabricated by writing gratings on the core of an optical fibre. The idea is to engrave, at the core of the optical fibre and for a short length for about 1cm, a periodic modulation of its refractive index. This will behave as a series of weak partially reflecting mirrors, which will by diffraction, reflect back the optical wavelength that is exactly proportional to grate spacing.

Fibre optic Bragg grating (FOBG) strain sensors are extensively used to measure strains as an alternative to strain gauges. Essentially, when a broadband light is launched into a fibre core to pass through a Bragg grating, a narrowband light at the Bragg resonance wavelength are reflected back by the periodic refractive index variation as explained above. This optical fibre is then attached to or embedded into the surface of the structure. Basic operating concept of FOBG can be described as follows; when the fibre grating is expanded or compressed the grating period expands or contracts changing the spectral filter response of the grating. The strain measurement is done by measuring the corresponding spectral shift in the peak position of the reflection band from the FOBG by spectrum analysis. This sensing principle of the FOBG strain sensing system is shown in **Figure 2.7**.

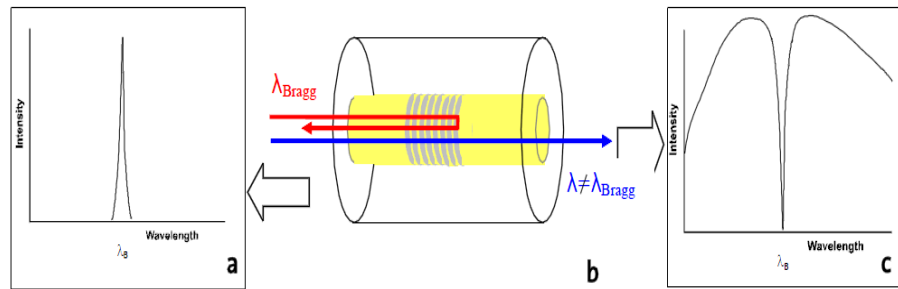


Figure 2.7 Light propagates through FBG, spectral response in reflection (a) and transmission (b) (FIXTER 2006)

2.1.2.1.2.3 Phase Modulated Optical Fibre Sensors, or Interferometers

Interferometry is the most accurate laboratory technique or precise distance measurements. It has to be borne in mind that direct phase measurements, or the display of the electrical field versus time, as is done with oscilloscopes for low frequency electrical signals, cannot be done for an optical wave; only the intensity of the light, the average power of the electromagnetic field, can be measured.

Interferometers are the devices that can be used to produce this phase information. If a continuous monochromatic light wave is divided into two beams (by a partial mirror in conventional optics or by a coupler in the case of optical fibres) and these waves travel through different paths before being recombined, any slight difference in path-length will cause a delay between one wave and the other, and consequently their electromagnetic fields will not sum up; they may even oppose one another, so that the final result is that the output intensity may be reduced to zero.

Interferometer output will change from the power input level to zero each time the length of either of the two paths increment or decrement by half a wavelength (380 nm, if the red light of a He-Ne laser is used). So the resolution would be half light wave length or multiples of 380 nm.

In other words, the functional principle of the system consists of a pair of single mode fibres installed in the structure to be monitored. One of the fibres, called the measurement fibre, is in mechanical contact with the host monitored structure itself, while the other one, the reference fibre, is placed loose in a neighbouring pipe. All deformations of the structure will then result in a change of the length difference between these two fibres. To make an absolute measurement of this path unbalance, a low-coherence double Michelson interferometer (Appendix-D) is used. Light Fringes indicate wavelength deformation. This technique is very stable and highly precise. It has the drawback of being invasive and of high cost compared to foil strain gauge (INAUDI 2000).

The extreme sensitivity causes that any perturbation in the optical path of any of the two arms makes measurements difficult outside because a local temperature change alone may cause a drift of several maxima and minima. Fortunately, the sensor is the whole length of the optical path of one arm; it is an "averaging distributed sensor". Another drawback is that measurements are related to the path differences when the equipment is switched on and any interruption will mean that the reference is lost. In addition, there is no direct indication whether an increment (tension) or a decrement (Compression) is occurring, and a quadrature technique is needed to identify this as explained in (BARLOW 1989).

2.1.2.1.2.3 Foil Strain Gauges (FSG)

After nearly 70 years of the discovery of metallic wire/foil gauge principle, application in measurement has been widely spread for sensing dynamometric quantities (force and torque) or geometric quantities. Although some arising and promising technologies are emerged to the market, still about 50% of all the sensors rely on the strain gauge principle (BETHE 1989). The change of the electrical resistance of the foil wire is proportional to the applied strain. Among the various kind of sensors used in SHM, FSG remains the least expensive and the most widely used.

However, they become less attractive when sensor driving electronics is far from the strain gauge location. This is because the low level of signal these sensors produce make coupling of electromagnetic and electrostatic signals on long wires incisive on the strain signal precision and quality. The aim of this study is to provide higher signal to noise ratios by adopting another strain gauge technology like Thick Film. Thick film sensors in mass production are much cheaper and have the possibility of integrating driving electronics on the same substrate beside many other advantages described in Chapter one. The single resistor Foil Metal Strain Gauge price is about 10 times higher than the equivalent TF piezo-resistive sensor. In addition, engineering cost is much lower.

Typically, the metallic wire/foil gauge consists of a very fine wire or metallic foil, mounted on a resin backing film called carrier. The applied load, which is normally parallel to the gauge, results in the change of the gauge length and the corresponding strain is measured in terms of the electrical resistance of the wire/foil, which varies linearly with strain. The gauge is not sensible to loads applied perpendicularly on the gauge like TF strain gauges.

Common strain gauge has relatively low gauge factor around 2, nominal resistance values from 30 to 3000 Ω , and shows good temperature dependent gauge factor and resistance as mentioned in **Table 1.1**. The hysteresis of the adhesive material between the sensor gauge and the object needs to be considered for strain measurement in SHM applications. As with all other sensors, the primary design considerations for the success of applications are working temperature, the nature of the strain to be detected, and the material under test.

Metal foil strain gauges are the sensors normally used in laboratories to measure strain on building materials. Because of the accumulated experience and the long industrial deployment history for designing all kind of strain measurement devices like load cells, it is the reference

technology in the field. The deployment in SHM is a natural consequence or expansion of this long history.

Remarkable application is what (TEGTMEIER et. al. 2000 and 2003) accomplished and patented; FSG was used to build a multi-component strain and stress transducer to be embedded in structures to monitor Change of forces in different directions. The transducer was protected with an adequate packaging technique to assure long term stability. **Figure 2.8** depicts the conceptual idea behind the transducer construction, which was made of steel.

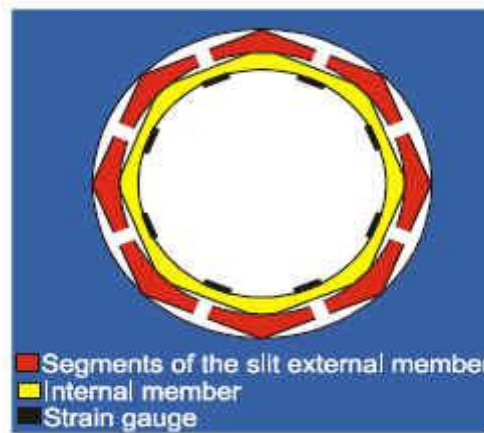


Figure 2.8 Multi-component strain stress transducer

Recommendations for the application of FSG in general on building materials for SHM purpose is reported by (ISIS-Canada 2001).

2.1.2.1.2.4 Self-Sensing Materials

Damage has been successfully detected in CFRP (Carbon fibre-reinforced polymer) composites by monitoring the change in resistivity of the highly conductive carbon itself (WANG 1999). Strain levels can also be monitored, and agreement with foil strain gauges has been obtained to within approximately 7%, although the change in resistance is usually

attributed to geometrical changes in the fibres, rather than an intrinsic material resistivity change (De TERESA 1991). However, it has been possible to relate the change in resistance to an increase in crack length in propagation tests (IODOROKI 1995)

Using the electrical resistance of the material itself requires the mounting of electrodes on two surfaces of the structure. Even if the process merely requires the connection of a simple grid of connection terminals; for example, each point must be abraded and the wire adhered to the surface. Clearly, this can be extremely time-consuming if a large area is to be monitored. Furthermore, protecting the resultant wiring loom from damage is difficult under laboratory conditions; for a structure in service, it would require an additional surface layer to protect the electrical connections. This introduces additional processes into the manufacture of the structure, and additional mass from the wiring used.

The contact electrical resistance between two interfaces of carbon plies can be used to provide information regarding the structure at this interface. The inter-laminar interface is susceptible to delamination and is commonly associated with the failure of Polymer Matrix Composites (PMC) structures. Research has been conducted, measuring the contact resistance across this interface, providing information on strain, damage, temperature, and moisture because of resistance change. Although it has been demonstrated that a resistance change is associated with each one of these parameters, for measuring more than one parameter, complicated compensation methods would be required (WANG 2004).

Another resistive method utilizes two electrodes positioned either side of the composite, displaced by a distance so they are not back to back. When a current is passed between the electrodes, cracks can be detected by measuring the change in resistance. This technique has been demonstrated as a wireless technique using a ceramic oscillator connected to the electrodes. This transmits the electrical resistance change as an

oscillating frequency that is picked by a receiving transmitter (MTSUZAKI 2005).

2.1.2.1.2.5 Magnetostrictive Sensors Including Amorphous Wire Sensors

In accordance with the theory of magneto-elasticity, the magnetic properties of ferromagnetic materials depend dramatically on the stress level. As an engineering application of the said theory, the magneto-elastic (ME) stress sensor has been used in the stress monitoring of civil infrastructure. Through the application of ME stress sensors in representative infrastructures, their promising engineering advantages have been demonstrated, which is a prelude to a viable application stage (WANG 2009).

Magnetostrictive materials are broadly defined as materials that undergo a change in shape due to change in the magnetisation state of the material. Nearly all ferromagnetic materials exhibit a change in shape resulting from magnetisation change. In most common materials, nickel, iron, and cobalt, the change in length is on the order of 10 parts per million. In addition, the change in volume is very small. This type of magnetostriction has been termed Joule magnetostriction after James P. Joule's discovery in the 1850's. The relatively small change in shape of these materials limited their use in engineering. Initial sonar designs contemplated exploiting the magnetostrictive effect, but were left unexplored due to advances in piezoelectric materials such as quartz and Rochelle salt, and later Lead Zirconium Titanate (PZT).

Amorphous wires and ribbons have been extensively researched over the last few years, primarily because of their suitability for use as magnetic field and strain sensors, due to a combination of their mechanical performance and magnetic softness (ATKINSON 2000), (MILNE 2001), (MAYLINE patent), (BOWELS 2005). Cobalt-rich and iron-rich amorphous alloys have been used for these types of sensors and the characteristic property that changes with applied stress (through the phenomena of the

'magnetostrictive' or 'magneto-elastic' effect) is magnetic permeability. This change in magnetic permeability may be detected in a number of ways. One method uses the amorphous ribbon as the core for an induction coil (KRAUS 2002), whilst another method monitors the high frequency electrical impedance of the material (HERNANDO 1988) The change in impedance that is observed in these materials with applied stress can be very high (>100%) which can result in a very sensitive strain sensor. For instance, conventional metal foil strain gauges have gauge factors of the order of 2, semiconductor strain gauges have a gauge factor value of 100, whilst the magnetic amorphous strain sensor can have a value of 1500 (BITER 2001).

Another major advantage of amorphous wires (and ribbons) sensor type, is its size. The diameter of the conducting (copper) wire can be, for example, 75-125 microns. This makes them suitable for embedding in composite as the thickness is close to a ply thickness (<http://www.mdatechnology.net/techprofile.aspx?id=530#listing> 2010).

Magneto-elastic technology is a novel approach to monitoring cable forces in pre-stressed structures and bridge cables. With a theoretical basis in magneto-elasticity, magneto-elastic sensors have been employed in health monitoring for infrastructures (WANG G and WANG M 2006]. Relative permeability is used to monitor the tensile stress. This technology overcomes the drawbacks of the current available NDT while retaining the advantages of normal NDT methods. They measure the internal stress in steel tendons and cables directly. Easy installation for new structures and in-situ installation adaptability for existing structures are some key characteristics of this method. Other attractive points include being compact, easy to operate, accurate, and a theoretically unlimited service lifetime (WANG M L 2009)

2.1.3 Some Universities Research on the Subject

There are different institutions and research centres undertaking studies to investigate the best possible solution for structural health monitoring with aids of sensors and electronic means. Here are some examples:

2.1.3.1 Bristol University

Bristol University installed instrumentation on one of its buildings as part of the research study. One interesting motivation for this study is to apply monitoring on prototype buildings, which is more adequate for laboratory testing and analysis. The instrumentation employed for load, strain, temperature, deflection and environmental monitoring using traditional methods utilizing vibrating wire, load cells, LVDT, and slope measuring technologies. A series of load tests were carried out in selected areas of the structure enabling the structure and instrumentation to be calibrated and, in effect, become a transducer providing an indication of the service load of the floor where this instrumentation were installed. Artificial Intelligence was used for the analysis of the revealed data (Vann 1996 and Bristol university web site).

2.1.3.2 University of Delaware

The possibility of adopting MEMS technology for micro crack monitoring in concrete was explored, delving into both technical and technological issues. Micro-electro-mechanical systems (MEMS) are miniature sensing or actuating devices, which can interact with their environment to either obtain information or alter it. With remote query capability, it appears that such devices can therefore be embedded in concrete to monitor distresses such as cracking. MEMS technology could result in several sensors smaller than today's computer chips being embedded in structures. These sensors could then relay messages via wireless technology and the Internet about the performance of a bridge or a building or work in tandem with actuators to perform in-situ repairs of cracks or other

structural anomalies. These devices being in-situ and distributed through the structure will give continuous information on the integrity of the infrastructure. The actuation or sensing ability of MEMS depends on some intrinsic properties of the components such as piezo-resistivity, piezoelectricity or thermoelectricity. Piezoresistivity relies on the electrical resistance changing in response to mechanical stress. Piezoelectricity produces an electric field in response to strain and vice versa. The objective of sensing is to transduce a specific physical parameter to electrical energy. Integrated circuit technologies are the foundation of sensors and actuators as well as of MEMS. Integration of sensors, revelation of signals, elaboration and transmission can then be accomplished with semiconductor technologies (ATTOH-OKINE 2003).

2.1.3.3 Berkeley University

On the same trend for getting benefit of the integration of sensors, actuators and electronics in semiconductor development process, interesting research was carried out by Berkeley to build an autonomous wireless array of MEMS (BRETT 2002). MEMS are used to build tiny sensor nodes that can be rapidly deployed in massive distributed networks to allow unobtrusive, spatially dense, sensing and communication components. Volume and energy consumption of these components are fundamental for reliable autonomous performance. The technology used was standard integrated circuit process that could inherently integrate sensors to sense a few phenomenon such as light and temperature in a compact area. Micro-machining has allowed researchers to shrink many types of sensors into small volumes while often maintaining similar, or even exceeding, performance levels of conventional transducers. Examples include thermal sensors, accelerometers, gyroscopes, pressure sensors, microphones, radiation detectors, magnetic sensors, flow sensors, and chemical and biological sensors.

Several factors need to be considered when selecting sensors for use in tiny wireless sensor nodes: volume, power consumption and suitability to power cycling (power on/off). Some sensors require more time when switched on to generate a stable measurement. Other difficulty is to have sensors to be in contact

with the external environment as a primary request for their functionality to sense environment measured parameters. This adds fabrication packaging and assembly constraints for compatibility with other components of the system.

In cooperation with Berkeley, The University of Michigan built a number of small MEMS-based wireless sensor node systems (Mason, et al 1998). The multi-sensor micro-cluster that measures pressure, temperature, humidity, and vibration/position, includes a microcomputer, and has a 50m RF (radio frequency) link. The work starts from discussing the primary components useful to build complete electronic system, called node and the consideration of technologies helpful to optimize energy consumption, normalizing the energy consumption by unit volume. The project name was Smart Dust project in which 16-mm³ nodes were designed and built (BRETT 2002).

2.1.3.4 The University of Michigan

The university has a “Laboratory for Intelligent Structural Technology (LIST)”. The laboratory publications are available for down load directly from:

<http://www-personal.umich.edu/~jerlynch/pubpage.html> 2010.

The university is dedicated to the creation of smart structure technologies for the next-generation of engineered structures. Main areas of focus are the design of wireless sensors, distributed data interrogation algorithms for dense sensor networks, micro-electromechanical system (MEMS) sensors and multifunctional materials tailored at the micro- and nano-scales. Other laboratory research thrusts include the exploration of decentralization in control and damage detection algorithms.

2.2 Summary

From the literature review, two main stream branches could be found; the dominant one is the global acoustic Lamb wave SHM, in which properties of the structure is altering the return frequency in a technique similar to radar scanning, The second one is strain measuring under which falls fiber optics, Magnetostrictive, self sensing materials, foil strain gauges etc..

TF piezo-resistive sensors are part of the second category and literature does not show any previous research on this subject for SHM. The present work is the first investigation on the possibility of using ceramic thick film strain measurement sensors for structure health assessment.

Literature review of work on TF force and pressure sensors brought to the light the different kinds of GF that TF may experience. This fact was useful in defining the deployment methods for SHM, which are discussed and experimented through this thesis.

3. Sensor Design and Validation Tests

The main topic in this chapter is to design the Thick Film Sensor to satisfy the deployment requirements to measure strain in civil structures.

The designed sensor will be described, simulated and tested in the two deployment methodologies; glued on material and mounted on PCB in Surface Mounting Technology (SMT). Four Point Bending Test will be used to, first examine feasibility of application like metal foil strain gauges, and secondly, to evaluate the sensor response and gauge factor. In this later case, metal foil strain gauge will be used as reference to measure strain. Uniform loading will be applied to Surface Mounted Thick Film sensor to evaluate the response and the maximum supportable load. Following test elements will also be described: Simulation software tool, Foil Strain Gauge, data acquisition system 5000, and the Wheatstone bridge.

3.1 Piezoresistive Thick Film Sensors

Thick Film piezoresistive sensors are formed by placing stress-sensitive resistors on highly stressed parts of a suitable mechanical structure. The piezoresistive transducers are usually attached to cantilevers, or other beam configurations, and are connected in a Wheatstone bridge circuit. The beam may carry a seismic mass to form an accelerometer or may deform in response to an externally applied force. The stress variations in the transducer are converted into an electrical output, which is proportional to strain, by the piezoresistive effect.

Thick Film sensors are commercially available in Wheatstone bridge configuration on AL₂O₃ ceramic membrane as shown in **Figure 3.1**. An overview of Wheatstone bridge is shown in Appendix A.

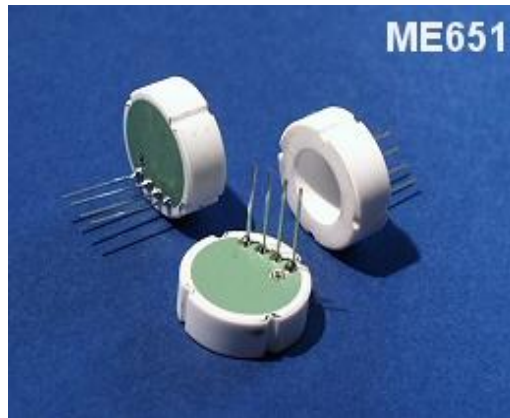


Figure 3.1 Ceramic pressure transducer membranes (Metalux)

Such configuration is of a little benefit for the scope of this investigation. To be able to examine the applicability on building materials and on structures, the designed sensor has to meet the followings application requirements:

1 - Could be glued on building structures to produce an electronic signal proportional to the stress applied to the structure as in **Figure 3.2**. This kind of application is similar to applying foil metal strain gauges;

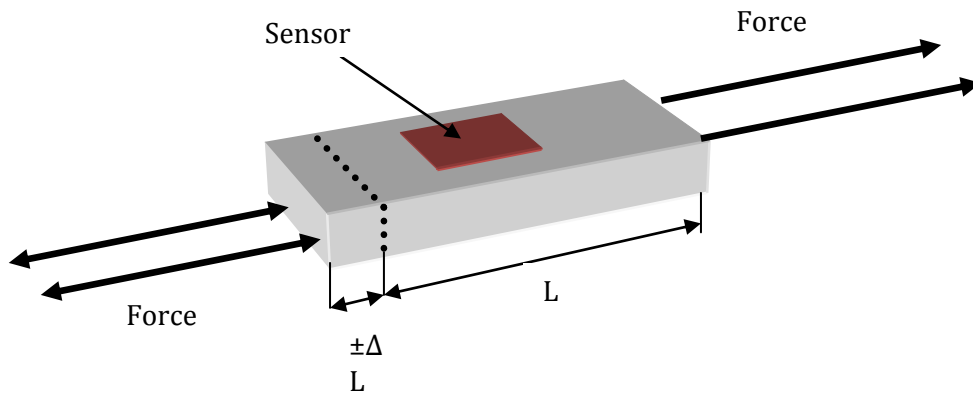


Figure 3.2 Thick Film Sensor glued on sample building block under stress

2- To work as a tactile sensor (Appendix-D) embedded into the structures to produce an electronic signal proportional to the load applied on the structure, like in **Figure 3.3**.

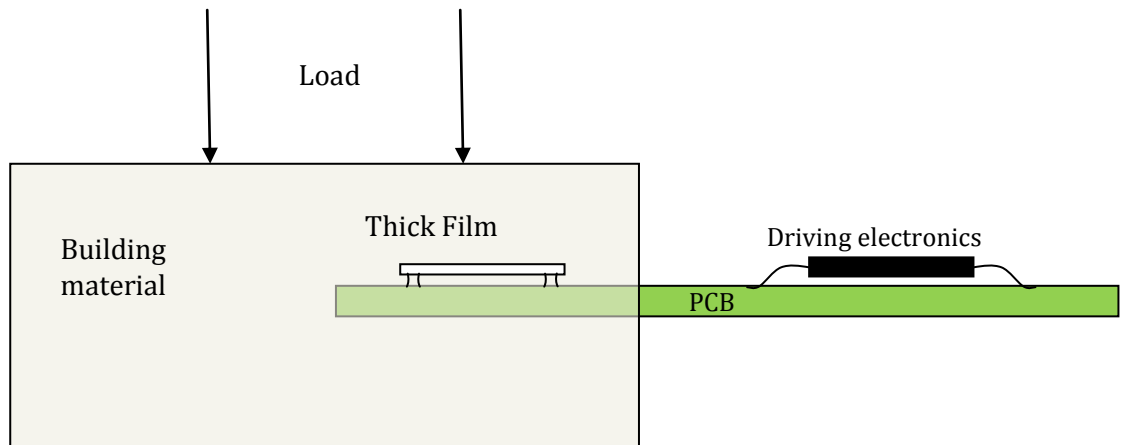


Figure 3.3 Thick Film force sensor embedded in building material

3- To be configured and used as an array for the scope of

a) Improvement of signal magnitude

b) To cover major number of possible configurations on different structure layouts like being in different angles of a concrete block, etc.

c) Reading sequentially the array of sensors to evaluate the response to load or strain long the covered area of the array.

4- Must be useable in laboratory on sample building materials and structures as a first approach to evaluate the feasibility of such application.

3.2 The Designed Thick Film Piezoresistive Sensor

The sensor was designed to meet the above points mainly to be deployed in laboratory on sample building material to evaluate the feasibility and response. **Figure 3.4** shows views of the designed sensor.

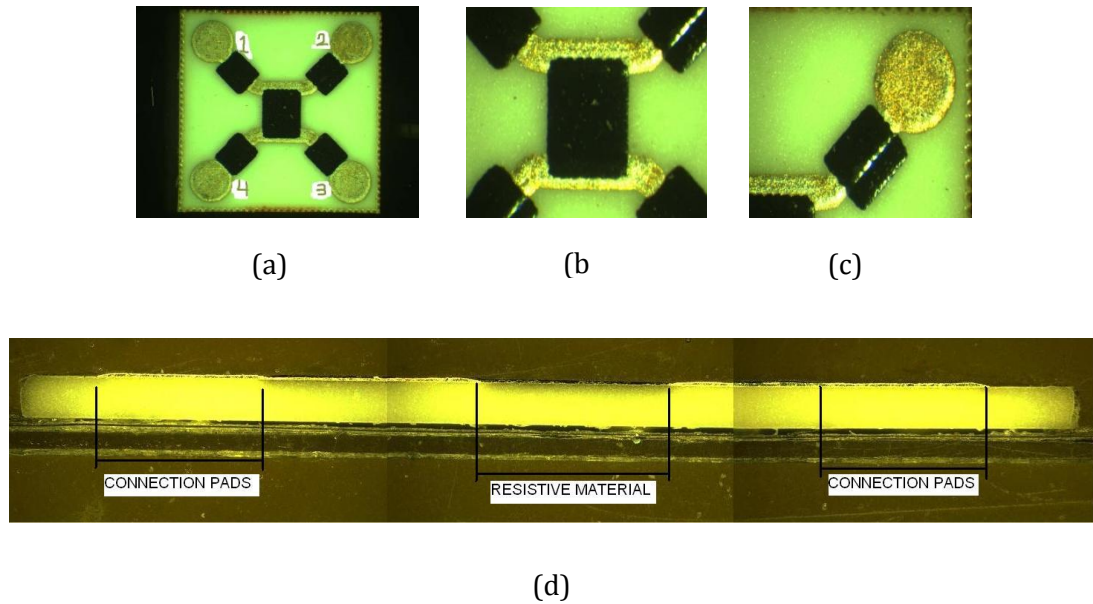


Figure 3.4 (a) Thick Film piezoresistor on ceramic (b) only the resistive part without terminals (c) one connection terminal (d) magnified side view

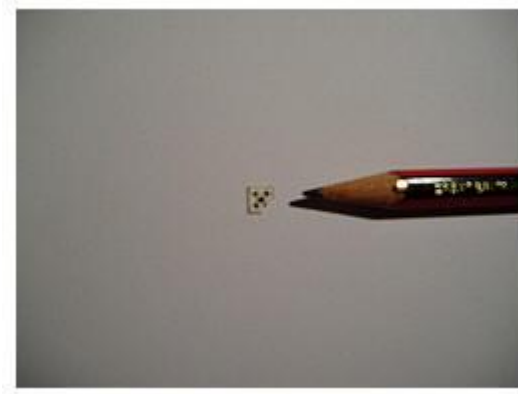
3.2.1 Sensor Description and Properties

The sensor is made of the widely used substrate material; Alumina (AL₂O₃) of 96% purity which has Young's modulus of 270-300 kN/mm² (270- 300 GPa).

Chosen Alumina sheet thickness is 0.3 mm allowing it to be sensitive enough for all the predetermined application methods.

Sensor should be small enough to be suitable for different deployment scenarios either alone or combined with other similar sensors so the final dimensions L x W x T are of 5 x 5 x 0.3 mm.

Tolerance of dimensions is 5% and the actual measured sample dimensions are 4.9 X4.9 X 0.275mm. **Figure 3.5** shows the sensor compared to a pencil



Actual sensor Dimensions
4.9mm x 4.9mm x 0.275mm

Figure 3.5 Thick film ceramic sensor (TFCS) compared to the tip of a pencil

As can be seen from **Figure 3.4a** , the sensor has four soldering pads which are useful to connect it to the external circuitry and are also used as a mechanical and electrical connection pads on PCB when the sensor is mounted in Surface Mounting Technology SMT. The distance between these pads has a decisive impact on the SM sensor response. The pads inter distance is 3.5mm.

3.2.1.1 Resistor Value

The piezo-resistor aspect ratio; $W: L$ is 1.3. The importance of aspect ratio will be evident after reading the coming paragraph; the per Square Concept. The paste used is the widely used DuPont Paste, which has a gauge factor of 10. Sheet resistance used was $10\text{K}\Omega/\text{sq}$ and the approximate resistance value obtained was in the range of $7.2 - 8.5\text{K}\Omega$ and a medium value of $7.5\text{k}\Omega$.

3.2.1.2 The per Square Concept

The “per square” concept eases the calculation of the resistance of uniform thickness areas by knowing the sheet resistance.

The sheet resistance is a measure of resistance of films that have a uniform thickness. It is commonly used to evaluate the outcome of semiconductor doping, metal deposition and resistive paste printing like in this case. In a

regular three-dimensional conductor, the sheet resistance can be derived from Equation 3.1 as follows:

$$R = \rho (L/A) \quad 3.1$$

Where ρ is the resistivity, A is the cross-sectional area and L is the length. A in Equation 3.1 is equal to the width W multiplied by the sheet thickness (t). Therefore, Equation 3.1 can be written as follows:

$$R = \rho [L/Wt] \quad 3.2$$

By grouping the resistivity with the thickness, the resistance can then be written as:

$$R = (\rho/t) (L/W) = R_s (L/W) \quad 3.3$$

ρ and t are both constants and their ratio is another constant called sheet resistance. Sheet resistance R_s is then:

$$R_s = \rho/t = \frac{R}{\frac{L}{W}} \quad 3.4$$

In Equation 3.3, L/W is a dimensionless ratio called the aspect ratio (AR) of the resistor. The aspect ratio is a term used to define the number of square shaped areas contained in the resistor body, no matter how big is this square or in other words all squares has the same resistance. For example, a resistor 0.15cm long and 0.075 cm wide would have an L/W or aspect ratio of 2 and would contain two square-shaped areas. It would be called a two-square resistor.

Paste manufacturers provide the paste specification in Ω/sq and hybrid circuit manufacturers design screen masks to deposit pastes to give certain resistance value based on the covered area or shape.

The sheet resistance used to develop our TFCS was 10000 Ω/sq . The sensor element area is a rectangle with approximate length $L = 1.0\text{mm}$ and

width $W = 1.3\text{mm}$ therefore the resistance for the TFCS used in the present investigation is as follows:

$$R = R_s (L/W) = 10000 \times (1/1.3) = 7692\Omega \quad \mathbf{3.5}$$

Due to small variation in thickness during deposition, the piezo-resistance values have a spread of resistance around the value indicated in equation.3.5 . In fact, sample values range from 7200 to 8500 Ω . These values could be optimised for a production lot and can be selected after production to values within a specified tolerance window.

3.2.1.3 Thick Film Conductor

Hybrid microelectronics utilizes conductive pastes to interconnect different discrete devices on a common substrate like Alumina in this case. The alloy used for interconnection is Silver Palladium (Ag-Pd) which is widely used as the metal inclusion component in conductive pastes.

The single thick film piezoresistive sensor, like any resistor, has two terminals one on each side. Each terminal is split in two connection points, (**Figure 3.4a**) where two conductors can be distinguished, one connecting pins 1 and 2 , the other connecting pins 3 and 4.

This way of connection allows for:

- a) The use of the connecting pads as a mechanical anchoring points to satisfy mounting the sensor on PCB to be embedded in building materials as in **Figure 3.3** and more clearly in **Figure 1.3**.
- b) Resistor terminals bridged this way will allow for more freedom of connectivity in Row column area configuration of arrays on PCB

3.2.1.4 Substrate Material and Thickness

Substrate dimensions and properties are decisive in defining sensor response. The cheapest and widely used substrate for hybrid technology in general and sensors in particular is Alumina. Alumina is a ceramic material with chemical formula Al_2O_3 , or in other words it is an oxide of Aluminium. Aluminium oxide

is an electrical insulator and has a relatively high thermal conductivity. Aluminium oxide hardness makes it suitable for use as an abrasive and as a component in cutting tools.

Aluminium oxide is responsible for resistance of metallic aluminium to environmental conditions. Pure metallic aluminium is very reactive with oxygen, and a thin layer of alumina (4 nm thickness) forms in about 100 picoseconds on any exposed aluminium surface (CAMPEL 1999). This layer protects the metal from further oxidation. The thickness and properties of this oxide layer can be enhanced using a process called anodizing. A number of alloys, such as aluminium bronzes, exploit this property by including a proportion of aluminium in the alloy to enhance corrosion resistance.

Alumina for hybrid circuits is available commercially in different plate thicknesses. The thickness is decisive in setting the sensitivity of pressure or force of piezoresistive sensor. Typical plate thicknesses are 0.3, 0.6, 0.95...etc. **Figure 3.4(d)** shows the designed sensor side view where it can be distinguished the piezo resistor area and connecting pads. The choice was for the thinnest possible sheet thickness of 0.3mm to be able to evaluate better stresses and load effects on various kinds of materials, even those with high modulus of elasticity. **Table 3.1** gives the most important property values of Alumina.

96% Aluminum Oxide			
Mechanical	Units of Measure	SI/Metric	(Imperial)
Density	gm/cc (lb/ft ³)	3.72	(232.2)
Porosity	% (%)	0	(0)
Color	—	white	—
Flexural Strength	MPa (lb/in ² x10 ³)	345	(50)
Elastic Modulus	GPa (lb/in ² x10 ⁶)	300	(43.5)
Shear Modulus	GPa (lb/in ² x10 ⁶)	124	(18)
Bulk Modulus	GPa (lb/in ² x10 ⁶)	172	(25)
Poisson's Ratio	—	0.21	(0.21)
Compressive Strength	MPa (lb/in ² x10 ³)	2100	(304.5)
Hardness	Kg/mm ²	1100	—
Fracture Toughness K _{IC}	MPa·m ^{1/2}	3.5	—
Maximum Use Temperature (no load)	°C (°F)	1700	(3090)
Thermal			
Thermal Conductivity	W/m·°K (BTU·in/ft ² ·hr·°F)	25	(174)
Coefficient of Thermal Expansion	10 ⁻⁶ /°C (10 ⁻⁶ /°F)	8.2	(4.6)
Specific Heat	J/Kg·°K (Btu/lb·°F)	880	(0.21)
Electrical			
Dielectric Strength	ac-kv/mm (volts/mil)	14.6	(365)
Dielectric Constant	@ 1 MHz	9.0	(9.0)
Dissipation Factor	@ 1 kHz	0.0011	(0.0011)
Loss Tangent	@ 1 kHz	—	—
Volume Resistivity	ohm·cm	>10 ¹⁴	—

Table 3.1 Alumina Substrate Properties (Accutatus)

3.2.2 Sensor Mechanical Simulation

The developed sensor is a rectangular mechanical element of ceramic, which can be treated as a beam that are either free, supported on hinge, or on fixed supports.

To find the generated strain on the sensor, classical static beam mechanics can be used. Another easy way is to use simulation software that has all these features.

The software used is the Framesolver from ESADS. In the coming paragraph, a description of the software and simulation results and setup is discussed.

3.2.2.1 Simulation Tool

Framesolver software is a simple two dimensional way to model and analyze planar frames, trusses, and multi span beams. It has graphical modelling capabilities with a Flexible Graphical User Interface (GUI) for pre and post-processing. Here are the important Features:

- Full GUI (Graphical User Interface)
- One interface for all model editing, model solution, and results browsing
- Direct manipulation of the basic modelling components
- Quick zooming capabilities
- Support for all units systems & conversions at any time
- Printing and copying of images
- Linear static analysis planar frames
- Linear static analysis trusses
- Linear static analysis multi-span Beams
- Internal hinges
- Load types include point and distributed loads
- Support types include pinned, fixed, roller and Elastic supports
- Flexible mode element drawing
- Graphical selection of model components
- Computation of spring and constraint reactions
- Computation of node displacements and rotations
- Drawing of deformation diagram
- Axial force diagrams
- Shear force diagrams
- Bending Moment diagrams

3.2.2.2 Simulation Results

3.2.2.2.1 Gluing Sensor on the Material

Assuming high rigidity of the structural adhesive gluing the sensor to the building material, a rectangular member of the dimension of the TF designed sensor was created. Dimensions and geometry of the sensor is shown in **Figure 3.6**. X-axis has 0.5mm per quadrant.

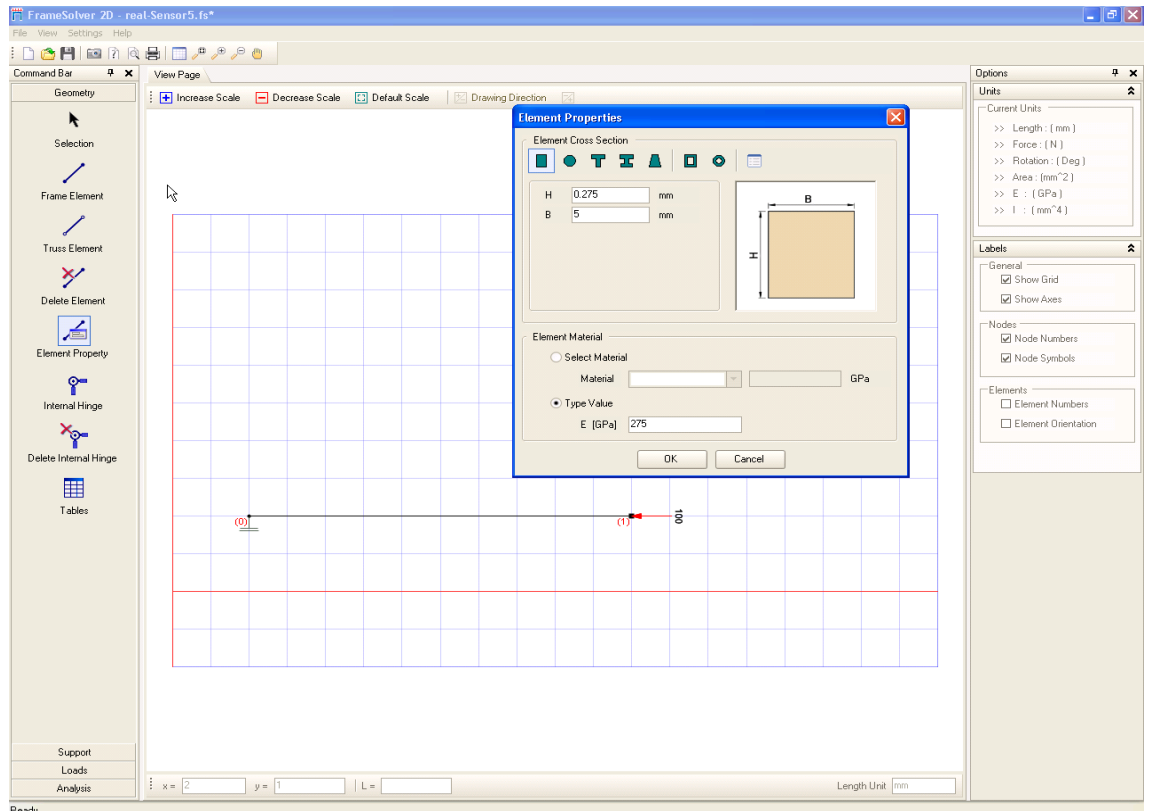


Figure 3.6 TF sensor 4.9X4.9X0.275mm 275GPa loaded with 100N

As an example, if a force of 100N is applied to the sensor on one end, parallel to the x-axis, while the other end has a fixed support, the change in length is 0.00132 mm which if divided by the original length; 5mm gives a strain of 264μ strain. This can be noticed in **Figure 3.7**. This result could also be obtained by applying Hook's law.

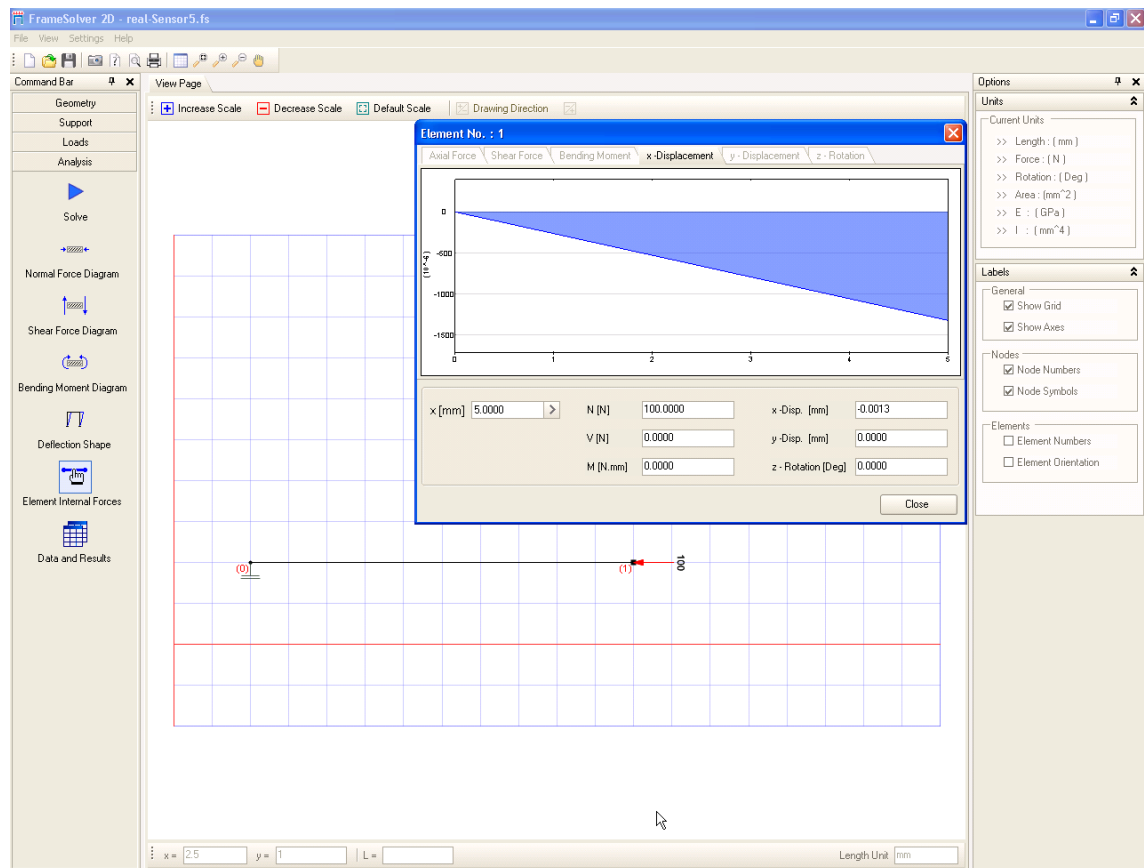


Figure 3.7 Sensor with applied 100N has a change in length of $\Delta x=0.0013\text{mm}$

3.2.2.2.2 Embedding Sensor in Building Material

The sensor can be mounted in Surface Mounting Technology (SMT) on PCB as in shown in **Figure 1.3**. Being embedded in building material, the sensor will have most likely a distributed load over the active surface as in **Figure 3.8**. However, the choice might be to put a cushion of a suitable size and rigidity to accentuate or alleviate the force effect as appropriate.

The 2D simulation capability of the used software is not enough because the sensor is soldered in four points and should be simulated in Finite element as a slab. The strain – load relationship in the 2D model is however indicative to the generated strain at the side middle of the sensor where the TF resistor is located. The strain, which results from the 2D model, is always less than slab central strain.

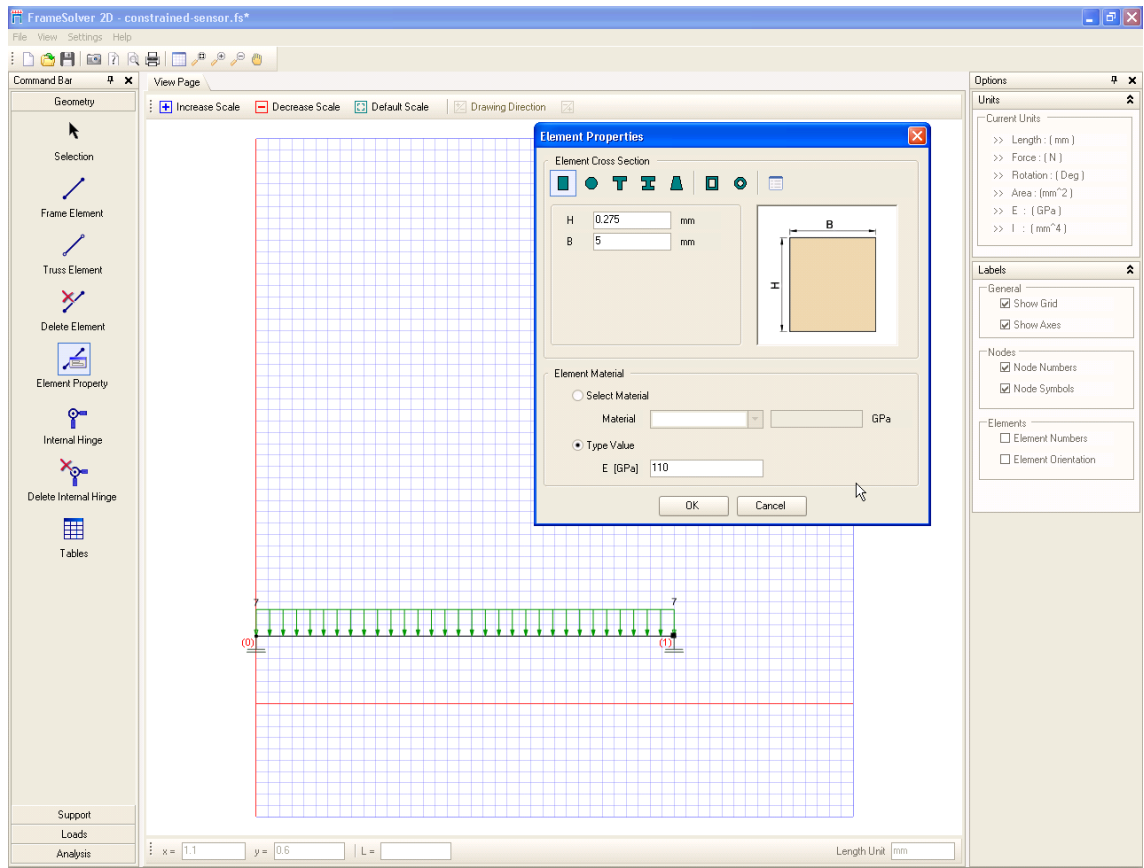


Figure 3.8 Distributed load on sensor area

In **Figure 3.8**, The sensor is considered as a constrained beam of length 3.5mm , which is the distance between the soldering pads and has a shear modulus of $G=110\text{KN}/\text{mm}^2$. Shear modulus is approximately 2.5 less than the Young's modulus.

Having a distributed load of $7\text{N}/\text{mm}$, the sensor will have maximum deflection response shown in **Figure 3.9**.

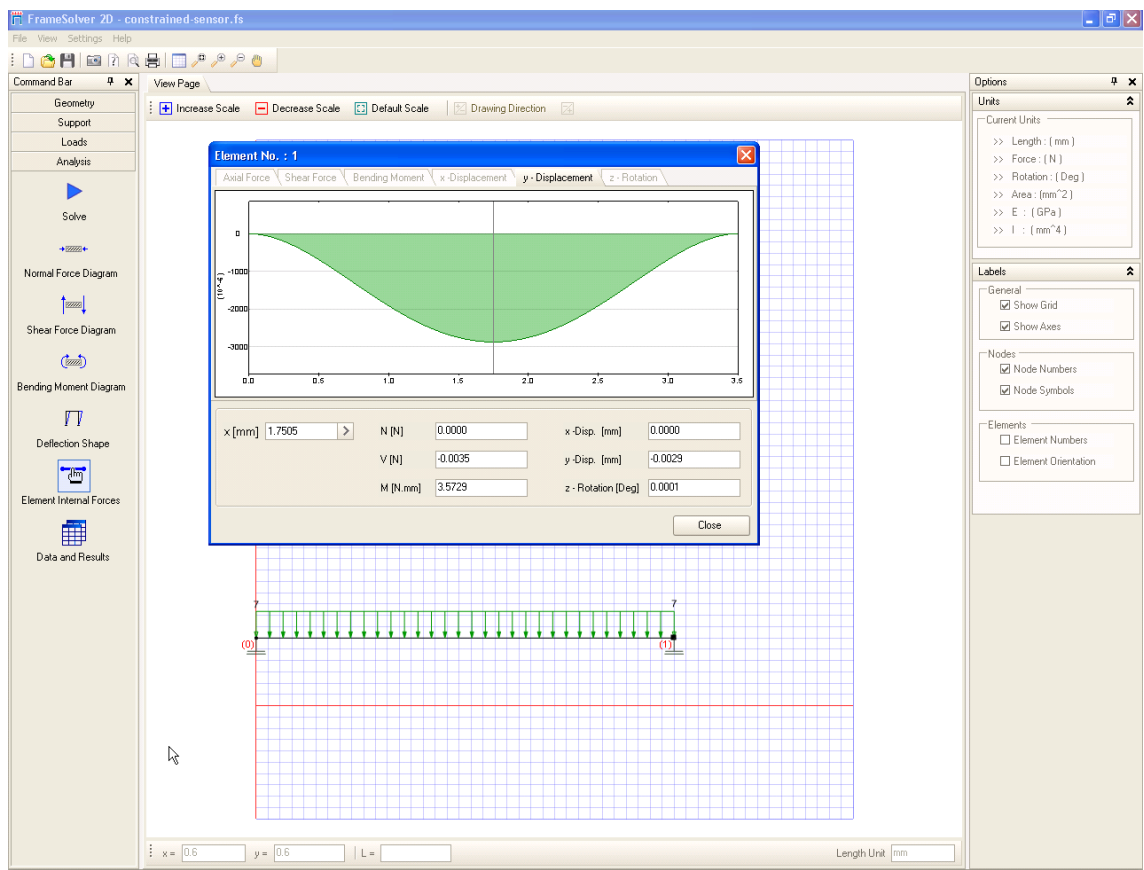


Figure 3.9 Constrained TF sensor response to 7N/mm distributed load

The maximum deflection that can be seen from **Figure 3.9** in the Y direction is of about 0.003mm and a maximum bending moment of 3.5694 N.mm giving rise to a strain of:

$$\epsilon = 736 \mu\text{strain}$$

Calculated from the formula

$$\epsilon = \frac{cM}{EI} \quad 3.6$$

Where:

c = maximum stress point which is sensor thickness over two

M= Maximum Moment

E = Young's shear modulus, the shear load will make the sensor to bend

I = Moment of inertia of area of the sensor (Appendix – D)

Alumina maximum supporting strain limit, before rupture, is $1000\mu\text{starin}$ (PRODUNZIATI 1994).

The bending moment diagram is shown in **Figure 3.10**.

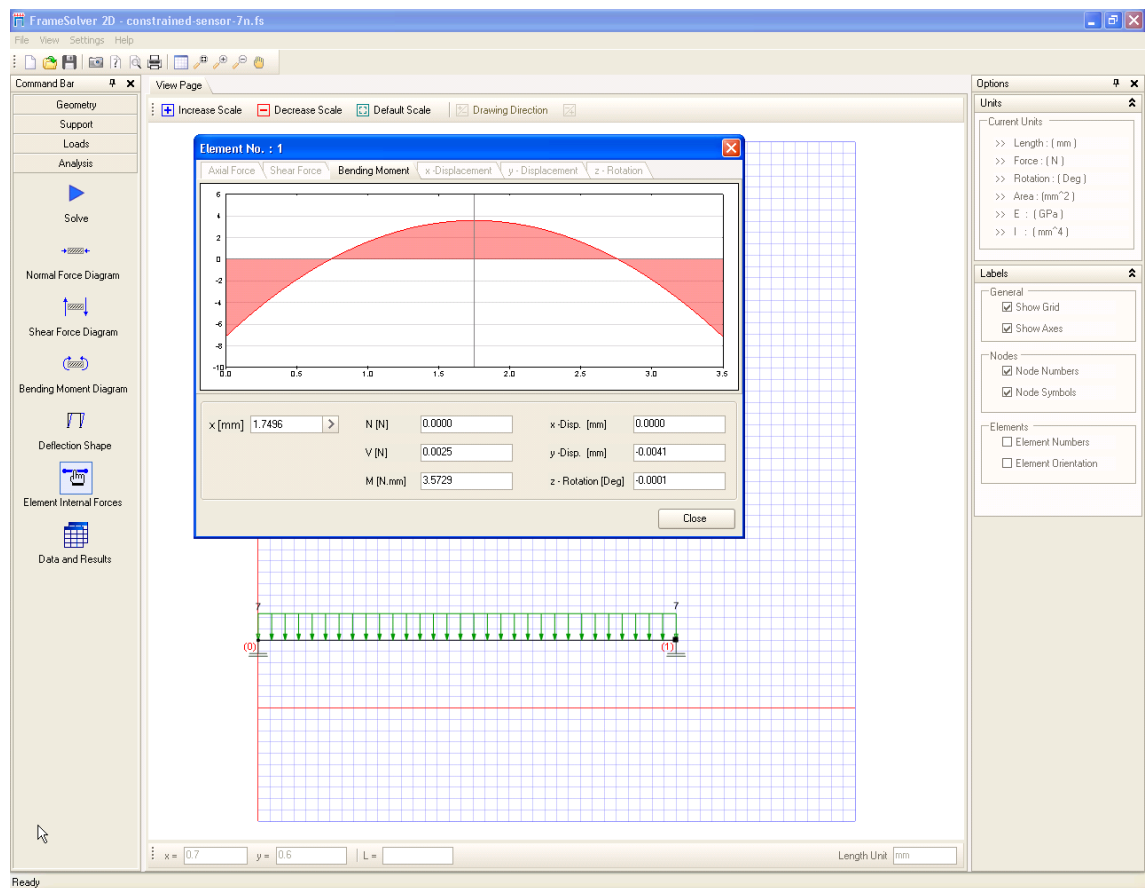


Figure 3.10 Constrained TF sensor bending moment diagram

This sensor configuration may have a better sensitivity to load by just soldering one side of the SMD Thick Film sensor. **Figure 3.11** shows a double deflection with respect to the previous configuration which would cause double strain for the same load.

Figure 3.11 and **Figure 3.12** show the deflection and bending moment diagram of this configuration.

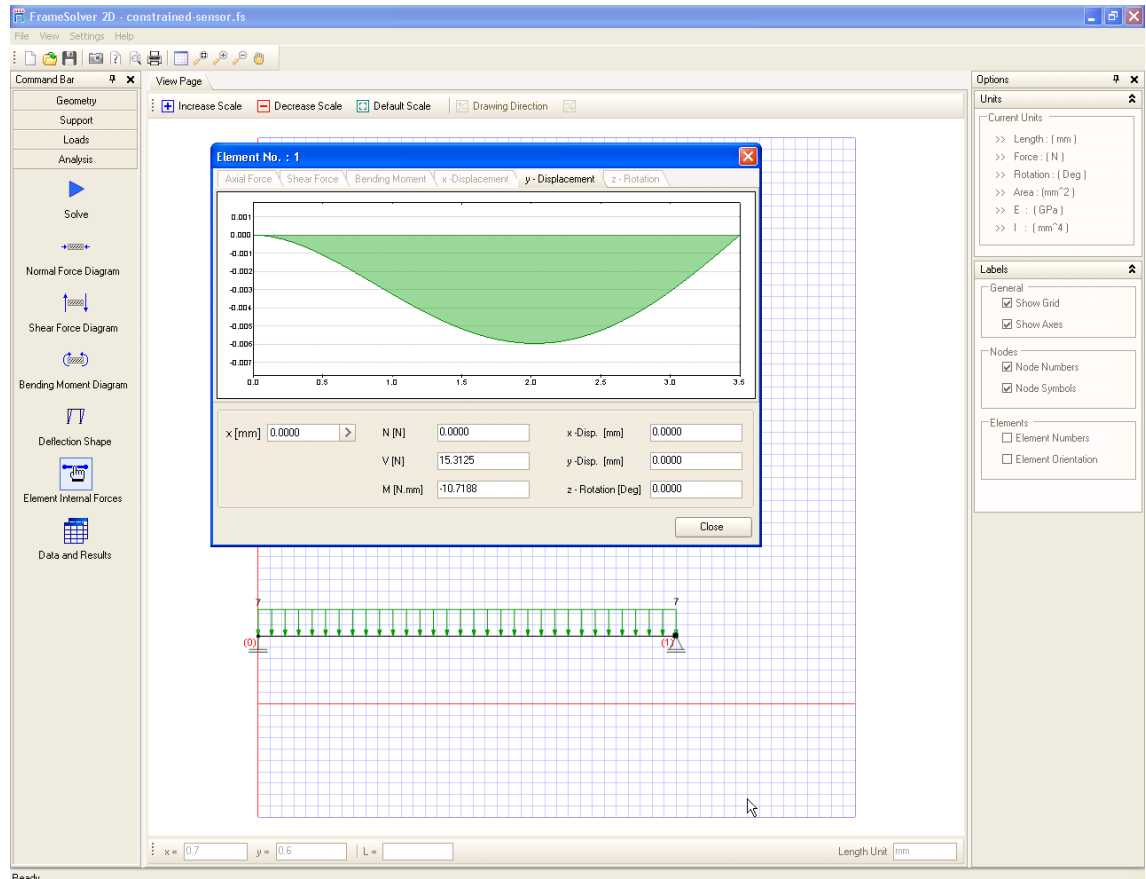


Figure 3.11 TF sensor sensitivity enhancements by soldering only one side

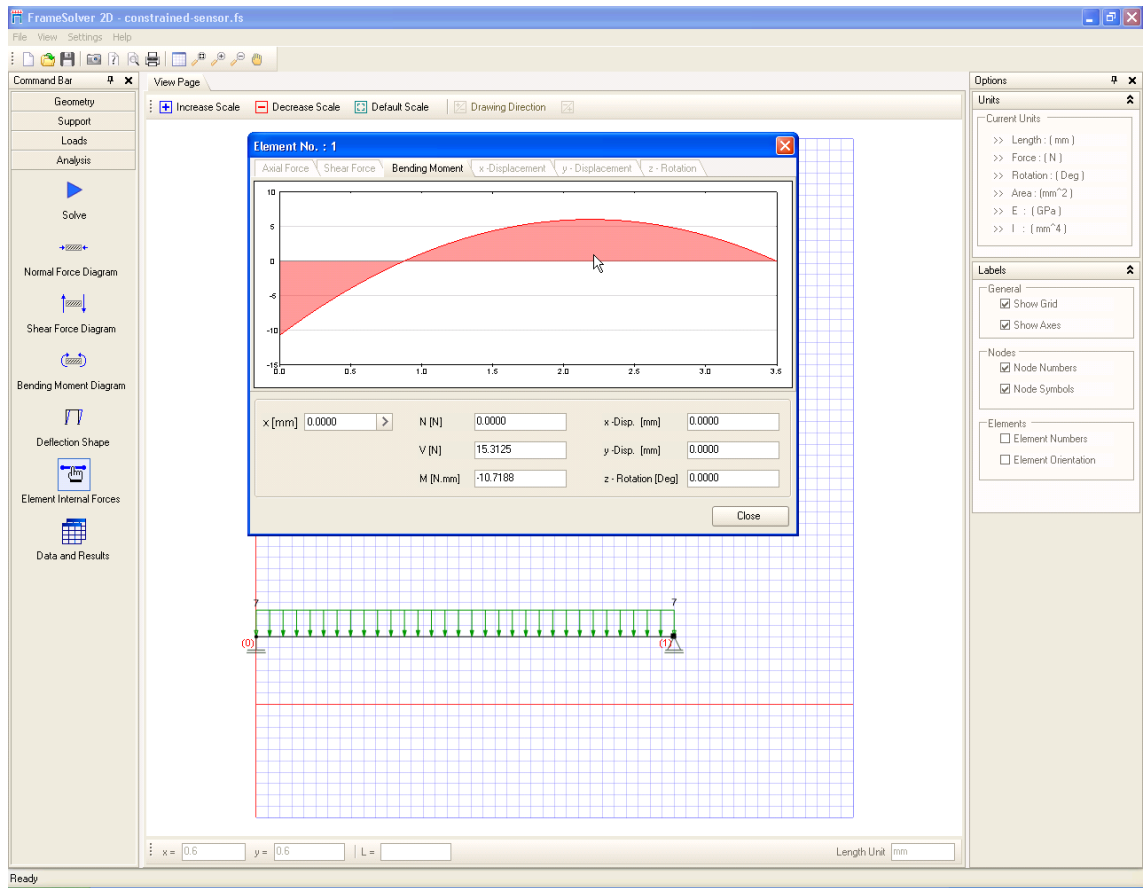


Figure 3.12 Bending moment diagram of the sensor soldered on one side

3.2.3 Thick Film versus Foil Metal Strain Gauges

As a first approach to evaluate the designed Thick Film sensor response, thick film and foil metal strain sensors were glued on a steel bar and a Four Point Bending (4PB) test was carried on. In this section, a description of the elements and devices used in this test will be given first. Results will be shown and discussed at the end.

3.2.3.1 Metal Foil Strain Gauge (FSG)

The widely used sensor to measure strains in civil engineering is the metal foil strain gauge, denominated usually as “strain gauge” (**Figure 3.13**). Metal strain gauge technology has been highly developed and used over the years and is the premier testing device for applications such as the testing of building materials. The accumulated experience of application of

FSG to building materials allows using it as a reference to evaluate the new TFCS in terms of response to strain.

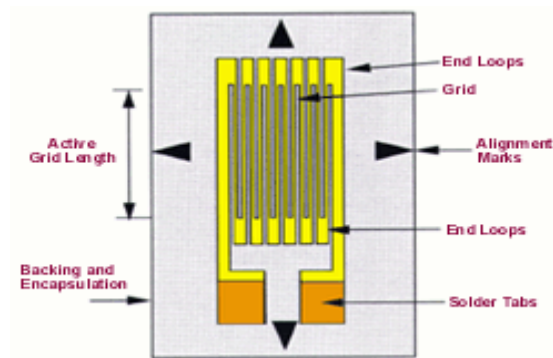


Figure 3.13 Typical Foil Strain Gauge (FSG)

3.2.3.2 System 5000

The System 5000 is a hardware and software for data acquisition and recording for strain gauges response. It has a linear displacement transducer control and a load cell to be used during specimens testing. System 5000 controls the application of load on specimens and reads sensor response. The hardware provides stable, accurate, low-noise signal conditioning for input channels. The number of channels ranges from 5 to 1200. These channels can be scanned with a settable scanning interval that can be as short as 0.1 seconds.

The software is Windows-based and provides interface to set up, monitor and calibrate all the strain gauge channels. It also provides presentation, recording, and post-test analysis of data. In general, System 5000 is composed of:

- Data conditioning and acquisition unit (**Figure 3.14**).
- Personal computer.
- Software package.



Figure 3.14 Data acquisition unit of System 5000

During the test phase of this research, the system was used to read the data received from both the FSG and TFCS. The system measures load/strain values by taking the number of AD (analogue/digital) counts and multiply them by a constant to give a value of load or strain for a specimen. The acquired measured data are stored in text files. This data was used for the generation of graphical representation of the measurements.

3.2.3.3 Circuit Electronics Used to Interface System 5000

Each TFCS in tests performed with System 5000, was connected as part of what is known as “quarter bridge” configuration as shown in **Figure 3.15**.

In the bridge of **Figure 3.15**, the strain-sensing gauge of interest appears in only one position (out of four). A constant ± 5 Volts DC excitation voltage coming from System 5000 was used. With $\Delta R=0$, the bridge is perfectly balanced and hence the output voltage, $V_o=0$. The change of ΔR will unbalance the bridge with a voltage proportional to strain on TFCS. System 5000 channels amplify the signal and provide the readings to the user. The FSG used as reference in our tests are connected directly to

dedicated and calibrated channels of the System 5000. The interface electronics for FSG are part of these dedicated channels.

The derivation for the output voltage difference change with strain or change in the strained resistor can be found in Appendix A.

Equation 3.7 is the result of this derivation:

$$V_o = \frac{V}{4} \times \frac{\Delta R}{R} \quad 3.7$$

Where V is the bridge excitation voltage and V_o is the output unbalance voltage.

Since:

$$GF = \frac{\frac{\Delta R}{R}}{\epsilon} \quad 3.8$$

Hence:

$$GF = \frac{4V_o}{V\epsilon} \quad 3.9$$

Equation. 3.9 relates the piezoresistive sensor GF, to the quarter bridge output unbalance voltage V_o and the exerted strain (ϵ). By having the GF of the sensor, the bridge output voltage can be used as a direct indication of strain.

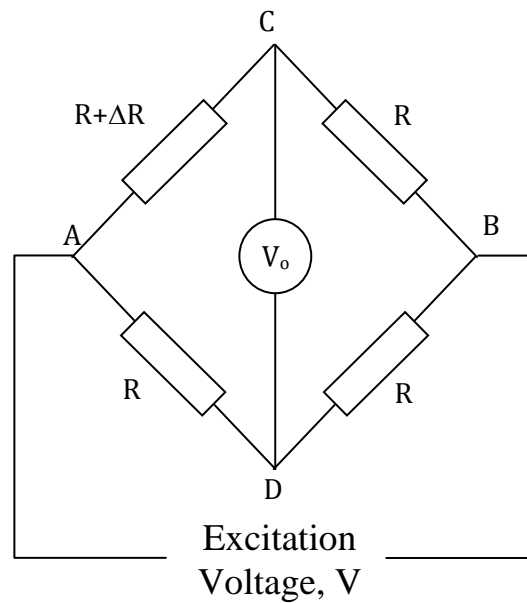


Figure 3.15 Quarter Wheatstone bridge

3.2.3.4 Four Point Bending Test (4PBT)

Figure 3.16 depicts the setup for the well known “Four Point Bending Test”. This test is widely used for flexural material testing Following the testing conventions specified in (ASTM D6272-00 2001). This later is a Standard Test Method for Flexural Properties of Unreinforced and Reinforced Plastics and Electrical Insulating Materials. With the Four-Point Bending, transverse vertical loads are applied to horizontal beams such that a constant bending moment results between the two inner load locations.

By simulating this Four Point Bending Test with the Framesolver software, a constant bending moment can be observed in the centre where the sensors are glued, a pure bending moment without shearing force. The constant moment at the centre and the deflection with an applied force of 100N is shown in **Figure 3.18**.

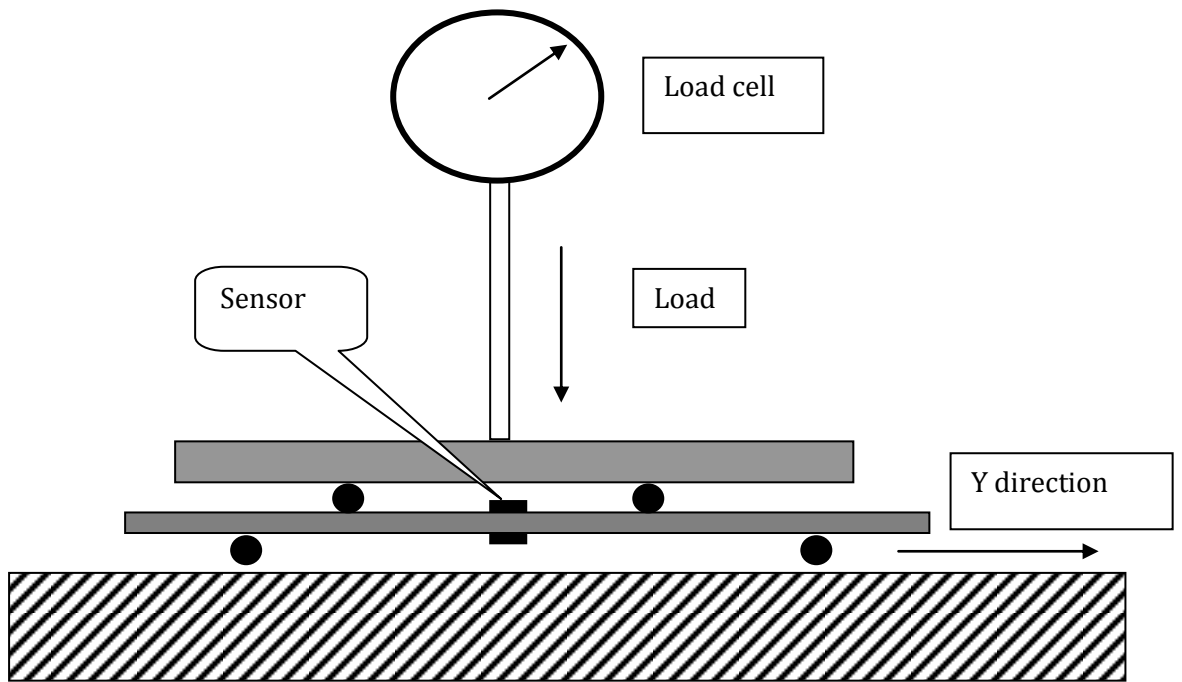


Figure 3.16 Four point bending test

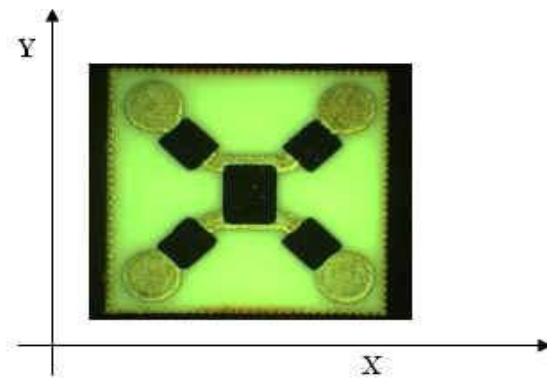


Figure 3.17 TFCS orientation

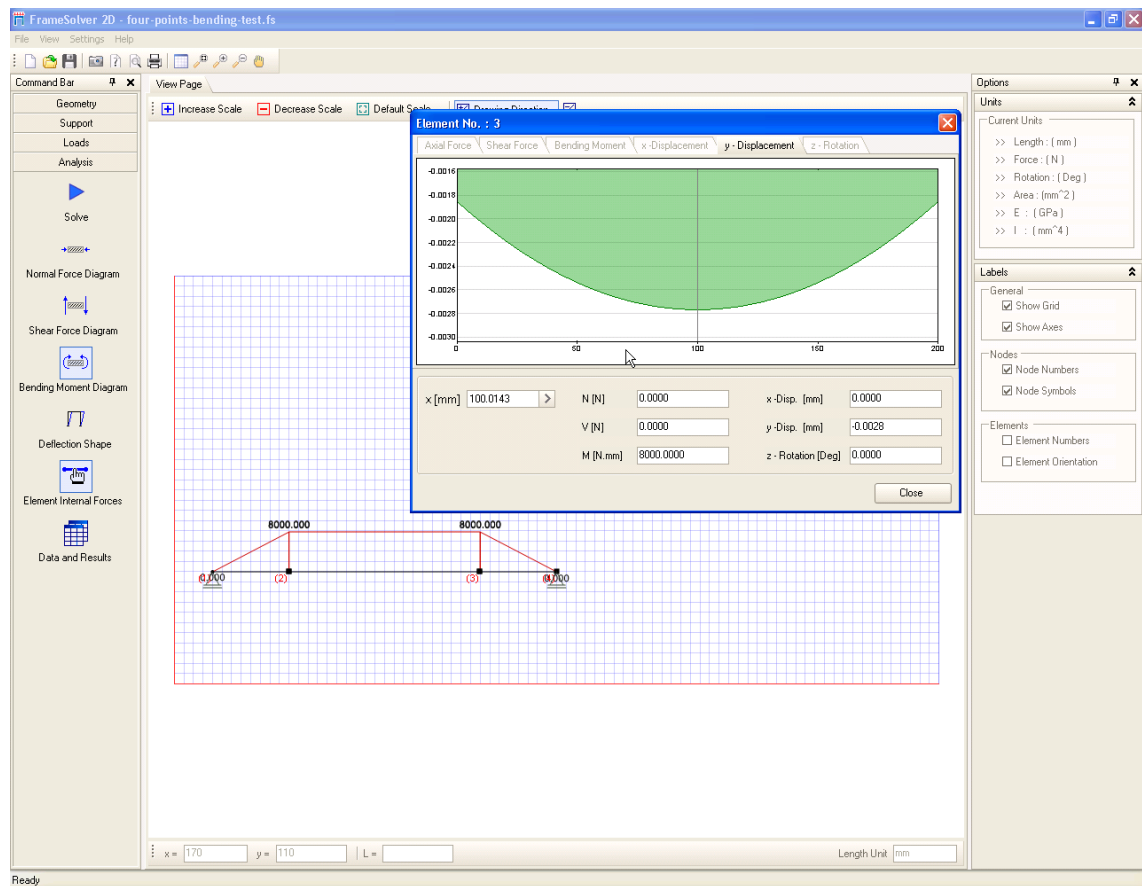


Figure 3.18 Four point bending test simulation results

Two ceramic sensors are glued on top and bottom of the steel bar, which has 20 X 20 X 500mm dimensions. The Y direction in **Figure 3.16** and **Figure 3.17** indicate the sensor orientation with respect to the applied load and beam axis. Another beam is used to apply the load equally on both sides of the beam under test.

Foil strain gauges are also glued parallel and in the same direction to each TFCS (**Figure 3.19**). Each TFCS sensor was connected to a Wheatstone bridge, which has been connected to System 5000. The sensors are glued using the normal foil strain gauge adhesive (M-bond 200 Cyanoacrylate ester made by Measurements Group Inc). This kind of adhesive uses a catalyst called Catalyst C. **Figure 3.20** shows detailed electronic connections of one Single sensor to the steel bar and System 5000.

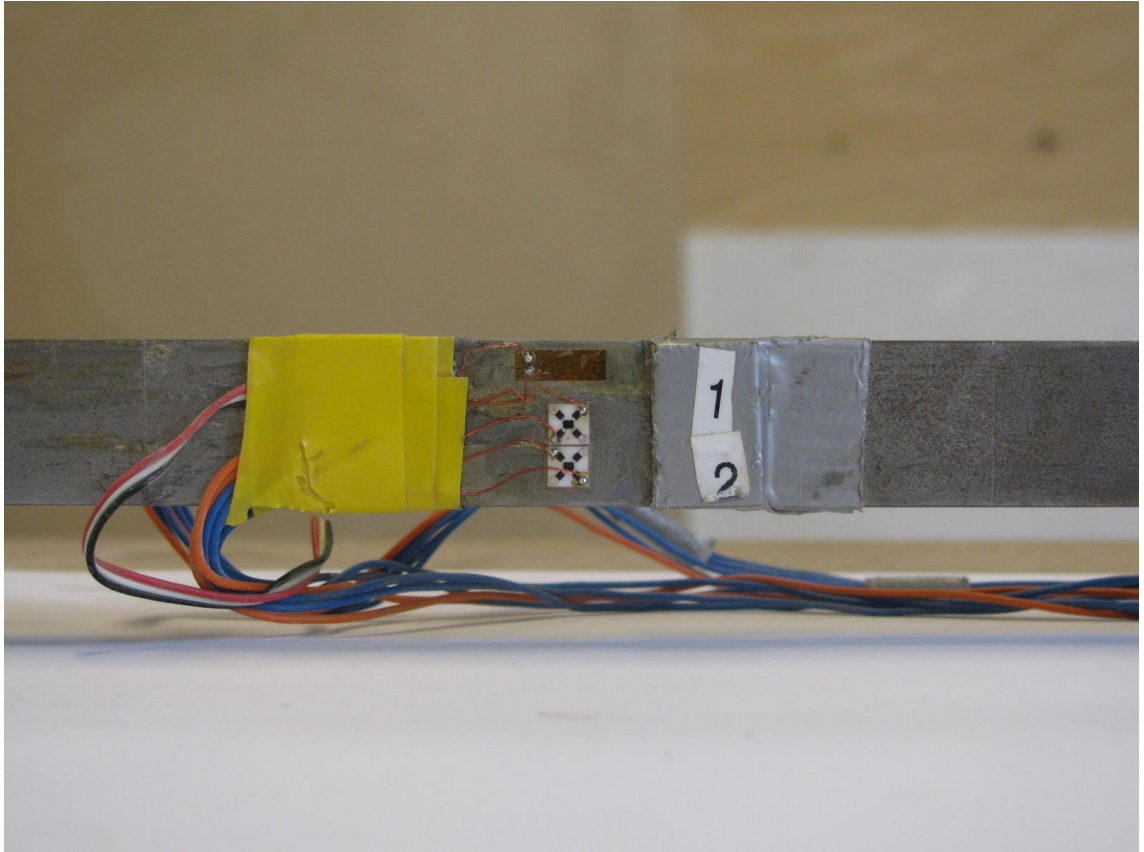


Figure 3.19 Image of TF sensors together with foil strain gauge in 4 PBT

Foil strain gauge has a calibrated reading for strain in System 5000 and were used as reference for strain measurement to characterize the TFCS.

System 5000 controls also an actuator to apply load to the steel bar and has a load cell to measure the applied load. System 5000 generates a table of mV/V output of TFCS versus load and a table of strain versus load of the foil strain gauges.

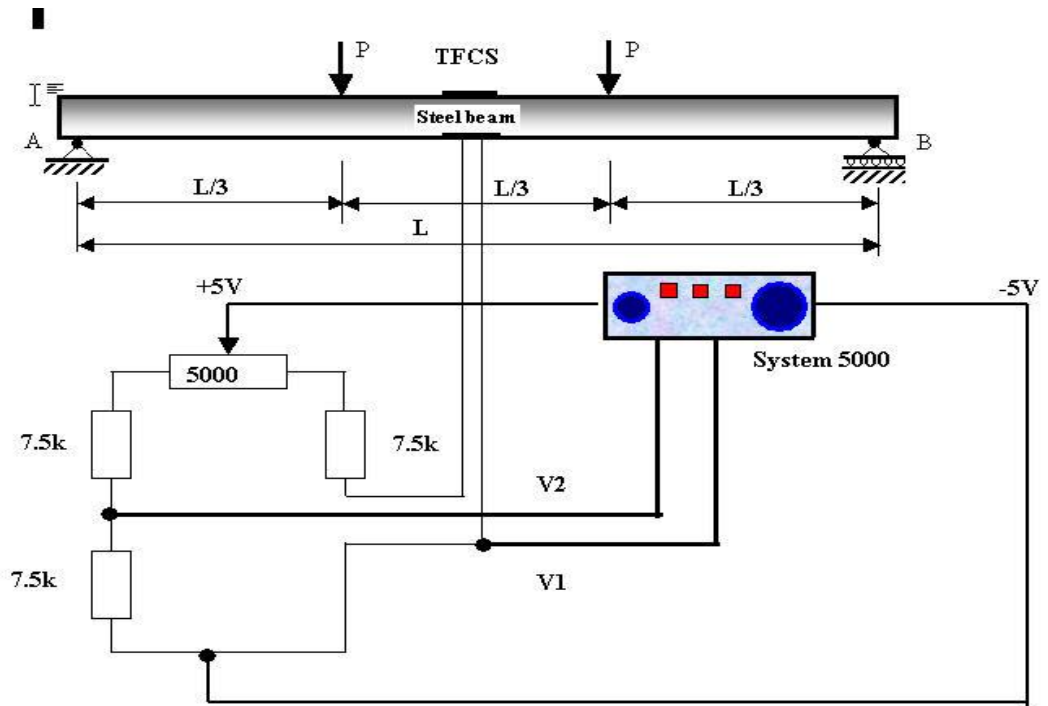


Figure 3.20 TFCS bridge circuit connection to the steel bar and system 5000

3.2.3.4.1 Test Results

Test was carried on for one single sensor placed during the first run on the upper side of the steel bar and during the second run on the lower side of the steel bar. When the sensor is on the topside it is in compression and when it is on the lower side it is in tension. The two readings were put together on the same graph shown in **Figure 3.21**. Both TF and FSG response are reported on the graph. The TF response is $0.0018/0.0005 = 3.6$ times higher the metal FSG. So since the GF of FSG is known to be 2, the Gauge Factor of thick film sensor should be $2 \times 3.6 = 7.2$.

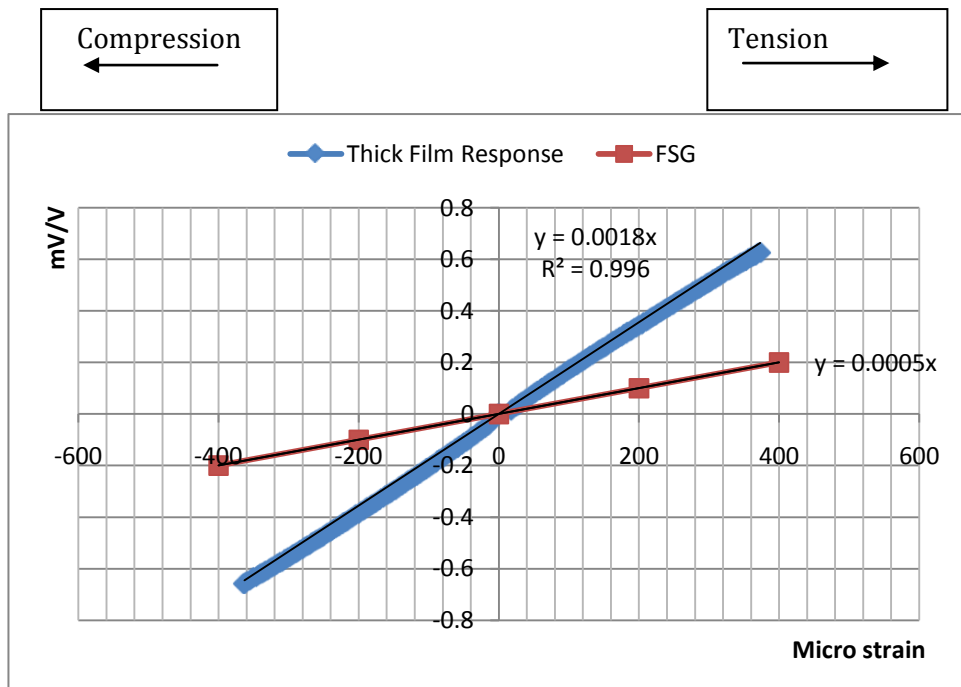


Figure 3.21 Thick-Film ceramic Sensor in tension and compression

Test was repeated several times, loading and unloading, and results were almost the same and within the thick line in the graph for the Thick Film sensor. TF in the Graph in **Figure 3.21** shows a maximum Hysteresis of around 6.5%.

3.2.3.4.2 TF Sensor Gauge Factor Calculation

As mentioned, in Quarter Bridge configuration the relationship between strain and bridge output unbalance voltage due to the application of load is:

$$GF = (4V_o/V) \times (1/\epsilon) \quad \mathbf{3.10}$$

Where:

GF = Sensor Gauge factor

V = Bridge excitation voltage

V_o = Bridge voltage unbalance due to load application

ϵ = Material strain

The linear equation relating strain to bridge output unbalance voltage is given from the graph in **Figure 3.21** as:

$$V_o = 0.0018\epsilon \quad 3.11$$

Re-arranging (3.10), and substituting from (3.11):

$$GF = \frac{4}{V} * \frac{V_o}{\epsilon} \quad 3.12$$

Hence, TF sensor Gauge Factor is 7.2, which is more than three times bigger than the Foil Strain Gauge GF mounted on the same beam as mentioned before.

3.2.4 Test of SMT Mounted Sensor

In an operation of serigraphy, paste type Sn62Pb36Ag2 was deposited on PCB and sample sensors were mounted. The PCB was then put in a kiln and heated to 240 Cent degrees which is the melting point of the mentioned paste and then cooled, the result is in the image of **Figure 3.22** where sensor is shown mounted on PCB and tested by applying a uniform load on its surface. A 5 and 1/2 digits multi meter type HP 3468A was used to register change in resistance with load. The load was measured with a 1 g precision scale which is the platform in **Figure 3.22**. The response is shown in **Figure 3.25**.

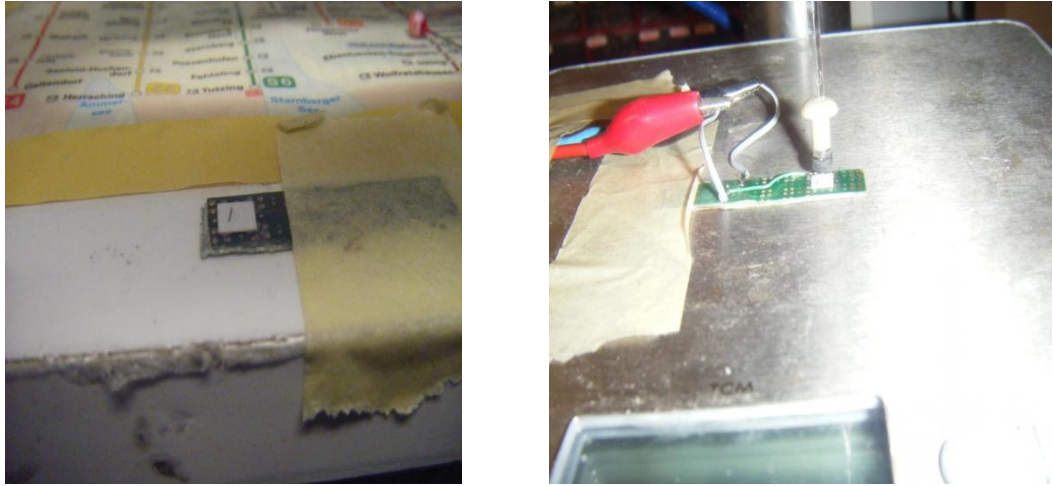


Figure 3.22 Test of TF sensor mounted on PCB in SMT

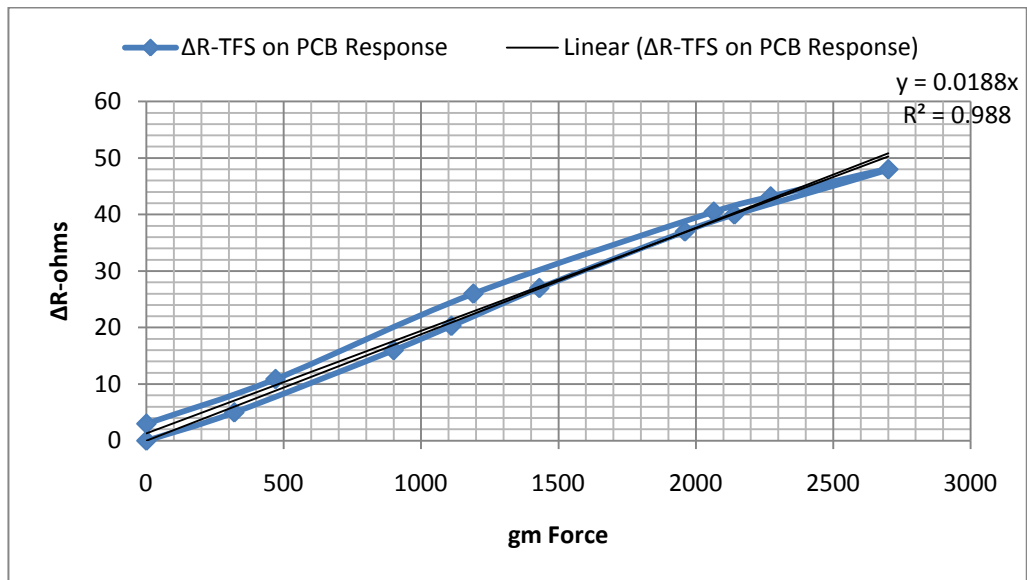


Figure 3.23 SMD mounted TF sensor response to uniform load

The response shows an offset from zero after load application. This offset returns back to zero after some time (several minutes).

To be able to compare the simulation result with the measured response, the distributed load has to be 7N/mm.

Substituting 7000 in the linear trade equation 3.13 of **Figure 3.23**;

$$\Delta R = 0.0188 * load \quad 3.13$$

$\Delta R = 131 \Omega$ which is 1.5% of the initial value (8510 Ω)

The gauge factor would be from 3.8 ;

GF= $(\Delta R/R)/\epsilon = 0.015/736 \mu\text{strain} = 21$ which is double the specified paste GF. As mentioned in paragraph 3.2.2.2.2, the sensor simulation in 2D is not enough to represent the sensor centre deflection, but can give an idea about the side strain. The sensor mounted in this way is similar to a circular edge-clamped diaphragm; response to pressure of which is shown in **Figure 3.24**.

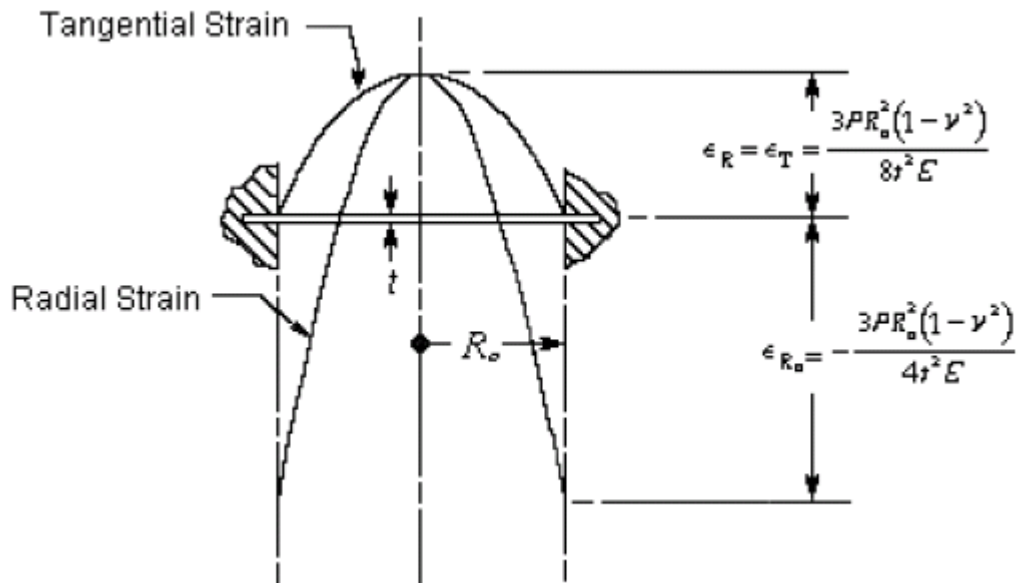


Figure 3.24 Circular edge-clamped diaphragm Response (Measurement Group)

At the diaphragm centre, the maximum tangential and radial strains are equal;

$$\epsilon_t = \epsilon_r = \frac{3wr^2(1 - \nu^2)}{8h^2E} \quad 3.14$$

Where:

w= distributed load which is 7N/mm

r= diaphragm radius which is 3.5 mm

ν = Poisson's ratio for Alumina (0.21)

h= diaphragm thickness which is 0.275mm

E= shear modulus of elasticity 110000/mm²

The calculated strain would be;

$$\epsilon_r = \epsilon_t = 1054 \mu\text{strain}$$

The GF of the sensor is $(\Delta R/R)/\epsilon = 14.23$ which is the value confirmed by amount of change of TF resistance (1.5%) deducted from **Figure 3.23** .

3.2.4.1 Maximum Allowable Supported Load

To find the maximum allowable load which the designed TF sensor can support, equation 3.14 can be written as follows;

$$w = \frac{8h^2\epsilon E}{3r^2(1 - \nu^2)} \quad 3.15$$

Maximum load which will produce a strain of 1000 μstrain is $w=1.894$ **N/mm** and the total load would be then $1.894 \times 3.5=6.63$ N.

3.3 Direct Load Application of TFS

During beam test, it has been observed that glued TFCS was sensitive to the strains developed on ceramic surface. The phenomena was accentuated by merely touching TFCS surface with a pencil or any other hard pointer.

By having the ceramic substrate sensible to load, a new viable way of deployment of TF sensors could be exploited like in **Figure 3.25**.

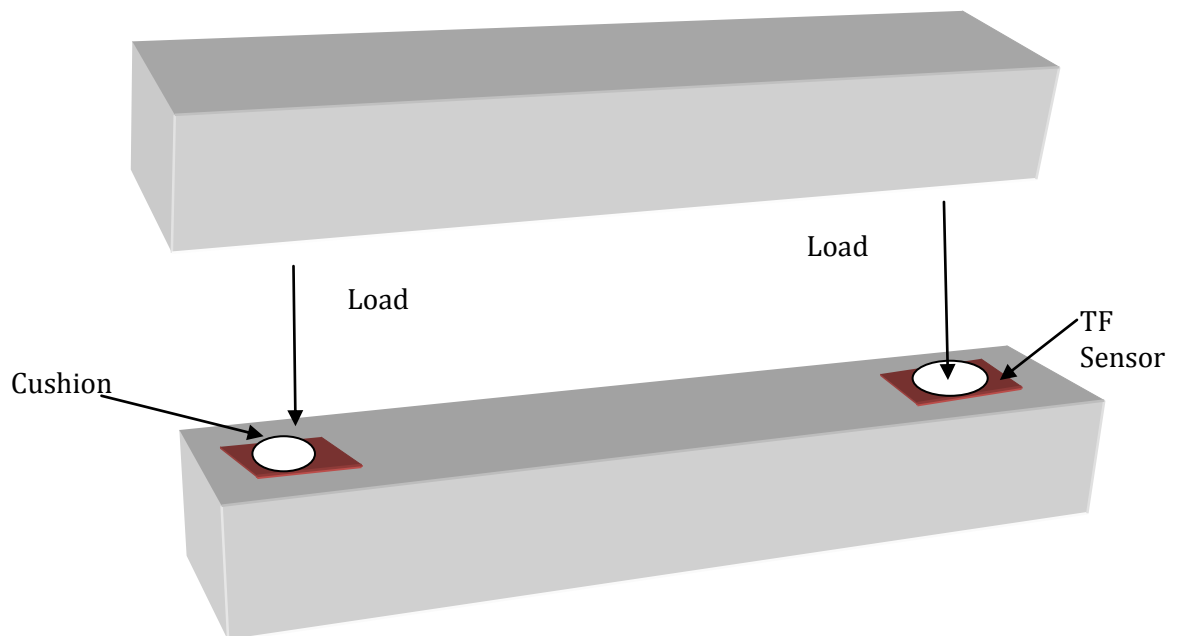


Figure 3.25 Direct application of load on Thick Film substrate

3.4 Summary

A Thick Film Ceramic piezoresistive sensor was designed and a number of samples was manufactured. The designed sensor is suitable for two different employment methodologies;

- 1- To be glued on civil structures to measure strain when structures are under load stress and load is symmetrical and parallel to the gauge.
- 2- To be embedded into the building material for direct monitoring of loads.

Sensor response in both deployment methodologies has been simulated with mechanical simulation software.

For the second deployment methodology, sensor was mounted singularly on Printed Circuit Board in Surface Mounting Technology.

As a first approach to examine the sensor response to strain, four point bending test was conducted on a steel bar on which TF sensors were glued together with metal foil gauge sensors. The metal foil strain gauge connected to system 5000 is a reference to give direct reading to strain and by having thick film sensor response together; the TF gauge factor could be measured and found to be 7.2, which is more than three times bigger than the gauge factor of foil metal strain gauge mounted on the same beam.

A test on sensor mounted in SM technology was carried on and from the equation of the response curve; the strain at the designed load was calculated and found to be divergent from simulation. Circular edge-clamped diaphragm equation was then applied on sensor properties and found to be correspondent to the test results.

It was also found that TFS glued on building material is sensitive to directly touching its substrate. This phenomenon suggests a new way of deployment by direct load application that will be examined in the coming chapters.

4. Sensor Interface

This chapter has the objective to assess the application of TF sensors on building materials and to prove consistency of response of this sensor with the various building material types. Alternative interface circuits will be introduced, derived mathematically, simulated and tested with TF sensors applied on building materials.

The chapter will start with an introduction to sensors and their characteristics and specification.

Here are the main constituent parts of this chapter:

- 1- To propose new alternative interface circuits to Wheatstone bridge where op-amps would boost sensor sensitivity. A mathematical comparison of the two interfaces will be shown.
- 2- One of the proposed alternative circuits will be simulated and compared to the mathematical derived solution.
- 3- The proposed circuit will be used to perform tests on two sample building material; brick and concrete.

4.1 Sensor Definition

A sensor is a device that measures a physical quantity and converts it into a signal, which can be read by an instrument or data acquisition system. Data from the outside world are usually acquired through sensors. Depending on how accurately the reality is to be gauged, the sophistication of the sensors increases and the relationship is not usually linear or simple. Thus, the sensors are an important part of the acquisition systems that, in providing an interface between the system and the outside world,

have to comply with the requirement of both environments. This puts stringent requirements on the chemical, mechanical, and electrical characteristics of the sensors, especially in corrosive, harsh, or delicate environments. These situations are normally encountered in Structural monitoring applications. Hence, a reliable and systematic characterization of the sensor is of utmost importance in today's rapidly advancing field of sensors.

In the specific case of TF sensors applied to monitor structures, the physical phenomenon is the stress on the structure, which would generate a strain or deformation of the structure. The TF sensor element has an intrinsic response to strain and the conversion constant is gauge factor of the sensor.

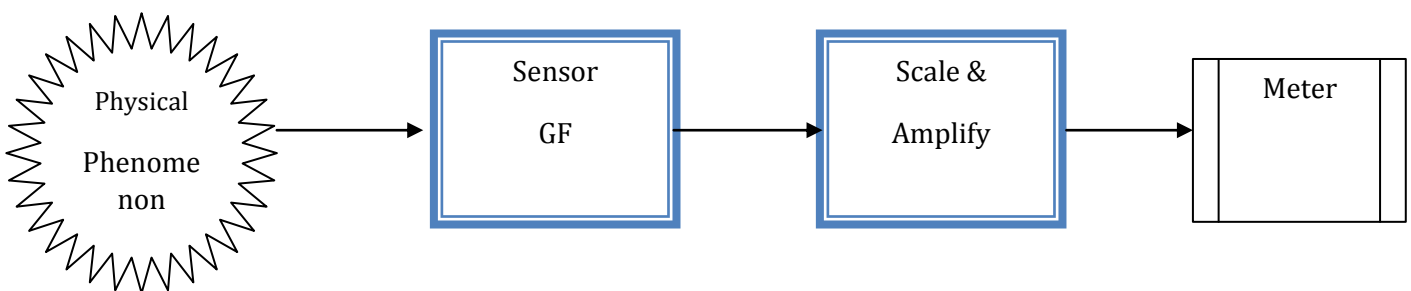


Figure 4.1 Sensor interface to measure a physical phenomenon

As can be seen from **Figure 4.1** the conversion factor of the sensor is the sensor GF that will provide a signal to be scaled and amplified appropriately to suit the reading instrumentation or data acquisition system. A good sensor obeys the following rules:

- Is sensitive to the measured property
- Is insensitive to any other property likely to be encountered in its application
- Does not influence the measured property

Ideal sensors are designed to be linear or to have some simple mathematical function of the measurement like logarithmic or simple polynomial. If sensor response is linear then output signal of such a sensor

is linearly proportional to the value or simple function of the measured property. The sensitivity is then defined as the ratio between output signal and measured property. For example, if a sensor measures strain and has a voltage output, the sensitivity is a constant with the unit [mV/ μ strain]; this sensor is linear because the ratio is constant at all points of measurement.

4.2 Sensor Classes and Specification

In general, there are many specifications and performance characteristics defining the sensor class. The most important sensor characteristics which have direct impact on its performance are here described:

Accuracy: A measure of how closely the result of the experiment (sensor output) approximates the true value. Since the true value of the unknown (measurand) is not known a priori, a comparative measurement is needed in specifying the accuracy of a transducer.

Sensitivity: It is the incremental ratio of the output (e.g. mV) to the input (e.g. strain).

Precision: Describes how exactly and reproducibly an unknown value is measured. It has nothing to do with how accurately the measured value represents the unknown parameter. For example, when using a ruler to measure the length of a rod, accuracy refers to how closely the measured value represents the true length of the rod. The precision refers to how carefully the number is read from the ruler or how carefully the ruler is set next to the rod. Clearly, accuracy without precision does not have any meaning and precision does not imply accuracy.

Resolution: The resolution of a sensor is the smallest change it can detect in the quantity that it is measuring, the smallest increment in the value of the measurand that results in a detectable increment in the output. It is expressed as a percentage of the measurand range (%MR). For example, if a strain sensor yields an increment of ΔV output voltage in response to a

$\Delta\epsilon$ change in the strain (or load) of an object, then the maximum resolution is the smallest $\Delta\epsilon$ that yields a detectable ΔV and it is expressed as percentage of the measured range; MR.

Nonlinearity: A measure of deviation from linearity. For a linear device, if $Y_1 = f(x_1)$ and $Y_2 = f(x_2)$, then $Y_1 + Y_2 = f(x_1 + x_2)$ of the sensor, which is usually described in terms of the percentage deviation in FSO at a given value of the measurand. The method used in this work to quantify linearity is the deviation from best-fit straight line, which is most commonly used by researchers and expresses the deviation of the transducer output from a best-fit straight line. It is the method already available in Microsoft Office tools.

Hysteresis: Difference in the output of the sensor for a given input value X when X is reached from two opposite directions. i.e., in the case of strain gauges in general; when strain is increasing approaching point X is different than when it is decreasing and reaching the same point X . The Hysteresis in mechanical sensors is usually caused by a lag in the action of the sensing element.

Repeatability: An important property of sensors is the repeatability which means to have the same readings for the same excitation. In General, it is the difference in the output readings at a given value of the measurand X . X is consecutively reached from X^- (or X^+).

Noise: Random fluctuation in the value of the measurand that causes random fluctuation in the output. Noise at the sensor output is due to either internal noise sources, such as resistors at finite temperatures, or externally generated mechanical and electromagnetic fluctuations. AC power line interference (50 or 60 Hz) and other external interferences are also considered as noise, even though they are not random. The external noise will become more important as the transducer size is made progressively smaller. The external noise in sensors is primarily associated with the random fluctuation of the particular measurand which

usually has several different components. Most of these components can be identified as the equivalent of one of the following internal noise mechanisms. Internal noises, which are usually electrical in nature, are of four types: shot noise, Johnson (or thermal) noise, recombination-generation (r-g) noise and 1/f (or flicker) noise. Shot noise is caused by charge carriers crossing a barrier at random. It is present in Schottky barrier diodes, p-n junctions (including n + - p + tunnel diodes) and in thermionic emission. Johnson noise is caused by random motion of charge carriers which produce a fluctuating emf at the output terminals. It is present in all resistive components. Recombination-generation (r-g) noise in semiconductors is caused by trapping and de-trapping of charge carriers causing a random fluctuation in the number of carriers and resistance. Among commonly encountered r-g noise is burst noise. 1/f noise has a spectral density that varies inversely with frequency, being very large at very low frequencies. The origin of 1/f noise is not yet well understood and recent experiments suggesting fluctuations in the number of charge carriers (essentially an r-g type of process) or fluctuation in the carrier mobility are still inconclusive. Dominant in TF piezo-resistive sensor is the thermal noise, which is proportional to resistance value. In second place comes the 1/f noise. A possible way to avoid these noise sources is by exciting the TF sensor with a pulse and filtering low frequencies.

A practical sensor is not ideal and it has many factors that deviates its performance from the ideal response. Here are the most important:

- The sensitivity may in practice differ from the value specified. This is called a sensitivity error, but the sensor is still linear.
- Since the range of the output signal is always limited, the output signal will eventually reach a minimum or maximum when the measured property exceeds the limits. The full scale range defines the maximum and minimum values of the measured property.

- If the output signal is not zero when the measured property is zero, the sensor has an offset or bias. This is defined as the output of the sensor at zero input.
- If the deviation is caused by the rapid change of the measured property over time, there is a dynamic error. Often, this behaviour is described with a bode plot showing sensitivity error and phase shift as function of the frequency of a periodic input signal.
- If the output signal slowly changes independent of the measured property, this is defined as drift.
- Long-term drift usually indicates a slow degradation of sensor properties over a long period of time.
- The sensor may, to some extent be sensitive to properties other than the property being measured. For example, most sensors are influenced by the temperature of their environment.
- All these deviations can be classified as systematic errors or random errors. Systematic errors can sometimes be compensated for by means of some kind of calibration strategy. Noise is a random error that can be reduced by signal processing, such as filtering, usually at the expense of the dynamic behaviour of the sensor.

4.3 Choice of Suitable Interface Circuit

In designing sensor interface, the aim of the designer is to get as much as possible of useful signal with respect to the surrounding noise(S/N ratio) without losing linearity and without altering the fundamental parameters like repeatability and temperature stability. By just using an amplifier may end up in amplifying noise or introducing instability or drift. Best result is obtained by having the sensor element to have intrinsically a high sensitivity to the measured parameter, which means high Gage Factor for strain gauge. Another possibility is to have better pre-amplification interface circuitry.

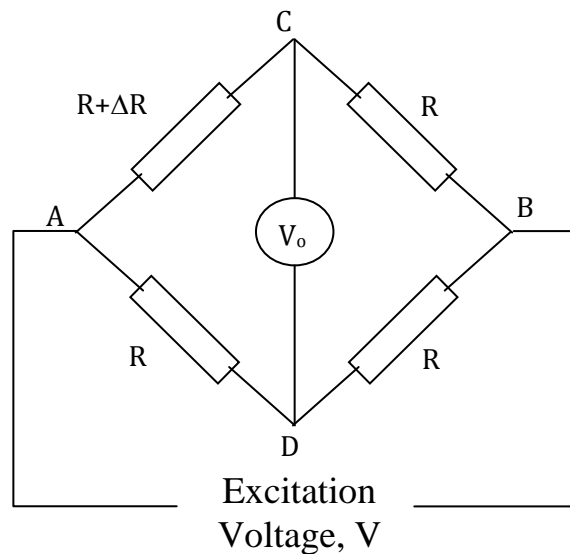


Figure 4.2 Wheatstone bridge Circuit

An interface circuit which would provide better sensitivity to strain will be proposed. A comparison to the typical circuit used in strain gauges; the Wheatstone bridge will be made.

An interface circuit to drive an array of sensors will be also mathematically derived and simulated. This circuit allows the addition of the response of several TF sensors in an array.

4.3.1 The Quarter Wheatstone Bridge

As mentioned in CHAPTER 3, equations 3.7, 3.8 and 3.9, in the quarter bridge circuit shown in **Figure 4.2**, strain-sensing TF gauge resistor appears in only one bridge position out of four. $R+\Delta R$ are the change in TFS resistance due to stress-strain relationship.

When the bridge is balanced (i.e. $\Delta R=0$), and any offset is eliminated the voltage difference $V_o=V_{AB}=0$. By applying stress on the TF sensor, its

resistance will change and cause V_{AB} to change. From equation. 3.7, the output voltage change or unbalance across the bridge V_o is:

$$V_o = \frac{V}{4} \times \frac{\Delta R}{R} \quad 4.1$$

Noting that previously we related change in resistance to axial strain, $\Delta R/R=GF\epsilon$, hence:

$$\epsilon = \frac{4V_o}{V} \times \frac{1}{GF} \quad 4.2$$

This equation relates mechanical strain measurement to the bridge unbalance voltage (V_o). Excitation voltage (V) and Gauge Factor (GF) are considered constants.

4.3.2 Operational Amplifier as Current Source

The simple inverting operational amplifier in **Figure 4.3**, can be used to increase output voltage variation with strain. The TF (R_{TF}) sensor is placed as a feedback resistor of the operational amplifier.

Due to the virtual ground at op-amp input, the voltage at the inverting input is forced to be equal to the voltage at the non-inverting input and a constant current will be flowing through sensor. Current value is decided by two constant values; namely V_{ref} and $R_{current}$,

$$I = \frac{V_{ref}}{R_{current}} \quad 4.3$$

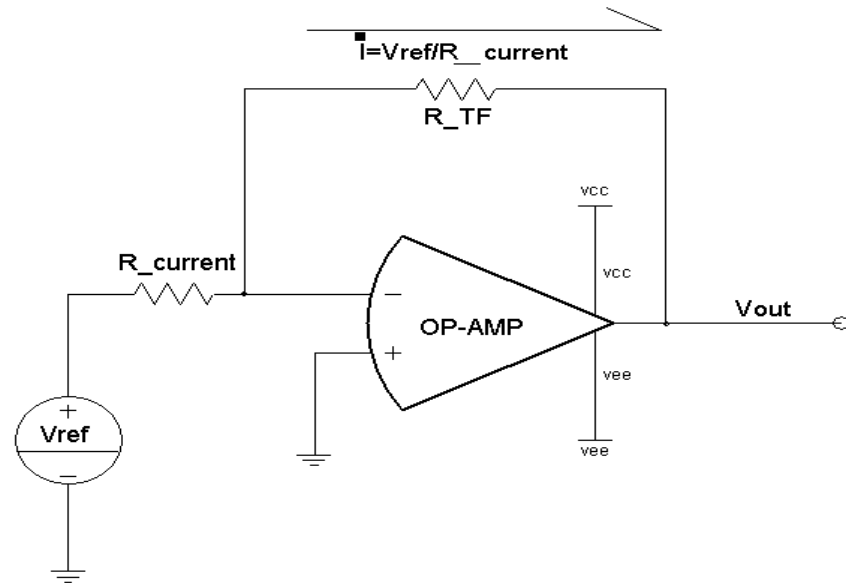


Figure 4.3 Op amp as current source

Only a negligible part of the current will go into the op amp input due to its high input impedance. The constant current is forced to go through the Thick Film piezo-resistor. The change in R_{TF} will be a change in the voltage across it and consequently the op amp output voltage V_o will change following this equation:

$$\Delta V_o = I \times \Delta R_{TF} \quad 4.4$$

Equation 4.5 results from dividing both sides of 4.4 by R_{TF} :

$$\frac{\Delta V_o}{I \times R_{TF}} = \frac{\Delta R_{TF}}{R_{TF}} \quad 4.5$$

To be able to compare equation 4.5 to equation 4.1, $(I \times R_{TF})$ is replaced by the excitation voltage V , i.e. The maximum output voltage swing;

$$\frac{V_o}{V} = \frac{\Delta R}{R} \quad 4.6$$

Higher is the current more is the voltage variation with strain. However current must be as high as allowed by the amplifier dynamic range thus $I \cdot R_{TF}$ is almost the excitation voltage V . Output voltage swing is a function of the op amp technology. Certain op-amps using Complementary Metal Oxide Semiconductor (CMOS) transistors may have rail-to-rail output swing capability (Appendix-D).

From equation 3.8;

$$\frac{\Delta R}{R} = GF \epsilon \quad 4.7$$

$$\frac{V_o}{V} = GF \epsilon \quad 4.8$$

$$V_o = V \cdot GF \cdot \epsilon \quad 4.9$$

This equation relates mechanical strain measurement to the op-amp output voltage (V_o). Excitation voltage (V) and Gauge Factor (GF) are considered constants.

4.3.2.1 Wheatstone Bridge Versus Op-Amp Outputs

Equation 4.2 is written simplified as in the following equation 4.10;

$$V_o = V \cdot GF \cdot \epsilon / 4 \quad 4.10$$

Comparing 4.9 with 4.10, it is obvious that the piezo-resistive change with strain of one single sensor resistor, the output voltage swing in the op-amp configuration is four times bigger than the common quarter Wheatstone bridge setup at the same excitation voltage.

4.3.2.1.1 Verification by Simulation

To verify the derived mathematical conclusion before deploying the op-amp solution in real measurements, the two solutions were simulated with Saber simulator to which an introduction will be given. The convention used in the circuitry is by having TF sensor resistances in compression denoted by R_c while those in tension are denoted by R_t . Saber simulator is a system level multi domain simulator which has a graphical user interface to enable user to draw the system to simulate. One important reason for adopting this simulator is the availability of the models of the widely used electronic components like integrated circuits and transistors. In the specific case, the amplifiers models used in the experimental work through this thesis were available in Saber.

4.3.2.1.2 Saber Simulator

Saber simulator is a single kernel, mixed-signal simulator. A built-in event algorithm, full mixed-signal hardware description language (HDL) and continuous-time, differential-equation algorithms simultaneously accommodates event processing, Boolean logic, and continuous mathematical expressions and relationships.

Saber simulator can simulate analogue, event driven analogue (such as Z-domain), digital, and mixed-analogue/digital devices in the same simulation, while allowing interaction between analogue and digital domains.

For simulating designs that include models written in Verilog or VHDL, Saber simulator can be linked with popular digital simulators. Another advantage is that Saber simulator is designed to perform simulations

based on very few preconceptions about the target system; consequently, the simulator can analyze designs containing multiple technology disciplines, using the analysis units native to these technologies:

- Electronic
- Power electronics
- Electro-mechanical
- Mechanical
- Electro-optical
- Optical
- Hydraulic
- Control systems
- Sampled-data systems
- Thermal

Given this capability, models can be created directly using the actual equations and relationships that govern the behaviour of devices not just an equivalent electrical model. At the beginning of this work the intention was to use Saber also for mechanical simulation and to deploy eventually digital circuits. The simulator offers the possibility to mix technologies and all simulation results will be output in the corresponding units.

4.3.2.1.3 Wheatstone Bridge Simulation

The signal conditioning circuit usually used to interface strain gauges in general is the Wheatstone bridge shown in **Figure 3.15**. The unbalance voltage that will develop due to change of resistances in the bridge is usually amplified to be suitable for an A/D converter or any other data acquisition system.

The full Wheatstone bridge of **Figure 4.4** shows four mechanically excited TF resistors. Resistors in the bridge are marked R_t for resistors in tension and R_c for resistors in compression. Those resistors must be positioned on

the structure under test in a way to be excited mechanically in an opposite sense to enhance the signal output product.

To verify the quarter bridge equation 4.1 , only resistor R_{t1} will be varied. The TF typical initial value resistance will be assumed to be 7500Ω similar to the manufactured samples typical value. . A GF of 10 for a maximum strain of 1000 will produce maximum amount of piezo-resistance change of 1%, i.e. 75Ω . In reality, almost 1.5% could be observed with all the developed samples thus the R_{t1} will be swept from 0 to 100Ω .

The instrumentation amplifier has a fixed gain of 10. During simulation cycles, instrumentation amplifier (LT1101) gives an immediate reading of the voltage difference across the bridge and it is actually of the type that was used in some of the experiments. Datasheet of LT1101 is available on the web.

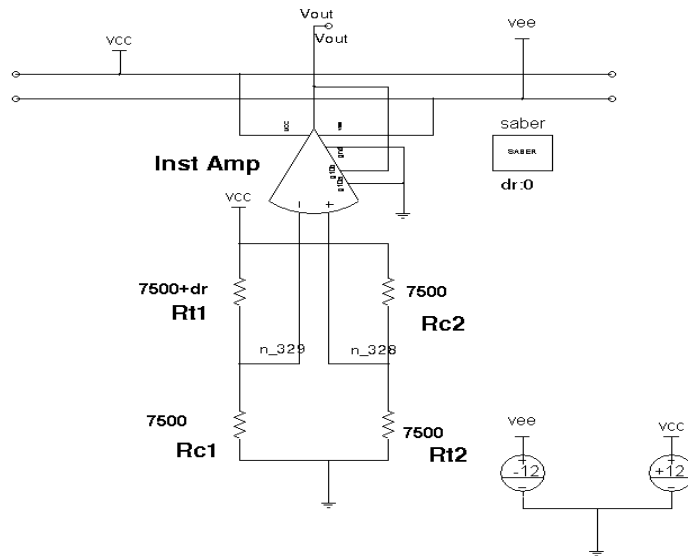


Figure 4.4 Wheatstone bridge voltage amplified by an inst. Amp

Transient analysis simulation of the circuit was setup for $100\mu s$. R_{t1} is made to change by steps of 10Ω and for each value of R_{t1} ; the simulator resolves the circuit equations to find the output voltage of the instrumentation amplifier.

Figure 4.5 shows the output voltage on the waveform viewer of Saber named Cosmoscope. In the plot, there is one waveform for each value of R_{t1} . The maximum obtainable voltage, ΔY can be seen from the measurement on the waveform to be $= 0.397/10= 0.0397V$. The division by 10 is for the LT1101 amplifier fixed gain. After dividing by 10, the measured voltage is across the bridge.

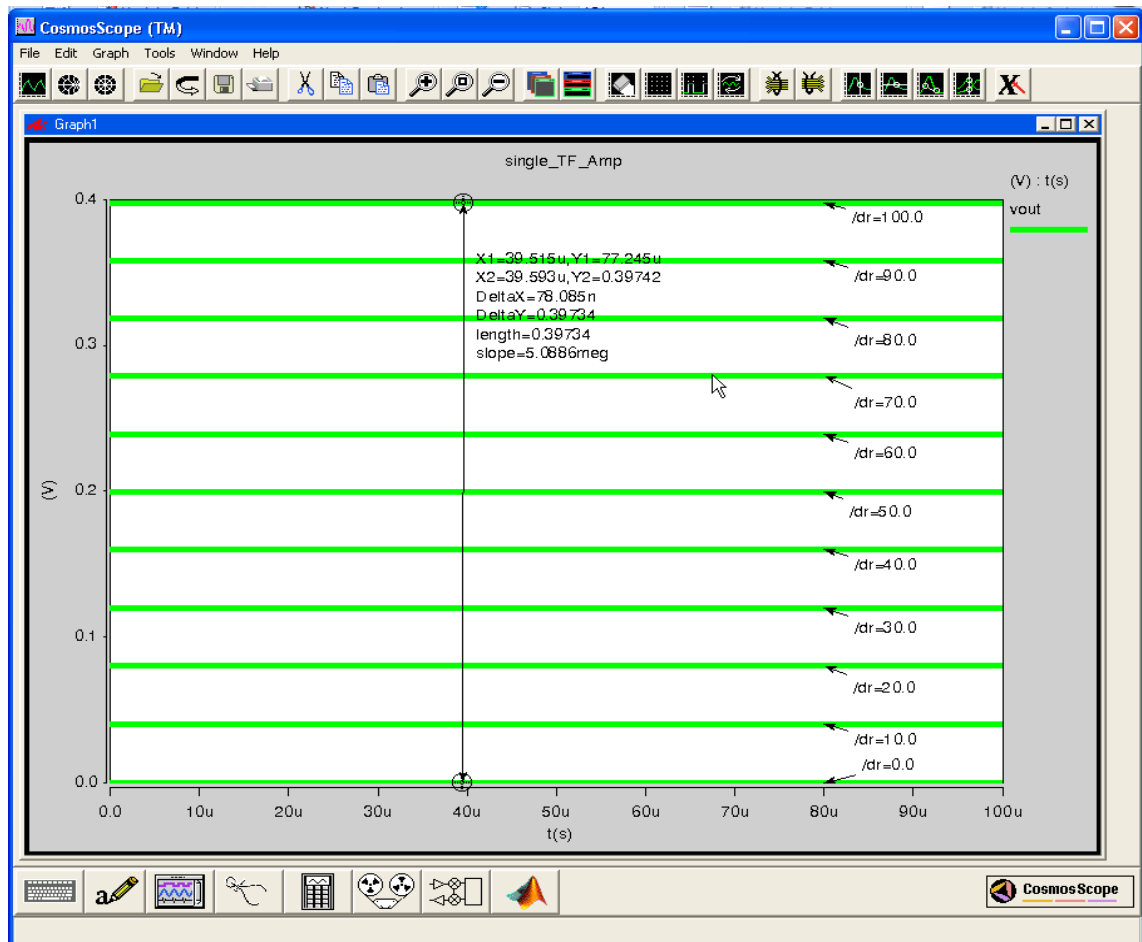


Figure 4.5 V_{out} vs. TF R_{t1} change, ΔY should be divided by 10

4.3.2.2 Op-Amp Simulation

The same single TF resistor is made to change in a rail-to-rail operational amplifier configuration as shown in **Figure 4.6**. The amplifier is of type LMC6482 (Data sheet is available on the web). Maximum allowed input

current of $(11 \text{ V}/7500 \ \Omega)$ A is made to flow through the TF feedback resistor. The output is still in the allowed linear amplifier dynamic range.

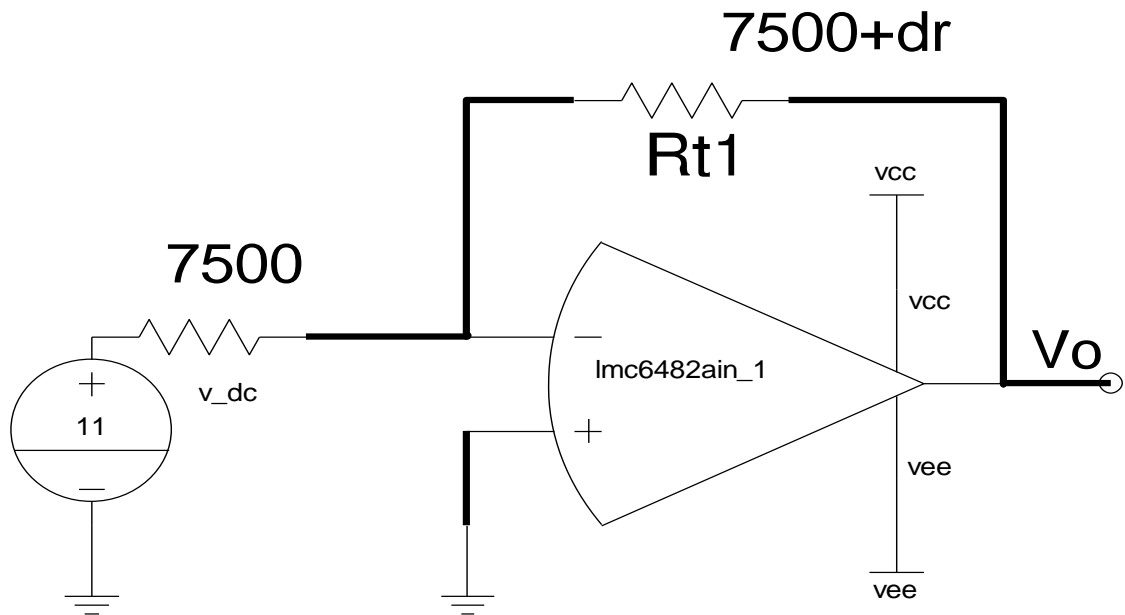


Figure 4.6 TF sensor resistor in op-amp LMC6482 configuration

Simulation for $100 \ \mu\text{s}$ result with R_{t1} changing in steps of $10 \ \Omega$ is shown in **Figure 4.7**. The measured voltage change $\Delta Y = 0.14666 \text{ V}$.

The ratio of the op-amp configuration to the quarter bridge configuration is thus

$$\frac{V_o \text{ (op - amp)}}{V_o \text{ (bridge)}} = \frac{0.14666}{0.039} = 3.69 \quad 4.11$$

The output in the op-amp case is negative and increasing negatively with resistance increase. This is due to the inverting op-amp configuration and the positive supply applied at the input.

4.3.2.3 Full Bridge with Amplifiers Simulation

In **Figure 4.7**, the small output voltage change, is offset by 11 volts from zero while the waveform in **Figure 4.5** swings to almost 0.4 V from zero.

One of the advantages of Wheatstone bridge is its elimination of the offset by having two branches or two voltage dividers that when subtracted, the difference is almost at zero level. This differential mode of functionality eliminates all non-desired common signals like noise and DC voltage.

In addition, by using similar elements on opposite sides of the bridge temperature drift of the sensors can be significantly reduced.

To collect the advantages of both solutions, The circuit in **Figure 4.8** was simulated with Saber simulator to examine the output voltage maximum swing with 1000 μ strain applied on all four bridge resistors R_{t1} , R_{t2} , R_{c1} and R_{c2} . R_{t1} and R_{t2} are supposed to be under tension hence increasing and R_{c1} and R_{c2} are supposed to be contemporarily under compression hence decreasing. ΔR changes in steps of 10Ω .

A maximum voltage change of 5.3 Volts can be observed at instrumentation Amplifier output as shown in waveform of **Figure 4.9**. The differential amplifier removes the DC offset voltages at op-amps outputs thus its output swing starts from zero to 5.3 V. The noise and temperature drift of the sensors will be also cancelled by the differential final stage. This way, besides signal improvement by using op-amps, the advantage of having a differential output is maintained.

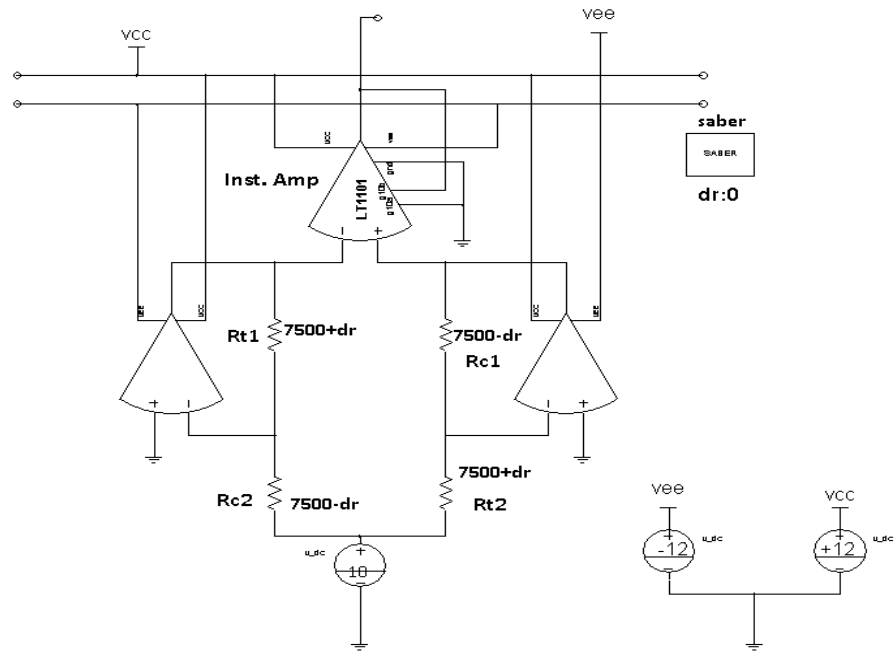


Figure 4.8 Op-amp boosted Wheatstone bridge

The transfer function of the circuit in **Figure 4.8** after letting $(\Delta R/R)^2$ to zero is :

$$V_o = 4V_r G \times \frac{\Delta R}{R} \quad 4.12$$

Where V_r : input reference voltage (10 V in the Figure)

G= Instrumentation amplifier gain (set to 10)

R= Nominal TF resistance value and ΔR is the change in resistance due to strain

To notice here that the final output is a multiplication of a DC reference voltage and instrumentation amplifier gain.

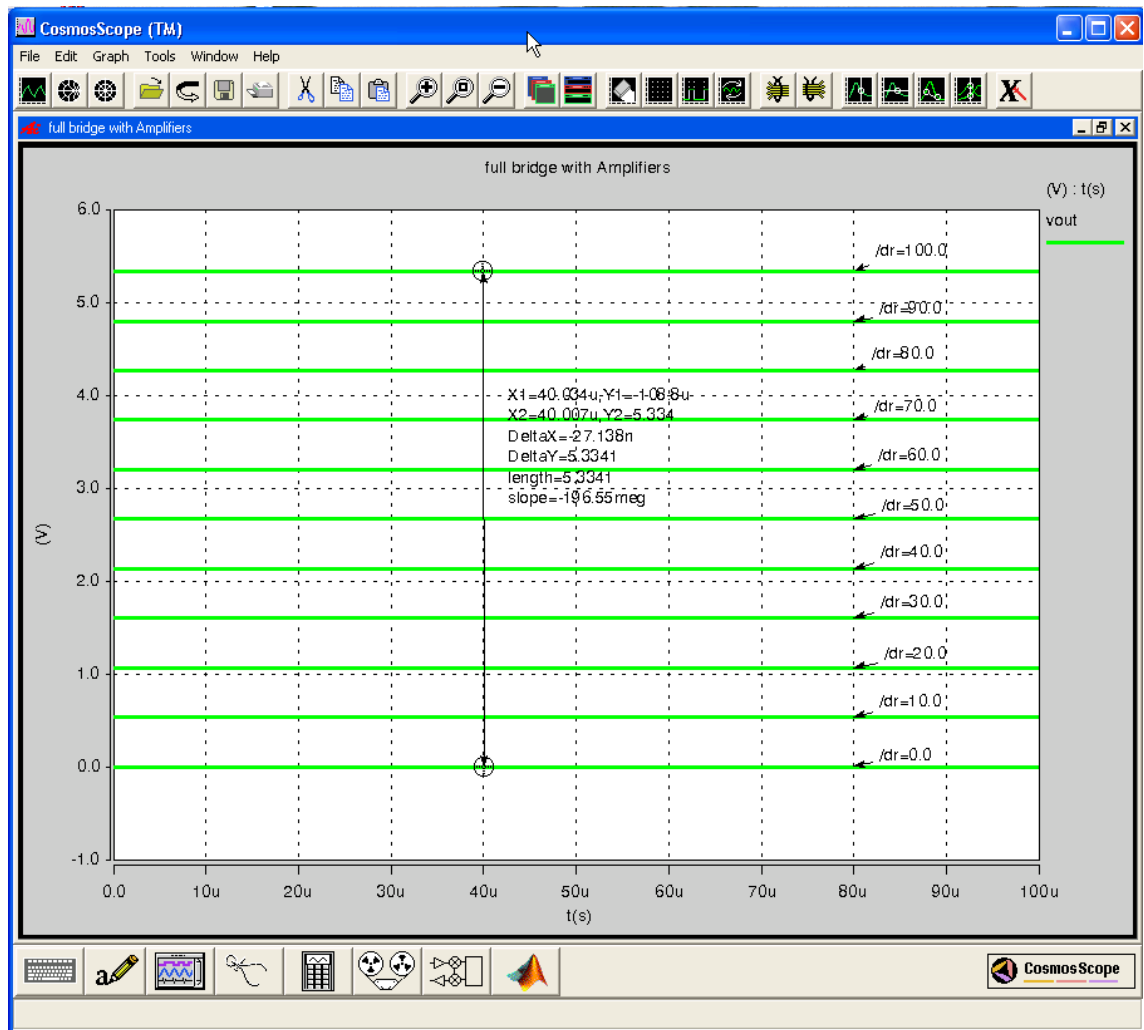


Figure 4.9 Op-amp driven Wheatstone bridge max output voltage swing

4.3.3 Sensor Array Interface Circuit

The designed sensor is suitable for an array of sensor application. Example of such array is shown in **Figure 4.10**.



Figure 4.10 Two arrays of four TF sensors mounted on PCB

These sensors can be connected in parallel branches as in **Figure 4.11** to enhance the output signal per strain. One single current source formed from an op-amp and a bipolar transistor sinks current from the four sensor branches. Having a bipolar driving voltage allows to make voltage variation around zero volt at the input of the four op-amp buffers. The buffers output is added together and shifted by the final op-amp.

The transfer function of this configuration is:

$$V_{out} = (4 \times i \times \Delta R) \times G \quad 4.13$$

Where:

G= gain of the summing amplifier

i= current in each branch

$$i = \frac{V_r - V_{ee}}{R_{28}} \times \frac{1}{4} \quad 4.14$$

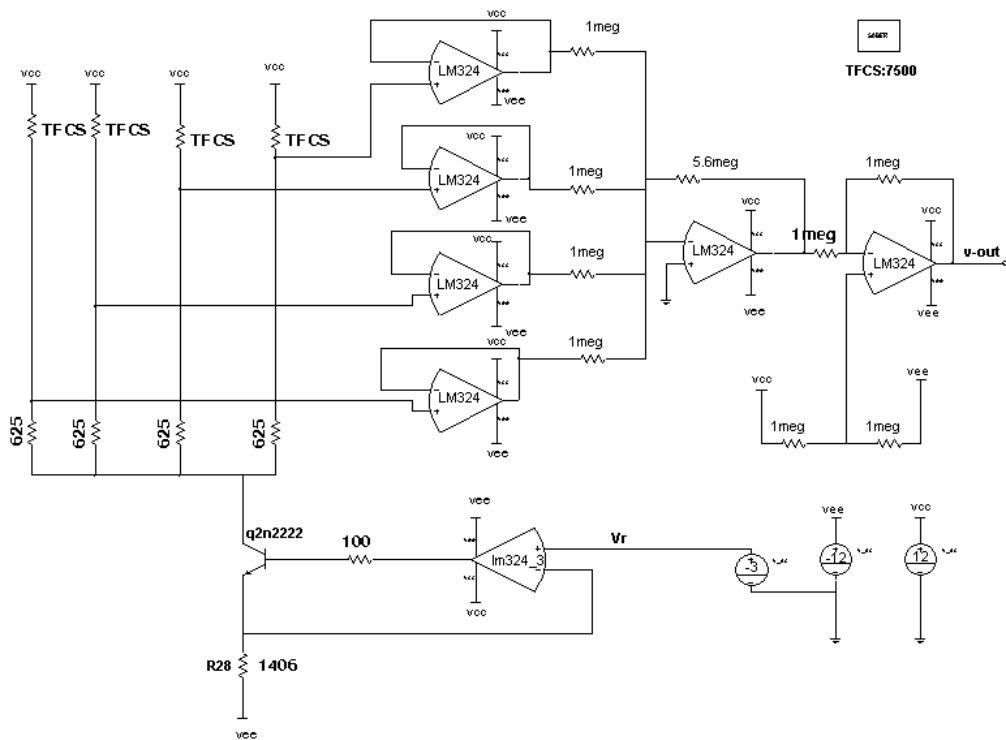


Figure 4.11 Array of four TFCS driven by one current source

In piezoresistive sensors, a constant current is made to flow through the sensor resistor. A change in the resistance will cause a voltage change. This voltage is amplified and level shifted before reaching the final output. Sensitivity of the sensing element is $I \times \Delta R$. When the sheet resistivity is high, like in the case of our sample sensor, the amount of current which can be made to flow through the sensor is limited by the supply voltage, i.e. it is allowed to let only 1.6 mA to flow through the 7500 TF sensor when the supply voltage is 12 V. i.e. In numbers, $1.6\text{mA} \times 7500\Omega = 12\text{V}$.

The circuit in **Figure 4.11** gives a way around this limitation by making the current to flow in four branches and then sum their effect, which will result in signal to strain sensitivity mitigation.

Another advantage of this circuit is to collect the distributed load on various geometrical form areas in direct load application on sensors. A practical implementation for SHM will be shown in Chapter 6.

4.3.4 Sensor Array Simulation

From equation 4.14, the current in each branch is about 1.6mA. Summing amplifier gain, G , is $5.6/1=5.6$ and in case of $1000 \mu\text{strain}$ applied to the four TF sensors, causing the piezo resistors to change by 100Ω . From equation 4.13, $V_{\text{out}}= 3.584 \text{ V}$. The stress applied on all four sensors could be either compressive or tensile stress. Transient analysis simulation results for $100 \mu\text{s}$ are shown **Figure 4.12** .

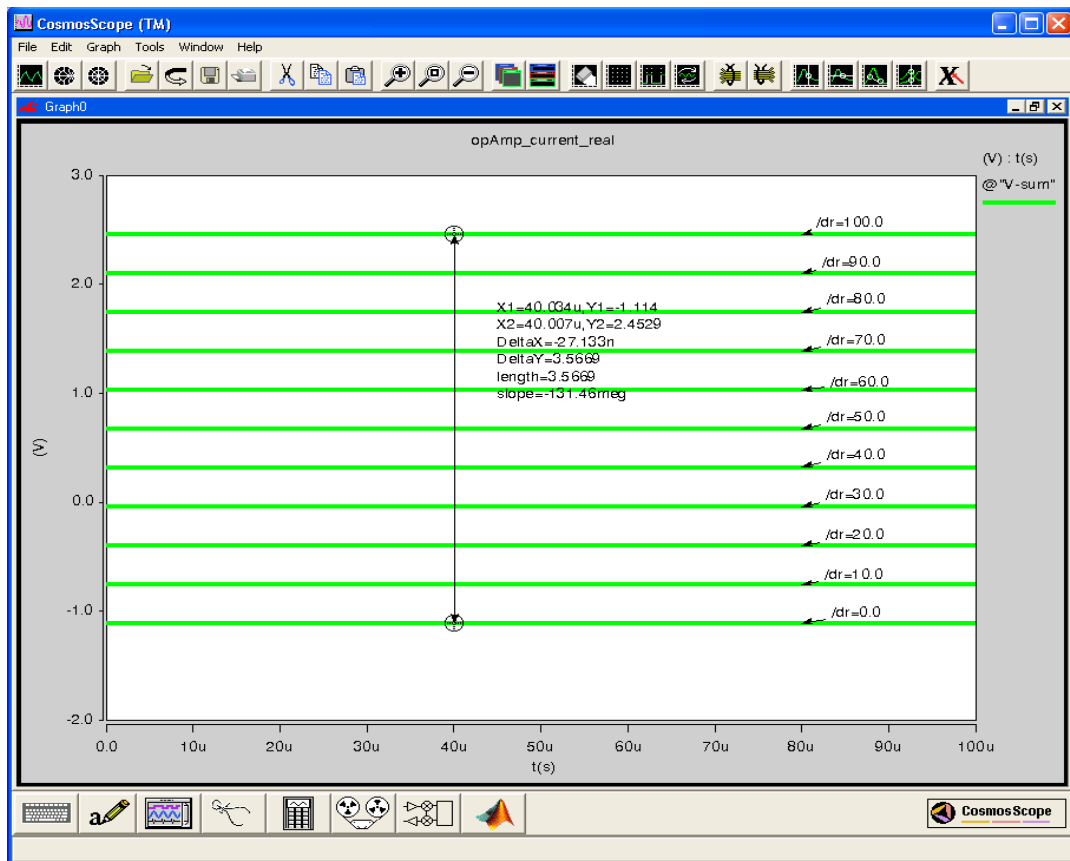


Figure 4.12 TF sensor array output response , $\Delta Y=3.56 \text{ V}$

4.4 Application of TF Sensor on Building Materials

In the circuit of **Figure 4.8** , even if sensors are under same mechanical excitation they could be placed appropriately in the right place in the circuit to sum the effect at the output. In other words, it is possible to use the two resistor sensors in compression only while the sensors in tension

eventually increase the gain to 100. The analogue switch control is from LABVIEW through DAQPod1200 **Gain_control** digital output pin.

To verify applicability of thick film sensors on different building materials and to evaluate their response as a function of the different materials, a test was carried on:

- 1- sample brick of dimensions 12.4x16.7x34.7 mm **Figure 4.14**



Figure 4.14 Sample brick 12.4x16.7x34.7 mm

- 2- Sample concrete dimensions 23.3x22.3x50 mm **Figure 4.15**

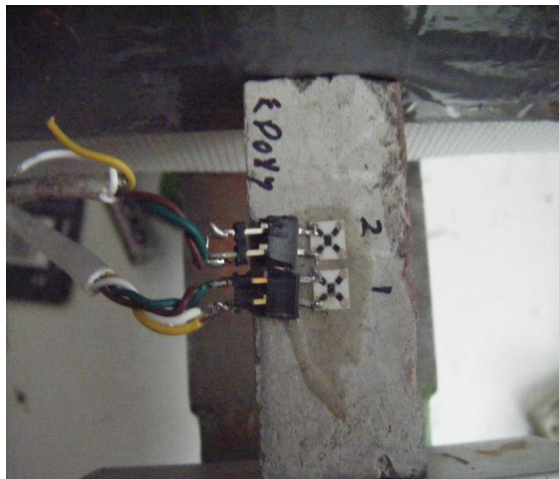


Figure 4.15 Sample concrete block 23.3x22.3x50 mm

The aim of the test was to verify:

- 1- The applicability and functionality of TF sensors on concrete and bricks in general.
- 2- To test the circuit and examine the possibility of adding the effect of two adjacent sensors glued on the same side of a structure and that the linearity is maintained i.e. if $Y_1 = f(x_1)$ and $Y_2 = f(x_2)$, then $Y_1 + Y_2 = f(x_1 + x_2)$.
- 3- To verify output entity and the proportionality of response of TF sensors as a function of the material modulus of elasticity when applied to different materials like in the specific case, red brick and concrete.

The two TF sensors were glued to the two samples with a two components epoxy adhesive and were put in the locations indicated by R_{c1} and R_{c2} on the schematic. The other resistors; R_{t1} and R_{t2} were replaced with a fixed resistor as shown in **Figure 4.13**.

Following is the transfer function equation of the circuit;

$$V_{out} = [V_r (\frac{R_{c1}}{R_{t1}} - \frac{R_{t2}}{R_{c2}})] \times G \quad 4.15$$

Where, $V_r=10$ V, $R_{t1}=R_{t2}=7500$ Ω .

The mV reading of V_{out} is directly proportional to the compressive strain.

4.4.1 Experimental Result

4.4.1.1 Overview of the Experiment

The brick and concrete samples were put one at a time under pressure against an electronic linear scale in a bench vice as shown in **Figure 4.16**. The load was increased a step by step up to 100 kg Load. Here are the experiment steps:

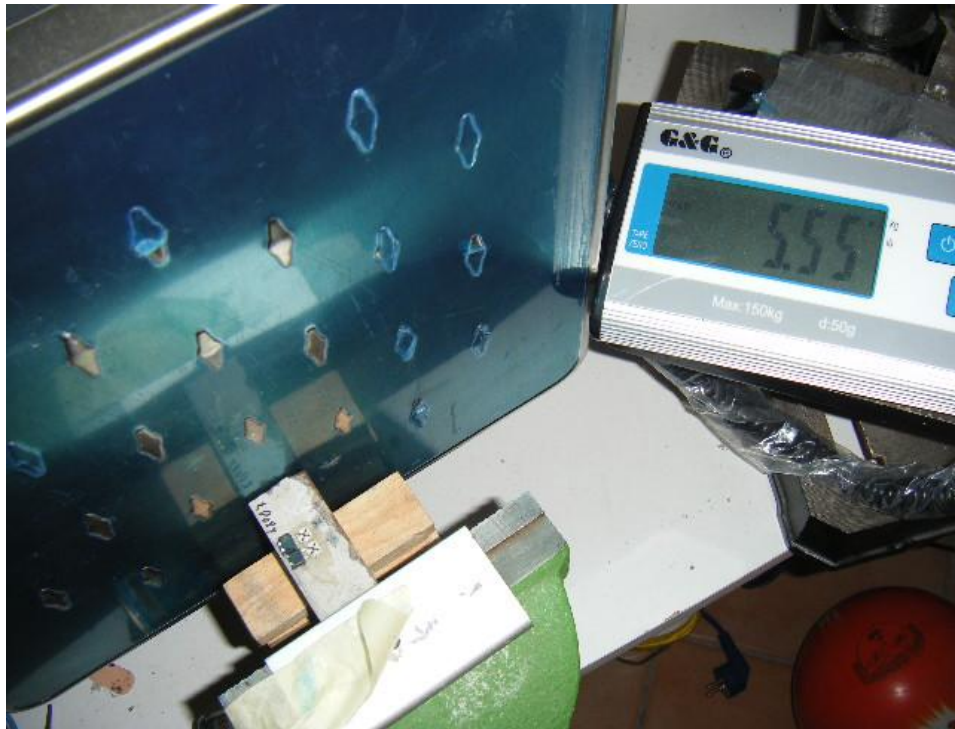


Figure 4.16 Concrete block sample stressed on a linear scale

- 1- The response of one single sensor at a time was considered first on red brick sample,
- 2- The response of both sensors in compression at the same time on red brick was then registered,
- 3- Mathematical sum of the two sensors compressed singularly was compared to experimental result of both sensors compressed contemporarily.
- 4- The response of both sensors in compression at the same time on concrete sample was then registered,
- 5- Comparison of TF response of the two sensors on both samples was then considered based on the difference in the two materials modulus of elasticity.

Step1: **Figure 4.17** shows S_1 response with S_2 replaced by a fixed resistor of 7500Ω .

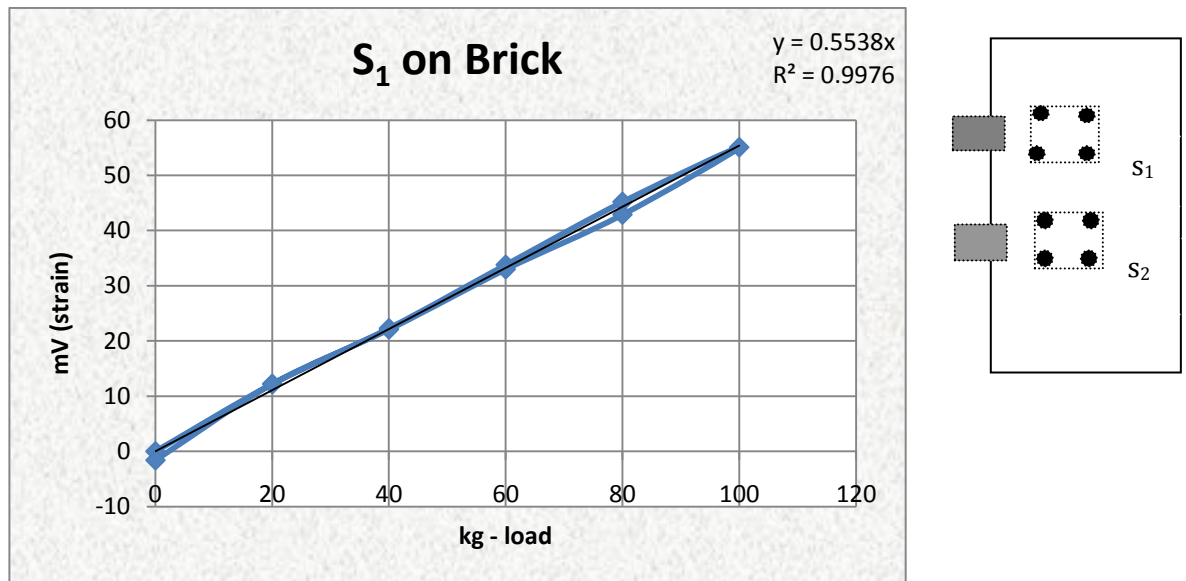


Figure 4.17 S₁ response vs. compressive force

Figure 4.18 shows S₂ response with S₁ replaced by a fixed resistor of 7500 Ω.

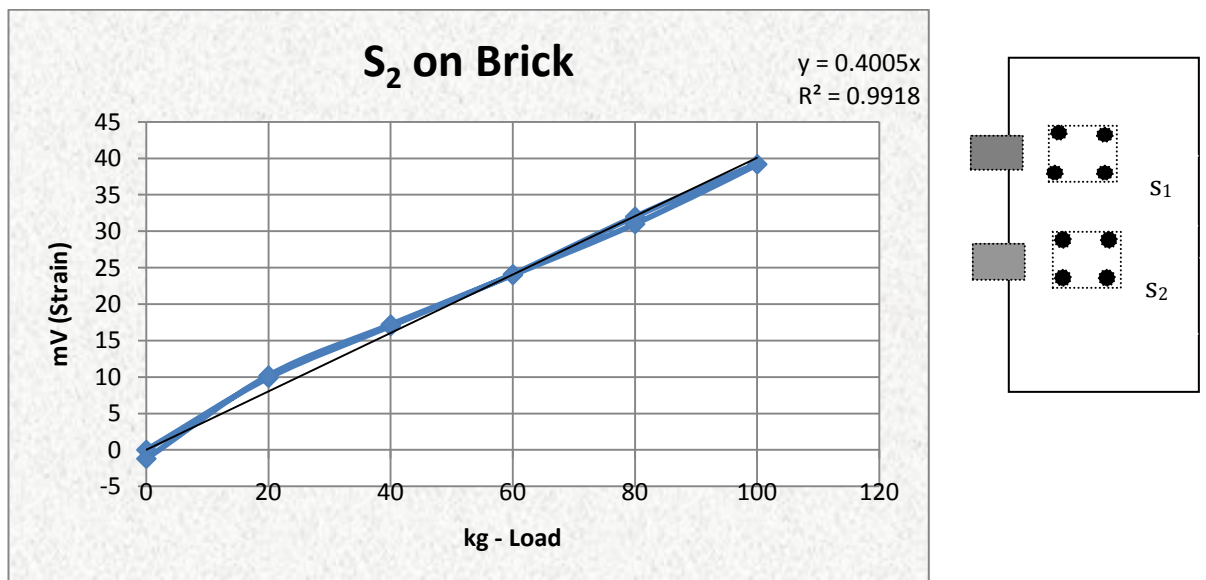


Figure 4.18 S₂ response vs. compressive force

Step2: Figure 4.19 shows the response of both S₁ and S₂ under mechanical compressive stress at the same time.

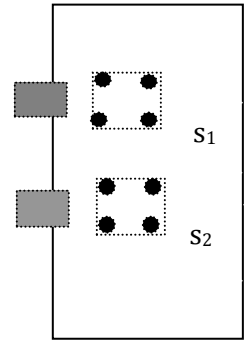
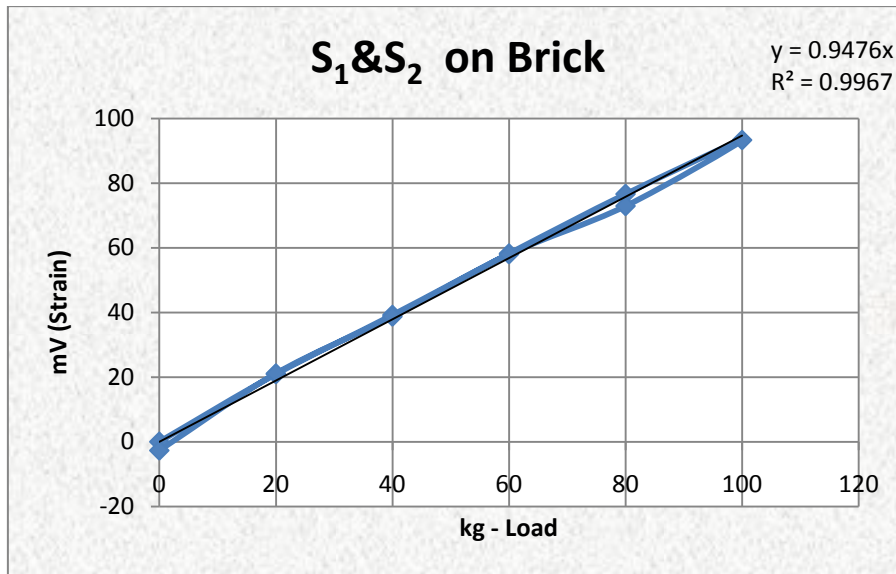


Figure 4.19 S₁ and S₂ response vs. compressive force

Step 3: From the linear equations of response of S₁ and S₂ in **Figure 4.17** and **Figure 4.18**, it is clear that the sum of the two equations will produce the equation of the experimental sum in **Figure 4.19**, i.e. $0.4005x + 0.5538x = 0.9543x$. The x in these graphs is the applied load and y is the mV output proportional to strain.

Step 4: **Figure 4.20** shows the response of other TF sensors S₃ and S₄ on concrete block.

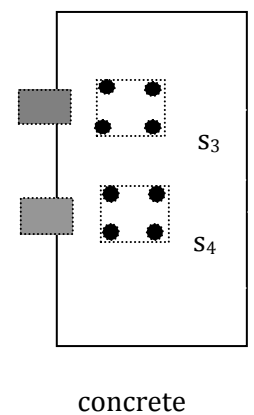
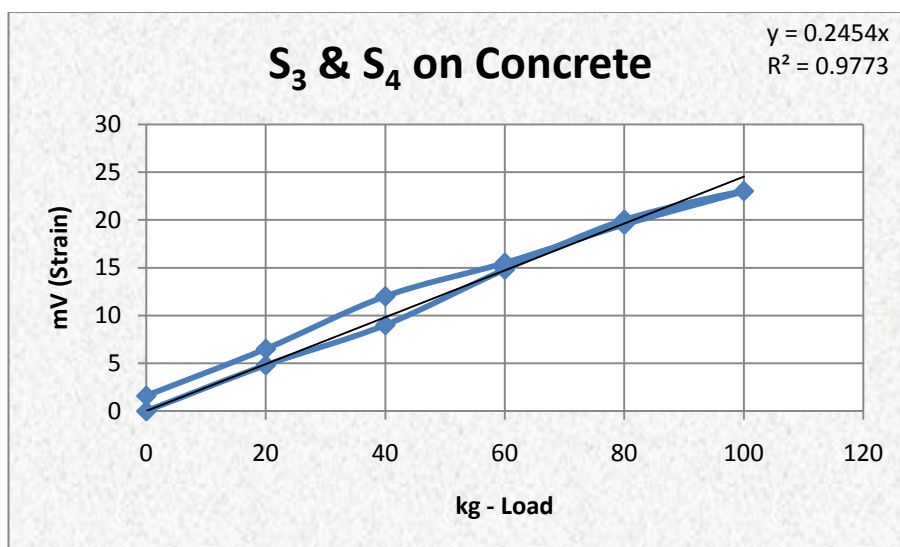


Figure 4.20 S₃+S₄ on concrete

Step 5: Figure 4.21 shows the response of TF sensors on the brick and concrete blocks put on the same graph for comparison.

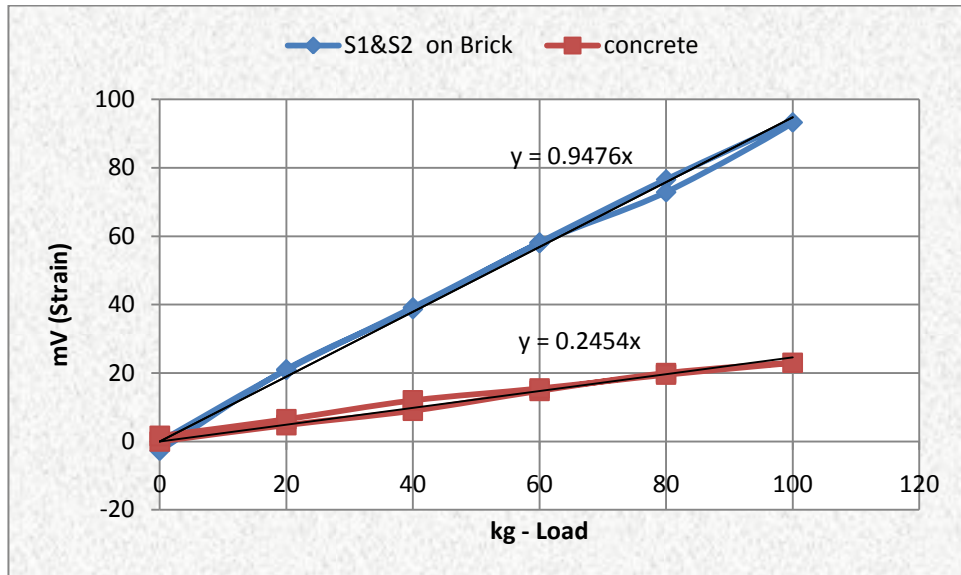


Figure 4.21 TF sensors response on red brick and concrete

4.5 Proportionality of Response

The sensor used to measure strain on material should have a response consistent with different materials under test.

Following is the proof from the measurement curves of **Figure 4.21**:

If we consider Hook's law $E = \sigma / \epsilon$ and apply this on the two samples; red brick and concrete where subscripts c=concrete and b=brick;

$$E_c = \frac{\sigma}{\epsilon_c} \quad 4.16$$

$$E_b = \frac{\sigma}{\epsilon_b} \quad 4.17$$

By dividing 4.16 by 4.17 and considering the application of the same force change on both samples:

$$\frac{E_c}{E_b} = \frac{\frac{\Delta F}{A_c \times \epsilon_c}}{\frac{\Delta F}{A_b \times \epsilon_b}} = \frac{A_b \times \epsilon_b}{A_c \times \epsilon_c} \quad 4.18$$

Since the output voltage is linearly proportional to strain, and the applied ΔF for the two samples is the same,

$$\frac{E_c}{E_b} = \frac{A_b \times \Delta V_b}{A_c \times \Delta V_c} \quad 4.19$$

Considering the coefficients in the generated equations from the curves in **Figure 4.21** for the same 100Kg force change, and Substituting the values for the different sample areas; $A_b=205\text{mm}^2$, $A_c=545\text{mm}^2$,

$$\frac{E_c}{E_b} = \frac{205 \times 0.9476}{545 \times 0.2454} = 1.4524 \quad 4.20$$

To evaluate the left side of the above equation 4.20, values elastic moduli need to be substituted. From (Su et. Al 2002) , concrete elastic modulus depends on the ration of sand to aggregate (S/A) and it varies from 22 to 25 kN/mm² The sample under test has almost no aggregate and hence the modulus is around 22-23 kN/mm² (page 12 Figure 5 of the same reference). The experimental modulus of elasticity of red brick is around 15 kN/mm² (NICHOLS 1997) .

Hence:

$$\frac{E_c}{E_b} = \frac{22000}{15000} = 1.466 \quad 4.21$$

The reason for the small difference is due to a) the different sensors which have been chosen randomly from a production lot. Thick Film piezoresistive sensors production allows for a window of different sensor

response that might reach $\pm 20\%$ spread. The manufactured samples were screened after production to have a window of $\pm 5\%$, b) Exact modulus of elasticity of the samples, which could be different from the values considered in the calculation. However, result shows that response is consistent and proportional with material elastic modulus.

4.6 Summary:

In this chapter, the following alternative interface solutions to boost sensor response were introduced:

- 1- Operational amplifier as current source
- 2- Sensor Array interface circuit

The first alternative was compared mathematically with Wheatstone bridge and found to be four times bigger and was verified by simulation.

The second was shown mathematically to multiply the output by the number of sensor elements in the array and was also verified by simulation.

Sensors were applied on sample brick and concrete blocks and their response were tested experimentally.

The sum of the sensor response singularly measured was verified to be equal to the experimental sum of the two sensors. Thus since $Y_1 = f(x_1)$ and $Y_2 = f(x_2)$, and $Y_1 + Y_2 = f(x_1 + x_2)$, the sensor elements and electronics are linear.

The response of TF sensors on the two materials were compared as a function of the elastic modulus of each. The TF sensor response was found proportional to the modulus of elasticity.

5. Sensor Application on Building Materials

In this chapter, a comparison between different TF sensors coming from the same production lot will be experimented and a method to measure TF GF before deployment will be proposed. TF sensors will be applied on different materials and in different methodologies.

5.1 Thick Film Piezo-resistive Sensor Intrinsic Discrepancies

The TF strain gauge production procedure has intrinsic limitations that make each TF sensor different than the other in two aspects; initial resistance value and gauge factor, the first is due to the tolerances of the deposited paste thickness. Deposition of paste needs a strict control of the viscosity of the paste in time; before, during and after deposition which is almost impossible and the result is always a compromise.

Strain sensitivity of thick film resistors is related in a complex way to their compositional and micro structural properties, which, in turn, are related to the composition of the paste, the firing process, as well as interaction of the films with substrate and terminations. Examples of dependency of GF on firing temperature and dwell time are shown in (PRUDENZIATI 1994). Also, the substrate thickness, TF resistor geometry, and aspect ratio have a considerable effect on GF as shown experimentally by (KERNS et. al 1989).

During this study, other factors were noticed to effect sensor GF like for example the nature of the specimen surface and the kind of used glue. gluing on a polished smooth surface of steel is different from gluing on a rough brick surface. Surface preparation, drying and cleaning are of great importance in the case of steel and similar surface materials and less important in the case of concrete and brick.

If there is a need for precise readings, then each sensor should be tested before deployment to measure its GF and to standardize on a methodology of application, which would include defining the type of glue to use for which surface and how this surface should be treated before the application of TF sensors. One of the issues that was investigated also is the applicability of the measured GF on every deployment methodology i.e. is the measured GF valid in all three ways of deployment whether it is glued on the specimen with load parallel to gauge, embedded in the material and glued with direct load application on the substrate?

In the coming paragraphs, ways for characterizing TF sensors before deployment will be introduced.

5.2 Gauge Factors in a Thick Film Piezoresistive Sensor

The relationship 5.1 mentioned in chapter one, show that the GF is dependent on two terms; one is due to change in resistivity with strain and

$$GF = \frac{\Delta R}{R\epsilon} = \frac{\Delta \rho}{\rho\epsilon} + 1 + 2\nu \quad 5.1$$

the other is for geometrical alteration. The Poisson's ratio expresses the interrelationship between transverse and longitudinal strains. When a longitudinal strain occurs, there should be a transverse strain due to the constant volume of the stressed body. The ratio between these two strains is the Poisson's ratio, which is a property of the material. Thick film resistors actually exhibit different gauge factors, depending on the direction of the applied strain with respect to the direction of the current flow. If the two are parallel, it is referred to as the longitudinal gauge factor GF_L , whilst if they are orthogonal, the transverse gauge factor GF_T has effect (WHITE et. al. 1997). Under simplified assumptions, this difference is $GF_L - GF_T = 2(1 + \nu)$ (MORTEN 1997).

Typically, the transverse gauge factor is about 70% of the longitudinal gauge factor. This has been verified with the manufactured TF sensor in many kind of application on building material and is also mentioned by many references.

An additional and important gauge factor also exists through the thickness of the resistor. This is the so-called Z-axis gauge factor and it has been shown to be about twice the longitudinal gauge factor value for strains parallel to the thickness of the gauge (WHITE 1997). In fact, this has been noticed also during the first tests of the manufactured sensor and has been mentioned in chapter three. Further measurements will be conducted during this chapter to examine the relation between the z-axis gauge factor and the material on which the sensor is applied.

5.3 Experimental Comparison between Response of Two TF Sensors

To compare the response of the two TF sensors on the sample brick used in the previous chapter on which, two sensors were glued, the same circuit interface was used. Assuming the brick undergoes same compressive stress, the two sensors should indicate same strain. Material is assumed homogeneous and isotropic.

In the circuit of **Figure 5.1**, TFCS (R_{c1}) is in the feedback loop of one of the amplifiers. This resistor position was used to test the two sensors glued on the sample red brick one at a time. The entire circuit is the same and the strain in the brick material is assumed to be the same, so the difference in response would be only an intrinsic response difference between the two sensors. The sensors have different initial resistance value. The offset balance equates the two op-amp outputs in a way to get zero output voltage at zero loads on the brick.

From **Figure 5.2** , it is obvious that the two sensors have different gauge factor response.

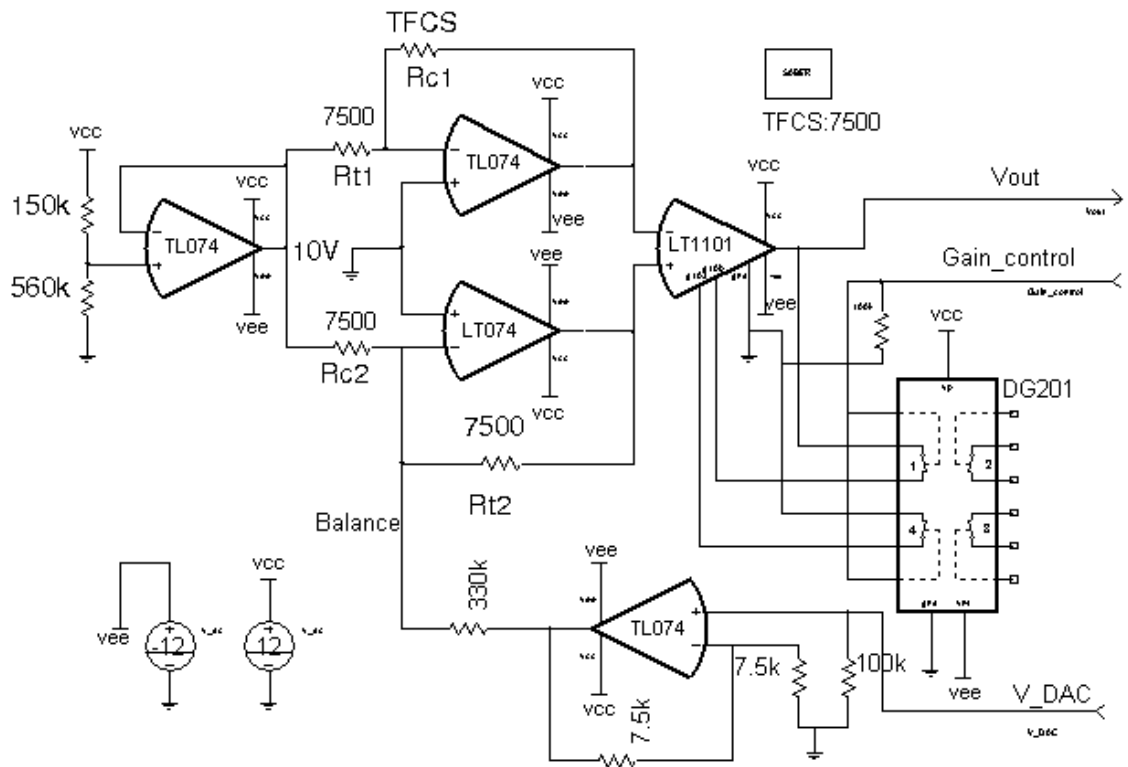


Figure 5.1 Circuit used to compare two TF sensors response

By placing the two sensors on the two op-amps in position R_{c1} and R_{t2} and making the brick subject to compressive stress, only the difference would be effective at the instrumentation amplifier output.

In fact, in **Figure 5.3** the response of this configuration shows that the trend line equation is very close to the difference between the two curves in **Figure 5.2**. i.e. $0.493x - 0.3202x = 0.1733x$.

The ripple in the curves is because readings were taken with load tolerance of ± 1 kg in both directions; increasing and decreasing. From the many tests done, it is obvious that the response is linear and the best-fit line precision is very little affected.

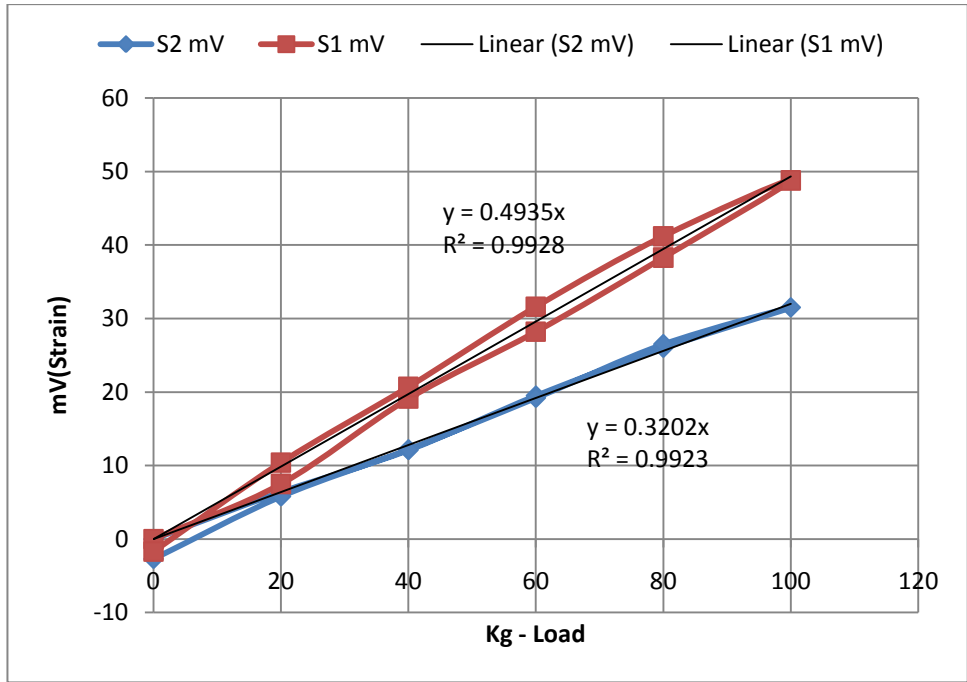


Figure 5.2 Response of two TF sensors subject to same strain

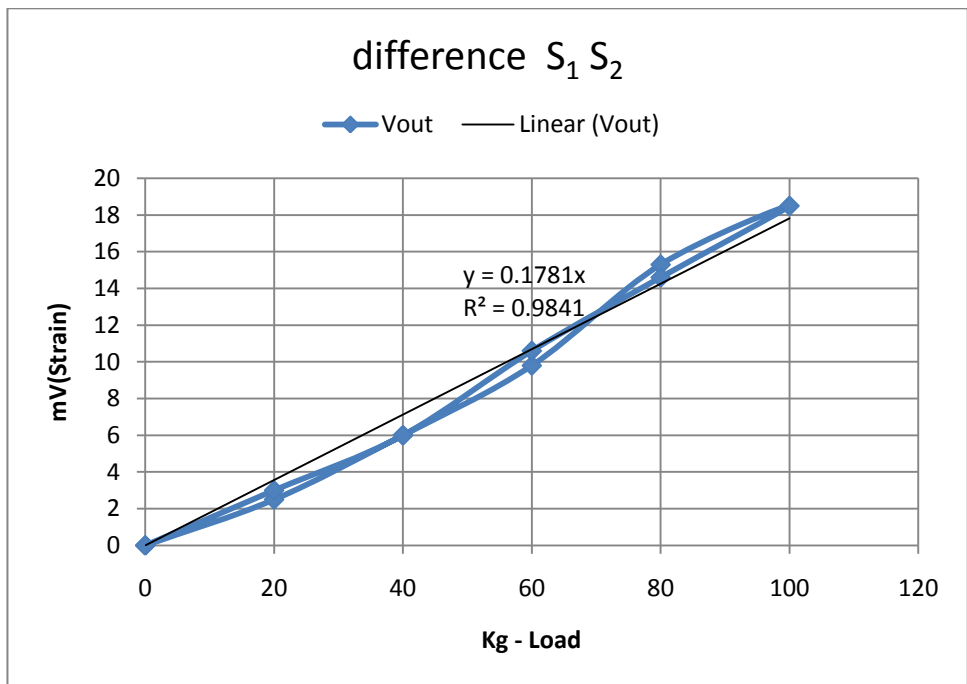


Figure 5.3 Difference response of two TF sensors subject to same stress

5.4 TF Sensor Characterization

For applications requiring high precision which are mainly lab testing experiments, a well known response of the sensor is necessary. This is required to be able to assess the conditions of the specimens. Two methodologies to measure the GF of TF piezoresistive sensors will be introduced.

Thick film piezo-resistive sensor is a strain gauge on a predefined mechanical substrate. This fact has the advantage that any sensor can be measured before deployment. (Kerns et. al 1989) used Three Point Bending Test (3PB) to measure the effect of resistor layout geometry on TF gauge factor. It is possible to use 3PB test from beam mechanics to measure the GF of thick film sensors.

The change in the TF resistance is due to the strain induced on the TF substrate. However, as mentioned in paragraph 5.2, there are different kinds of GF dependent on the way of deployment.

5.4.1 Three Point Bending Test

The three point bending flexural test provides values for the modulus of elasticity in bending G (Appendix-D), flexural stress σ , flexural strain ϵ and the flexural stress-strain response of the material. The unknown in our case is only the strain.

In principle, $\Delta R/R$ is easily measurable by a precision meter and to find the gauge factor from $GF = (\Delta R/R) / \epsilon$, strain ϵ must be found also. This can be accomplished with 3PB test.

5.4.1.1 Testing Method

Force is applied at the centre of the sensor which is supported at both ends as in **Figure 5.4**.

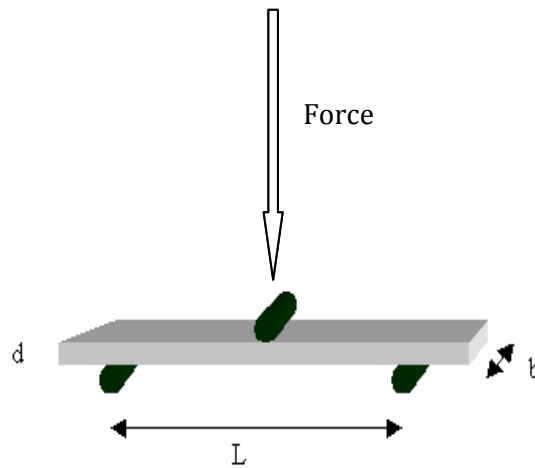


Figure 5.4 Three Point Bending test to measure sensor GF

The strain is calculated from the beam flexural formula and the change in TF resistance due to bending is registered. Hence, from the equation $GF = (\Delta R/R)/\epsilon$, the gauge factor of the sensor could be calculated.

5.4.1.2 Summary of Beam Theory

The derivation for the calculation of strain in beams taken from text book (SINGER 1980) indicates that the stresses caused by the bending moment are known as bending or flexure stresses, and the relation between these stresses and the bending moment is expressed by the flexure formula. The elastic deformations plus Hooke's law determines the manner of stress variation, after which the conditions of equilibrium then establish the relation between stress and load.

Figure 5.5 shows two adjacent sections, ab and cd , separated by the distance d_x . Because of the bending, caused by load P , sections ab and cd rotate relative to each other by the amount $d\theta$, as shown in **Figure 5.5**.

Fibre ac at the top is shortened, and fibre bd at the bottom is lengthened. Somewhere between them is located fibre ef , whose length is unchanged. Drawing the line $c'd'$ through f parallel to ab shows that fibre ac is shortened an amount cc' and is in compression, and that fibre bd is lengthened by an amount $d'd$ and is in tension.

The plane containing fibres like ef is called the neutral surface because such fibres remain unchanged in length and hence carry no stress. This neutral surface contains the centroids of all transverse sections.

Consider now the deformation of a typical fibre gh located y units from the neutral surface. Its elongation hk is the arc of a circle of radius y subtended by the angle $d\theta$ and is given by

$$\delta = hk = yd\theta \quad 5.2$$

The strain is found by dividing the deformation by the original length ef of the fibre.

$$\epsilon = \frac{\delta}{L} = \frac{y d\theta}{ef} \quad 5.3$$

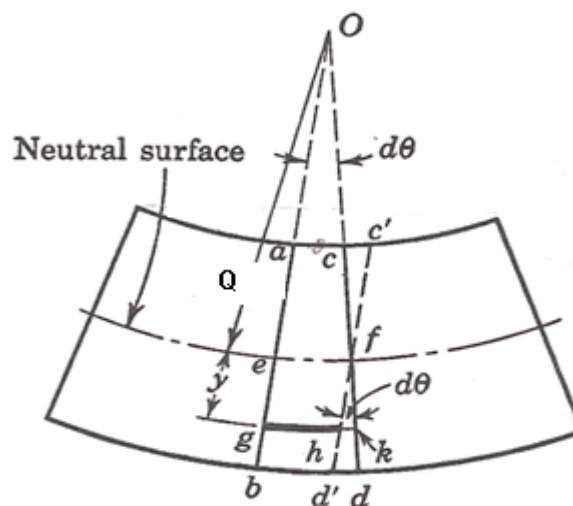


Figure 5.5 Deformation of a beam subject to force

If the radius of curvature of the neutral surface is denoted by Q , the curved length ef is equal to $\rho d\theta$; whence the strain becomes

$$\epsilon = \frac{y d\theta}{Q d\theta} = \frac{y}{Q} \quad 5.4$$

Assuming the material is homogeneous and obeys Hooke's law, the stress in fibre gh is given by

$$\sigma = E\epsilon = \frac{E}{Q}y \quad 5.5$$

The final condition of equilibrium, $\Sigma M_z=0$, requires that the bending moment be balanced by the resisting moment; that is $M=Mr$. The resisting moment about the neutral axis of typical element being $y(\sigma x dA)$, this condition requires that

$$M = \int y(\sigma x dA) \quad 5.6$$

which, by replacing σx by E_y/Q from equation 5.5;

$$M = \frac{E}{Q} \int y^2 dA \quad 5.7$$

The term $\int y^2 dA$ is defined as I , moment of inertia of the area (Appendix-D) about the reference axis, which here is the neutral axis, finally;

$$M = \frac{EI}{Q} \quad 5.8$$

This formula is used to calculate the deflection in beams.

From equation 5.5, and 5.8,

$$\frac{E}{Q} = \frac{M}{I} = \frac{\sigma}{y} \quad 5.9$$

Which leads to the formula;

$$\sigma = \frac{My}{I} \quad 5.10$$

5.4.1.3 Strain Calculation in 3 PBT

From the beam mechanics table for the case of a beam with free ends supported as shown in **Figure 5.4** and loaded in the middle with a force P ,

$$M = \frac{PL}{4} \quad 5.11$$

And maximum deflection δ is;

$$\delta = \frac{PL^3}{48EI} \quad 5.12$$

By simplification from equations 5.4 and 5.8 substituting in 5.12 we obtain the relationship between maximum deflection δ and maximum strain ϵ ;

$$\epsilon = \frac{6 \times \delta \times h}{L^2} \quad 5.13$$

If the load is uniformly distributed over the sensor then another formula for M and ϵ should be used.

Figure 5.6 shows the built setup for 3PB test.

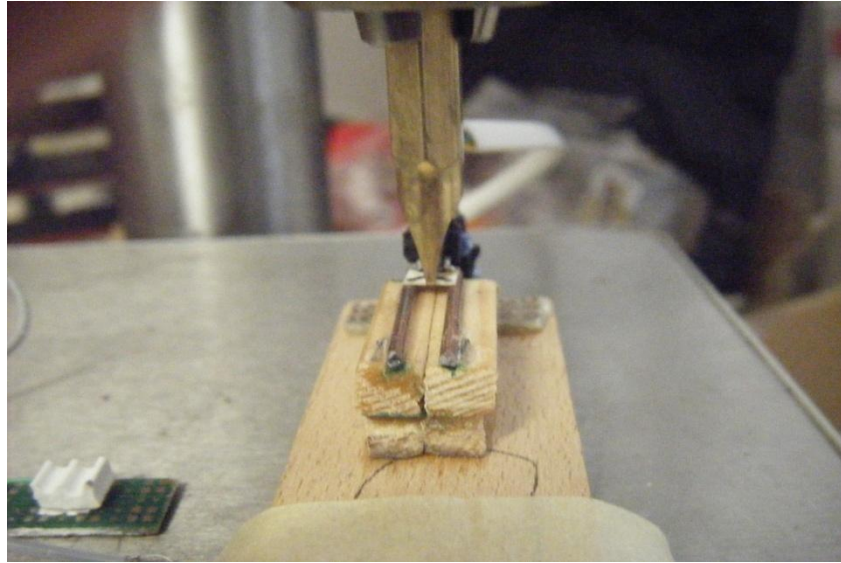


Figure 5.6 Three point bending to measure TF sensor GF

The measured GF in both cases, with distributed load and point load were from 7 to 10. The small manufactured sensor is difficult to handle to perform a reliable mechanical setup for characterization. Tolerances have big impact on the measurement. Bigger sensors can be easier to measure. However, the distributed load method is less error prone.

5.4.1.4 Pressure Chamber Characterisation

In CHAPTER THREE, a distributed load was used to measure the strain on a surface mounted thick film sensor. It was found that edge-clamped diaphragm is a good representation of the sample TF sensor mounted on PCB. For the purpose of finding the response of an array of sensors, a chamber of uniform pressure was built. A fluid (oil) pumped over an area under which, an array of TF sensors mounted on PCB as in **Figure 5.7**, is covered. The fluid inflates a balloon. The pressure can increase in steps and the response of the array could be registered. Connecting cables come out of the chamber to be read sequentially by a data acquisition system. **Figure 5.8** shows the response of the array in **Figure 5.7**.



Figure 5.7 An array of TF sensors mounted in SM technology

The chamber has also an attachment for a pressure transducer so that a graph or a table of resistance versus pressure can be registered and saved for each sensor. The response could then be used by a microprocessor system to find the exact pressure after reading the sensor output value.

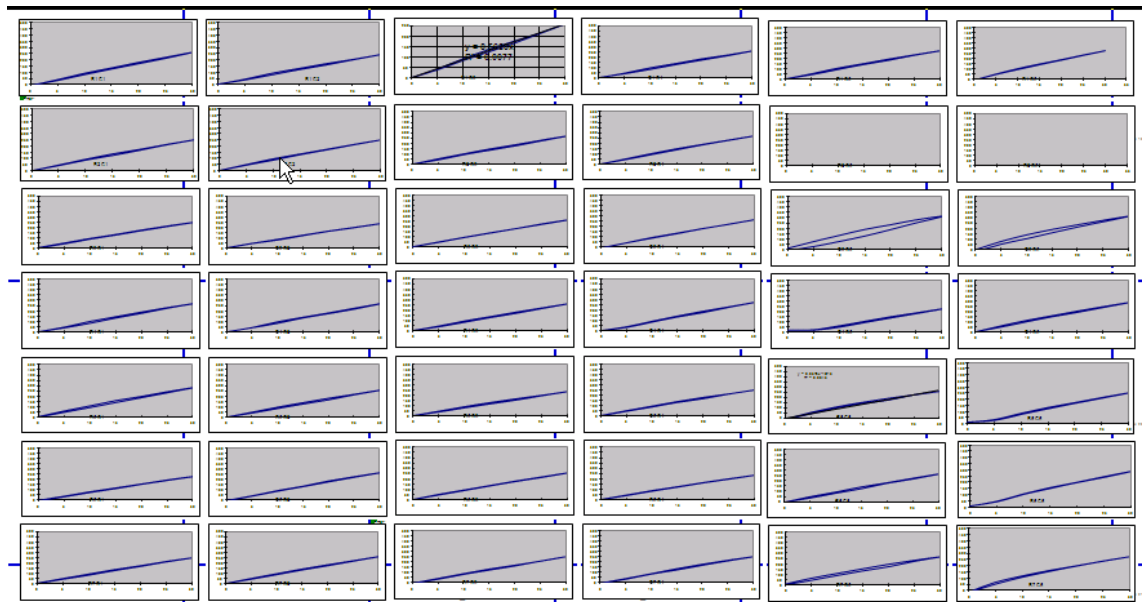


Figure 5.8 response of an array of TF sensors subject to uniform pressure

5.5 Application of TF Sensor on Building Material

5.5.1 Gluing on Material Surface

This methodology has been introduced and tested on steel bar and brick. It is mainly by gluing the TF sensor on the structure as it is commonly used with metal film strain gauges (FSG). For the case of the beam in 4PBT, the load is not parallel to the gauge and would cause the sensor to bend while in the case of brick and concrete the load is parallel to the gauge. The two methodologies have two different GF responses. In chapter three, it has been shown that TF sensor applied on steel bar works like FSG in bending. The response for the constant bending moment in the 4PB test was measured and the GF was found to be 7.2. In chapter four, TF sensors were glued on sample brick and concrete and it has been shown that the response of TF sensors is consistent with the kind of material on which it is applied. Here this application will be extended to other materials, namely wood and gypsum (Plaster) and a methodology to find GF will be proposed.

5.5.1.1 On Wood

Wood is a generic building material and is used in building just about any type of structure in most climates. Wood can be flexible under loads, keeping strength while bending, and is strong when compressed vertically. There are many differing qualities to the different types of wood.

To be able to measure the sensor under tension, a cube of soft wood was compressed to 50 Kg load then a TF sensor was glued on it with a fast adhesive from Henkel (Cyanocrylate), the load was then increased to 95 kg and then decreased to 0. The sensor in this case underwent to compressive stress first then to tensile stress when the force became lower than the initial 50 kg load.

Resistance change was registered during this operation then the zero coordinate was moved to reflect two signs, positive for compression and negative for tension as shown in **Figure 5.9**.

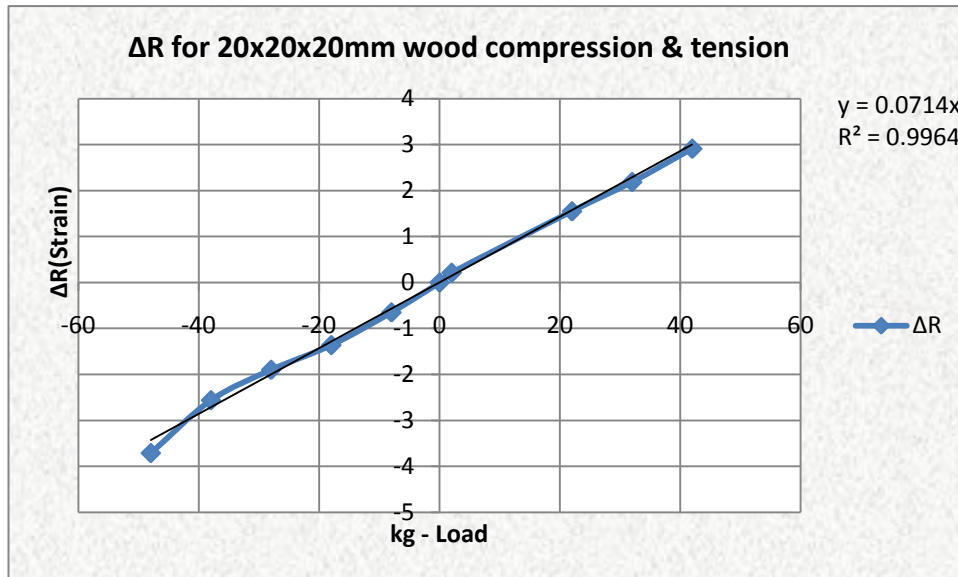


Figure 5.9 20x20x20 wood block under compression and tension

This kind of wood was soft and elastic and did not show hysteresis in sensor response. In compression, the resistance was increasing which means that the sensor was bending up because of Poisson's effect.

5.5.1.2 On Gypsum Plaster

Gypsum or plaster is a natural occurring material that is widely used in construction. It is an optimum material for finishing in particular for facades.

As a building material, plaster is a durable, attractive, and weather-resistant wall covering. It was traditionally used as both an interior and exterior finish applied in one or two thin layers directly over a solid masonry, brick or stone surface. The finish coat usually contained an integral colour and was typically textured for appearance. It was also a wood substitute in the ancient world; for example, when wood became

scarce due to deforestation on Bronze Age Crete, gypsum was employed in building construction at locations where wood was previously used.

It hardens in few hours thus it gives possibility of building plaster bricks or any other shape. Plaster has high compressive stress that may reach 69 N/mm² at low water to plaster ratio. It is relatively weak in tension and has very low impact strength. In other words, it might break on impact because of the brittle nature.

The TF sensor was applied on a 19.6x23x70 mm plaster brick with a two components epoxy adhesive. The single TF sensor was connected to the input of the differential configuration of **Figure 5.1** and the relative response at the instrumentation amplifier output is shown in **Figure 5.10**

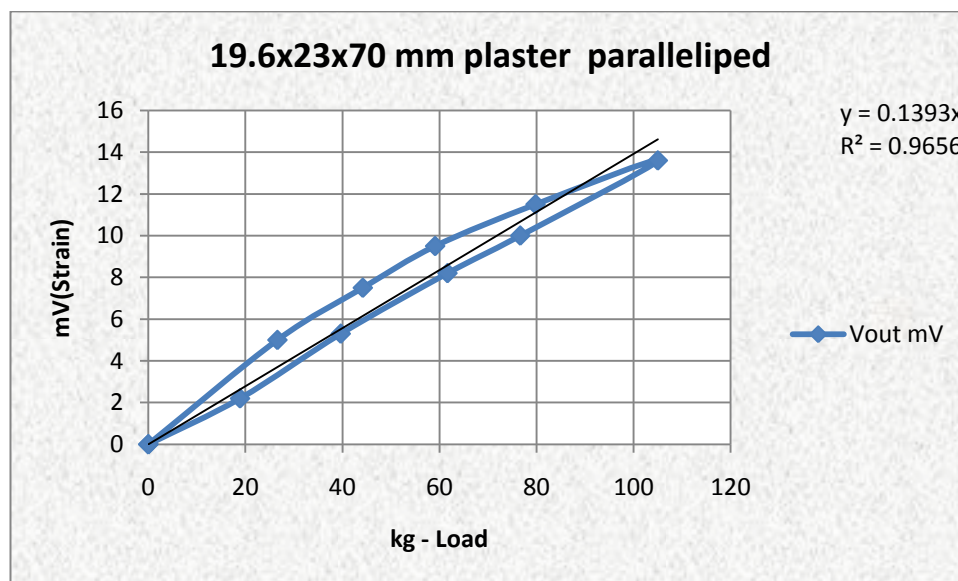


Figure 5.10 TF sensor on sample plaster compressive stress

Gypsum shows a hysteresis of about 14%. The block has lagging response to compressive stress. Also, the sensor shows a kind of curvature response when load increasing and it is linear when relaxing the pressure on the sample.

5.5.1.3 TF Gauge Factor When Glued on Material

As has been mentioned in chapter three, there was direct measure of strain by having the foil strain gauge attached side to side with the thick film sensor. The measured bending GF in the 4PB test was 7.2.

The gauge factor when the sensor is bending is different from the gauge factor when the load is parallel to the TF gauge resistor. The FSG has no substrate and is made of a very soft foil, thus it deforms like the specimen to which it is attached. TF ceramic sensor has a modulus of elasticity of 270000N/mm^2 (270GPa) and it resists the deformation. Actually, there is a combination of three materials, the specimen, the glue, and the sensor. Each one of these members has different rigidity and modulus of elasticity. The resultant GF of the TF ceramic sensor is much lower when glued on the material and force is parallel to the thick film sensor. The deducted GF for wood, plaster, brick and concrete is about 1.25. Next paragraph is showing a methodology to come to this conclusion.

5.5.1.4 Methodology for Finding GF

Four sample building materials were used in compressive stress. Namely, Wood, Red Brick, Plaster and Concrete. These samples had different sections. The load that was applied on all four samples was from 0 to 100kg. The resistance was measured for each at 100kg load.

From the previous chapter, it is known that TF response is consistent and proportional to the modulus of elasticity.

First step was to normalise the stress on all samples and the ΔR values were changed proportionally to the values at the common normalised stress of all four materials as shown in **Table 5.1**

Material	ΔR	E for GF=1.16	E for GF=1.25
wood	12.43	1407	1508
brick	1.25	14000	15000
gyps	0.928	18857	20204
concrete	0.913	19167	20536

Table 5.1 TF sensor GF calculation table

Since the response is linearly proportional with modulus of elasticity, it is enough to know one of these materials to deduce the others. Red brick published modulus of elasticity is 14000 N/mm² (14GPa) so the table shows the other calculated elasticity moduli for the other four materials. In the last column of the table, it shows the change if red brick were of a modulus of 15000 N/mm² (15GPa) as was experimentally measured by (Nichols 1997). By having the normalized stress and elasticity modulus, strain can be calculated and used to find the gauge factor. The gauge factor is 1.16 for red brick modulus of 14000 N/mm² (14GPa) and is 1.25 for the case of a modulus of 15000 N/mm² (15Gpa). These values of GF explain the results of hundreds of measurements done on this TF ceramic sensor during the research.

It would be also possible to apply a FSG and have it a as a reference as was done in the 4PB test. This could introduce other issues of; which FSG and which glue for which specimen introducing other uncertainties.

5.5.2 Embedding in Structures

As mentioned in chapter three, one of the requirements for the designed TF sensor is to have the possibility of being embedded into the building material to measure the compressive stress to which a structure is subject to. In fact, tests in chapter three were conducted on the sensor working as a tactile sensor (Appendix-D) mounted in SM technology on PCB and its response could be modelled and predicted.

Two requirements are to be satisfied in this application:

- 1) To be embedded in already erected structures like in the observation of monumental buildings.
- 2) To be embedded during construction like in concrete, clay, mortar etc. In the first case, a slot needs to be cut in specific location on the supporting structure and then the SMD mounted TF sensor has to be buried in. The setup in
- 3) **Figure 5.11** is a solution to make the sensor work in both senses i.e. tension and compression.

After drilling a hole for the sensor in the column, it is to be first glued to the upper surface of the hole with fast glue like Cyanoacrylate then the remaining space beneath the PCB to be filled with another material, which functions as filling, and gluing material at the same time. This material is available in the market and it is a two component Epoxy that can be mixed to become like modelling clay and then to be pushed into the hole. This glue will harden in minutes.

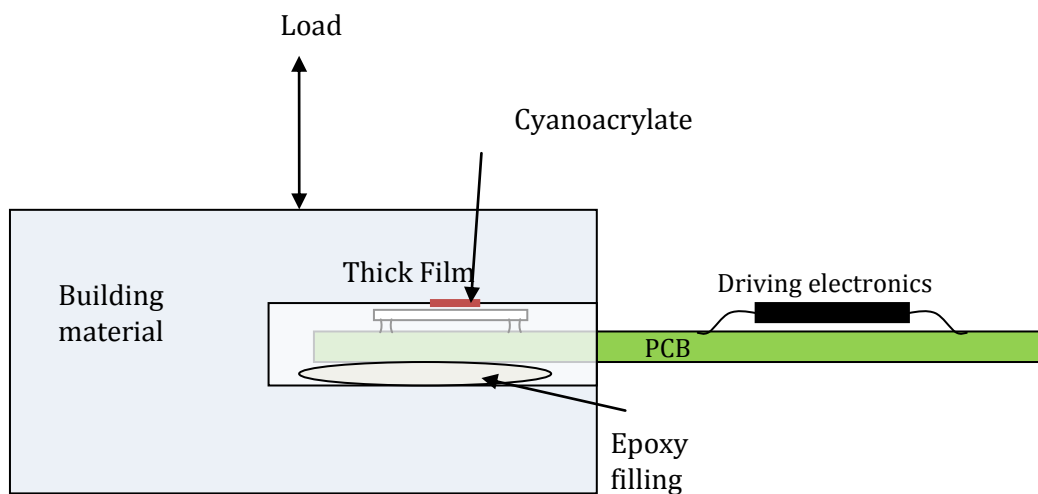


Figure 5.11 Embedded TF sensor for column stability

The technique is not needed if the building material adheres naturally to the sensor substrate and to the PCB. More investigation is required on this front. The PCB could be replaced by a ceramic Alumina substrate in hybrid technology. This

technique was successfully experimented with wood and will be described in the coming paragraph.

5.5.2.1 Embedding in wood

Figure 5.12 is an image of the experiment performed on embedding the surface mounted sensor on PCB, in wood. After having created the slot for the sensor, it was glued in the wood and the remained empty space was filled with a two-component epoxy, as can be seen form **Figure 5.13**.



Figure 5.12 TF sensor embedded in wood with bi-component adhesive

The sensor was connected in one position at the input of the differential op-amp configuration of **Figure 5.1**. Before applying load, the circuit output was reset to zero by the V_DAC input from DAQPod1200.



Figure 5.13 Surface Mounted sensor embedded in wood

As can be seen from **Figure 5.12** , a 2kg load was applied on a T-shape wood structure. The load was moved in steps from -20 cm to + 20 cm with respect to column centre. The sensor in one sense works in compression and in the other sense works in tension. **Figure 5.14**, shows the output response of the differential op-amp configuration. The response is almost symmetrical. This result is very helpful in observing stability of walls and almost any structure by just making a slot and embedding a TF sensor as above. The slot can be big enough to accommodate two sensors, mounted side to side on PCB, one glued on the structure as described above and the other is free without any mechanical excitation.

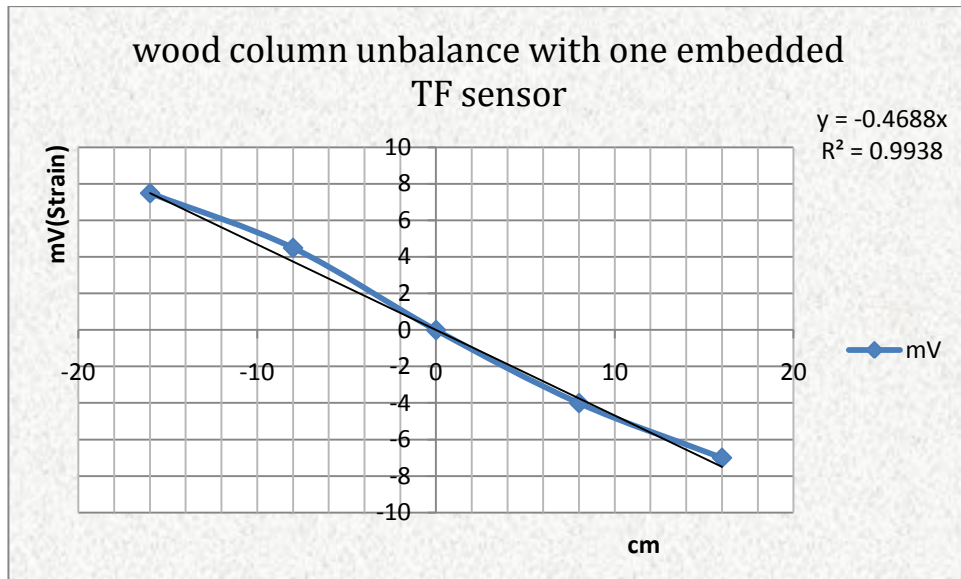


Figure 5.14 Load unbalance with one sensor in wood

This second sensor is useful for removing any environmental effect and noise by differentiating its output with the other glued sensor.

A second experiment was conducted to measure the response of the structure when load is increasing at plus 20 cm and at -20 cm. 1, 2, and 3 kg load was applied at the mentioned distances. **Figure 5.15** and **Figure 5.16** is the response.

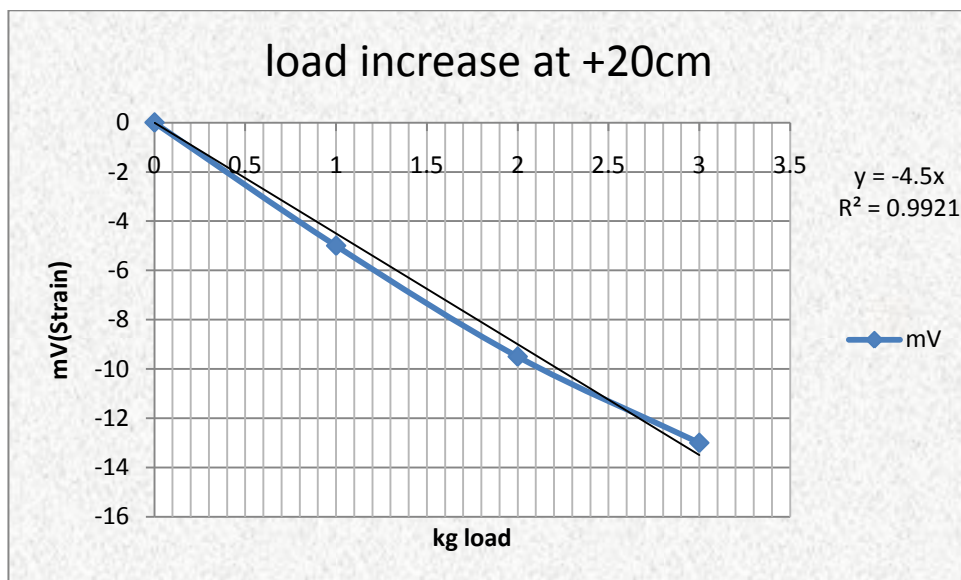


Figure 5.15 Load increase at +20 cm from centre

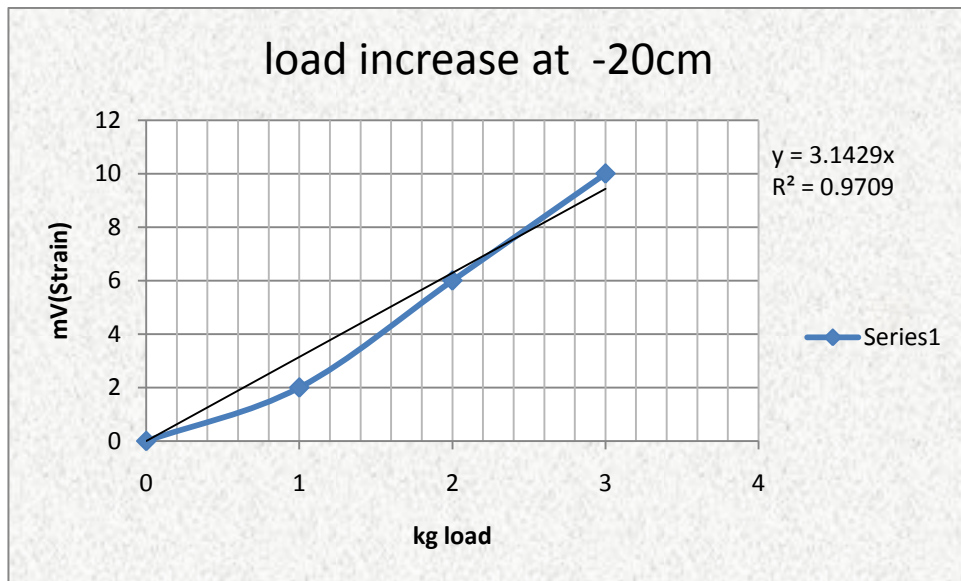


Figure 5.16 Load increase at -20 cm from centre

5.5.2.2 Embedding in Gypsum Plaster

For the second case, in which sensor should be embedded during construction of the structure, the sensor should work in water or at least should not undergo fundamental changes when immersed in water. From the first tests on TF piezoresistive sensors, it was noticed that the sensor continues to work even if it emerged in water. However, its initial resistance value changes by 5 to 10% when it's fully immersed in water.

On a test in Gypsum Plaster, the sensors returned to 2% of their initial value after the Plaster dried completely.

Figure 5.17 shows a plaster column with two TF sensors embedded on opposite sides. Plaster is the ideal material for modelling and test as it does not require much time to cure and is cheap and easy to prepare and has a high compressive strength comparable to bricks or even higher when water to Gypsum ratio is low.

A plastic mould was prepared with two slots suitable for sensor insertion at two opposite sides. After mixing the Gypsum with water as specified by manufacturer, the material was put into the mould and after 5 minutes, the sensors were inserted through the slots. The column complete cure and drying took some days. However, it was strong enough after 20 minutes for removing the mould and handling the column alone. The column dimensions were 28x20x107mm.



Figure 5.17 Plaster column with two embedded TF sensors

A test of loading on the column was carried on and the following main problem was found; after applying a uniform load on the column, each

sensor starts to sense the load at a different threshold. The explanation could be that as sensors are randomly accommodated in the structure and there is no information on the evolution of the internal movement and positioning of the sensor with respect to the surrounding material, the material starts to act on the central sensitive part of the sensor at different threshold loads.

Figure 5.18 reports the response of one side sensor to load. The sensor starts to work at about 80 N.

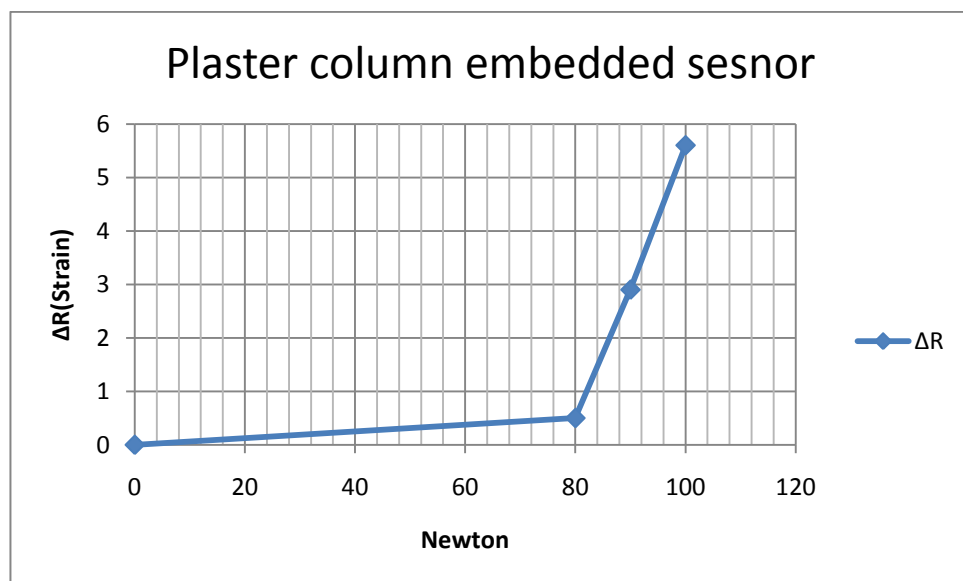


Figure 5.18 Response of embedded TF sensor in Plaster column

After reaching the threshold, the response is linear with load.

Another column was constructed to test response on a column structure and will be shown in chapter six.

5.5.2.3 Embedding in Concrete

Two SMD mounted TF sensors were embedded in a 50mm cube of concrete. The concrete mixture was without aggregates to avoid anomalous sensor- concrete interface.

Similar to Gypsum, a mould was also prepared to build a concrete cube as shown in **Figure 5.19**. The concrete mix was 1 part of cement for every 4 parts of sand and water/cement ratio was 0.83. Sensors were inserted in opposite sides as shown.

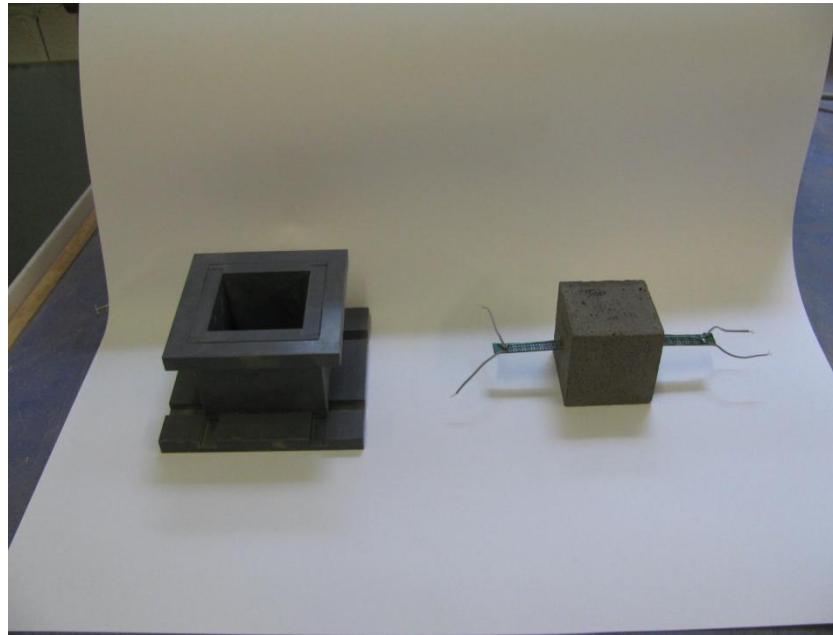


Figure 5.19 Mould and concrete cube with embedded TF sensors

The value of the sensor resistance before insertion in the concrete and during concrete curing period was registered many times for the first days and once every day until one month. One of the sensors showed an increase in the resistance in time as shown in **Figure 5.20**. The curve is minutes starting from casting the concrete and sensor insertion. Reported in the graph are only the first 9 days. After this, the sensor stabilised on the value of 8022Ω . When the humidity is high the sensor piezo-resistor decrease for the first day then concrete curing in time increase the stress on the sensor causing it to steadily increase for the successive eight days. However, this needs more investigation and experiments.

The concrete block was subject to loading but the sensors did not show any change. This could be a problem of the same nature as what was faced in Plaster column test with the exception that this time the material is harder.

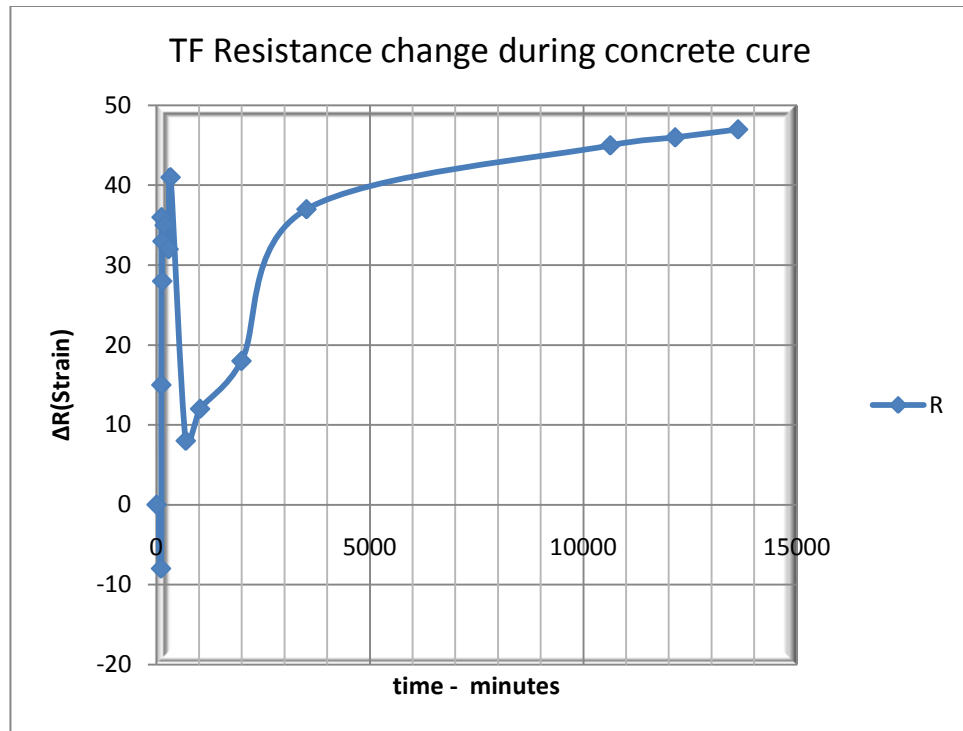


Figure 5.20 TF resistance change during concrete cure time

5.5.3 Direct Force Application

It has been noticed through the sensor validation test process of this study that sensor is sensitive to touching its surface and when connected to electronic circuitry, it was showing significant output change by applying small forces on the surface. Literature confirmed the existence of the so-called z-axis gauge factor (PUERS et al. 1987). (SION 1993) thesis was on using the z-axis gauge factor to build a compact rigid accelerometer.

This fact is of great help in Structural Monitoring and stability control where direct load sensitivity is appreciated to estimate load and load differences on side of a structure. This solution is also an alternative for embedding sensors in building material.

5.5.3.1 Four Different Sensors on a Steel Block Angels

As a first approach to evaluate the functionality of the sensors, four sensors were glued at the upper surface of a steel cube as shown in **Figure 5.21**.

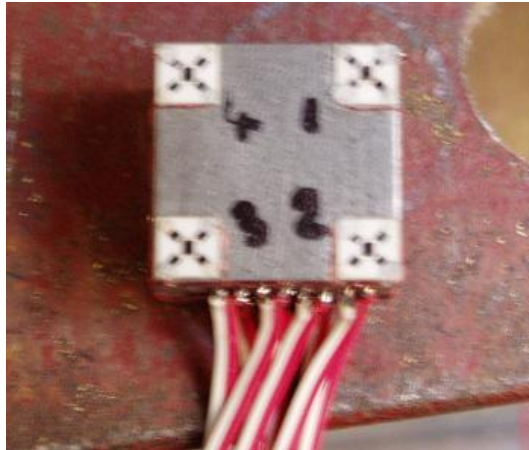


Figure 5.21 Four TF sensors on upper surface of steel cube

The cube with the sensors was then put in the middle between two other steel cubes and load was applied on top. The four sensors were connected individually with a Wheatstone bridge to system 5000. System 5000 accepts only this kind of interface circuitry. A TF sensor was also glued to the side of the steel cube as shown in the setup is shown in **Figure 5.22**.

During this test the upper of the three cubes does not sit directly on the TFCS' s but requires having a layer of material to act as a shield or cushion so that the TFCS is not damaged. There are various options available for such material. Rubber, wood, or paper could be used. In our experiment, a thin layer of balsa wood was used (Appendix-D).

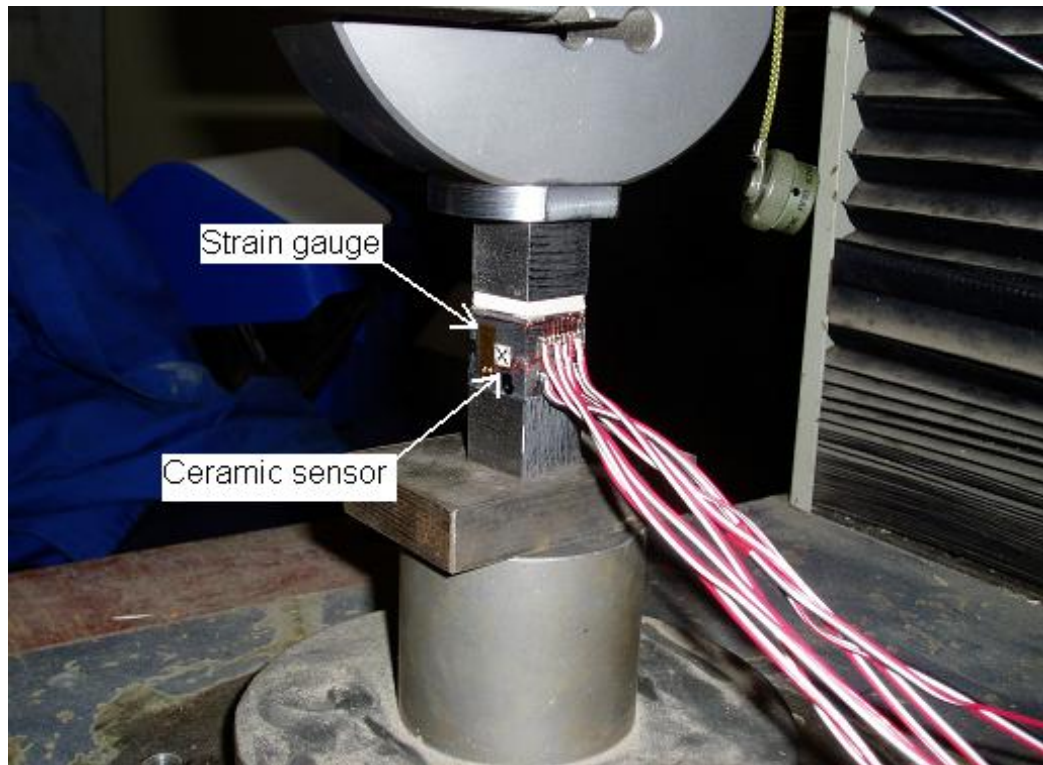


Figure 5.22 Direct load application in steel cube compression test

This material provides enough protection to the TFCS but is also soft and compressible enough not to impede the TFCS when reading. The cushion material is of great importance to define the full load scale operation of the system. Rigid materials has different response curve than a soft material and in reality can be any mortar material. The response as a function of this cushion material will be shown in curves here after. The application of the Balsa wood is visible in the image showing the test set-up and it appears as a white layer.

The load is distributed uniformly on the cube surface and sensors at the same time. From **Figure 5.23**; sensors seem to have almost the same response, which deviates at higher loads because of the different angles of response, i.e. different gauge factor.

The sensor is a sandwich between two materials, the building material and the cushion material. A quantification of the effect of the cushion material was carried out as explained here after.

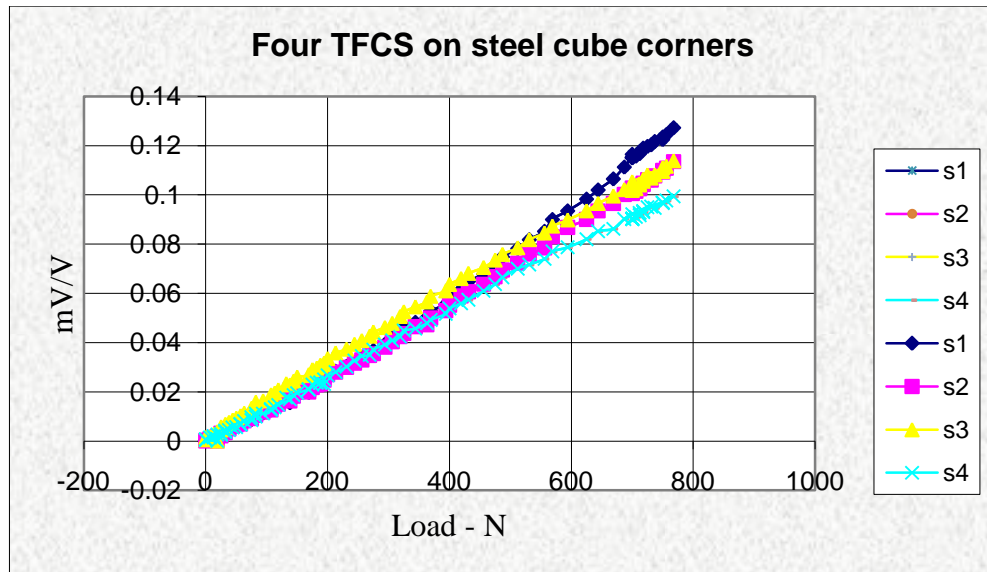


Figure 5.23 Four sensors response in direct load application on steel cube

5.5.3.2 Effect of Cushion Material Test

In direct load application on TF sensors method. The sensor is squeezed between two materials, one is the cushion material the other is the building material itself. To evaluate the effect of the kind of building material on the response the sensor, three building materials were considered as follows; three of the samples shown in **Figure 5.24** were used. Namely wood, plaster and steel. A 2mm diameter Teflon pin was used to load the TF at centre where the TF resistor is located, (**Figure 5.25**).

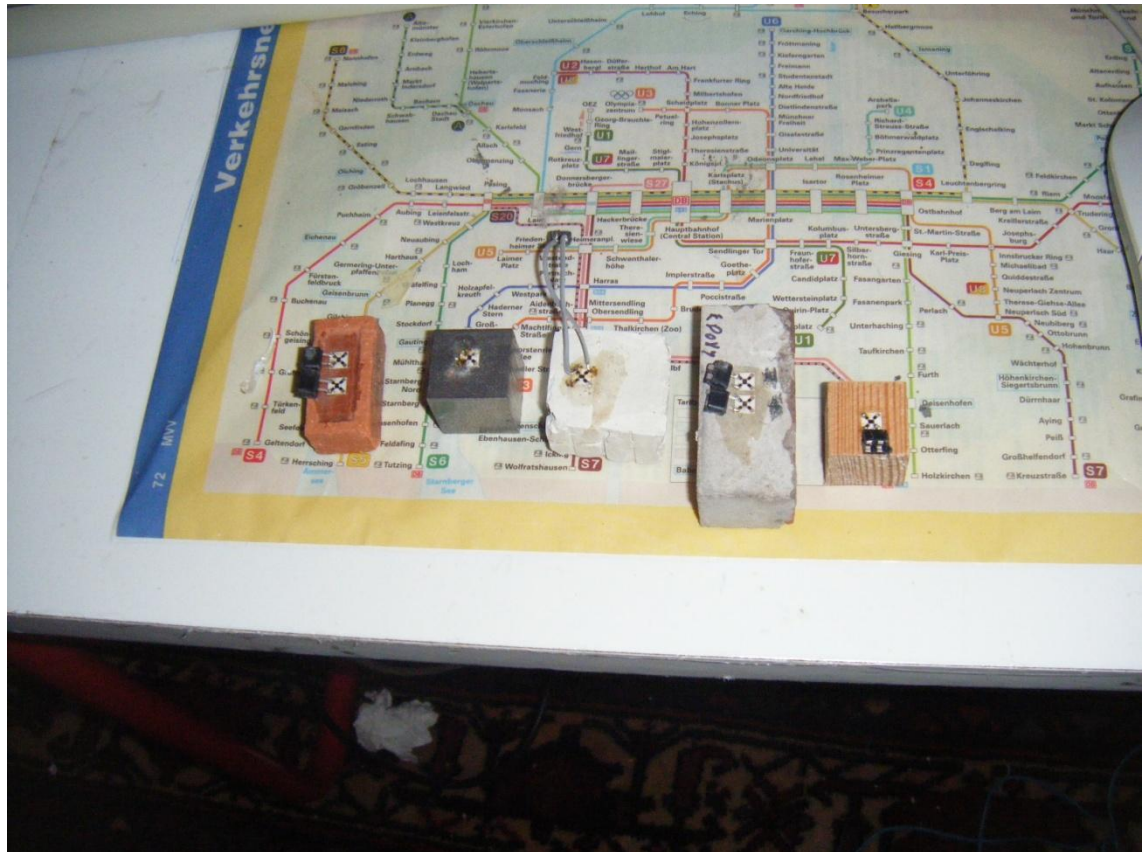


Figure 5.24 Sample-building materials with TF glued

The load was increased gradually up to 4000 gm force (12.5 N/mm² stress) then it was decreased to zero again.

Results are shown in **Figure 5.26**. It can be noticed the effect of rigidity of the building material on the response. Higher is the modulus of elasticity of the building material lower is the effect of loading on the TF resistor. When the material is soft, the TF substrate centre can more easily bend in the middle causing the resistor to decrease. In the Figure it can be noticed a first load stabilisation range, after which the response follows a second linear envelop. The hysteresis is due to the limited rigidity and to deformability of Teflon as it might change shape due to loading. Other pointing pins might confirm this but for the purpose of our study it is enough to show the dependency of response on building and loading materials.



Figure 5.25 TF on steel cube loaded with Teflon pin

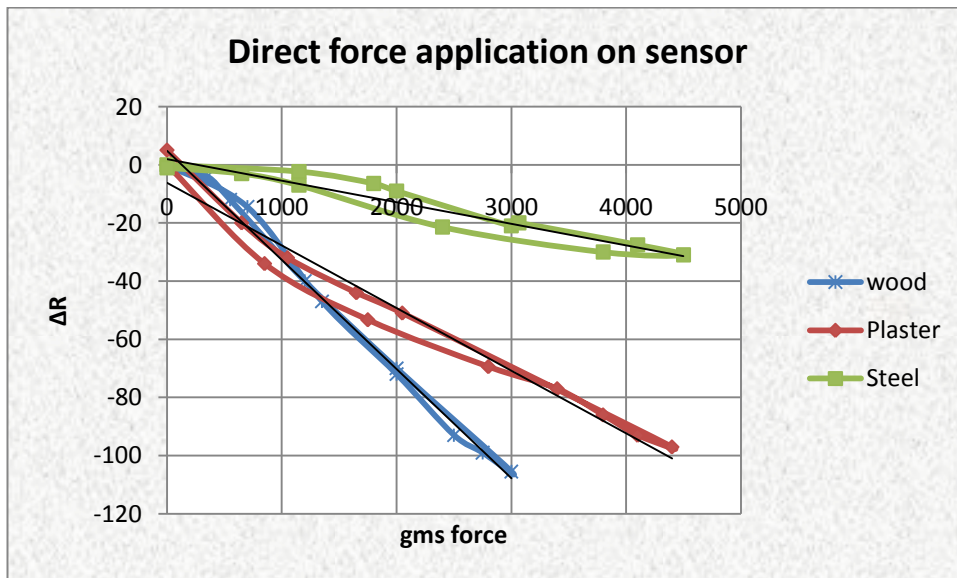


Figure 5.26 Response of TF directly loaded on wood, plaster, steel

This kind of functionality with direct application of load on substrate is one of the advantages of having the strain gauge built on a predefined substrate like alumina. The same functionality is not possible with metal foil strain gauges.

5.5.3.3 Current Source to Sum Effect of TF Array

In chapter four, the circuit in **Figure 5.27** was proposed. The transfer function of the circuit is

$$V_{out} = G\Delta R \times \frac{V_r - V_{ee}}{R_{28}} \quad 5.14$$

In this circuit, we can increase the number of branches and sum the effect of the resistor change due to strain at the output. This will allow the output voltage swing to remain within the circuit dynamic range limited by supply voltages. The circuit was simulated for a $\Delta R = 100 \Omega$ and the output was as expected from the transfer function.

A simple application for this circuit is the direct loading of sensors on a brick shown in **Figure 5.28**, where Silicone rubber was used as cushion in the first time and then replaced by hard rubber in a second time.

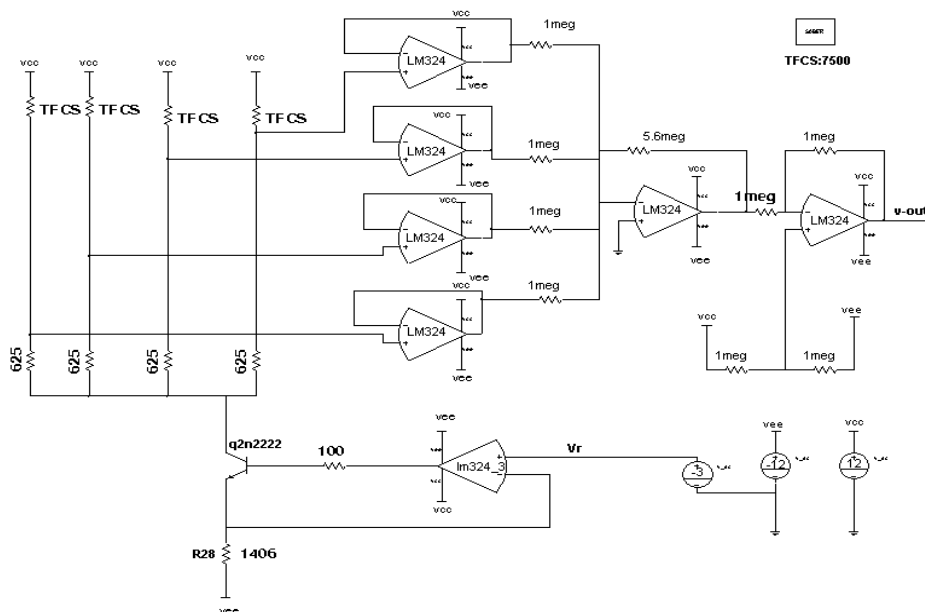


Figure 5.27 Array of four TFCS driven by one current source

Each TFCS is located in one branch and shares the current drawn by the current source formed by V_r , op-amp, R28, and the 2N2222 bipolar transistor. The output is decreasing because of the last level shift amplifier stage, which is configured as inverter stage. The result of loading the brick in both cases are shown in **Figure 5.29**.

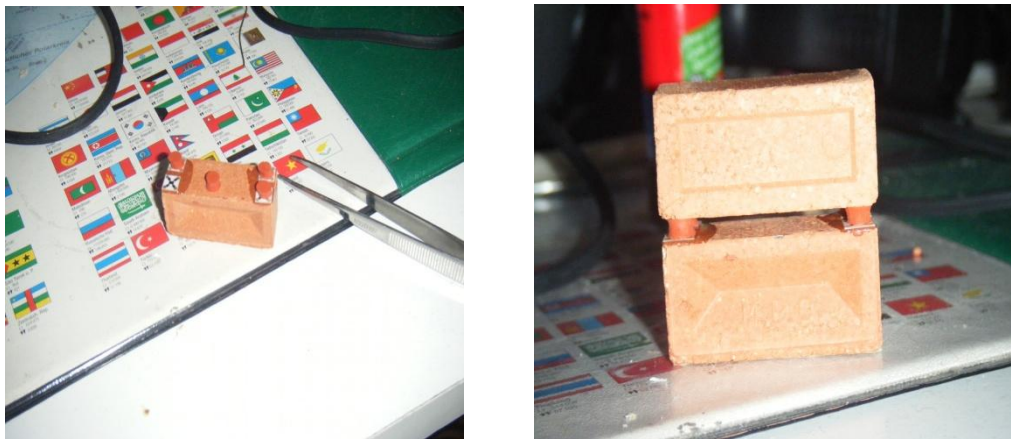


Figure 5.28 Silicon rubber on TF sensors on the angles of sample red brick

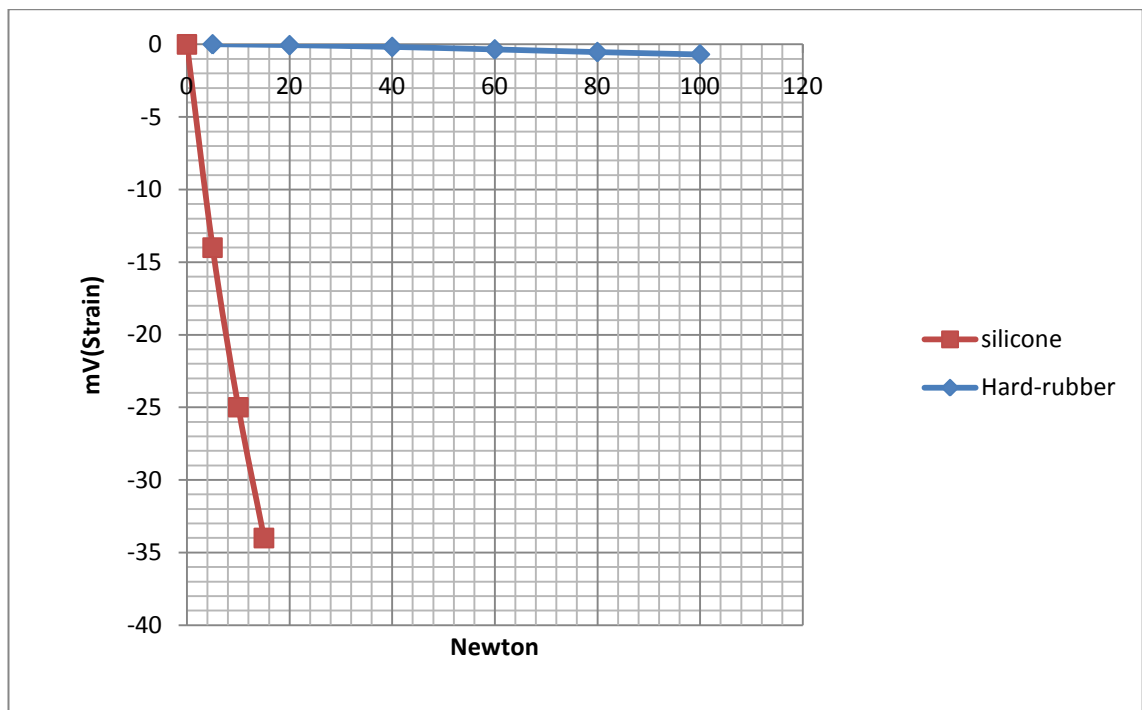


Figure 5.29 Response of silicone and hard rubber in direct load on brick

The load on soft cushion would saturate in very short range of force applied while harder materials can have more smooth grow of the 1000 μ strains of ceramic per load unit.

This circuit was also tested configured with single supply operation, which is a more practical deployment. One single battery with sufficient TF sensors can be a practical circuit for monitoring stability of structures and for many other applications for load calculation.

The noise and drift for environmental effects like temperature makes this circuit less stable per se. These effects will add up together with adding up the signal. Better if this configuration is followed by a differential amplifier stage to observe stability between two structures, which will be proposed in the following chapter.

5.6 Summary

In this chapter, gauge factors for piezo resistive thick film sensors was introduced and related to TF application for SHM. An experiment showed the response difference between two TF sensors. Methodologies to characterize TF sensors before deployment were discussed and applied to find GF of the designed TF sensor.

A methodology was shown for how to find the GF of TF sensor when is glued on material and is under stress parallel to the sensor.

Three ways of deploying TF sensors on building materials were discussed and experimented and these are: Gluing on material surface , embedding in structures and direct load application. A technique for using the embedded sensor in tension and compression on erected structures was proposed and experimented successfully.

6. Thick Film for Practical SHM Application

This chapter will focus on the practical system implementation and difficulties for implementing TF sensors to assist Structural Health Monitoring. A description of the environmental requirements will be described then a simple circuit to monitor the stability of an erected structure like a column will be introduced and experimented with recommendations for a final product based on a microprocessor system will be given.

6.1 The Environment

Structures, including bridges, buildings, dams, pipelines, aircraft, ships, among others, are complex engineered systems that ensure society's economic industrial functionality. To design structures that are safe for public use, standardized building codes and design methodologies have been created. Unfortunately, structures are often subjected to harsh loading scenarios and severe environmental conditions not anticipated during design that will result in long-term structural deterioration (LYNCH 2006).

SHM is predicted on the ability to integrate sensors within a structure in such a way that the overall system reliability is increased. This requires that not only the sensors able to detect the damage and algorithms are in place to recommend appropriate intervention, but that the sensors themselves are sufficiently reliable so that they do not require replacement at intervals less than the economic life time of the part they are monitoring (KESSLER et. al. 2004). Civil structures present a well-known engineering problem which is the fundamental challenge for the ability to capture the system response on widely varying length- and time-scales comparable to man or medium structure life.

TF sensor technology for measuring force related to deformation is applicable in automotive, industrial, medical and sport apparatus fields. Long-term stable thick-Film pressure transducers are commercially available (DJINSTRUMENTS 2010). The Thick-Film materials are known for their survival, longevity and reliability in harsh environments, extreme temperatures and high mechanical stresses, such as those present in automotive applications (WADA et. al. 1997). This fact makes Thick-Film technology a good candidate for civil engineering applications.

One of the main obstacles for deploying a SHM system for in-service structures is the environmental and operational variation of structures. In fact, these changes can often mask subtler structural changes caused by damage. Often the so-called damage-sensitive features employed in these damage detection techniques are also sensitive to changes in environmental and operational conditions of the structures.

Best candidate technology for such harsh environment is the hybrid circuits production technology. The TF sensor or array of sensors could be developed on the same substrate together with its driving electronics.

A sensor per se, is not enough to monitor structures, it needs intelligence to be able to tune, compensate and communicate with other sensors and with a central control unit through a network.

6.2 Hybrid Technology for Packaging and Long Term Functionality

Here after is a description of the Hybrid technology and the packaging solutions available to provide a protection for the electronic circuitry.

6.2.1 Technology Overview

Hybrid micro circuits have been in use for over fifty years. In the early sixties, hybrids were extensively used in weapons systems such as the Minuteman Intercontinental Ballistic Missile (LICRAI 1998). Reliability and reduced size were behind the use of hybrids instead of printed circuit boards. In the late sixties and early seventies, the fast-growing monolithic integrated circuits began to replace

hybrid functions; many predicted the demise of the hybrid technology. In fact, Large Scale integrated circuits (LSI) began to replace hybrid products. However, it soon became evident that the usefulness of ICs could only be optimized by integrating them with other ICs, resistors and capacitors in a multi chip hybrid circuit. Hybrid circuits have thus outlived these predictions. Hybrids are found in almost every military system and in most commercial products. Commercial products include home computers, calculators, radios, televisions, aircraft equipment, heart pacemakers, etc. These are but a few of the commercial applications of hybrids. Hybrids are used mainly to save weight and space; however, in the commercial field, cost is usually the deciding factor, because the commercial market is very competitive and will settle only for the lowest cost packaging approach. Only when a commercial application requires a more reliable circuit, such as a heart pacemaker, cost is overridden. While Thin-film hybrids are better suited to high-frequency applications, both thin and thick-film technologies can be used up to 500 MHz, above that limit thin film technology dominates (LICRAI 1998).

6.2.2 Commercial Applications

Similar to structural health monitoring, medical electronics (which is for Human health monitoring) is one segment of the commercial market that requires long-term reliability, along with dense circuitry. Similarly, to SHM, irregularly shaped substrates may be needed to fit the package. Medical hybrids must pass even more stringent tests than military hybrids and must be free of contaminant in order to be implanted in humans. The broad field of medical electronics includes instrumentation for life support, patient monitoring, hearing aids, and pacemakers. The pacemaker market especially has developed rapidly, and hybrid circuits along with it as the logical approach for packaging. As stated above, the restrictions in size and materials have made medical electronics a very challenging area for the hybrid engineer (LICARI 1998).

6.2.3 Military and Space Applications

In addition to the less demanding commercial market, Hybrids are the best choice for military and space applications. Every military weapons system uses one form of hybrid or another. Hybrids are used in missiles, satellites, aircraft, helicopters, submarine navigation instruments etc. A military system that benefited from the reduced size of hybrids was an airborne data processor built by Hughes Aircraft for the F-14 and F/A-18 aircraft (LICRAI 1998)

As reported by (LICARI 1998), the original version of the computer consisted of eighteen 13 X 13 cm printed circuit boards. Redesigning these boards and partitioning them into hybrids condensed them to one 15 X 23 cm, ten-layer board containing eight hybrids, 13 discrete less, and some capacitors and resistors. Besides the reduction in space and weight, the hybrid version also increased the computer's speed by a factor of 1.5 by shortening the signal paths. One of the hybrids was packaged in a 5 X 5 cm case and had 1601 Inputs/outputs. It consisted of a fifteen layer ceramic substrate with integrated circuits in open chip-carriers that dissipated 20 watts. A later version, designed with gate arrays to replace some of the integrated circuits missions dissipated only 10 watts not surprisingly; one of the biggest users of hybrids has been NASA for the space shuttle. Each shuttle uses over 10,000 hybrids for their reduced size, weight, and reliability. Over one thousand power hybrids are used on each orbital..

6.2.4 Hybrid Technology Reliability

As was described in the overview, it is a well-known fact among the electronic industry that Hybrid technology is intended for high quality systems known for their reliability and high performance. Hybrid technology has made major contributions to the wide range of low-cost, high performance microwave components available worldwide. Components in this category include wide-bandwidth amplifiers, microwave oscillators, filters, directional couplers and others. Thick film

resistor networks are finding widespread use in analogue-to-digital and digital-to-analogue converters. With constant advances in multilayer hybrids, packaging techniques and diagnostic abilities it is becoming feasible to put many Integrated circuits on a single hybrid. This is finding applications in many areas, which make this technology a good candidate for structural health monitoring. **Figure 6.1** is an example of a packaged hybrid circuit.

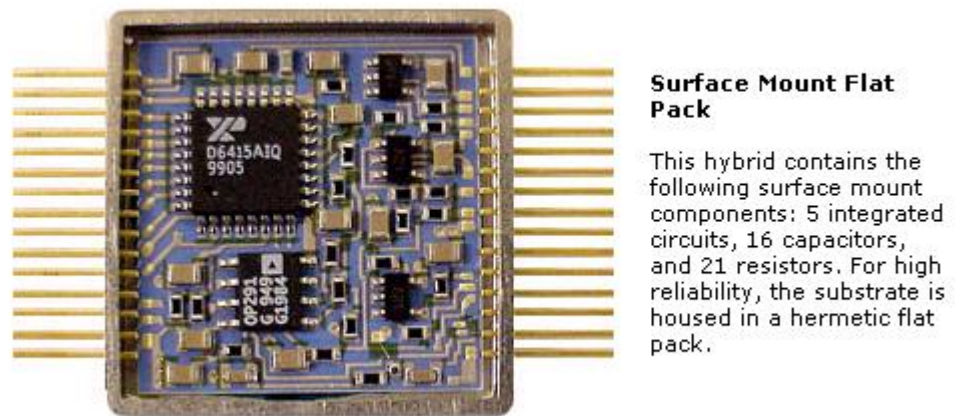


Figure 6.1 Example of Hybrid circuit (Sanchez Hybrids)

6.2.5 Packaging

To monitor structure health, sensors within a structure need to be integrated in such a way that the overall structure reliability is increased. This requires that not only are the sensors able to detect the damage and algorithms are in place, to recommend appropriate intervention, but that the sensors themselves are sufficiently reliable so that they do not require replacement at intervals less than the economic lifetime of the part they are monitoring (KESSLER 2004). This requirement is a major consideration in the integration and packaging of the SHM sensors into the overall structure. The packaging has to perform multiple functions. First, it must provide an interface between the SHM sensors and the structure they are integrated within. This requires that there is a direct connection

suitable for ensuring that the measured property is transmitted faithfully to the sensor. Second, the electrical connections to and from the sensor for signal and power must be guaranteed and thirdly, the sensors must be protected from the environment so that temperature moisture and local damage events (such as impact) do not compromise the ability of the sensors to fulfil their function. Finally, these connections must be achieved in a way that they are not subject to durability issues (fatigue, creep, moisture.etc.). All these points can be achieved with the hybrid circuit's production technology.

In Hybrid technology, choosing the right package that meets all the application needs is of primary importance to achieve adequate system performance. Careful consideration must be given to the seal type, package style, and package size before committing a package to production. In selecting the package, an early decision must be made as to the degree of protection that the package is expected to provide; for example, should the package be hermetic or non-hermetic in the sense of meeting definite helium leak rate requirements, which is a standard method for leak detection. Most military, space, and some medical applications, require hermetic packages while most commercial applications can use lower cost expendable, non-hermetic packaging such as epoxy plastic-encapsulation or transfer moulding (LICARI 1998). Due to the SHM long term deployment requirement and environment conditions a hermetic encapsulation should be foreseen. Moisture and humidity is the major cause of failures in electronic system and special consideration for SHM systems packaging is a prerequisite. Hybrid packages are of many types and they are differentiated by the connectivity with respect to the substrate and the materials used; flat-pack, plug-in, Epoxy sealed, cavity package, ball grid, plastic encapsulated. Each serves different market and application requirement.

Even if Hybrid circuits looks very promising technology in many terms including packaging , more research need to be conducted on the ways of

deployment of TF sensors; i.e. on surface parallel to force, direct load application, and embedded to assure reliability of response. Burn-in technique should be used to accelerate aging and evaluate long term functionality.

For multilayer packaging, a new promising technology emerged. It belongs to the hybrid electronics world and offers higher level of integration, compactness and is adequate at the same time for harsh environment. The Low-Temperature Co-fired Ceramic, LTCC technology that will be introduced in the coming paragraph.

6.2.6 Low-Temperature Co-Fired Ceramic, LTCC Technology

For multi-layer packaging, The low-temperature co-fired ceramic process (LTCC) offers significant advantages over the high temperature process (HTCC) and provides a new dimension for engineers to design both high-density multilayer interconnect substrates and advanced packages for high-speed and microwave circuits. The key feature of the LTCC process is a "green tape" that can be fired at 850°C in a conventional furnace instead of at 1600°C in a hydrogen environment required by the conventional HTCC process. The lower firing temperature and air ambient of LTCC permit the use of the conventional thick-film conductor pastes such as gold and silver whose high electrical conductivities are vital to high-speed circuits. Furthermore, in the LTCC process, passive components such as resistors, capacitors, and inductors, can be co-fired with the ceramic tape and embedded in a monolithic structure. On the other hand, the HTCC process is limited to refractory metal conductors because the high temperatures involved would melt gold and other non-refractory metals. Resistors, capacitors, and inductors comprised largely of mixed metal oxides would also be reduced and degraded by the hydrogen reducing atmosphere required of the HTCC process.

Very low profile packages can be produced with LTCC by designing the interconnect substrate integral with the package and leads. Cavities can be

formed in the ceramic simultaneous with its fabrication so that ICs or other chip devices can be inserted into recessed areas, producing a very low profile package. The package-substrate combination can be hermetically sealed or encapsulated with high performance plastics such as epoxies or silicones. A further advantage of LTCC over HTCC is that it lends itself to producing contoured or three-dimensional electronic circuits and packages since the tape can be processed over a shaped mandrel before firing. This is of special interest in producing "smart skins" where electronics and sensors are integrated with the structure.

However, advantages of HTCC include mechanical rigidity and sealing, both of which are important in high-reliability and environmentally stressful applications. Another advantage is HTCC's thermal dissipation capability, which makes this a microprocessor packaging choice, especially for higher performance processors which is not stringent requirement for SHM application.

As an example of the suitability of LTCC and classical thick film technologies to work in harsh environment, (JACQ et. al. 2009) reported practical examples of devices where reliable operation in harsh environments such as high temperatures, high pressures, aggressive media and space, poses special requirements for sensors and packages, which usually cannot be met using polymer-based technologies.



Figure 6.2 Liquid level sensor

Ceramic technologies, especially LTCC offer a reliable platform to build hermetic, highly stable and reliable sensors and packages. The examples are discussed in terms of performance, reliability, manufacturability and cost issues. **Figure 6.2** is an image of ceramic module of liquid level sensor.

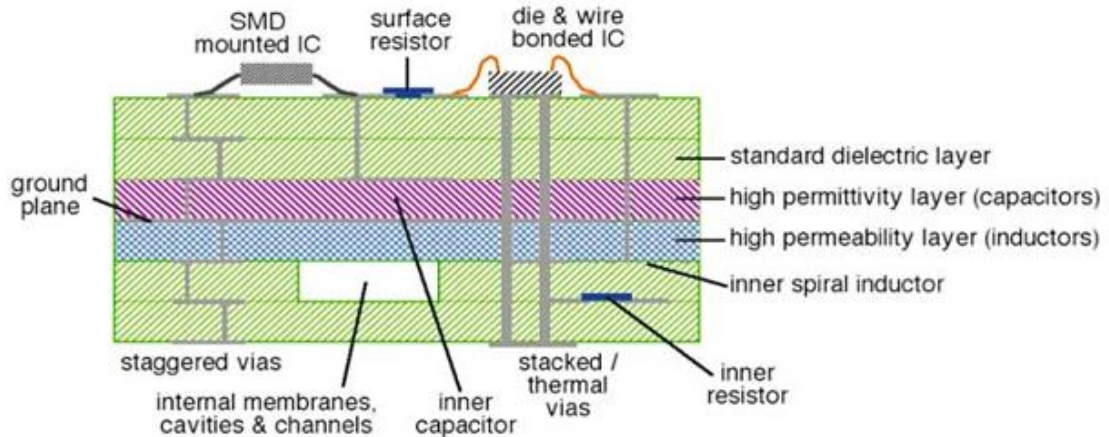


Figure 6.3 3D structure of LTCC and example of possible features (JACQ 2009)

Figure 6.3 is a representation of the possible complexities involved in multilayer LTCC structures.

One of the alternative substrates to Alumina, (MAEDER et. al. 2005) considered LTCC. The lower strength of LTCC vs. alumina (120-180 GPa) is more than compensated for by the lower elastic modulus (80-120 GPa) (SCRANTON 2000). Further improvements can be gained through the excellent 3D structuring capabilities of LTCC. Therefore, the LTCC can be an alternative to Alumina to:

- 1- overcome the $\pm 1000 \mu$ strain limitation
- 2- Offer more electronic integration and better packaging capability,
- 3- Resist to the harsh SHM environment

6.3 Structural Stability in SHM

Stability represents a fundamental problem in solid mechanics, which must be mastered to ensure the safety of structures against collapse. The theory of stability is of crucial importance for structural engineering, aerospace engineering, nuclear engineering, ocean and arctic engineering. It plays an important role in certain

problems of civil structures, geotechnical structures, geophysics and materials science.

The importance of the subject is evident from the history of structural collapses caused by neglect or misunderstanding of the stability aspects of design. The most famous among these is perhaps the collapse of the Tacoma Narrows Bridge in 1940, due to aerodynamic instability, and the collapse of Quebec Bridge over St. Lawrence in 1907, but numerous other disasters provided important lessons.

Stability analysis in solid mechanics began with Euler's solution of buckling of an elastic column (Euler 1744). Most basic linear elastic problems of structural stability were solved by the end of the 19th century, although further solutions have been appearing as new structural types were being introduced. The twentieth century has witnessed a great expansion of the stability theory into nonlinear behaviour, caused either by large deflections or by nonlinearity of the constitutive law of the material. In the second half of this century, dynamic stability, important especially for non-conservative systems, became reasonably well understood. (ZSENEIK et. al 2000).

6.3.1 Column Stability

The strength and stability of steel columns have been the subject of many studies since the original work of Leonhard Euler in 1744 and 1759. Numerous examinations of elastic buckling of perfectly straight columns were conducted during the 19th century, the most famous being the studies of Engesser and Considère (JOHANSTON 1981), with several series of column tests attempting to find agreement between theory and physical behaviour. The research work continued in the 20th century, examining the influence of material and member imperfections, including the famous tangent modulus work of Shanley, and the resolution of the effects of material non-linearity, residual stress and column out-of-straightness. The definitive solutions were only obtained in the 1970-s, when modelling and numerical solutions allowed for the incorporation of all nonlinear effects. Since that, time reliability and probabilistic solutions have provided state-of-the-art criteria for limit state treatment of the column problem. These principles

are now the bases of the design standards for columns in all of the countries in the world (BJORHOVDE 2010).

A simple and practical application to measure column stability using TF sensors will be proposed. The scope is to show the effectiveness and feasibility of applying TF technology to Structural Health Monitoring.

6.3.2 TF Sensors Glued on Surface for Structures Stability

To examine the stability of a sample column-supporting floor, TF sensors were glued on opposite sides of a column made of bricks. The sample structure is shown in **Figure 6.4**. A T – shape structure constructed with a column of 55mm height made of sample red Brick and a supporting plane of wood. TF sensors were glued with two components epoxy on opposite sides at three different heights; 0.5, 2.5 and 5 cm. The wood was marked for each 5 mm until 30 mm on both sides to enable a dead weight of 2Kg load to move from +30 mm to -30 mm in steps of 5mm.

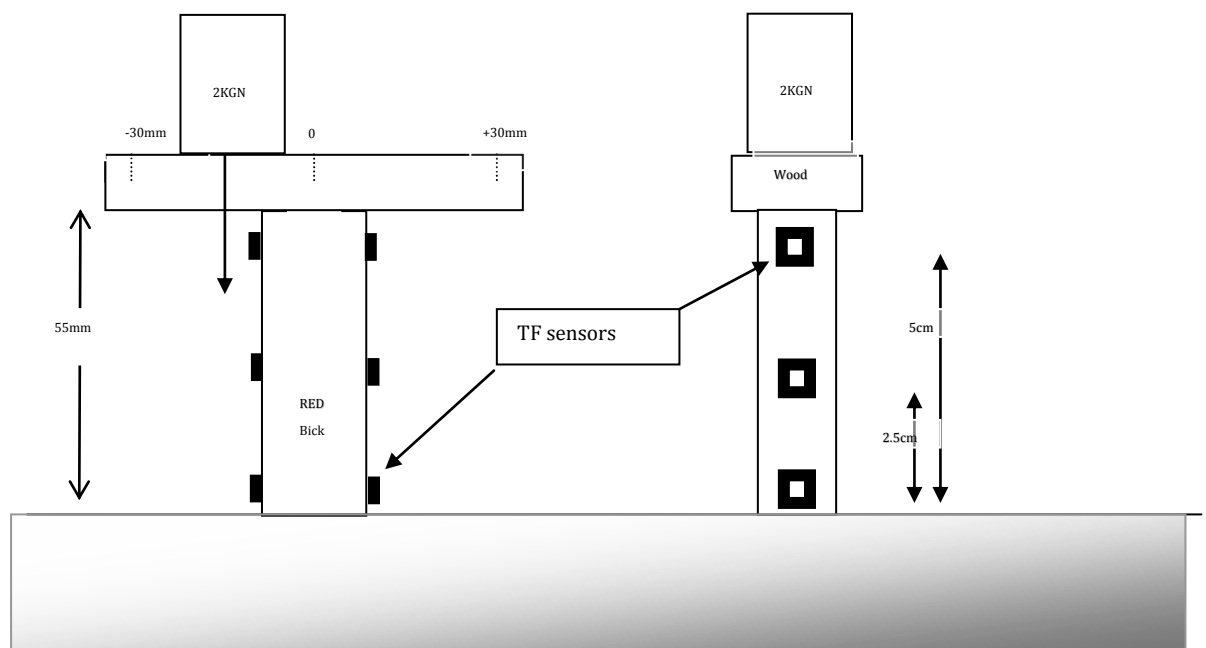


Figure 6.4 Sketch of the column stability test setup

The circuit used is the differential amplifiers configuration shown in **Figure 6.5**.

In this schematic diagram, Side-1 and side-2 are the two TF sensors allocated on opposite sides of the column. The test was performed for each height of sensors and results can be seen in **Figure 6.6**. The 5cm height result is not reported in this figure because it has a weak signal.

The procedure is always to reset the difference between the two op-amp outputs by injecting current in one side through the V-DAC coming from the D/A converter output of DAQPod1200 and LABVIEW software. The instrumentation amplifier gain is 10.

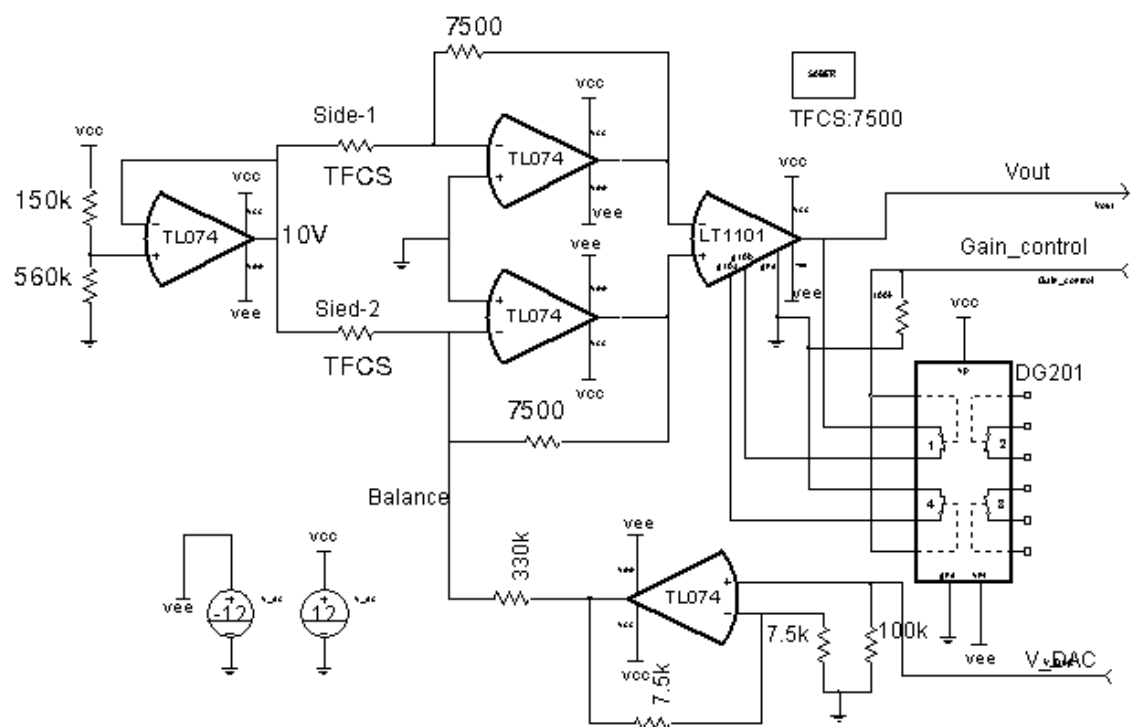


Figure 6.5 Circuit to observe column stability

Figure 6.7 is an image of the test.

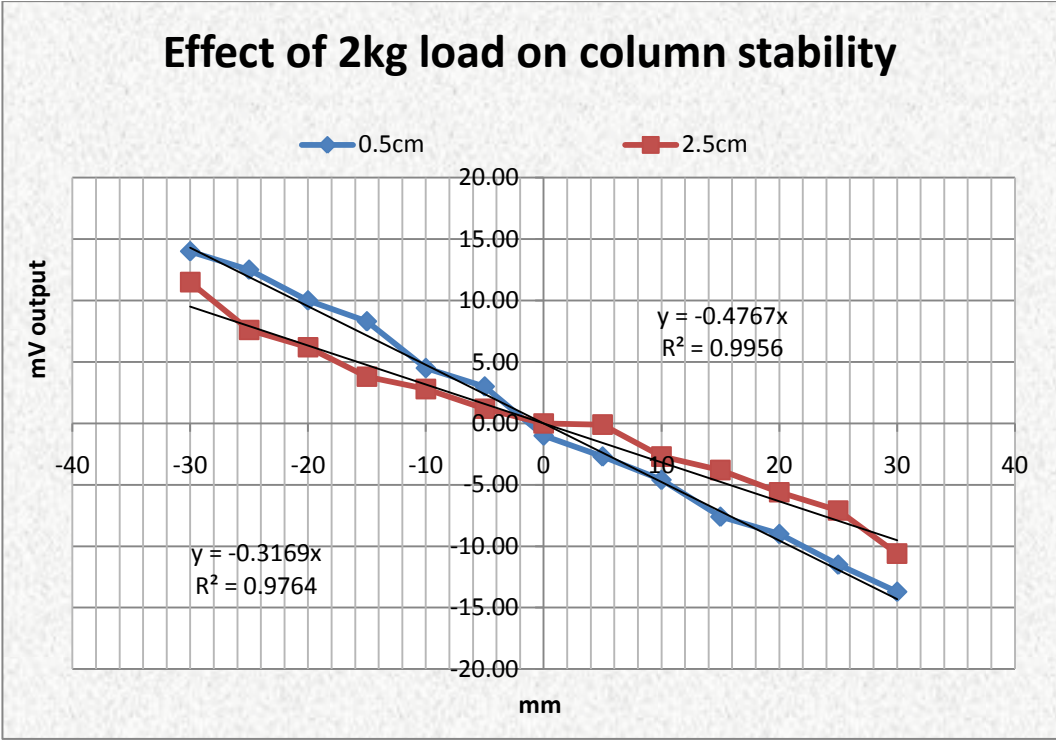


Figure 6.6 Brick column response as function of load movement



Figure 6.7 TF sensors on sides of Brick column with moving load

6.3.3 Mechanical Simulation of the Column Structure

The structure in **Figure 6.7** is simulated mechanically with Framesolver software. Point (0) on the mechanical diagram will move in X and Y directions and the displacement can be seen from **Figure 6.8** and **Figure 6.9** to be X=0.0004 mm and Y=0.0124 mm.

There are different ways to find the solution for the strain on the internal side of the column. Since the displacement of point (0) is already available from the mechanical simulation, the column behaviour is similar to a cantilever beam and the total strain has two components, one is from the bending moment of a cantilever beam and the second is the compressive strain long the column axis = P/A .

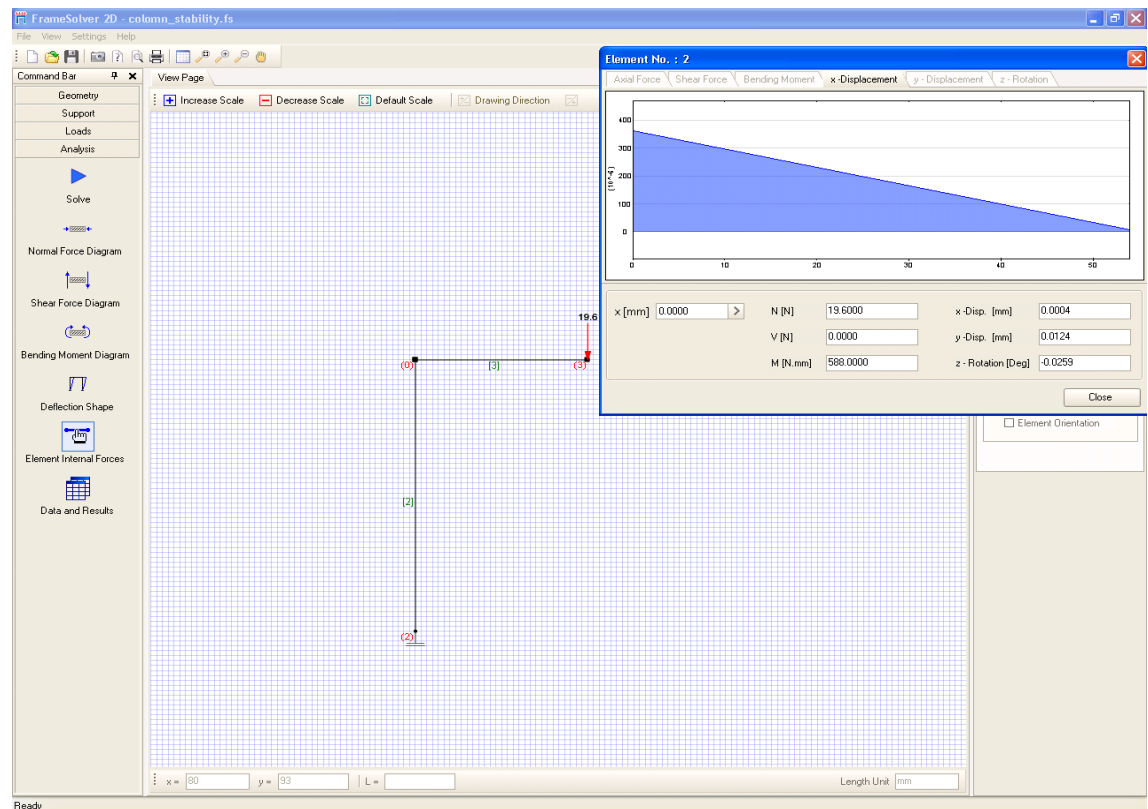


Figure 6.8 Simulation of brick column loaded with 2Kg at 30mm

$$\epsilon_t = \epsilon_1 + \epsilon_2$$

6.1

From cantilever equations;

$$\epsilon_2 = \frac{6 \cdot x \cdot \delta \cdot h}{4l^3} \quad 6.2$$

Where x is the sensor position from the point (0) of load = 50mm.

δ is the deflection in the x-direction = 0.0004mm

h is the column thickness = 17mm

l is the total cantilever length = 55mm

As a result, the strain, ϵ_2 at 50mm from point (0) is found to be about 3 μ strain.

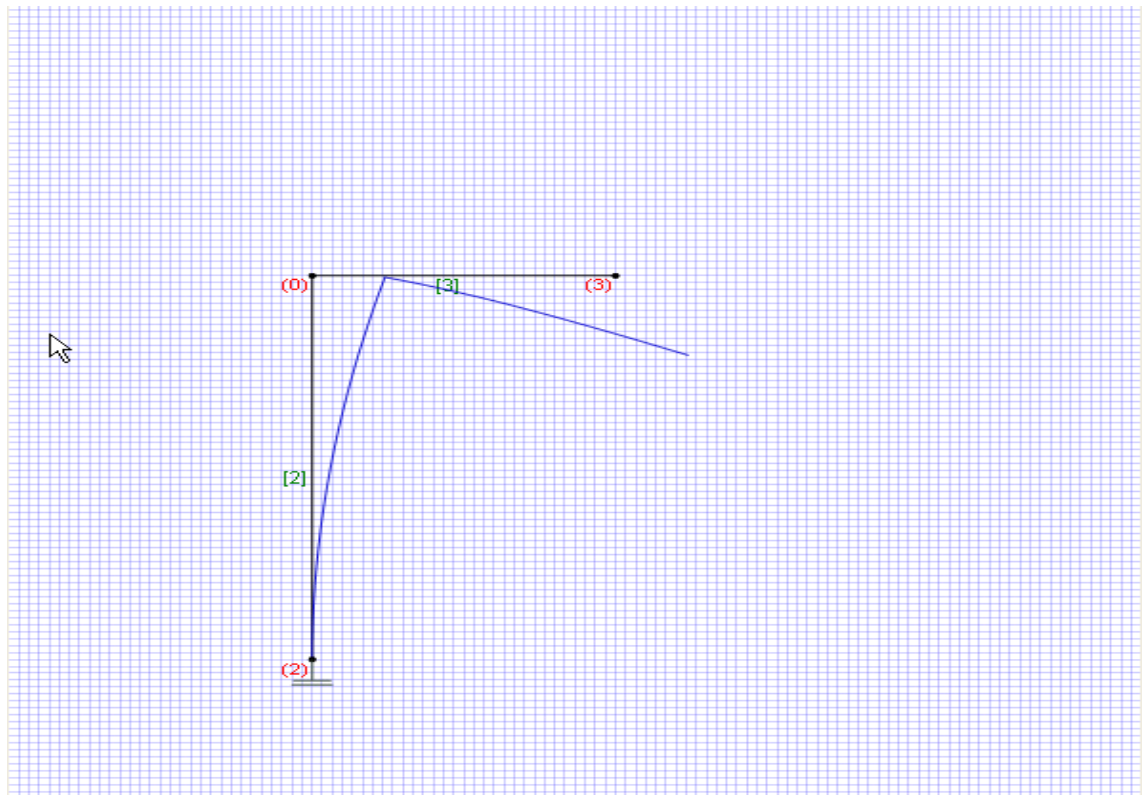


Figure 6.9 Column side loading behavior

By considering a GF of 13-14 in bending, the corresponding $\Delta R/R$ can be calculated from:

$$GF = \frac{\frac{\Delta R}{R}}{\epsilon} \quad 6.3$$

The other strain component is from the compressive force long the column which is From Hook' law,

$$\epsilon_1 = \frac{\frac{P}{A}}{E_b} \quad 6.4$$

The GF considered in this case is 1.25 and the corresponding $\Delta R/R$ could be calculated also from 6.3. Finally, from 6.5,

$$V_o = 2V_r G \times \frac{\Delta R}{R} \quad 6.5$$

The voltage swing was found to be about $\pm 10\text{mV}$, which is similar to experimental results with small difference that could be due to GF, modulus of elasticity and distances tolerances. In addition, the column is not one piece of brick but it is made of two joined sample bricks. In the equation, two was used instead of four, as there are only two sensors in the bridge.

6.3.4 Current Source to Improve Signal

The current source circuit introduced in chapter three can also be used in differential mode as shown in **Figure 6.10**. The advantages of using this configuration is first to allow covering various points on each side of the monitored structure and secondly to increase the sensitivity of the system to strain. The side-1 block contains four TF ceramic sensors allocated as appropriate on the column. This number can increase according to the need of sensitivity, which is dependent on the column material and size, and on the column floor and forces involved.

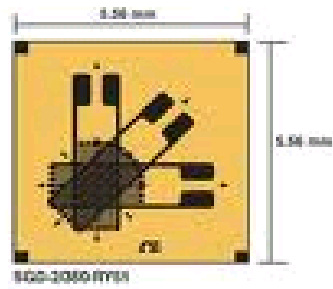


Figure 6.11 Rosette Foil Strain Gauge

Similar technique may be used in TF sensors either by printing three TF piezoresistive sensors on the same substrate or to use different single sensors oriented appropriately. (KERNS et. al. 1989) showed experimentally how the TF resistor geometry affects GF_T with respect to GF_L . This experimental work can be used as a guideline to increase directivity or direction selectivity of a newly designed sensor useful for structure stability monitoring.

6.3.6 Embedded TF for Structure Stability

In the experiment of **Figure 6.7**, the TF sensors were glued on the brick surface.

As shown in chapter four, the sensor can also be embedded in the structures.

Two TF sensors were embedded in two opposite sides of a 30 x 30 x 106 mm column made of plaster. The two sensors mounted on PCB were embedded during column construction. Two slots in the mold allowed for sensor insertion. Plaster requires short time to harden. As shown in **Figure 6.12 and Figure 6.13**, a plane was glued on top of the column with its base fixed to see the effect on moving a load on the plane. The same circuit that was used for the brick column in **Figure 6.5** was also used in this experiment. A 3 kg load was moved in steps of 20 mm long one axis from -100 to 100 mm and the resulting output voltage is shown in **Figure 6.14**.



Figure 6.12 An experiment on a column supporting a floor



Figure 6.13 TF sensors embedded and on surface of plaster column

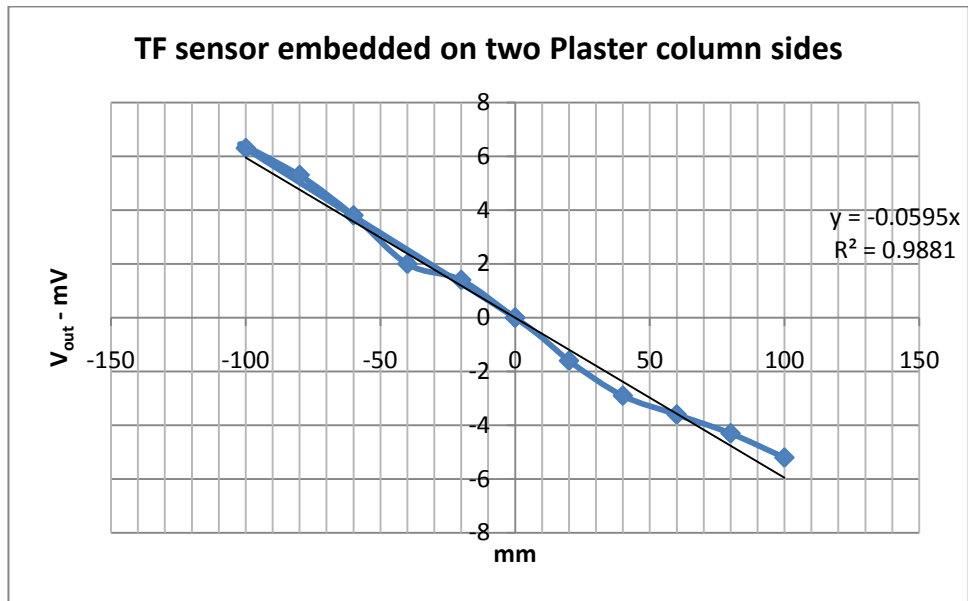


Figure 6.14 Response to load of two embedded TF sensors in plaster column

The linear equation of the best-fit straight line; $V_{out} = -0.0595 X$ describes the sensitivity of this structure to load decentralization.

Lower output voltage with respect to **Figure 6.6** is due to:

- a) The bigger dimensions of the column and
- b) Higher modulus of elasticity of plaster.
- c) Sensors are working only in tension (bending down) i.e., when the load is on the other side with respect to the sensor, the column material is not pulling up the sensor to make it work in compression.

6.3.7 Direct Load Application for Structure Stability

Similar to gluing sensors on side of a structure to observe unbalance load, direct load application on TF sensors can also be used. The four sensors applied on steel and brick in **Figure 6.15** can be used to monitor stability in the x, y directions and measure also load contemporarily.

Either the circuit in **Figure 6.5** or **Figure 6.10** can be used to monitor stability of a structure with for direct load application by assigning two sensors of **Figure 6.15** to one instrumentation amplifier input and the other two for the other input. At the same time, the four outputs may indicate the vertical component of the load.

When the differential output is around zero, the structure (column, wall or similar) is stable and the total sum of the sensors is the applied load.

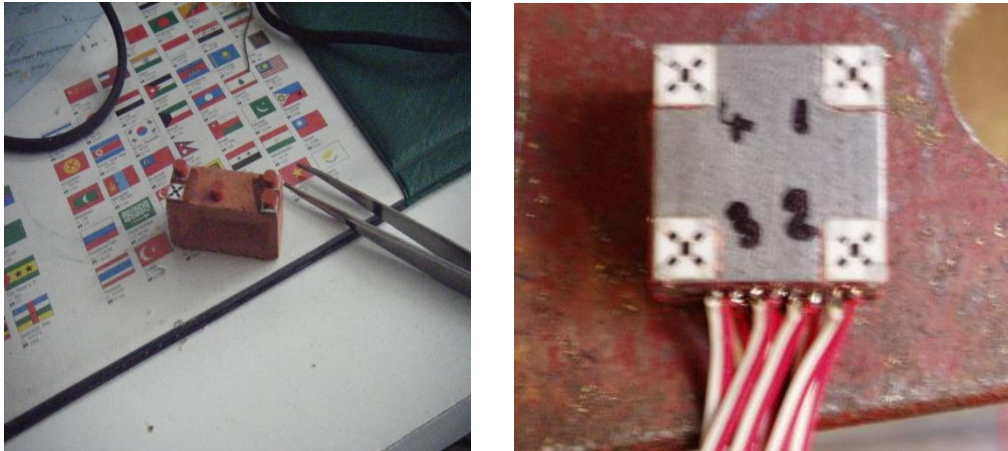


Figure 6.15 Four TF sensors used to monitor load and stability

6.4 Floor Stability

The response shown in **Figure 6.4** is due to the movement of the load on one axis like X. On the same column, it would be possible to observe the force decentralization on a floor plane by adding other sensors to signal the strain on the other axis, Y. This way, it would be possible to have $\pm X$, $\pm Y$ signals to indicate stability or load Bari centre of a floor. This application is extendable to any erected structures. **Figure 6.12**, shows an experiment of a plane supported by a Plaster column. **Figure 6.16** is a block diagram showing four current sensor groups allocated on each side of a column. Their output is differentiated with the other side one time to monitor stability in the x and y directions and at the same time the sum gives an indication of the total load supported.

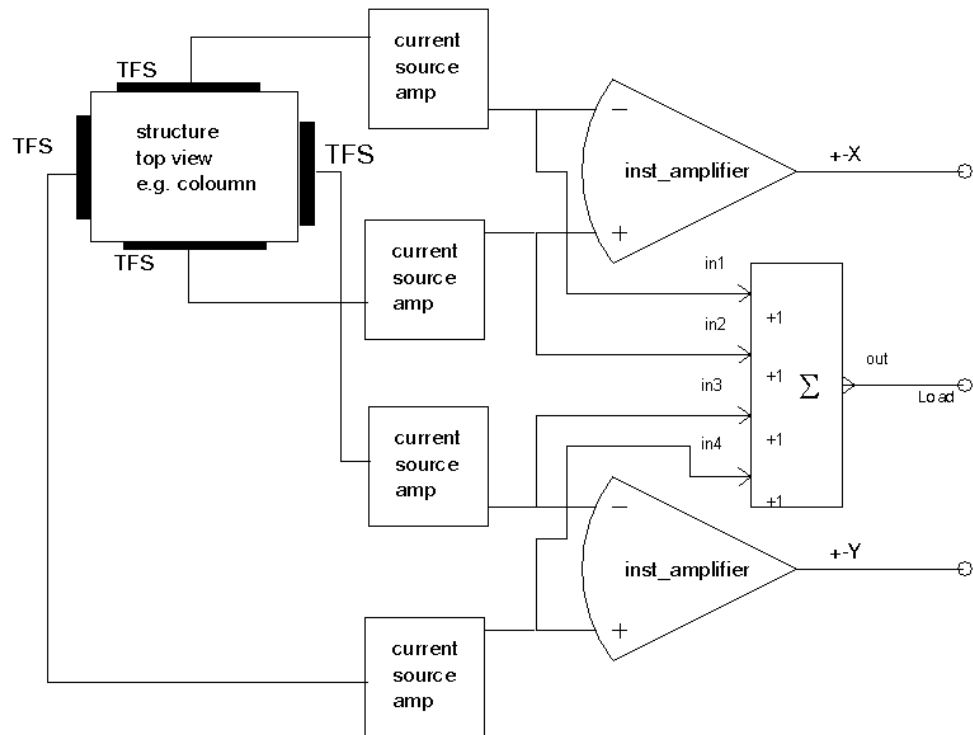


Figure 6.16 Block diagram of load and stability measuring system

6.5 Microcontroller Based System

It has been shown so far that the three ways of application of TF piezoresistive sensors are viable to assess local conditions of a civil structure. Buildings, bridges, and towers are typically large and complex. Information from just a few sensors is inadequate to accurately assess the structure condition. The dynamic behaviour of these structures is very complex both in spatial and time scale.

Several sensors, superficial or embedded, need to be implemented in a network. These sensors could be connected in a wireless network to give a global vision of structure status. It could also be combined with the systems monitoring the dynamic frequency response of the structure by using Lamb waves. Local strain sensors constitute a significant aid to comprehend the dynamic behaviour.

However, a local sensor system implementing TF technology will need to be “smart”. The essential difference between a smart sensor and a standard

integrated sensor is its intelligence, i.e., the on-board microcontroller which is essentially a microprocessor plus other peripherals like A/D, D/A, Timers, Memory, etc. integrated on the same chip. Programs can be embedded in the microcontroller, which allows smart sensors to save data locally, perform desired computations, make decisions, scan necessary information, send results quickly, schedule multiple tasks, coordinate with surrounding sensors, etc.

The on-board microprocessor can also control the time and duration that the sensor will be fully awake so as to efficiently manage power consumption. The smart sensors can arrange autonomous networks to achieve multiple tasks, such as SHM, power saving, multi-hop communication, self-configuration and self-healing of the network, dynamic routing, etc.

Here are some of the tasks that a smart sensor should handle:

- Be able to monitor on timely basis, e.g. once or twice a day, the status of stability of the structure
- To set a baseline of the structure and to use this memorised base line as a reference for future readings and alarms.
- To manage communication protocols with a central data base or neighbouring sensor systems.
- To compensate for environmental effects
- To set alarms in case of exceeding certain memorised limits
- To manage the power of the system.

A practical implementation of what has been said and showed so far is shown in **Figure 6.17**. A microcontroller system to monitor the stability and load of a structure like a column or wall. The minimum requirements for the microcontroller are as follows:

- At least three A/D converter inputs, for $\pm X$, $\pm Y$ and load readings. These can be three multiplexed A/D channels. The number of bits depends on many factors like the material, power supply, precision, etc. The load is the sum of the outputs of the four TF sensors on the four sides of the column.

- Three D/A converters to reset the outputs to zero at power up and to memorize this value for future readings. Other less expensive techniques could be used like Pulse width Modulation.
- One reference voltage. In this schematic, reference voltage is made with simple partitioning resistors. It would be better to use a very stable voltage reference.
- The analogue switch (DG201) will eventually set the gain of the amplifier to 100 in case smaller signals need to be monitored.
- RF communication is necessary to integrate the system in a network and to allow for changing configuration on demand like e.g. increasing gain.
- Power need to be comparable to structure life and it is the one essential critical part in SHM systems. A separate paragraph will be dedicated to power consideration.

6.6 Power in Structural Health Monitoring

A major concern with any embedded wireless sensing networks is their long term reliability and sources of power. If the only way to provide power is by direct connections, then the need for wireless protocols is eliminated, as the cabled power link can also be used for the transmission of data. However, if one elects to use a wireless network, the development of micro-power generators is a key factor for the deployment of the network. Possible solutions to the problem of localized power generation are technologies that enable using ambient energy to power the instrumentation. Although energy gathering for large-scale alternative energy generation using wind turbines and solar cells is mature technology, the development of energy gathering technology on a scale appropriate for small, low-power embedded sensing systems is still in the developmental stages, particularly when applied to SHM sensing systems.

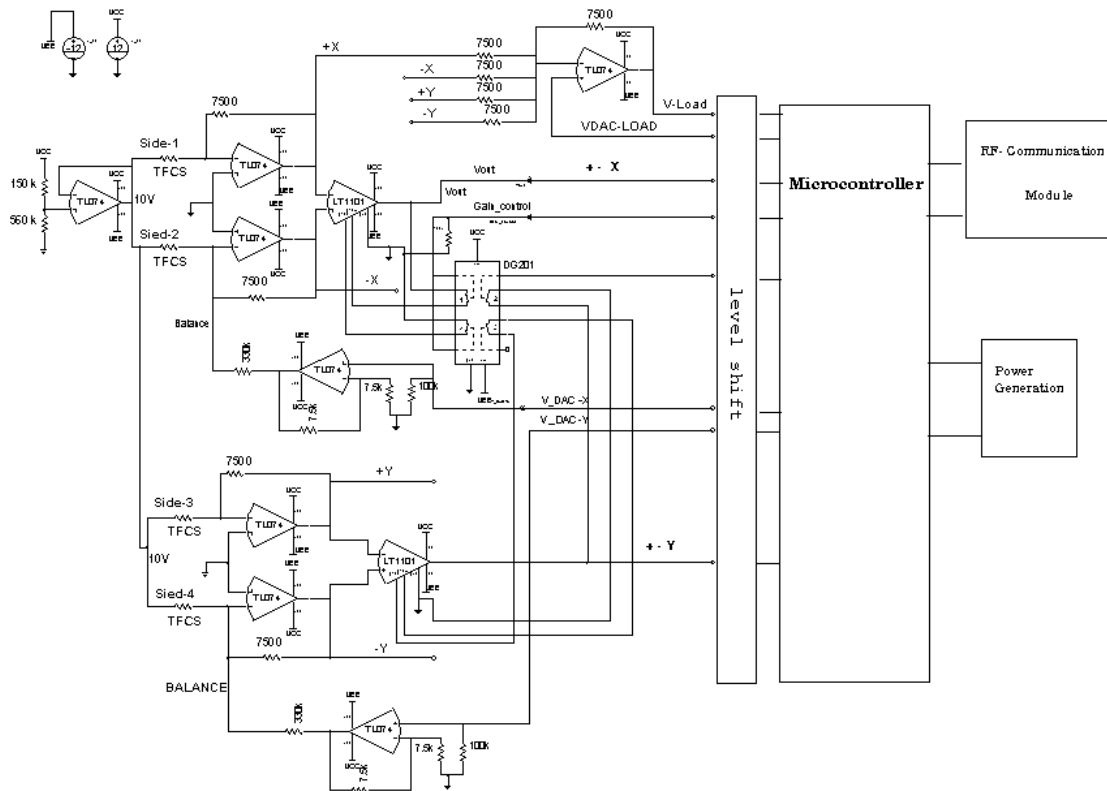


Figure 6.17 Microcontroller system to monitor structure stability

Given these reasons, the amount of research devoted to energy gathering has been rapidly increasing, and the SHM and sensing network community have investigated the energy harvesters as an alternative power source for the next generation of embedded sensing systems.

Besides the usual technologies like solar energy, some intelligent measures might be used to save energy like to power on demand or in case of exceeding certain stress limits settable by the wireless network. Another way is to power on any stress activity. Similar technique was used by the author in an athlete power device mentioned in (JABIR 2001), the prototype of this system is still working after 10 years.

The most interesting application is mentioned in (PFEIFER et. al. 2001) where the stresses in a structure themselves are used to generate power for the instrumentation. A piezoelectric device converts the mechanical energy to electrical energy to be stored. The amount of this energy is also an indication of the entity of the stress. Recently, Linear Technology, which is a semiconductor

manufacturer, introduced a chip dedicated to exploit the piezoelectric phenomenon for power harvesting.

6.7 Summary

In this chapter, practical considerations for deploying TF technology in real structural health monitoring systems were given. After having underlined and described the environment in which SHM has to work, hybrid technology and packaging technique were described as a solution to overcome these environmental difficulties.

TF piezoresistive sensors were deployed to monitor the stability of a column structure. Sensors were glued on column sides in one case and embedded in the column in another case. Response of moving load on the column supported floor was shown. The motivation for using smart sensors with a microcontroller was introduced and a circuit monitoring structure stability with a microcontroller was proposed. Finally, power in SHM systems and its importance was described and last innovations in this field were underlined.

7. Discussion, Conclusions and Recommendations

7.1 Discussion

The main objective of the study was to evaluate using Thick Film Ceramic sensors to measure strain on building material in the hope that this will give an aid to the vast field of Structural Health Monitoring.

In chapter one under research objectives, specific questions with regard to the suitability of using TF piezo-resistive sensors on building materials were posted. Those questions have been answered through this thesis as follows:

1. *Is a piezo-resistive thick film sensor suitable for measuring strain on building materials?*

The work through this thesis confirms the feasibility of using TF technology for strain and load measurements on building materials. Results are summarised in the conclusions of this research.

2- *How to interface TF sensors to measure loads in a reliably way and for a period comparable to the civil structures life?*

Two new interface circuits were proposed, verified mathematically and by simulation to give higher response with respect to the classical Wheatstone bridge. The current source circuit provides a way to add sensors gauge factors and to collect strain from different geometrical structure scenarios. The proposed circuits maintain the differential functionality advantages of Wheatstone bridge. However, Thick film strain sensor can also work with a Wheatstone bridge.

3- What are the advantages of using Thick Film technology?

Thick film technology is defined by a particular manufacturing process. This process is screen-printing and firing. The range of materials available, therefore, is determined by their capability of being both printed and fired. Research and development brought all sorts of materials that reveal sensitivities to various physical and chemical phenomena. Besides the availability of materials, TF fabrication technology allows physical forms to be realised which by constitution and shape facilitates appropriate interaction with the physical world.

Thick-film hybrid technology is also an interconnection technology that allows different electronic components of various degrees of complexity to be assembled to form systems capable of signal elaboration. This process does not require big investment compared for example to semiconductor manufacturing. An estimation of the cost of small size semiconductor production line is from one to two million USD compared to 0.1 to 0.2 million USD of thick film. The process of semiconductor manufacturing often requires hundreds of sequential steps, each one of which could lead to yield loss. Consequently, maintaining product quality in manufacturing facility often requires the strict control of hundreds or even thousands of process variables. Production in thick film technology has much less parameters and hence yield is less susceptible to process variation. Basic material cost is also lower; in TF technology e.g. 40 cm² 0.3 mm thick Alumina substrates price is around 1 USD compared to the 300 USD of a 12 inch diameter wafer (730cm²) which means a cost per square cm of TF of 2 cents/cm² compared to 41 cents/cm² of Silicon wafers. (prices were found on the web in February 2011).

Thick film hybrid technology responds to the need of civil and industrial structures of different kinds of sensors, to measure various physical and environmental entities, relevant to building security monitoring like

temperature measurement [FERRARI 2002], (MAHAYEER 2001), Gas (DAE 2002)], and chemical biosensors (VOSKERICIAN 2005).

An important topic in SHM is the power supply for the intelligent sensors. The supply is necessary to drive electronics and the networking to monitor a structure during its life, which might last for tens of years. It is well known that cadmium sulphide can be screen printed and sintered to form films that display photosensitivity. Photoconductive sensors based on screen-printed cadmium sulphide and cadmium selenide Thick Films printed over standard silver-palladium conductors are feasible. Simple photoconductive arrays and a potentiometric position sensor have been fabricated with Thick Film Technology (ROSS 1994, NICOLL 1955) and (VOJDANI 1973).

Substrates made of ceramic material or steel has outstanding mechanical and thermal properties, which make them adequate on one hand to have stable electronic circuits and to withstand harsh environmental conditions on the other.

Compatibility with Hybrid circuit technologies like LTCC enables packaging techniques and compactness suitable to work in the SHM harsh environment.

4- How can Thick Film piezo-resistive sensors be employed?

It has been shown that TF sensor can be deployed on building materials in two methodologies; glued on the surface or embedded into the building material. Differences of these applications are summarized in the conclusions.

5- What are the limitations of the technology and what are the recommendations to improve the usage?

- Thick Film sensor glued on material with load parallel to sensor, showed a very low signal response to stress. The gauge factor was about 1.3, which is lower than foil strain gauges GF known to have a value of 2. This is due to the fact that ceramic is a harder material than both the epoxy and the specimen.

The strain in the ceramic will be relatively small in accordance with its higher modulus. However, the crucial area will be the edge of the joint, where there will be a large increase in strain at the edge. This behaviour is similar to a bolted joint where the majority of load is taken by the first few threads.

The modulus of elasticity of epoxy is around 70 GPa, the mismatch between brick and ceramic will be accommodated by the epoxy; provided the latter can accommodate the large strains experienced near the joint edge. The force on the ceramic is only partial with respect to the total. **Figure 7.1**, shows how would the glue behave in the middle between ceramic and specimen.

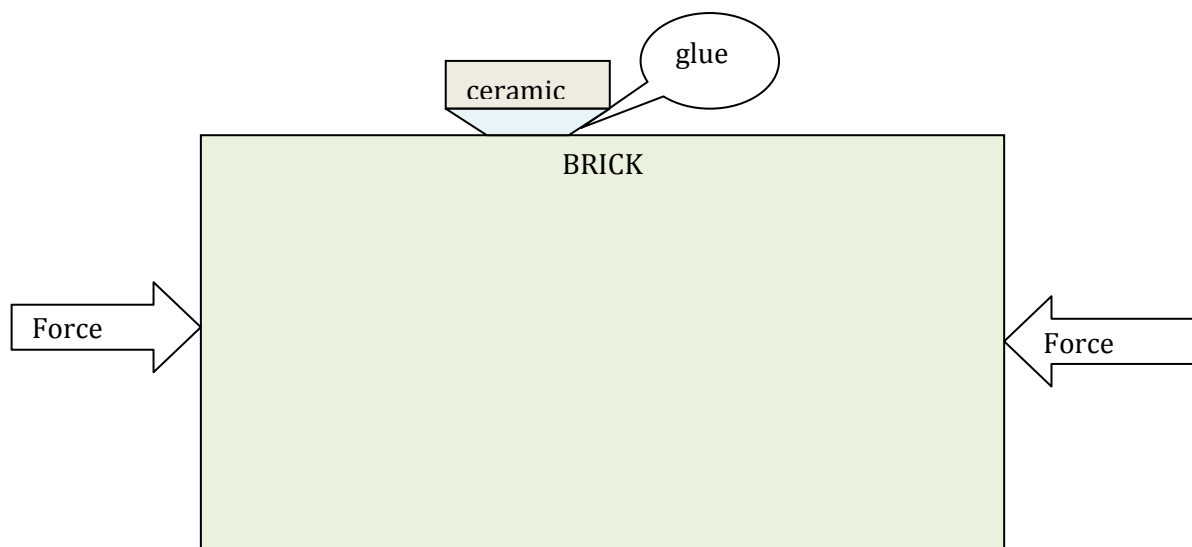


Figure 7.1 TF Ceramic sensor glued on sample Brick

The epoxy rigidity must be much higher than ceramic. This is a big limitation for ceramic substrate as there is almost no epoxy or other glue with such high modulus. In the recommendation, other substrates will be suggested. However, even with this limitation, TF sensor showed a consistent response with the kind of material on which it is glued and it maintained linearity.

The load on the ceramic is partial with respect to the total load and depends on the modulus of sensor, glue and the specimens. The following equation learned from adhesive industry (MAXWELL 2010) gives approximate results:

$$P_c = \frac{E_c \cdot h_c}{E_c h_c + E_b h_b + E_e h_e} P_{total} \quad 7.1$$

Where:

P_c = Shear Force on ceramic sensor/metre

E_c = Shear modulus of elasticity of ceramic

E_b = Brick elasticity modulus

E_e = Epoxy elasticity modulus

h_c, h_b, h_e = are thicknesses for ceramic, brick and epoxy

P_{total} = total force applied to the brick/metre

- The output voltage of **Figure 4.13** when applying the compressive stress on brick and concrete samples was of different sign, i.e. with concrete was positive while with brick was negative. This means that R_{c1} and R_{c2} were in one case increasing with compressive stress while the in the other case was decreasing. The expectation would be that the TF sensors resistor will be shortened and its resistive value decrease. The explanation for this phenomenon could be in the Poisson's ratio.



Figure 7.2 Bulge occurs in the middle in relatively flexible material

From the web site of University of Wisconsin, <http://silver.neep.wisc.edu/~lakes/PoissonIntro.html>, we learn that the material is constrained at contact surfaces by the compression device, so the Poisson effect cannot freely occur. Bulge occurs in the middle as shown in the image in **Figure 7.2**, causing the thick film resistor to bend up. This same phenomenon was also encountered with soft wood cubes.

The effect of bending the middle prevails on the contraction effect. This phenomenon is due to the hard substrate material on which thick film resistor is implanted. Bulge is related to the stiffness (Appendix-D) of the compressed material. In general, elastic modulus is not the same as stiffness. Elastic modulus is a property of the constituent material; stiffness is a property of a structure. That is, the modulus is an intensive property of the material; stiffness, on the other hand, is an extensive property of the solid body dependent on the material and the shape and

boundary conditions. For example, for an element in tension or compression, the axial stiffness is

$$K = \frac{AE}{L} \quad 7.2$$

where

A is the cross-sectional area,

E is the elastic modulus (or Young's modulus),

L is the length of the element.

For the special case of unconstrained uni-axial tension or compression, Young's modulus can be thought of as a measure of the stiffness of a material. This phenomenon and how it is related to TF substrate requires more investigation as the TF response to the property of the material is maintained however even if it has a different sense. Tests on Wood with higher L and less A gave the expected result, i.e. to decrease resistance in compression.

- The attempt to characterise TF sensor before deployment, works only for the case when the specimen is under bending moment and when the sensor is mounted in SMD on PCB or hybrid. The expectation is that when gluing on material surface, the ceramic substrate has a maximum supportable strain of $\pm 1000 \mu\text{strain}$ which is a big limitation on one hand and a feature on the other; the limitation is because the desirable range in building materials may exceed $\pm 2500 \mu\text{strain}$. Nevertheless, this limitation could be used in certain scenarios as a predefined alarm limit. The intelligence of the system has to take different actions when the sensors are within their operating limit and to take other actions in case of a break recognized by an open circuit.

Strain gauges can be printed on an elastic deformable structure to realize low-cost, high-sensitivity mechanical sensors, such as displacement, force,

acceleration, torque, pressure sensors. The use of a metal substrate in TF mechanical sensors has been already proposed (PRUDENZIATI 1982). The metal substrate insulation is simply obtained by screen printing and firing a dielectric layer on the substrate. This solution has some advantages over conventional alumina substrates: the maximum elastic strain is generally much higher than in a ceramic substrate, the value depending on the metal substrate used. In addition, metal substrates can often be worked simply in various shapes and sizes to obtain more complex structures and constraints can be easily implemented avoiding excessive stress and shocks (MIROLI 1994).

Besides alumina, there are other substrate materials which are of interest for various reasons. These are; zirconia, zirconia-toughened alumina (ZTA), LTCC and printed circuit board (PCB) fibreglass reinforced epoxy laminates substrates that are Flame Retardant FR4. These polymer substrates are a particular class, as they require polymer thick-film compositions, which can also use epoxy resins as a matrix, combined with silver and graphite fillers for conducting and resistive compositions (MAEDER 2005). Compared to other substrates, they potentially allow the highest strains, as they have strength comparable to that of alumina at a far lower elastic modulus. This substrate might resolve the gauge factor issue when gluing on building materials and load is parallel to the sensor substrate plane.

7.1.1 Contributions to knowledge

Through the work to answer the posted questions in the research objectives, and by going through the literature to know the state of art of the technologies in SHM, the following contributions could be counted:

- Thick film piezo-resistive technology to measure strain has never been considered for civil structure health monitoring and the results of this investigation open new researches and many industrial applications in the SHM field in particular in light of the suitability of thick film

technology to develop many other kinds of sensors measuring different properties, useful for monitoring structure's health.

- A Thick Film sensor suitable for different ways of deployment on building materials was developed, simulated and validated to reach the prefixed objectives. The sensor is suitable for SM technology and can be organized in different arrays and arrangements on PCB or on hybrid circuit to cover different structural geometrical force measurement requirements. The sensor was deployed successfully on different building materials and helped in reaching study objectives and provided orientation for further research and development to realize a real system.
- Two alternative circuits to Wheatstone bridge were proposed, simulated and used to interface TF sensors, one is the op-amp boosted differential bridge and the other is the current source to collect strains from array of sensors.
- Both circuits can use multiple TF sensors allocated under the right mechanical excitation to suit the measurement need. In other words, structures which have points of compressive and tensile strains can use the appropriate resistors in the bridge to either mitigate the signal to strain or to observe stability of the structure like in case of columns.
- The op-amp boosted bridge has the advantage of better sensitivity and stability. The stability is improved due to the fact that a stable reference voltage is a multiplier of the total circuit gain (equation 7.3).

$$V_o = 4V_r G \times \frac{\Delta R}{R} \quad 7.3$$

A reference voltage V_r is used to multiply the gain G .

- Tests for embedding the surface mounted TF sensor in building material during construction can still work after drying with little change in the piezo-resistance. Sensor survives humidity and at least curing of two materials; concrete and plaster. This is an important fact

for building material testing and opens new fronts of research and development not only for strain measurement but also for other properties like chemicals, gas, etc..

- Direct application of load on the ceramic substrate together with the fact TF sensors glued on supporting angles of a structure withstands mortar humidity opens a new horizon for load stability monitoring in civil engineering. It has been shown experimentally through the thesis that sensor response in direct load application, depends on the building material and the loading cushion over the sensor. The cushion could be of the various building material types like gypsum, or any mortar.
- Direct load application is useable to monitor stability of civil structures by allocating symmetrically sensors on sides of the monitored structure and using a differential amplifier. To monitor loads in different directions, a geometrical shape can be constructed with sensors glued on faces perpendicular to loads directions. Shapes of any suitable material could be for example a cube, or a ring etc.
- A methodology has been proposed and experimented to embed the SM sensor in erected structures (wood) and to have it to work in both tension and compression. This method will enhance the response of the electronics working in differential mode used to monitor stability. This is due to the fact that a structure has always two sides; one side is in compression the other is in tension. Surface glued TF sensors responds to both tension and compression while embedded sensors will work only when the structure is in compression. The proposed and experimented technique will insure the sensor response in both senses.
- TF sensor has been applied on surface of sides of a sample column and showed to be working in tension and compression to reveal stability of the structure supported by column or by a wall.

7.2 Conclusions and Recommendations

7.2.1 Conclusions

The work through this thesis confirms the feasibility of using TF technology for strain and load measurements on building materials.

After going through a literature review of the technologies used for SHM and TF sensor force and pressure applications, a sample thick film resistor was developed, simulated and its response was validated experimentally.

It has been shown that the designed TF sensor can be deployed on building materials in two methodologies; glued on the material surface (like metal Foil Strain Gauges; FSG) and embedded into the material. When the TF sensors are glued on surface, the load can be applied in three ways, 1) directly on the sensor substrate 2) away from the sensor substrate like in beams and 3) parallel to the sensor gauge like in tension or compression of the building blocks. Each one of these methods has different response gauge factor. The glued sensor on material surface with load parallel to the gauge has a lower GF than FSG. For the used paste with nominal GF of 10, it showed a GF of 1.25. The response depends on the glue type and substrate. However, in this kind of application the response has been experimented and found to be linear and consistently proportional to the modulus of elasticity of the specimen.

On beams, TF sensor has a higher GF than its counterpart metal FSG and is predictable by characterisation before deployment by using three-point bending test.

It has been shown also that the sensor can be embedded in the building material where it is useful for assessing load on the structure and for stability monitoring. Embedding in erected structures has been shown to be feasible and predictable by characterization using a uniform load or pressure chamber.

Thick film sensors glued on the material with load directly applied on sensor substrate has been shown to have a response dependent on the 1) kind of building material, 2) kind of cushion on the sensor body and 3) the substrate.

Experiments were conducted on steel, brick, concrete, and wood where the TF sensor showed a linear and repeatable response dependent on the kind of material and way of deployment.

The circuits used to do the measurements were two new interface circuits verified mathematically and by simulation to give higher response with respect to the classical Wheatstone bridge. These circuits are 1) op-amp boosted Wheatstone bridge and 2) current source to sum effect of TF sensor array. The current source circuit provided a way to add sensors gauge factors and to collect strain from different geometrical structure scenarios. The proposed circuits maintain the differential functionality advantages of Wheatstone bridge.

This study is a first step investigation on the subject. The obtained results open several doors for further research and investigations. Followings are recommendations and directives for further research:

7.2.2 Recommendations

As a conclusion of the research, a sensor with different spec should be designed.

Here are the recommendations for future sensor:

- 1- Different substrates: A substrate like steel or fibreglass will allow for the measurement of higher strains suitable for building materials.
- 2- At least two resistors to be printed on the substrate, one in the centre and the other on the area of opposite strain as in **Figure 7.3**.
- 3- Three resistors to form the kind of rosette strain gauge would be of benefit to screen the lateral strains and have the possibility to define strain final direction.

- 4- To have the resistance geometrical shape longer in the direction of strain in a way to emphasize the longitudinal gauge factor GF_L as suggested by (KERNS 1989).

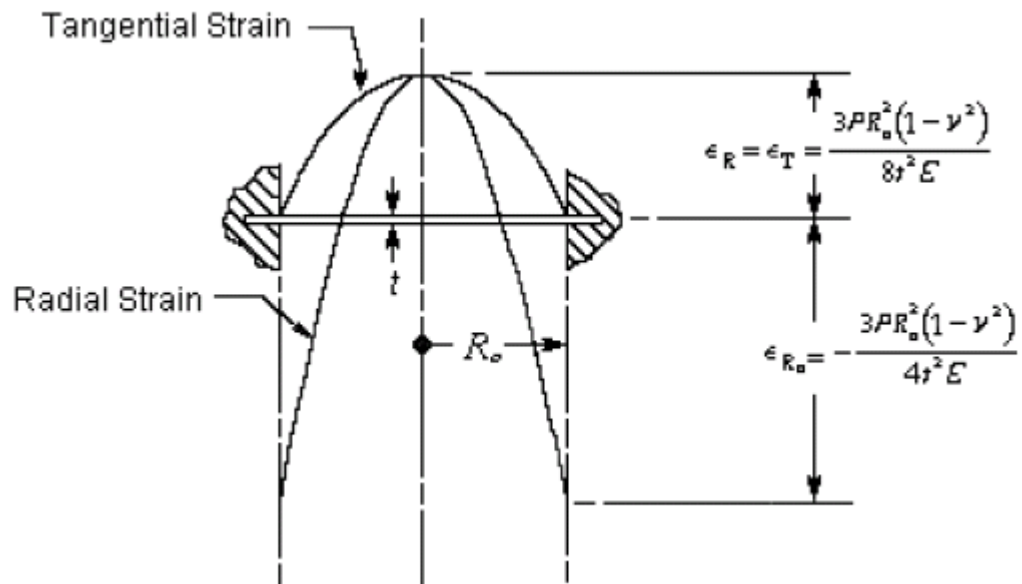


Figure 7.3 Edge clamped Diaphragm

To overcome the problem of low GF when glued on surface of building materials with load parallel to the gauge surface, following factors and their combination need to be investigated:

1. Using a fiberglass substrate
2. Experimenting different adhesives, which are on one side, more rigid than the substrate and on the other side are suitable to the kind of building material. This multi-discipline study requires chemical, mechanical and electrical knowledge and experience.
3. To increase the sensor substrate length to assure bigger adhesive lap area. The mechanics of stress-strain transfer through the joint is complex and not trivial.

4. One important deployment methodology to investigate is embedding the sensor parallel to the direction of load as in **Figure 7.4**.

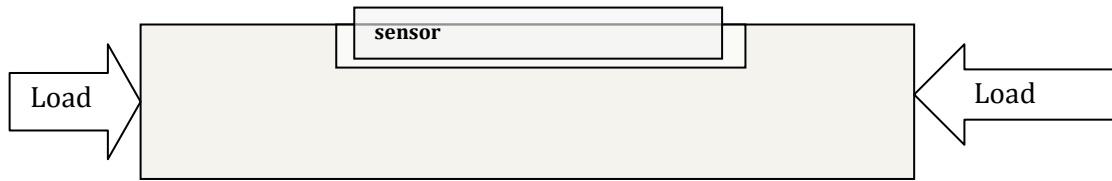


Figure 7.4 TF sensor embedded parallel to load

Other recommendations

- For the application of load directly on the sensor substrate, a mathematical model needs to be developed in a way to have the possibility to combine materials, loads and sensors. Finite element could be one approach.
- Burn in for life acceleration to investigate the reliability of thick film materials in the harsh building environment. This could be one part of a study on the compatibility of materials of this technology. The variables are many; pastes, substrates, adhesives, solders, and all building materials.
- The microcontroller circuit could be completed for a small system that can be interfaced optionally to all three kinds of deployment methodologies. The prototype should be of hybrid LTCC technology. The sensor and electronics could be on the same hybrid circuit. Typical application could be the monitoring of monumental historical structures.
- Embedding TF sensors in Plaster and concrete during structure construction showed a problem that sensors start to function at different loading thresholds.

To solve this problem, sensitivity of the PCB mounted sensor to loading might be increased by covering the central sensitive area of the sensor with another material like silicon or rubber. This active area is within the 3.5mm separating the soldering pads of the sensor. The 3D form of this material and its effect on sensor response could be a subject of future investigation.

8. REFERENCES

1. ALLEYNE, D. N. AND CAWLEY, P, "The Interaction of Lamb Waves with Defects", IEEE Transactions on Ultrasonic, Ferroelectrics and Frequency Control, Vol. 39, 381–397, 1992 ASTM D6272-00, American Society for Testing of Materials. 2001.
2. D6272-00 Standard Test Method for Flexural Properties of Unreinforced and Reinforced Plastics and Electrical Insulating Materials by Four-Point Bending, West, Conshohocken, Pennsylvania, 01-Jan-2000
3. ATKINSON D., SQUIRE P.T., GORE J.G. AND MAYILN RVTG., 'An integrating Magnetic Sensor based on the Giant Magneto-impedance effect, Sensors and Actuators 81 82-85, 2000.
4. ATKINSON D, GORE J, MAYLIN MG, SQUIRE PT 'integrating magnetic sensor', Patent No. GB2354593, US6747449., Application No. US 11/514793 filed on 01-Sep-2006
5. ASTM C 597-83, American Society for Testing and Materials, Standard Test Method for Pulse Velocity Through Concrete, West Conshohocken, PA, ASTM, 1991.
6. ATTOH-OKINE PHD, STEPHEN MENSAH NII O. "Civil Infrastructure Monitoring Using Microelectromechanical Systems (MEMS): A Case Study for Concrete Microcracking, Department of Civil and Environmental Engineering, University of Delaware, 2003.
7. BADCOCK RA, CURTIS PT, HUMBERSTONE L, KEMP RMJ " An initial investigation of Piezoelectric polymer composite films for 'Smart' sensing applications", DRA/SMC/CR963001, June 1996.
8. BALGAUGEAS D., FRITZEN C.P, GUEMES A., Structural Health Monitoring, Book, Publisher ISTE Ltd, 2006.
9. BARLOW J. , Quadrature Phase Shift Technique for Measurement of Strain, Optical Power Transmission, and Length in Optical Fibres, IEEE JOURNAL OF LIGHTWAVE TECHNOLOGY. VOL. 1. P. 1264, NO. 8. AUGUST 1989

10. BETHE KLAUS, "The Scope of The Strain Gauge Principle", VLSI and Microelectronic Applications in Intelligent peripherals and their Interconnection Networks Proceedings, pp.31-38, May 1989
11. BITER W. J., HESS S. M., OH S., "Magnetic Wire for monitoring strain in composites", Sensors, June 2001
12. BIRT EA, PERCIVAL WJ, "Large area damage detection in composite structures using ultrasonic Lamb waves ", insight: Non-Destructive Testing and Condition Monitoring, December 1996
13. BJORHOVDE REIDAR ,Evolution And State-Of-The-Art Of Column Stability Criteria Journal of Civil Engineering and Management ,16(2): pp159–165, 2010
14. BOWLES ADRIAN, GORE JON, TOMKA GEORGE 'An Amorphous AHoy Stress Sensor for Wireless, Battery-free Applications', Proceedings of SPIE, The International Society for Optical Engineering 5765 (PART 2), pp. 1104-1111,2005
15. Bristol university web site, in service structural behaviour of buildings 2005.
16. BRETT.A.WARNEKE, BRIAN S.LEIBOWITZ,MCHAEL D. SCOTT,LIXIA ZHOU, COLBY BELLEW, J. ALEX CHEDIAK, JOSEPH M. KHAN, BERNHARD E. BOSER, KRISTOPHER S.J. PISTER, "An autonomous 16mm³ solar-powered node for distributed wireless sensor networks", Berkeley sensor and actuator centre, University of California at Berekely. 2002
17. BROWNJOHN, J. M. W. , Structural health monitoring of civil infrastructure. Phil. Trans. R. Soc. A 365, 589–622. 2007
18. CARTZ, LOUIS Non-destructive Testing. A S M International. (1995).
19. CHANG F. K., M. LIN, 2nd International Workshop on Structural Health Monitoring, Stanford Univ., Technomic, pp. 603-611, 1999.
20. CHANG, F.-K. (1999), "Structural health monitoring: A summary report on the first International Workshop on Structural Health Monitoring", September 18-20, 1997.

21. CHEDLIZE D., CUSUMANO J., CHATTERJEE A., "Failure Prognosis Using Non-linear Short-time Prediction and Multi-Time Scale Recursive Estimation", Proc. of DETC '01, ASME 2001 Design Engineering Techn. Conf., Pittsburg, Pennsylvania, USA, Paper DETC2001/VIB-21407, 10 pages (published on CD), 2001.
22. CHEDLIZE D., "Dynamic System Approach to Material Damage Diagnosis", Proc. of DETC '03, ASME 2003 Design Engineering Techn. Conf., Chicago, Illinois, USA, Paper DETC2003/VIB-48452, 8 pages (published on CD), 2003.
23. CHITALE S.M., HUANG C.Y.D. AND STEIN S.J., "ESD Susceptibility of High Gauge Factor Thick Film Piezo-resistors", Electro-Science Laboratories, Inc., Presented at IMAPS, 1996
24. COHEN Y CAR ET. AL., Polymer Piezoelectric Transducers for Ultrasonic NDE NDT net, Vol.9,1996
25. DAE-SIK LEE, DUK-DONG LEE, SANG-WOO BAN, MINHO LEE, AND YOUN TAE KIM "SnO₂ Gas Sensing Array for Combustible and Explosive Gas Leakage recognition" IEEE SENSORS JOURNAL, VOL. 2, NO. 3, JUNE 2002.
26. DALTON RP, CAWLEY P, LOWE MJS, "The potential of guided waves for monitoring large areas of metallic aircraft fuselage structures" Journal of Non-destructive Evaluation. Vol20.No.1, 2001
27. DELL'ACQUA, "Thick Film Resistor Strain Gauges: Five Years After", Proc. IMC 1986, Kobe, Japan, May 28-30, pp. 343-351, 1986.
28. DETERESA S.J., "Piezoresistivity and failure of carbon filaments in axial compression", Carbon, V.29(3), pp397-410, 1991
29. DJINSTRUMENTS, <http://www.djstruments.com/> , 10 June 2010.
30. DOEBLING S.W., FARRAR C.R., PRIME M.B., SHEVITZ D.W., "Damage Identification and Health Monitoring of Structural Systems from Changes in The Vibration Characteristics: A Literature Review", report no. LA-12767-MS, Los Alamo National Laboratory, 1996.
31. Engineering and Mechanics-ISS (IMAC) EPFL-Swiss Federal Institute of Technology, CH-1015 Lausanne, Switzerland, 2000.

32. EULER, L., Methodus Inveniendi Lineas Curvas Maximi Minimive Proprietate Gaudentes (Appendix, De Curvis Elasticis). Marcum Michaellem Bosquet, Lausanne, year 1744
33. FARHAD ANSARI, Sensing issues in civil structural health monitoring, book, 2005
34. FARRAR CHARLES R AND WORDEN KEITH, An introduction to structural health monitoring, Phil. Trans. R. Soc. A 2007 365, 303-315, 2007
35. FERRARI VITTORIO, DANIELE MARIOLI, AND ANDREA TARONI Displacement Sensor Based on Pyroelectric Thick-Films and Contactless Light-Spot Cursor IEEE TRANSACTIONS ON INSTRUMENTATION AND MEASUREMENT, VOL. 51, NO. 4, AUGUST 2002.
36. FINLAYSON R.D., FRIESEL M., CARLOS M., Health Monitoring of Aerospace Structures with Acoustic Emission and Acousto-Ultrasonics, WeNDT, Roma 2000.
37. FIXTER L., WILLIAMSON C., "state of the art review – Structural Health Monitoring, QinetiQ , 2006
38. FRITZEN C.-P., JENNEWEIN D., KIEFER T., "Damage Detection Based Model Updating Methods", Mechanical Systems & Signal Processing 12 (1), pp= 163-186, 1998.
39. FRITZEN C. P., MENGELKAMP G., "In-Situ Damage Detection and Localization in Stiffened Structures", Proc. 23rd Intl. Modal Analysis Conference (IMAC), Orlando, FL, 2005, on CD-ROM.
40. GUEMES A. MENENDEZ M., chapter three, Book " Structural Health Monitoring", Publisher: ISTE Ltd,2006.
41. HALDAR ACHINTYA "Is the inverse problem technique appropriate for structural health assessment?" University of Arizona, Tucson, AZ 85721, USA, October 2009.
42. HERNANDO A. et al., "Metallic glasses and sensing applications", Journal of Physics E, V. 21(12}, pp1129,1988
43. HOLMES P. J. , MICROELECTRON. RELIABLIL. J. , 12(1973) 395, IHM J.-B., "Built-in Diagnostics for Monitoring Fatigue Cracks m Aircraft Structures", PhD Dissertation, Stanford University, Stanford, CA, 2003.

44. HOU Y., R. M. C. So, W. Jin, H. G. Xu and P. K. C. Chan, "Dynamic Strain Measurements of a Circular Cylinder in a Cross Flow using a Fibre Bragg grating Sensor", *Experiments in Fluids*, vol.27, pp.359-367, 1999.
45. IHM J.-B., CHANG F.-K., HUANG J., DERRISO M., "Diagnostic Imaging Technique for Structural Health Monitoring", *Proc. 2nd European Workshop "Structural Health Monitoring 2004"*, Munich, Germany, pp. 109-116, July, 7-9, 2004,.
46. INAUDI DANIELE ,BRANKO GLISIC, IAN SMITH " Towards Monitoring of Dynamic Deformations in Civil Structures using SOFO Sensors", *Structural Engineering and Mechanics-ISS (IMAC) EPFL-Swiss Federal Institute of Technology*, CH-1015 Lausanne, Switzerland, 2000.
47. IODOROKI A., KOBAYASHI H., "Application of electrical potential method to smart structures for detecting delamination", *Proceedings of ICCM-10*, Whistler, B.C., Canada, V. 5, pp.323-330 , August 1995
48. ISIS-CANADA, *Guidelines for Structural Health Monitoring, Design Manual n. 2*, September 2001.
49. JABIR SAAD , European patent app. N. WO2000IT00465 20001115 , "Detecting Device For The Forces Developing Under The Foot " 2001
50. JACQ C, MAEDER TH, AND RYSER P, "Sensors and packages based on LTCC and thick-Film technology for severe conditions", *Sadhana Vol. 34, Part 4*, pp. 677-687, August 2009
51. JOHNSTON, B. G.. Column Buckling Theory: Historical Highlights, *Journal of the Structural Division, ASCE 107(ST-4, April): 649-670*,1981
52. KERNS D.V., JR., KANG W.P., AL-ALI A.R., *Electrical Engineering Vanderbilt University Nashville, Tennessee*, "Piezoresistive Effects in Thick Film Resistors for Strain Sensing Applications", *IEEE Proceedings - South east conf*, 1989.
53. KESSLER, S. S., SPEARING, S. M. AND ATALLA, M. J, "In-Situ Damage Detection of Composites Structures using Lamb Waves Methods", In *Proceedings of the 1st European Workshop on Structural Health Monitoring, Ecole Normale Supérieure, Cachan, Paris, France*, 374-381 , 2002

54. KESSLER, SETH S., SPEARING, S.MARK AND DUNN, CHRISTOPHER T.
Packaging of structural health monitoring components. 219-229.(Proceedings of SPIE, 5391). (2004)
55. KRAUS L, FENDRYCH F, SVEC P, BYDZOVSKY J, KOLLAR M, "Cobalt Rich Amorphous ribbons for strain sensing in civil engineering" Journal of Optoelectronics and Advanced Materials, Vol 4, , p237-243 June 2002
56. LICARI JAMES J., ENLOW LEONARD R., "Hybrid Microcircuit Technology Handbook: Materials, Processes, Design Testing And Production", Book, 1998
57. LAMB, H, "On Waves in an Elastic Plate", Proceedings of the Royal Society of London, Containing Papers of a Mathematical and Physical Character, Vol. 93, 293-312.,1917
58. LEVASSORT F., LETHIECQ M. , DESMARE R., TRAN-HUU-HUE L.P., "Homogenization of Piezo-composites Containing Both 0-3 and 3-3 Connectivities" , Applications of Ferroelectrics, 1998. ISAF 98. Proceedings of the Eleventh IEEE International Symposium on, Page(s): 333 – 336,1998 ,
59. LIN MARK , QING XINLIN, KUMAR AMRITA, BEARD SHAWN J. „Smart Layer And Smart Suitcase For Structural Health Monitoring Applications, Acellent Technologies, Inc. 2005
60. LIN MARK, CHANG FU-KUO, "The manufacture of composite structures with a built in network of piezoceramics" Composites Science and Technology, p919 -939, 2002
61. LYNCH JEROME P. AND LOH KENNETH J., A Summary Review of Wireless Sensors and Sensor Networks for Structural Health Monitoring, 2006 SAGE Publications. April 17, 2008.
62. MAEDER THOMAS, FAHRNY VINCENT, STAUSS SVEN, CORRADINI GIANCARLO AND RYSER PETER," Design and characterisation of low-cost thick-film piezoresistive force sensors for the 100 mN to 100 N range", XXIX International Conference of IMAPS Poland Chapter Koszalin-Darówko, 19-21 September 2005

63. MAHAVEER K. JAIN AND CRAIG A. GRIMES, "A Wireless Magneto-elastic Micro-Sensor Array for Simultaneous Measurement of Temperature and Pressure", 2001.
64. MAXWELL JAMES DAVIS , <http://www.adhesionassociates.com/> , (July 2010)
65. 2022 IEEE TRANSACTIONS ON MAGNETICS, VOL. 37, NO. 4, JULY 2001.
66. MASON ANDREW, NAVID YAZDI, ABHIJEET V. CHAVAN, KHALIL NAJAFI, AND KENSALL D. WISE, "A Generic Multi-element Micro system for Portable Wireless Applications", IEEE 1997 revised 1998.
67. MATSUZAKI RYOSUKE, ODOROKI AKIRA T, "Wireless detection of internal delamination cracks in CFRP laminates using oscillating frequency changes" Composite Science and Technology, March 2005
68. MARIOLI D., ROLLA P. AND TARONI A.," THICK FILM STRAIN GAUGES ON INSULATED METAL SUBSTRATES FOR HIGH SENSITIVITY MECHANICAL SENSORS", IMTC 1994, IEEE 1994.
69. MARTIN TONY; FOOTE PETER; READ, IAN, "Acoustic-sensor-based detection of damage in composite aircraft structures", Proceedings of the SPIE, Volume 5272, pp. 341-348 , 1988.
70. MAYLIN MG, MILNE J, TOMKA JG, TREEN A 'Stress Sensor', Patent No. GB2390433, US6910384.
71. MEASUREMENTS GROUP TECH DESIGN , Note TN-510, Considerations For Diaphragm Pressure Transducers , 19/12/2000.
72. MILNE J., GORE J., TOMKA G., SKULL P " Effects of stress, temperature and annealing conditions on the transport properties of amorphous wires", Journal of Magnetism and Magnetic Materials 226 (SUPPL. 1), pp. 715-717, 2001
73. MORTEN, B., PRUDENZIATI M., "Piezoresistive Thick-Film sensors", Handbook of Sensors and Actuators vol. 1: Introduction, 1994.
74. MORTEN B., PIROZZI L., PRUDENZIATI M. And TARONI A., Journal of Physics D: Applied Physics 12, L51, 1997.
75. NICOLL F. H. AND B. KAZAN, Large area high-current photoconductive cell using cadmium sulphide powder J Opt Soc Am 45 647-650, 1955.

76. NICHOLS J.M., TOTOEV Y.Z., "Experimental determination of the dynamic Modulus of Elasticity of masonry units", Proceedings of the 15th ACMSM - 97, Melbourn, 1997
77. NORTON R.N., "Handbook of transducers for electronic measuring systems", Prentice Hall Inc, Englewood Cliffs, N. J. (1969) .
78. PEIL U., MEHIDIANPOUR R.SCHAREF R., FRENZM., " Life Time Assessment of existing Bridges", Proc. First European Workshop on SHM. Paris, France, pp9999-1006, 2002.
79. PFEIFER K. B., LEMING S. K., AND RUMPF A. N. , " Embedded Self-Powered Micro-Sensors for Monitoring the Surety of Critical Buildings and Infrastructure" , Sandia National Laboratories Albuquerque, New Mexico 87185 , 2001
80. PROSSER W. H., T. L. BROWN, S. E. WOODARD, G. A. FLEMING, AND E. G. COOPER, "SENSOR TECHNOLOGY FOR INTEGRATED VEHICLE HEALTH MANAGEMENT OF AEROSPACE VEHICLES, NASA Langley Research Centre, Hampton, VA 23681. 2002.
81. PRUDENZIATI M. B., Morten and A Taroni, Digest 1977 AEI Conference.
82. PRUDENZIATI M. "Handbook of sensors and actuators, Thick film sensors", 1994
83. PRUDENZIATI AND B. MORTEN, The state of the art in thick-film sensors Microelectronics Journal 23 133-141, 1992
84. PRUDENZIATI M., MORTEN B. AND TARONI A. , "Characterization of thick-film resistor strain gauges on enamel steel", Sensors and Actuators ,Volume 2, Pages 17-27, 1981-1982
85. PUERS B. SANSEN W. AND PASZEZYNSKI , Assessment of Thick Film Fabrication method for force (pressure) sensors, Sensors Actuators (1987)
86. POPOVICS SANDOR. "Analysis of the Concrete Strength versus Ultrasonic Pulse Velocity relationship", American Society for Non-destructive Testing. (American Society for Non Destructive Testing ,February 2001).
87. ROSS J. N. , Thick-film Photo-sensors, University of Southampton, <http://www.ecs.soton.ac.uk/publications/rj/1994/transduc/ross/ross.html>, 1994

88. RYTTER A., "vibration based inspection of civil engineering structures".
PHD thesis, Aalborg University, Denmark, 1993.
89. SARAVANOS, D. A., BIRMAN, V. AND HOPKINS, D. A., "Detection of
Delamination in Composite Beams using Piezoelectric Sensors", In
Proceedings of the 31st AIAA/ASME/ASCE/AHS/ASC Structures, Structural
Dynamics and Materials Conference, 181-191, 1994
90. SHAH J.S., IEEE Trans. Strain sensitivity of thick film resistors On
Component Hybrid and Manufacturing technology, 554, 1980.
91. SCHOESS J.N., "Conductive polymer sensor arrays: A new approach for
structural health monitoring", SPIE V. 4335, pp9-19, 2001
92. SCRANTOM C.Q. , GRAVIER G. J., " LTCC Technology Where We Are and
Where We're Going – IV, CMAC - Scrantom Engineering, Inc. June 2000
93. SINGER L. F, PYTEL A. Strength of material (Book), 1980
94. SION R. , A theoretical and experimental investigation of accelerometer
design using Thick Film technology, PHD Thesis, 1993
95. SMITH C.S, Phys. Rev. 94 (1954) 42.
96. SOEFFKER D., "Monitoring And Control of Reliability Characteristics as a
Base for Safe and Economical Operation of Technical Systems", Proc.3rd Intl.
Workshop on Structural Health Monitoring, Stanford, CA, Technomic Publ.
Co. Inc, pp.785-793, 2001.
97. SOHN H., WAIT J.R., PARK G., FARRAR C.F., "Multi-scale Structural Health
Monitoring for Composite Structures", Proc. 2nd European Workshop
"Structural Health Monitoring 2004", Munich, Germany, July, 7-9, pp. 721-
729, 2004.
98. STASZEWSKI W., BOLLER C., TOMLINSON G. (EDS.), Health Monitoring
Aerospace Structures - Smart Sensor Technologies and Signal Processing,
John Wiley & Sons, Chichester, 2004.
99. SU J. K., CHO S. W., YANG C. C., AND HUANG R. , Journal of Marine Science
and Technology, Vol. 10, No. 1, pp. 8-13, 2002.
100. STECHER, et al. G., "Integrated Hybrid Pressure Sensor Using a
Piezoresistive Thick Film Sensor Element", Sensors and Actuators,
Publisher SAE Inc., Warrendale, PA 15096, U.S.A., pp. 1-6. 1987

101. STEVEN R. ANTON thesis "Baseline-Free and Self-Powered Structural Health Monitoring" 2008.
102. SUN KE , "DESIGN AND CHARACTERIZATION OF PASSIVE WIRELESS STRAIN SENSOR" , master thesis , UNIVERSITY OF PUERTO RICO, 2006
103. SWARTZ R. ANDREW. "Active Sensing for Structural Health Monitoring", CEE619
104. VANN, AM, CAIRNS, J, DAVIS, JP & LINFOOT, BT. 'Intelligent Logging Strategies for Civil Engineering Applications', *Proc. ICE Structures and Buildings paper*, **116, Issue 2**, (pp. 194-203), 1996. ISSN: 0965-0911
105. TEGTMEIER, F.; PETERS, M.: "Determination structural damage to buildings using micro-sensors based on strain gauge technology" Proceedings of the IMEKO-XVI World Congress, Vienna, Austria, September 25-28, Volume VII, Topic28, 363-368, 2000.
106. TEGTMEIER FALK AND PETERS MANFRED, " Strain Gauge Based Micro-sensor For Spatial Stress Analysis In Building Structures", XVII IMEKO World Congress Metrology in the 3rd Millennium June 22–27, Dubrovnik, Croatia,2003
107. TOMKA G. J., GORE J., MILNE J., MAYLIN M. G., SQUIRE P. T., ATKINSON D. 'Properties of Giant Magneto-impedance material for a Novel Integrating Magnetic Sensor', Materials Research Society Symposium - Proceedings 577, pp. 499-504, 1999.
108. VOIGT THOMAS, SURENDRA P. SHAH. "Non-destructive Monitoring of Setting and Hardening of Portland cement Mortar with Sonic Methods", North western University, Evanston, USA ,NDT-CE international symposium 2003.
109. VOJDANI S., SHARIFANAI A. AND DOROUDIAN M., Photovoltaic junctions formed on silk- screened cadmium sulphide layers *Electron. Letts* 9 128-129, 1973.
110. VOSKERICIAN GABRIELA, CHUNG-CHIUN LIU, AND JAMES M. ANDERSON, "Electrochemical Characterization and In Vivo Biocompatibility of a Thick-

Film Printed Sensor for Continuous In Vivo Monitoring" IEEE SENSORS JOURNAL, VOL. 5, NO. 6, 1147, DECEMBER 2005

111. WALLASCHEK J., WEDMAN S., WICKORD W., „Lifetime Observer: An Application of Mechatronics in Vehicle Technology”, International Journal of Vehicle Design 28(2002), No. 1/2/3, pp.121-130, 2002.
112. WANG M L, North-eastern University, USA, Structural health monitoring of civil infrastructure systems, Book, Chapter 5, pp 153, 200, 2009
113. WARNEKE BRETT A., KRISTOFER S.J. “MEMS for Distributed Wireless Sensor Networks” Pister Berkeley Sensor and Actuator Centre, University of California at Berkeley . 9th IEEE International conference on electronics, circuits, and systems, Sept. 2002.
114. WEBSTER J.G Measurement , Instrumentation and sensors Handbook , CRC press, 1999 H.N. NORTON, Handbook of transducers for electronic measuring systems, Prentice Hall Inc, Englewood Cliffs, N.J. (1969).
115. WEDMAN S., WALLASCHEK J., The Application of a Lifetime Observer in Vehicle technology. Proc. 4th Intl. Conf. On Damage Assessment of Structures (DAMAS 2001), Key Engineering Material, Vol. 204-205. Uetikon-Zuerich: Trans Tech Publications, pp. 153-162, 2001.
116. WHITE N. M. AND. BRIGNELL J. E, A planar thick-film load cell Sensors and Actuators 25-27 313-319, 1991
117. WHITE N M AND TURNER J D Thick-film sensors: past, present and future , Measurement Science and Technology, Volume 8, Number 1 , 1997
118. WADA TAKESHI, STEIN SIDNEY J. STEIN MICHAEL ALA AND CHITALE SANJAY M., “the state-of-the-art of thick film technology for automotive sensors”, iemt/imc proceedings. 1997
119. WOLTERS K., SOFFKER D., "Control of Damage Dependent Online Reliability Characteristics to Extend System Utilization", Proc. 4th Intl. Workshop on Structural Health Monitoring, Stanford, CA, DesTech Publ, pp. 796-804., 2003.
120. X. WANG, S. WANG, D.D.L CHUNG, "Sensing damage in carbon fiber and its polymer-matrix and carbon-matrix composites by electrical resistance measurement", J. Mat. SeL 34{ 11) June 1999

121. WANG SHOUKAI, KOWALIK DANIEL P, CHUNG DDL, "Self-sensing attained in carbon-fibre-polymer- matrix structural composites by using the inter-laminar interface as a sensor, May 2004.
122. WANG M. L., WANG G. AND YIM J., "Smart Cables for Cable-stayed Bridge". Smart Structures Technology for Steel Structures, 16-18 November Seoul, Korea. (2006)
123. WANG G. AND WANG M. L., Application of EM Stress Sensors in Large Steel Cables, International Journal of Smart Structures and Systems, Vol. 2, NO.2. (2006)
124. WANG M. L. CHEN Z. KOONTZ S. AND LLOYD G. D., Magneto-elastic permeability measurement for stress monitoring, In Proceeding of the SPIE 7th Annual Symposium on Smart Structures and Materials, Health Monitoring of the Highway Transportation Infrastructure, 6-9 March, CA, Vol. 3995, pp. 492-500. 2000
125. ZDENEŤK P. BAZĪANT, Structural stability, International Journal of Solids and Structures 37 55±67,2000
126. ZHOU Y., SO R. M. C., JIN W., XU H. G. and CHAN P. K. C., "Dynamic Strain Measurements of a Circular Cylinder in a Cross Flow using a Fibre Bragg grating Sensor", Experiments in Fluids, vol.27,pp.359-367, 1999.

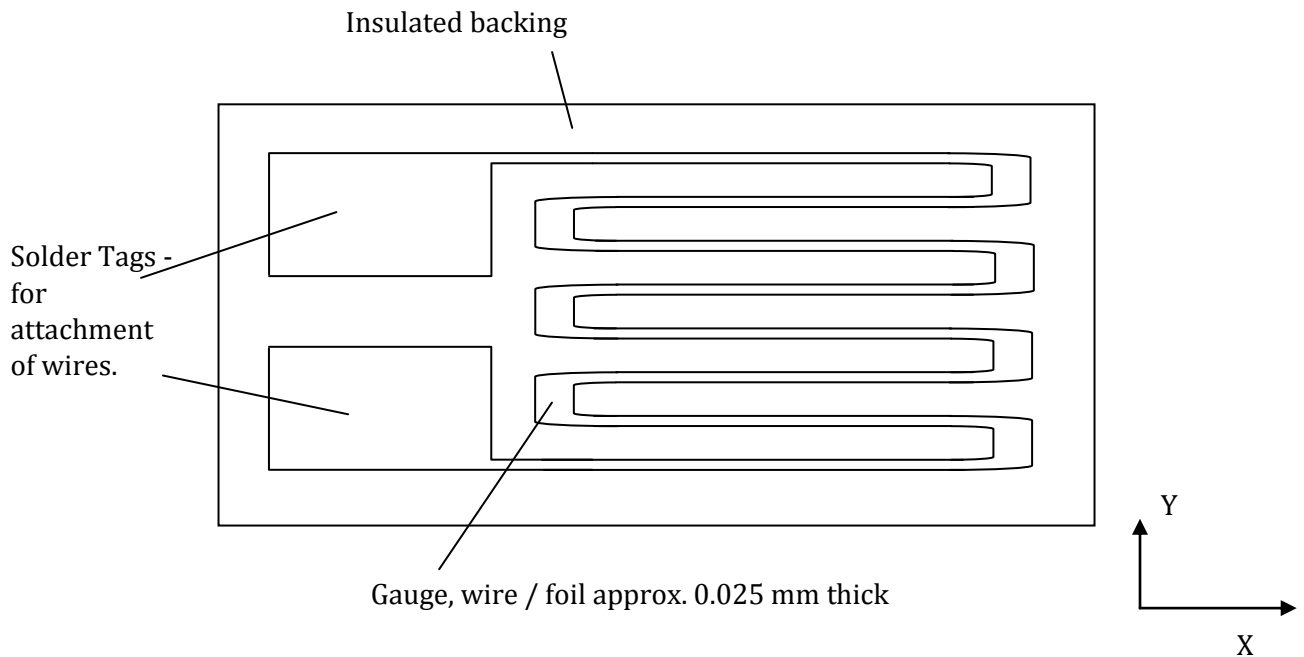
9. APPENDIX A-BASICS OF STRAIN GAUGES

9.1 Resistance of a Conductor

The resistance, R , of a conductor is defined in terms of its resistivity ρ (Ωm), length L (m), and cross sectional area A (m^2) by:

$$R = \frac{\rho L}{A}$$

If we consider an elongation of the wire, $L \rightarrow L + \Delta L$, by Poisson's effect there will also be reduction in cross sectional area, $A \rightarrow A - \Delta A$. From the expression for the resistance it can be seen that both effects contribute to an increase in the resistance.

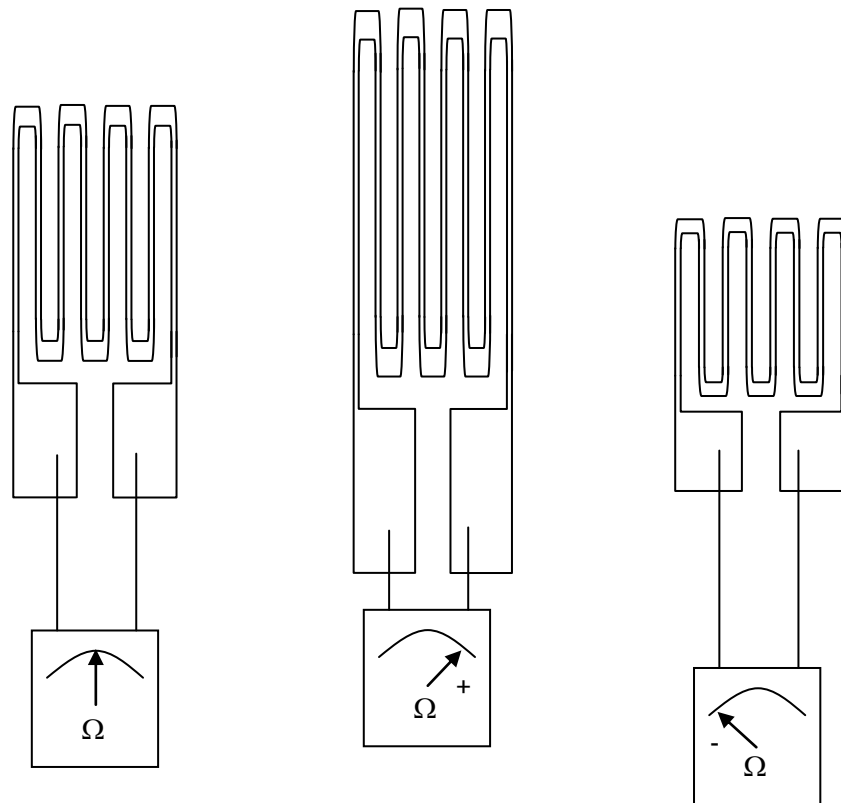


9.2 Strain Gauge Schematic

The gauge shown here is primarily sensitive to strain in the X-direction, as the majority of the wire length is parallel to the x-axis. There will be a small amount of cross-sensitivity, i.e. the resistance will change slightly for a strain in the Y-direction. This cross sensitivity is typically <2% of the primary axis sensitivity.

9.3 Strain Gauge Operation

This schematic shows how the strain gauge resistance varies with strain (deformation).



9.4 Relationship between Resistance and Strain

Starting with:

$$R = \frac{\rho L}{A}$$

If we consider a change in conductor length, ΔL , then:

$$\Delta R = \frac{\rho \Delta L}{A}$$

If we divide this expression through by R :

$$\frac{\Delta R}{R} = \frac{\frac{\rho \Delta L}{A}}{\frac{\rho L}{A}} = \frac{\Delta L}{L}$$

Allowing the resistance to vary through the other dependent parameters (A and ρ) and noting that as A is in the denominator such that for a positive change in cross sectional area ΔA , the resistance will decrease:

$$\frac{\Delta R}{R} = \frac{\Delta \rho}{\rho} - \frac{\Delta A}{A} + \frac{\Delta L}{L} \quad (\text{Eq. A.1})$$

The change in area can be related to the change in length via Poisson's effect. If the cross section is circular of initial diameter D , then as the area goes from A to $A + \Delta A$ and $D \rightarrow D + \Delta D$. If we define the axial strain as $\varepsilon_a = \frac{\Delta L}{L}$, and the transverse strain as

$\varepsilon_t = \frac{\Delta D}{D}$, Then

$$\varepsilon_t = \frac{\Delta D}{D} = -\nu \varepsilon_a = -\nu \frac{\Delta L}{L} \quad (\text{Eq. A.2})$$

Where ν is Poisson's ratio.

We can also expand the term for the area change in Eq. A.1 as:

$$\begin{aligned} \frac{\Delta A}{A} &= \frac{\frac{\pi}{4} \left\{ (D + \Delta D)^2 - D^2 \right\}}{\frac{\pi}{4} D^2} = \frac{D^2 + 2D\Delta D + \Delta D^2 - D^2}{D^2} \\ &\approx \frac{2\Delta D}{D} \end{aligned} \quad (\text{Eq. A.3})$$

By neglecting terms with the square of small quantities and combining Eqs A.2 and A.3:

$$\frac{\Delta A}{A} \approx -2\nu \frac{\Delta L}{L}$$

This can be substituted into Eq. A.1 to give:

$$\frac{\Delta R}{R} = \frac{\Delta \rho}{\rho} + 2\nu \frac{\Delta L}{L} + \frac{\Delta L}{L}$$

9.5 Relationship between Resistance and Strain (2)

From the previous page:

$$\frac{\Delta R}{R} = \frac{\Delta \rho}{\rho} + 2\nu \frac{\Delta L}{L} + \frac{\Delta L}{L}$$

$$\frac{\Delta R}{R} = \left(1 + 2\nu + \frac{\frac{\Delta \rho}{\rho}}{\frac{\Delta L}{L}} \right) \frac{\Delta L}{L}.$$

The bracketed term we define as the GF , giving:

$$\frac{\Delta R}{R} = GF \frac{\Delta L}{L} = GF \varepsilon_a.$$

This expression means that the change in resistance is directly proportional to the axial strain of the sample. The gauge factor is approximately constant and for most types of strain gauges has a value of a little greater than 2.

The component manufacturer will supply the gauge factor value. The material most often used for the conductor is constantan, because this material has a nearly identical gauge factor in both the elastic and plastic deformation regions of the stress-strain curve.

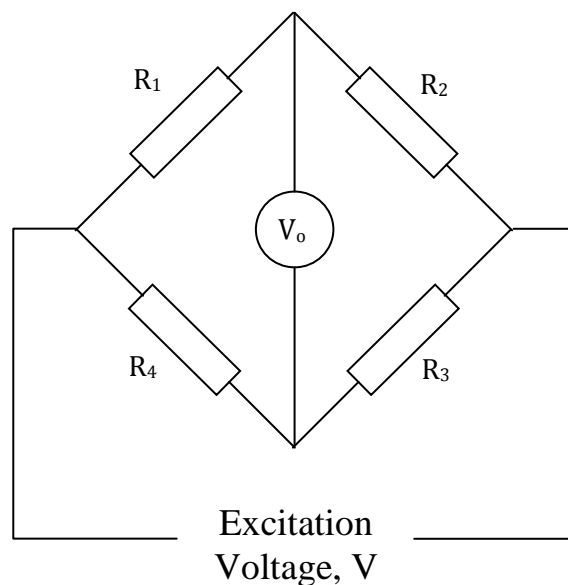
The measured values of strain vary between applications. The maximum measurable strain is typically 0.001, or 0.1%. Strain is most often expressed in microstrain, μ strain (10^{-6}). Therefore a strain of 0.001 is normally written as 1000 μ strain.

9.6 Signal Conditioning

The output of a strain gauge is therefore a change in resistance. This is normally detected as a change of voltage in a type of bridge circuit. It would appear that if we apply a large voltage to the bridge and have a large gauge factor that we would increase our sensitivity to strain. However, the gauges can withstand only a limited power, $\leq 25\text{mW}$, therefore we typically use low voltages and have to detect a small change in voltage which is proportional to the change in resistance. Therefore we often need to have an amplifier to increase the detected signal.

9.7 Wheatstone Bridge Circuit

Wheatstone developed a bridge circuit containing 4 resistances, one of which was the strain gauge, from the figure $R_{\text{gauge}} = R_1$.

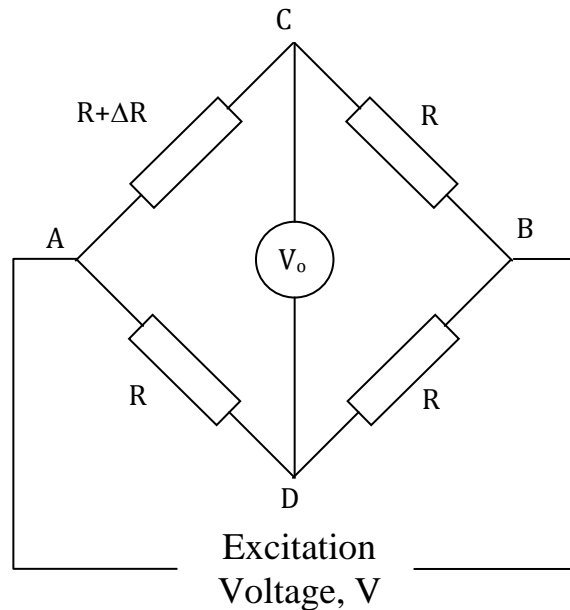


The excitation can be either DC or AC. DC voltages are normally used for sensitive measurements. AC voltages are used in electrically noisy environments with an

excitation frequency about a factor of 10 higher than the maximum strain variation frequency to be measured (typically excitations of >8 kHz).

Nominal resistance values are between 120Ω and 350Ω .

9.8 Output of a Wheatstone bridge



The circuit shown above is known as a 'quarter bridge' circuit as the strain-sensing gauge we are interested in appears in only one position (out of four).

We will consider a system with a constant DC excitation voltage, V , and where the input resistance of the voltmeter is infinite, i.e. no current flows through CD. With $\Delta R = 0$, the bridge is perfectly balanced and hence the output voltage, $V_o = 0$.

The current flowing through the upper half of the bridge is given by:

$$I_{ACB} = \frac{V}{2R + \Delta R}$$

Hence the potential difference across the strain gauge ($R + \Delta R$) is:

$$V_{AC} = \frac{V(R + \Delta R)}{2R + \Delta R}$$

The potential difference across AD is given by $V_{AD} = V/2$.

The output voltage of the system, V_o is given by:

$$\begin{aligned} V_o &= V_{AC} - V_{AD} = \frac{V(R + \Delta R)}{2R + \Delta R} - \frac{V}{2} = \\ &= \frac{V(2R + 2\Delta R - 2R - \Delta R)}{4R + 2\Delta R} = \frac{V\Delta R}{4R + 2\Delta R} \end{aligned}$$

Typically the change in resistance is low compared to the original resistance value, hence

$$V_o = \frac{V}{4} \times \frac{\Delta R}{R}$$

Noting that previously we related change in resistance to axial strain $\frac{\Delta R}{R} = GF\varepsilon_a$, we now obtain:

$$\varepsilon_a = \frac{4V_o}{V} \times \frac{1}{GF}$$

9.9 Characteristics of Quarter Bridge Strain Gauge Sensors

The strain is given by:

$$\varepsilon_a = \frac{4V_o}{V} \times \frac{1}{GF}$$

In most instruments this will be pre-calibrated to allow for the gauge factor and supply voltage.

The major disadvantage of the quarter bridge circuit is that changes in resistance of the gauge due to temperature cannot be differentiated from resistance changes due to strain. Several forms of temperature compensation can be introduced into the quarter bridge arrangement.

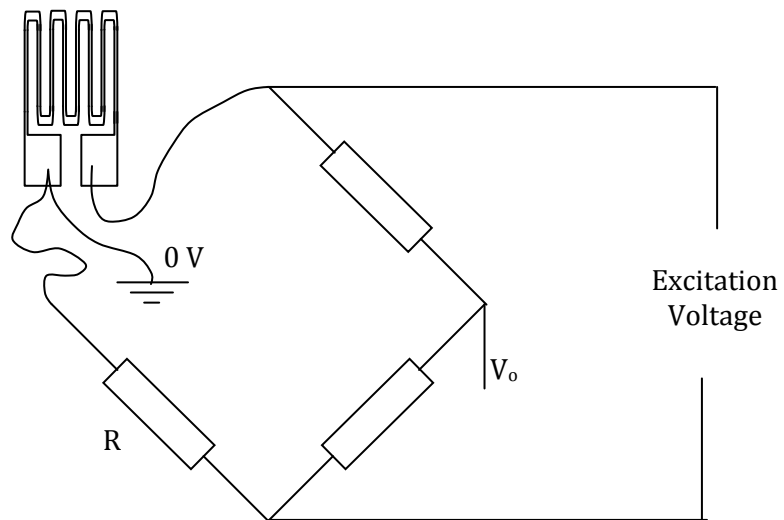
9.10 Temperature Compensation (1)

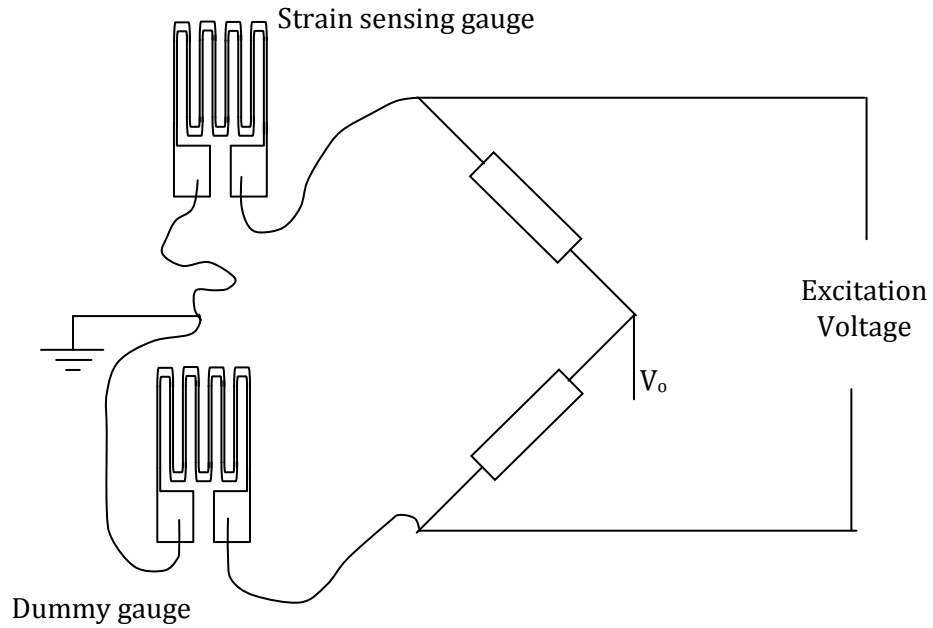
The diagram below illustrates how temperature (and hence resistance) changes within the leads going to the strain gauge can be compensated. This effect is common for lead lengths in excess of ~10 and normally both leads add to the resistance of the gauge in one arm of the bridge and hence are misinterpreted as a strain. Using a 'three lead wire' system, the resistance of one lead is with the gauge, and the resistance of the other lead is with resistor R in an adjacent arm of the bridge. Therefore any temperature and hence

resistance changes common to both leads are balanced in the bridge and do not affect the strain measurement.

Temperature Compensation (2)

Any temperature change of the gauge itself will also cause a resistance change and hence an erroneous strain measurement. This may be compensated by using a second, 'dummy' gauge. This dummy gauge is not under strain but is in situ and therefore experiences the same temperature fluctuations as the actual strain sensing gauge. The dummy gauge can be attached to an unstressed part of the component, or attached to a component of similar material as that under test. The diagram below illustrates this configuration. Careful assembly of dummy gauge systems can produce temperature compensation in both the gauge and the leads.





Particular combinations of gauges can be utilized in certain applications (see later) offering both increased sensitivity – with 2 sensing gauges in a half bridge – and simultaneously temperature compensated. Further, a full bridge can be used, offering 2.6 times the sensitivity of a quarter bridge.

9.11 Strain Gauge Installation

To correctly install a strain gauge all surfaces must be clean and free from grease before assembly.

Strain gauges can be protected from the environment in a number of ways. Techniques offering increasing protection are:

- Polyurethane varnish.
- Varnish + silicone rubber.
- Varnish + rubber + steel cover and sealed cable conduits.

In electrically noisy environments it is important that the wires leading to a gauge are made as a twisted pair. Hence any 'pick-up' (by induction) is common to both wires and the voltage difference is unaffected.

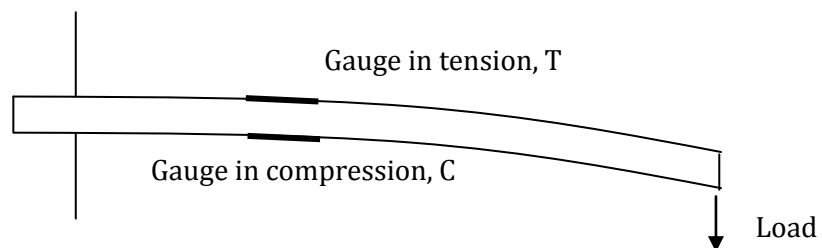
Installing strain gauges is a skilled art, it is easy to install gauges:

- In tension (by stretching).
- In compression.
- With poor adhesion.

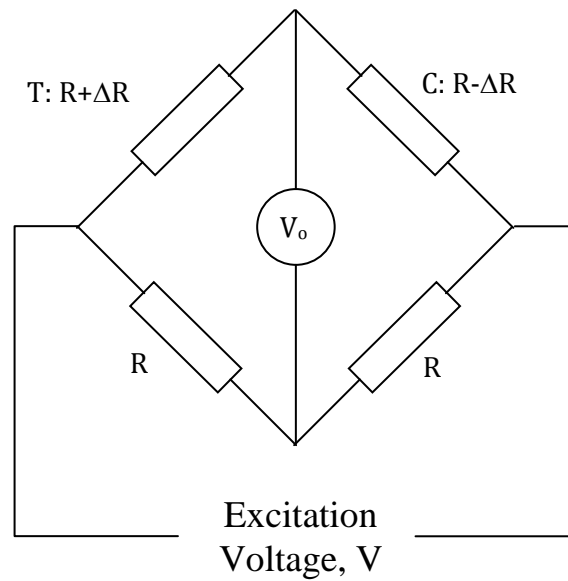
Calibration must be achieved in situ.

9.12 Measurement of Bending Strain

Consider measuring the bending strain in a cantilever.



If the two gauges are inserted into a half bridge circuit as shown and remembering that in tension the resistance will increase by ΔR , and in compression the resistance will decrease by the same amount, we can double the sensitivity to bending strain *and* eliminate sensitivity to temperature.



You can demonstrate that the output is given by:

$$V_o = \frac{V}{2} \times \frac{\Delta R}{R}$$

i.e. the output is double that from a quarter bridge circuit.

Further you can demonstrate that if the resistance of both gauges increases (due to temperature or axial strain) then the output voltage remains unaffected (try it by putting the resistance of gauge C as $R+\Delta R$).

10. APPENDIX B-MODULUS OF ELASTICITY

Material	Young's modulus (E) in <u>GPa</u>	Young's modulus (E) in <u>PSI</u>
Rubber (small strain)	0.01-0.1	1,500-15,000
Polystyrene	3-3.5	435,000-505,000
Nylon	2-4	290,000-580,000
Oak wood (along grain)	11	1,600,000
High-strength concrete (under compression)	30	4,350,000
Magnesium metal	45	6,500,000
Glass	50-90	7,250,000-13,000,000
Aluminium alloys	69	10,000,000
Brasses and bronzes	103-124	17,000,000
Titanium (Ti)	105-120	15,000,000-17,500,000
Carbon fiber reinforced plastic (unidirectional, along grain)	150	21,800,000
Wrought iron and steel	190-210	30,000,000
Tungsten (W)	400-410	58,000,000-59,500,000
Silicon carbide (SiC)	450	65,000,000
Tungsten carbide (WC)	450-650	65,000,000-94,000,000
Diamond	1,050-1,200	150,000,000-175,000,000

11. APPENDIX C- PUBLICATIONS AND ACHIEVEMENTS

PATENTS

1. Patent No. WO0135818. Detecting device for the forces developing under the foot, Inventor: Saad Jabir.
2. Patent No. WO0120284. Miniaturized device for sensing the surface force distribution, inventor; Saad Jabir.
3. Patent Nr. ITMI960829. Calzatura equipaggiata di elettronica, sensori, segnalatori, circuiteria particolarmente adatta per l'antifortunistica, la sicurezza , gli sport, per l'ortopedia e l' attivita' riabilitativa. Inventors : Saad Jabir and Dario Fiocchi.

LIST OF PAPERS RELATIVE TO THE THESIS WORK

1. Saad Jabir , N K Gupta, F Khalaf , "Application of Thick-Film Force Sensors on Building Materials ", measurements, Elsevier (Ref: MEAS-D-08-00218R2 accep). (accepted not published yet).
2. Saad Jabir, N K Gupta , "Thick Film Sensitive Strain Gauges for Structural Health Monitoring", issue 165/02 , 2011, EngineerIT journal, EEpublisher.
3. Saad Jabir, N K Gupta," Thick Film Ceramic Strain Sensors for Structural Health Monitoring ", IEEE Measurements , (to be published in coming issue).

LIST OF OTHER AUTHOR'S PUBLISHED PAPERS

1. Saad Jabir. "Simulation versus Emulation"; An article treating the advantages of simulation with respect to emulation of microprocessors was published in two magazines; EDAvision No. 9 September 2001 and the German magazine Elektronik, No. 11 of 28 May 2002. "Simulation versus emulation". <http://www.edavision.com/September2001/toc.php>
2. Saad Jabir. Simulation tools enhance Vehicle safety, Proc. Vehicle Technology Conference, UK – Coventry 2001.
3. Saad Jabir and Alexander Heubi. Mixed signal designs migration to new technologies in full custom design flow, Synopsys user Conference 2004.
4. Jan Sysr , Saad Jabir, "PLL characterization using HspiceRF in Custom Designer Environment" synopsys users conference.

SEMINARS AND OTHERS

1. Obtained European financial support for a feasibility study to improve FSR (Force Sensing Resistors) pressure sensors.
2. Obtained regional financial support for research on the implementation of sensors to study and improve sport action.
3. Covered the session for synopsys Analogue Mixed Signal Flow seminar in Munich May 2004.
4. Covered the session entitled. "Top-down design of a mixed signal audio chip in a mixed language environment" in a SoC (system on chip) seminar organized in Munich, November 2001.
5. Covered the session "analogue mixed signal design flow", synopsys seminar in Moscow November 2004.

MAIN REALISED PROJECTS

- 1- **Nuclear medicine** : Gamma camera for internal organs photography with the use of isotopes gamma rays instead of light. High speed Nuclear data acquisition system.
- 2- **Consumer** :
 - a. microprocessor based Automatic antenna positioning system , code deciphering and motor control.
 - b. Gate array for antenna control
 - c. Automatic testing equipment for antenna production final testing
 - d. Microprocessor based telex management system , three PC's to one telex machine
 - e. Microprocessor based centralized small building communication control
- 3- **Orthopaedics**: Three generations of foot print platforms for measuring body weight distribution and dynamic gate analysis.
- 4- **Industrial** :
 - a. Two generations of tyre footprint measurement system.
 - b. Two generation of hydraulic lift positioning system based on oil temperature.

- c. Firmware for underground voice communication microcontroller based system

5- Sport :

- a. on road cyclists power and energy measurement device based on force application on pedal .
- b. A tuning bench for force sensors controlled by LABVIEW.

6- Simulation and Modelling: A microprocessor model to debug hardware together with firmware. Model was written in Hardware Design Language MAST and C++.
<http://www.edavision.com/September2001/toc.php>

Balsa wood:

Ochroma pyramidale, commonly known as Balsa, (also *O. Lagopus*) is a species of flowering plant in the mallow family, Malvaceae. It is a large, fast-growing tree that can grow up to 30 m (100 ft) tall. Balsa trees are native from southern Brazil and Bolivia north to southern Mexico however Ecuador supplies 95 percent or more of commercial Balsa. In recent years about 60 percent of the Balsa has been plantation grown in densely packed patches of 50 to 100 trees per hectare (compared to about two to three per hectare in nature).[2] It is evergreen, or dry-season deciduous if the dry season is long, with large (30–50 cm/12–20 in) weakly palmately lobed leaves. Trees are classified as hardwood because of the shape of their leaves, so Balsa, with its large broad leaves is classified as hardwood despite being very soft. It is the softest commercial hardwood. The trees are harvested after 6 to 10 years of growth. The name Balsa comes from the Spanish word for "raft."

Balsa lumber is very soft and light with a coarse, open grain. The density of dry balsa wood ranges from 40–340 kg/m³ (2.5-21 lb/ft³), with a typical density of about 160 kg/m³ (10 lb/ft³).[3]

The light weight of the wood derives from the fact that the tree has large cells that contain water. After the water is driven off in an extended drying process (kiln dried for 2 weeks,) the large surface area of the resulting holes give strength. Unlike dry rotted wood, the surface is made of the usual strong cellulose/lignin mix.

As it is low-density but high in strength, balsa is a very popular material to use when making light, stiff structures in model bridge tests and for the construction of model aircraft as well as full-sized light wooden aeroplanes, most famously the World War II de Havilland Mosquito. Balsa is used to make wooden crank baits for fishing.

Birefringence, or **double refraction**, is the decomposition of a ray of light into two in two slightly different directions when it passes through certain anisotropic materials, such as

crystals of calcite or boron nitride. The effect is now known to also occur in certain plastics, magnetic materials, various non-crystalline materials, and liquid crystals. The names reflect the fact that if un-polarised light enters the material at a nonzero acute angle to the optical axis, the component with polarization perpendicular to this axis will be refracted as per the standard law of refraction, while the complementary polarization component will refract at a nonstandard angle determined by the angle of entry and the difference between the indices of refraction.

CMOS, Complementary metal-oxide-semiconductor: is a technology for constructing integrated circuits. CMOS technology is used in microprocessors, microcontrollers, static RAM, and other digital logic circuits. CMOS technology is also used for several analogue circuits such as image sensors, data converters, and highly integrated transceivers for many types of communication.

"CMOS" refers to both a particular style of digital circuitry design, and the family of processes used to implement that circuitry on integrated circuits (chips). CMOS circuitry dissipates less power than logic families with resistive loads. Since this advantage has increased and grown more important, CMOS processes and variants have come to dominate, thus the vast majority of modern integrated circuit manufacturing is on CMOS processes.

Besides digital applications, CMOS technology is also used in analogue applications. For example, there are CMOS operational amplifier ICs available in the market. Transmission gates may be used instead of signal relays. CMOS technology is also widely used for RF circuits all the way to microwave frequencies, in mixed-signal (analogue + digital) applications.

d33, piezoelectric coefficient:

Alternatively, Piezoelectric Modulus, quantifies the volume change when a piezoelectric material is subject to an electric field, or the polarisation on application of a stress:

$$d = \frac{P}{\sigma}$$

where P is polarisation, and σ is the stress. There are actually many Piezoelectric coefficients; D_{xy} .

Delamination: is a mode of failure for composite materials. Modes of failure are also known as 'failure mechanisms'. In laminated materials, repeated cyclic stresses, impact, and so on can cause layers to separate, forming a mica-like structure of separate layers, with significant loss of mechanical toughness. Delamination also occurs in reinforced concrete structures subject to reinforcement corrosion.

The cause of fibre pull-out (another form of failure mechanism) and delamination is weak bonding. Thus, delamination is an insidious kind of failure as it develops inside of the material, without being obvious on the surface, much like metal fatigue.

Delamination failure may be detected in the material by its sound; solid composite has bright sound, while delaminated part sounds dull, reinforced concrete sounds solid, whereas delaminated concrete will have a light drum-like sound when exposed to a dragged chain pulled across its surface. Other non-destructive testing methods are used, including embedding optical fibres coupled with optical time domain Reflectometer testing of their state, testing with ultrasound, radiographic imaging, and infrared imaging.

Flexural modulus

In mechanics, the flexural modulus is the ratio of stress to strain in flexural deformation, or the tendency for a material to bend. It is determined from the slope of a stress-strain curve produced by a flexural test (such as the ASTM D 790), and uses units of force per area. It is an intensive property.

$$E(\text{bend}) = L^3F/4wh^3d$$

For a 3-point deflection test of a beam, where: w and h are the width and height of the beam, L is the distance between the two outer supports and d is the deflection due to load F applied at the middle of the beam.

Michelson interferometer: is the most common configuration for optical Interferometry and was invented by Albert Abraham Michelson. An interference pattern is produced by splitting a beam of light into two paths, bouncing the beams back and recombining them. The different paths may be of different lengths or be composed of different materials to create alternating interference fringes on a back detector.

Morlet wavelet (Figure D-1)

In mathematics, the Morlet wavelet, named after Jean Morlet, was originally formulated by Goupillaud, Grossmann and Morlet in 1984 as a constant $\kappa\sigma$ subtracted from a plane wave and then localised by a Gaussian window.

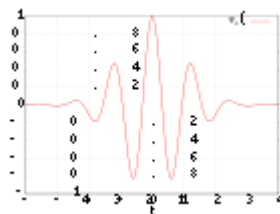


Figure D-1 Morlet Input Wave is a combination of sinusoid and Gaussian

Wavelet transform (WT) has gained popularity as an efficient means of signal processing in SHM, in which an optimal mother wavelet-based WT can carry out feature extraction with high precision enabling better diagnoses and localization of structural defects.

Moment of inertia of the area:

I is a property of a cross section that can be used to predict the resistance of beams to bending and deflection. The deflection of a beam under load depends not only on the load, but also on the geometry of the beam's cross-section. This is why beams with higher area moments of inertia, such as I-beams, are so often seen in building construction as opposed to other beams with the same area. It is analogous to the polar moment of inertia, which characterizes an object's ability to resist torsion. The second moment of area is not the same thing as the moment of inertia, which is used to calculate angular acceleration, although the calculations are similar. Many engineers refer to the second moment of area as the moment of inertia and use the same symbol, I , for both, which may be confusing. Which inertia is meant (accelerational or bending) is usually clear from the context and obvious from the units: second moment of area has units of length to the fourth power whereas moment of inertia has units of mass times length squared.

Moiré pattern in physics is an interference pattern created, for example, when two grids are overlaid at an angle, or when they have slightly different mesh sizes.

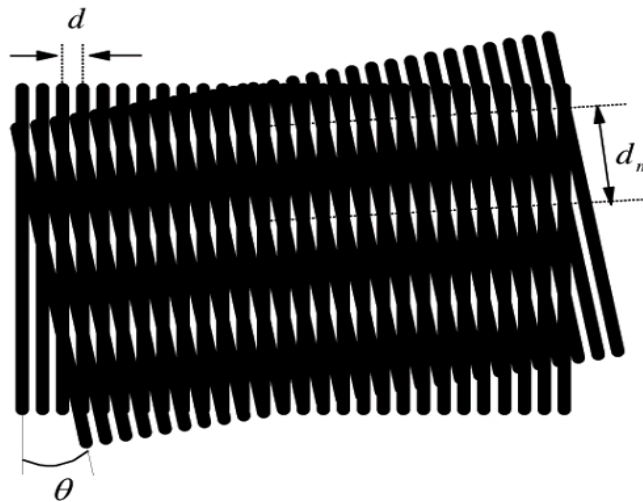


Figure D2 Moire' Pattern

In manufacturing industries, these patterns are used for studying microscopic strain in materials: by deforming a grid with respect to a reference grid and measuring the moiré pattern, the stress levels and patterns can be deduced. This technique is attractive because the scale of the moiré pattern is much larger than the deflection that causes it, making measurement easier.

Polyvinylidene Fluoride or PVDF:

is a highly non-reactive and pure thermoplastic fluoropolymer.

PVDF is a specialty plastic material in the fluoropolymer family; it is used generally in applications requiring the highest purity, strength, and resistance to solvents, acids, bases and heat and low smoke generation during a fire event. Compared to other fluoropolymers, it has an easier melt process because of its relatively low melting point of around 177°C.

Stiffness (rigidity):

is the resistance of an elastic body to deformation by an applied force along a given Degree of Freedom (DOF) when a set of loading points and boundary conditions are prescribed on the elastic body. It is an extensive material property. In general, elastic modulus is not the same as stiffness. Elastic modulus is a property of the constituent material; stiffness is a property of a structure. That is, the modulus is an intensive property of the material; stiffness, on the other hand, is an extensive property of the solid body dependent on the material and the shape and boundary conditions. For example, for an element in tension or compression, the axial stiffness is

$$k = \frac{AE}{L}$$

Where

A is the cross-sectional area,

E is the (tensile) elastic modulus (or Young's modulus),

L is the length of the element.

For the special case of unconstrained uniaxial tension or compression, Young's modulus can be thought of as a measure of the stiffness of a material.

Tactile sensor:

The term tactile sensor usually refers to a transducer, that is sensitive to touch, force, or pressure. Tactile sensors are employed where ever interactions between a contact surface and the environment are to be measured and registered.